

Thermal Analysis of the R7021 Radioactive Materials Transport Container

Report R5108-DRAFT2

March 2008

Thermal Analysis of the R7021 Radioactive Materials Transport Container

prepared for
REVISS Services (UK) Ltd.

M. Beiler
FTT Technology (Pty) Ltd

Summary

This report presents a thermal performance analysis of the R7021 transport container under IAEA normal and accident conditions of transport with an internal heat load of 2119W. Ambient temperature of 38°C and solar radiation from the top and sides was modelled for normal conditions of transport. The accident analyses modelled an environment simulating an 800°C furnace test with forced updraft around the flask in three different flask orientations, namely upright, vertical inverted and the flask on its side. The heating phase lasted for thirty minutes, followed by a cooling period in the normal conditions environment, which was continued until all temperatures were falling.

Salient temperatures are listed in the following tables, with reference locations included on page 7.

Normal Conditions (without insolation)

location	A ₁	A ₂	B ₁	B ₂	C ₁	C ₂	D	E	F	G	H	I	J
temperature	157	145	161	148	156	144	123	120	117	80	74	81	123

location	K	L	M	N	O	P	Q	R	S	T	U	lead max.
temperature	125	121	124	128	130	51	51	55	56	64	63	148

Normal Conditions (with insolation)

location	A ₁	A ₂	B ₁	B ₂	C ₁	C ₂	D	E	F	G	H	I	J
temperature	163	151	166	153	162	150	131	128	126	93	88	93	130

location	K	L	M	N	O	P	Q	R	S	T	U	lead max.
temperature	132	127	130	134	136	72	68	70	71	84	84	154

Accident Conditions

location	Accident 1: upright		Accident 2: inverted		Accident 3: side	
	peak temperature	time	peak temperature	Time	Peak temperature	time
A1	259	5100	251	5100	251	7500
A2	247	5100	239	5400	238	6900
B1	256	5100	256	5400	254	6900
B2	243	5100	243	5100	241	6900
C1	247	6000	253	5700	250	7500
C2	234	5700	241	5700	238	7500
D'	234	5400	225	5700	227	5700
E'	236	5400	221	5700	225	5400
F	240	3600	230	3300	232	3600
J	236	4500	223	4500	221	4500
K	240	2400	220	2700	216	4500
L	249	1800	244	1800	212	4200
M	215	3300	232	2400	219	5100
N	215	5700	226	5100	222	7500
O	216	6500	227	6500	222	7500
lead max.	251	2400	244	5400	243	6300
location	K		K		B ₂	

Contents

Summary	2
1 Purpose and Scope.....	4
2 R7021 Description and Specifications	4
3 Methodology	5
3.1 Modelling	5
3.2 Normal Conditions Analysis	6
3.3 Accident Conditions Analysis	6
4 Results	7
4.1 Normal Conditions	8
4.2 Accident Conditions	8
6 References	18
Appendix 1: Figures	19
Appendix 2: Grill Characterization	24

1 Purpose and Scope

The purpose of this report is to establish the thermal performance of the R7016 transport container and contents under IAEA normal and accident conditions of transport.

2 R7021 Description and Specifications

The R7021 transport container comprises an upright, cylindrical stainless steel flask mounted on a carbon steel pallet [1]. The flask has a central cavity holding the source capsules and a removable closure plug at the top. Lead surrounds the cavity. Voids in the flask corners and at the base are filled with ceramic fibre insulation. A cylindrical shield surrounds the flask. A second shield is mounted to the top of the flask. The cylindrical and parts of the top shield are filled with ceramic fibre insulation. Fins of different size are fitted to the cylindrical flask surface. A grill is positioned above the cylindrical shield. The flask comprises the following materials:

Flask and closure:	304L stainless steel
Lead:	pure lead
Insulation:	Superwool 607 blanket (64kg/m ³)
Pallet, jacket and top shield:	grey painted carbon steel
Bottom surface of top shield:	304L stainless steel

3 Methodology

3.1 Modelling

The CFD code Ansys CFX was used to model the heat transfer and gas flow processes involved. CFX is a leading general purpose CFD code. CFX is suitable to solve fluid flow, thermal radiation and heat transfer problems. It is used in research and industry and has been validated. Results of previously performed analyses of transport packages have been benchmarked against experimental data.

The model comprises different types of zones. The flask and shields comprise solid heat conducting regions and solid heat conducting and heat generating regions. Regions surrounding the flask were modelled as gas flow regions with thermal radiation. The voids of the top shield were modelled as gas regions with radiation heat transfer. Natural convection inside the voids was neglected. The grill was modelled as isotropic porous region with similar pressure loss characteristics (see Appendix 2).

The energy equation was solved for solid regions. Continuity, momentum, turbulence and energy equations were solved for the fluid flow domain. A Monte Carlo radiation model was used to calculate thermal radiation between free surfaces emitting, absorbing and reflecting long wavelength radiation.

Normal conditions steady state temperatures depend mainly on the free convection cooling. For the heating phase the container was tested in a furnace model. The analysis modelled the furnace test with air at 800°C blown into the domain continuously to simulate the air movement associated with a fire.

Continuous heat production was modelled in the cavity wall and lead shielding. Heat from the package contents was modelled as heat flux applied to the cavity wall. The rate of heat production in each component or region is:

Location	Energy deposition [W]
Cavity wall heat flux	547
Cavity wall	233
First 12mm radial lead	841
Remaining radial lead	498
Total	2119

Model characteristics:

1. A contact coefficient of 280W/m²K was applied between lead and stainless steel surfaces.
2. An emissivity of 0.4 was applied to stainless steel surfaces at normal conditions.
3. The jacket and top shield was considered to be in poor thermal contact with the flask.

4. The flask was placed upright on a horizontal, solid surface with an emissivity of 0.9.
5. The support structure within the top shield was in contact with the vertical wall. The internal vertical webs were removed as they are thermally insulated from the top and middle plates.
6. The thin volume between the side and base of the closure and the flask was assumed to be a solid with the properties of air.

3.2 Normal Conditions Analysis

Ambient air temperature of 38°C was assumed. Flask temperatures were calculated without and with solar insolation. The following directional heat fluxes were applied to model insolation:

1. Downward heat flux (-y direction): 800W/m²
2. Horizontal direction (-x direction): 200W/m²
3. Horizontal direction (+x direction): 200W/m²
4. Horizontal direction (-z direction): 200W/m²
5. Horizontal direction (+z direction): 200W/m²

3.3 Accident Conditions Analysis

The flask was placed in a furnace at temperature of 800°C for thirty minutes. An upward air flow at temperature of 800°C and flow rate of 6m/s was applied, which results in peak flow rates surrounding the flask of 7m/s to 8m/s. The steady state solution under normal transport conditions provided the initial container temperatures. External surface emissivity was changed to a value of 0.8. The furnace wall temperature was fixed at 800°C. The furnace wall emissivity was specified as 0.9. Insolation heat fluxes were excluded.

A cooling period at normal conditions followed the heating phase. The ambient temperature was 38°C and insolation heat fluxes were applied during the cooling phase.

Three flask orientations were considered:

Accident 1: Flask in upright position

Accident 2: Flask inverted

Accident 3: Flask on side, axis at 10° to horizontal with package base uppermost.

4 Results

The following measurement location references are used:

A1	Cavity wall (50mm below top)
A2	Lead adjacent to A1
B1	Cavity wall (mid-height)
B2	Lead adjacent to B1
C1	Cavity wall (50mm above base)
C2	Lead adjacent to C1
D	Lead (closure base centre)
E	Lead (closure top centre)
F	Closure flange (20mm below upper surface, 50mm from outer edge)
G	Lifting fin (100mm from top edge, 75mm from outer edge)
H	Lifting fin (40mm from top edge, 55mm from outer edge)
I	Lifting fin (135mm from top edge, 35mm from outer edge)
J	Lead (top chamfer top corner)
K	Lead (top chamfer bottom corner)
L	Flask wall (mid-height, midway between fins)
M	Lead (bottom chamfer top corner)
N	Drain point (centre of cylinder, 70mm from outer surface)
O	Lead (bottom chamfer bottom corner)
P	Flask foot (top surface, 30mm from outer edge)
Q	Jacket (mid height outer surface)
R	Jacket (top edge)
S	Jacket (inner surface, 40mm from top edge)
T	Top shield (mid height vertical face)
U	Top shield (half way across horizontal face)
V	Top shield (top surface centre)
W	Maximum lead temperature
X	Mean lead temperature
Y	Maximum lead temperature location

4.1 Normal Conditions

Table 1 shows steady state temperatures for normal conditions with and without insolation. Temperature and flow distributions on a vertical flask section are shown in Figure A1.2 and A1.3.

Table 1: Normal conditions temperatures [°C].

location	incl. solar insolation	excl. solar insolation
A1	163	157
A2	151	145
B1	166	161
B2	153	148
C1	162	156
C2	150	144
D	131	123
E	128	120
F	126	117
G	93	80
H	88	74
I	93	81
J	130	123
K	132	125
L	127	121
M	130	124
N	134	128
O	136	130
P	72	51
Q	68	51
R	70	55
S	71	56
T	84	64
U	84	63
V	87	63
W	154	148

4.2 Accident Conditions

Accident 1: Flask in upright position

The temperatures histories during heating and subsequent cooling at various locations are listed in Table 2 and plotted in Graph 1 to 3.

Table 2: Flask temperatures for accident 1.

time	temperature, °C													
s	A ₁	A ₂	B ₁	B ₂	C ₁	C ₂	D	E	F	G	H	I	J	K
0	163	151	166	153	162	150	131	128	126	93	88	93	130	132
300	163	151	166	154	162	150	131	129	126	283	399	304	130	137
600	164	152	167	154	163	151	131	129	127	494	590	498	132	148
900	167	155	169	158	164	153	131	129	134	631	716	613	137	165
1200	172	161	174	163	168	157	132	132	148	676	725	682	146	185
1400	177	167	179	168	171	160	133	135	159	703	737	693	153	199
1600	183	173	184	174	175	165	134	139	172	727	770	715	163	213
1800	190	181	190	180	181	171	136	145	186	732	770	719	173	226
2100	202	194	202	192	190	180	140	155	207	584	572	577	189	237
2700	227	218	225	215	210	201	155	179	232	425	400	432	215	240
3300	244	233	240	229	226	215	173	197	239	340	316	347	228	238
3900	253	241	249	237	236	224	191	210	240	284	264	291	234	236
4500	257	245	254	241	241	230	204	219	239	245	227	251	236	233
5100	259	247	256	243	245	233	215	224	236	217	201	221	236	230
5400	259	247	256	243	246	233	219	226	235	205	190	209	235	229
5700	259	246	256	243	246	234	222	227	233	196	181	199	234	228
6000	259	246	256	243	247	234	224	228	232	187	174	190	233	226
6300	258	245	256	243	247	234	226	229	230	179	166	182	232	225
6500	258	245	255	242	247	234	227	229	229	175	162	178	231	224
6600	257	245	255	242	246	234	227	229	229	173	160	175	230	223

time	temperature, °C													
s	L	M	N	O	P	Q	R	S	T	U	V	W	X	Y
0	127	130	134	136	72	68	70	71	84	84	87	154	136	B ₂
300	140	133	135	136	189	718	432	311	680	626	713	154	138	B ₂
600	158	140	137	136	346	767	647	544	717	757	776	157	141	B ₂
900	177	150	141	137	495	787	695	646	771	748	761	175	147	K
1200	201	163	147	138	581	764	745	635	782	775	739	197	155	K
1400	214	174	153	140	631	771	731	654	776	802	787	211	162	K
1600	234	185	160	143	664	802	725	689	799	778	779	225	170	K
1800	249	197	167	147	689	782	748	675	778	804	749	239	178	K
2100	247	209	178	154	588	416	519	536	471	473	444	248	190	K
2700	234	214	194	168	434	239	357	381	311	315	312	250	207	K
3300	225	214	203	182	341	173	277	293	243	245	250	245	217	K
3900	219	214	209	193	279	137	226	239	201	204	210	243	222	A ₂
4500	216	213	212	202	234	118	192	199	175	177	187	246	225	A ₂
5100	213	212	214	208	200	102	166	173	155	158	167	248	226	A ₂
5400	212	212	215	210	187	98	157	165	149	152	162	248	226	A ₂
5700	211	211	215	212	175	95	150	155	144	146	156	248	226	A ₂
6000	210	211	215	214	165	92	143	147	138	141	150	247	225	A ₂
6300	208	210	215	215	155	89	136	142	133	136	147	247	225	A ₂
6500	208	210	215	216	150	87	133	138	131	134	144	246	225	A ₂
6600	207	210	215	216	147	87	132	137	130	132	141	246	224	A ₂

A small air gap separates the closure lead from the flask body. Contact between flask and closure occurs at the closure top between the steel surfaces. As no heat is generated within the closure lead and no heat from the cavity is applied to the cavity base, heat flows from the hot flask body to the closure. This causes the temperature profile at location D and E to lag the surrounding body temperatures, which are declining. As the temperature difference between closure and lead is small (Figure 1) and the peak temperatures at location D and E will not exceed the peak temperatures at locations D' and E' (Figure 1), the peak conservative temperatures prevailing at D' and E' are presented instead of temperatures at D and E.

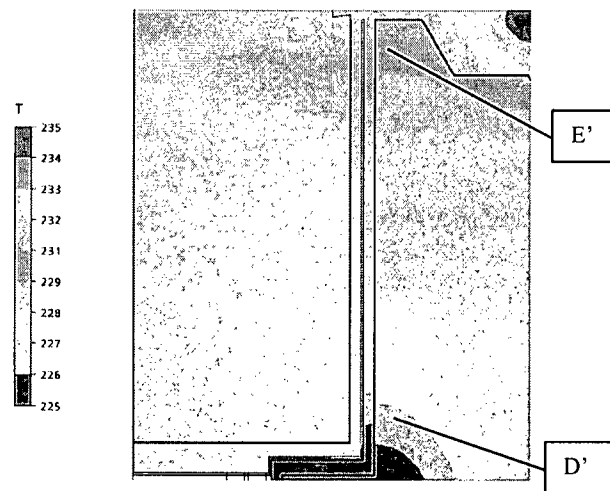
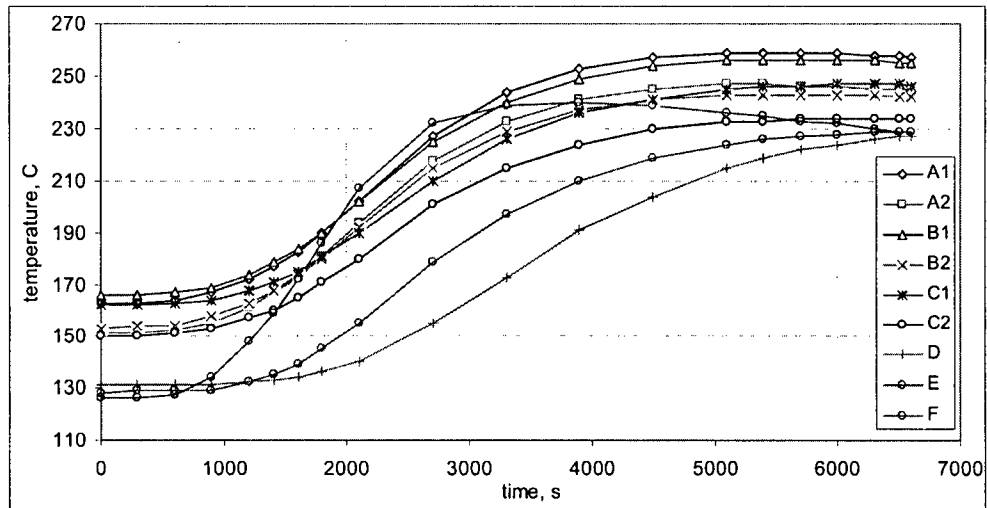


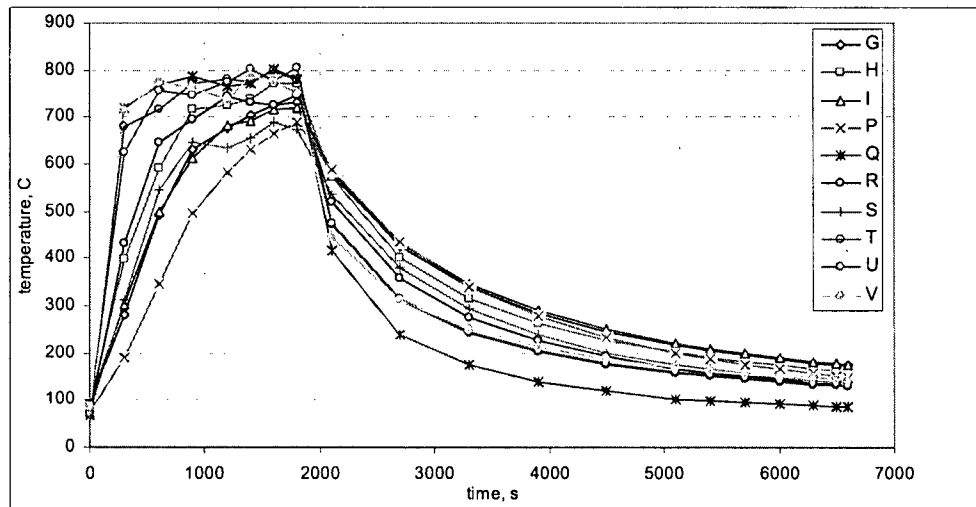
Figure 1: Closure and flask top temperatures at $t=6600s$ (Accident 1) [$^{\circ}C$]

Table 3: Temperatures at locations D' and E' for accident 1.

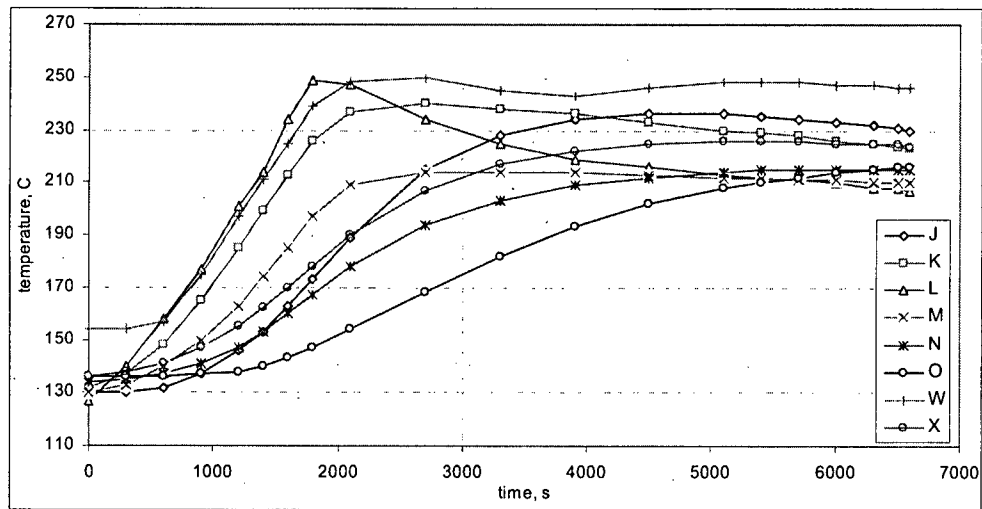
location	temperature [C]	peak [s]
D'	234	5400
E'	236	5400



Graph 1: Accident 1 temperatures.



Graph 2: Accident 1 temperatures.



Graph 3: Accident 1 temperatures.

Accident 2: Flask inverted

The temperatures histories during heating and subsequent cooling for accident 2 at various locations are listed in Table 4 and plotted in Graph 4 to 6. The flask temperatures after the heating period are slightly lower than for accident 1. The peak lead temperature initially occurs at the cavity (location B₂), while the peak is located at the flask wall (location M) during the heating and the initial cooling phase. At 3900s the peak lead temperature moves back to the location B₂ at the cavity.

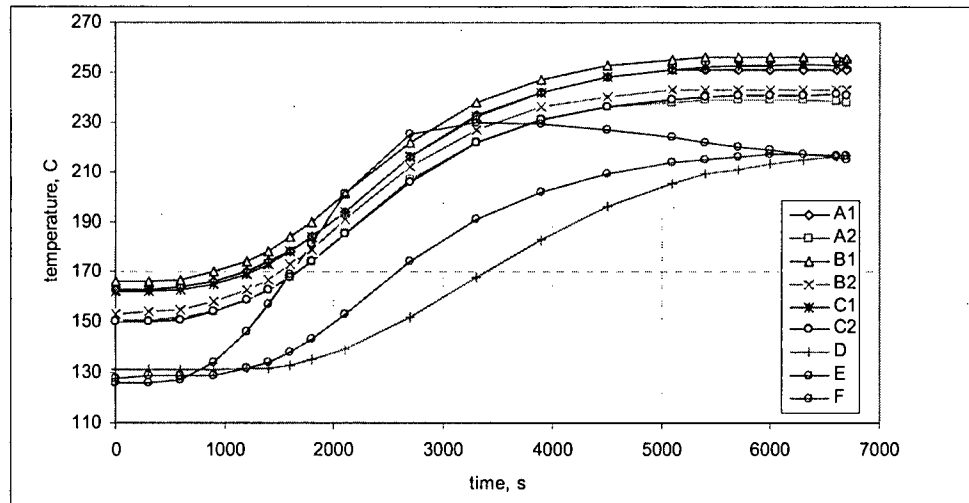
Table 4: Flask temperatures for accident 2.

time	temperature, °C													
s	A ₁	A ₂	B ₁	B ₂	C ₁	C ₂	D	E	F	G	H	I	J	K
0	163	151	166	153	162	150	131	128	126	93	88	93	130	132
300	163	151	166	154	162	150	131	129	126	285	357	261	130	136
600	164	152	167	155	163	151	131	129	127	458	579	418	132	143
900	166	154	170	158	165	154	131	129	134	564	666	552	136	155
1200	170	159	174	163	169	159	132	132	146	667	710	637	143	168
1400	174	163	178	167	173	163	132	134	157	682	724	653	150	179
1600	178	168	184	173	178	168	133	138	169	683	737	677	157	191
1800	184	174	190	179	184	174	135	143	181	716	730	699	166	203
2100	194	185	201	191	194	185	139	153	201	566	560	553	180	215
2700	216	207	222	212	216	206	152	174	225	400	380	398	203	220
3300	233	222	238	227	232	222	168	191	230	310	293	311	216	220
3900	242	231	247	236	242	231	183	202	229	253	237	255	221	219
4500	248	236	253	240	248	236	196	209	227	214	201	215	223	218
5100	251	238	255	243	251	239	205	214	224	184	172	186	223	217
5400	251	239	256	243	252	240	209	215	222	173	161	174	222	216
5700	251	239	256	243	253	241	211	216	220	163	152	164	221	216
6000	251	239	256	243	253	241	213	217	219	153	140	154	221	215
6300	251	239	256	243	253.5	241	215	217	217	143	130	145	220	214
6600	250.9	238.3	256.0	242.9	253	241.1	216.3	216.9	216	135	122	137	218	213
6700	250.8	238.1	255.8	242.8	253.4	241.0	216.7	216.8	215	133	120	135	218	212

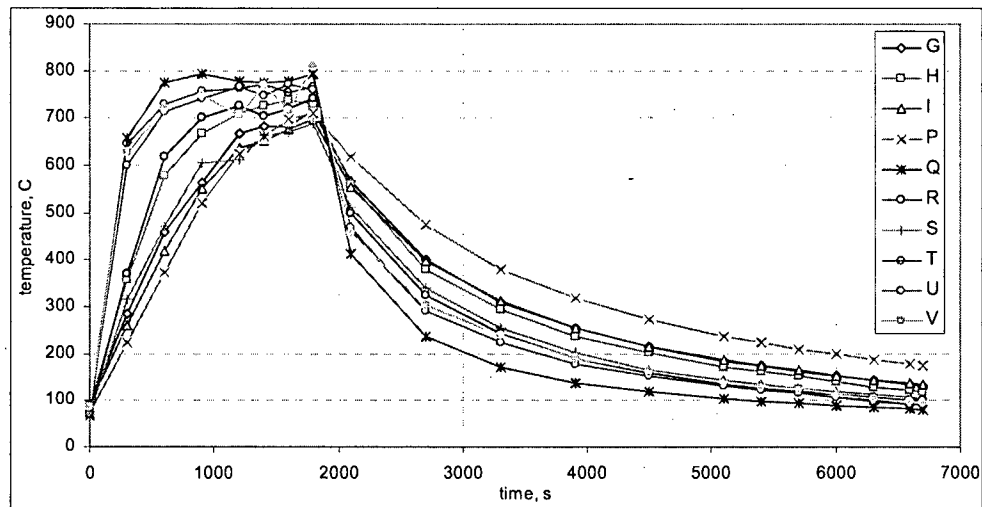
time	temperature, °C													
s	L	M	N	O	P	Q	R	S	T	U	V	W	X	Y
0	127	130	134	136	72	68	70	71	84	84	87	154	136	B ₂
300	143	136	135	136	222	659	370	315	645	599	628	154	138	B ₂
600	162	147	139	136	374	776	618	472	730	714	718	155	141	B ₂
900	182	162	145	137	520	792	700	607	757	742	748	167	147	M
1200	204	179	154	139	624	778	727	612	763	764	707	185	154	M
1400	217	191	161	141	662	776	705	663	771	748	767	198	160	M
1600	227	204	169	145	698	777	718	670	752	771	717	211	168	M
1800	244	216	177	149	710	794	741	688	764	760	807	224	176	M
2100	243	228	190	158	619	414	500	510	463	468	457	234	187	M
2700	232	232	206	176	474	236	323	339	292	292	302	236	204	M
3300	224	230	216	191	381	171	241	253	222	223	238	235	215	M
3900	219	229	221	204	319	138	191	201	179	179	191	236	220	B ₂
4500	216	227	224	213	272	119	159	166	153	153	163	241	223	B ₂
5100	214	226	226	219	237	105	136	144	131	131	140	243	225	B ₂
5400	213	225	226	222	222	99	127	134	122	122	131	244	225	B ₂
5700	212	224	226	224	209	95	120	127	116	116	125	244	225	B ₂
6000	211	223	226	225	198	90	112	119	107	106	114	244	225	B ₂
6300	210	223	226	226	187	86	106	114	102	99	105	244.1	225	B ₂
6600	210	222	225.9	226.8	178	82	102	106	93	93	97	244	224	B ₂
6700	209	222	225.8	227.1	175	81	100	104	92	91	94	243.9	224	B ₂

Table 5: Temperatures at locations D' and E' for accident 2.

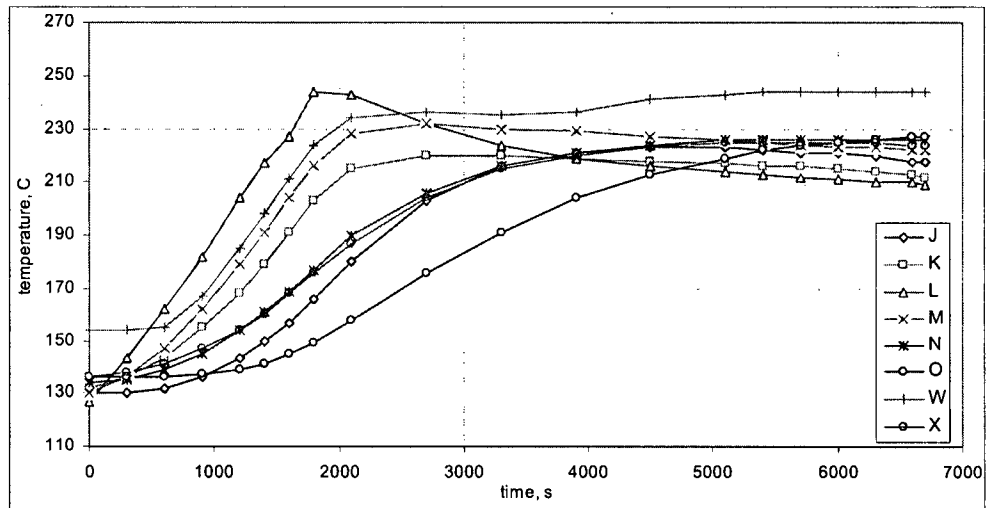
location	temperature [C]	peak [s]
D'	225	5700
E'	221	5700



Graph 4: Accident 2 temperatures.



Graph 5: Accident 2 temperatures.



Graph 6: Accident 2 temperatures.

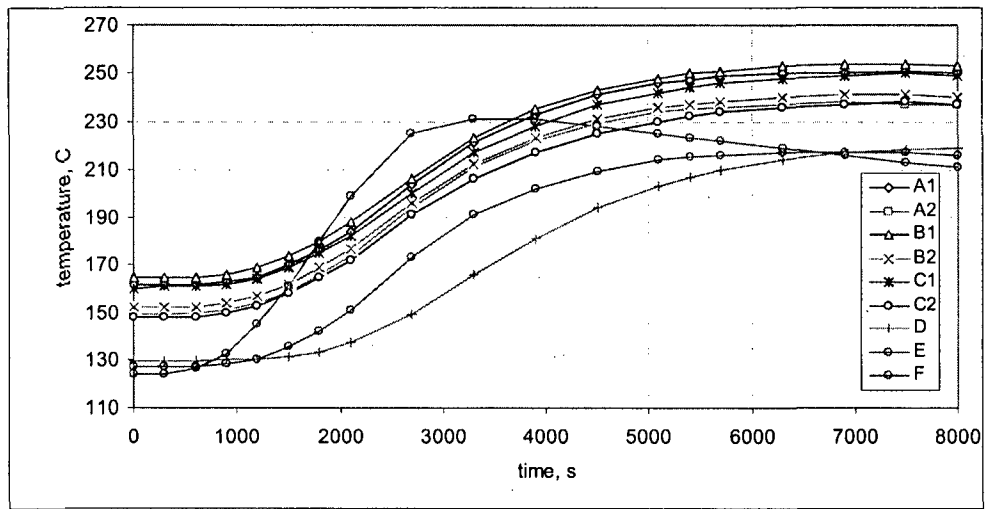
Accident 3: Flask on side

The temperatures histories during heating and subsequent cooling for accident 3 at various locations are listed in Table 6 and plotted in Graph 7 to 9. The cooling period for accident 3 extends over a longer period since the buoyancy effect is less effective when the finned cooling channels are not in upright position.

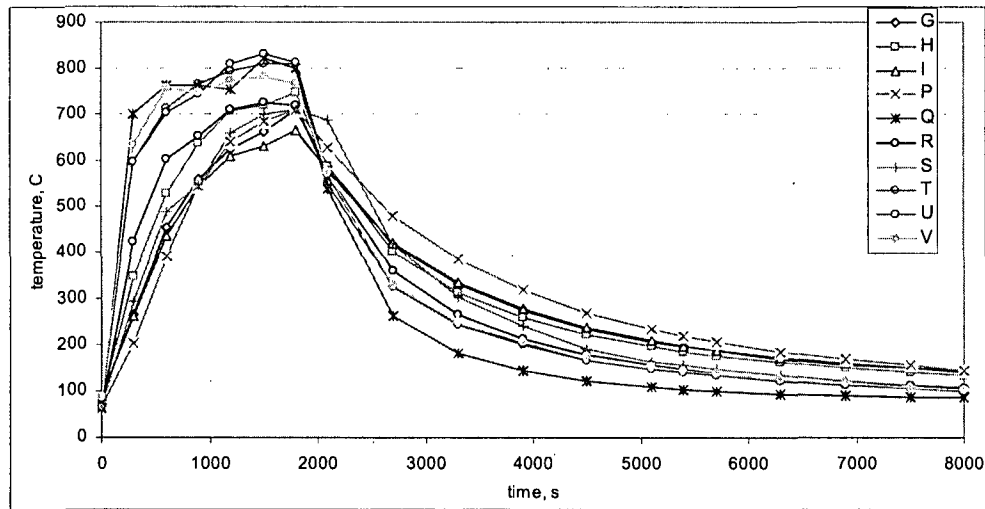
Table 6: Flask temperatures for accident 3.

time	Temperature, °C													
s	A ₁	A ₂	B ₁	B ₂	C ₁	C ₂	D	E	F	G	H	I	J	K
0	162	149	165	152	160	148	129	127	124	88	82	88	129	130
300	162	149	165	152	161	148	129	127	124	266	347	263	129	131
600	162	150	165	152	161	148	129	127	126	453	527	434	130	136
900	163	151	166	154	162	150	130	128	132	560	637	543	134	144
1200	165	154	169	157	164	153	130	130	145	625	706	609	141	152
1500	170	159	174	162	169	158	131	135	161	663	719	631	150	165
1800	176	166	180	169	175	165	133	142	180	710	747	665	162	179
2100	184	174	188	177	182	172	137	151	199	588	587	578	175	192
2700	204	194	206	196	200	191	149	173	225	417	400	418	198	206
3300	221	211	223	212	217	206	166	191	231	330	311	333	211	212
3900	233	222	235	223	228	217	181	202	231	274	259	278	218	214
4500	241	229	243	231	237	225	194	209	228	235	222	239	221	216
5100	246	234	248	236	242	230	203	214	225	207	196	210	221	216
5400	247	235	250	237	244	232	207	215	223	196	185	198	221	216
5700	249	236	251	238	246	234	210	216	222	186	176	189	221	216
6300	250	237	253	240	248	236	214	217	219	170	161	172	220	216
6900	250	238	254	241	249	237	217	217	216	157	149	159	219	215
7500	251	237	254	241	250	238	218	217	213	149	141	151	217	214
8000	250	237	253	240	249	237	219	216	211	142	134	144	215	212

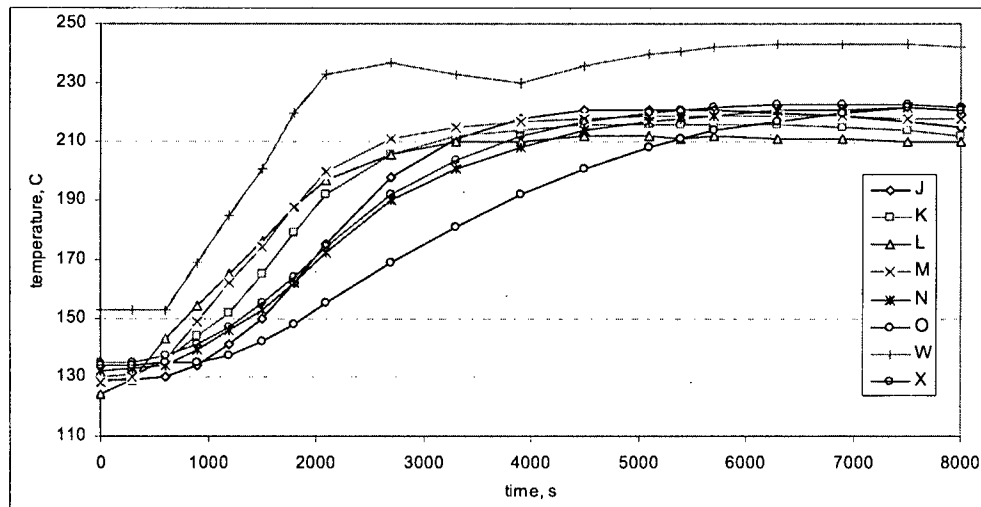
Time	Temperature, °C													
s	L	M	N	O	P	Q	R	S	T	U	V	W	X	Y
0	124	128	132	134	66	63	65	67	82	83	87	153	135	B ₂
300	129	130	133	134	204	700	421	294	598	597	635	153	135	B ₂
600	143	136	134	135	392	764	604	486	713	704	757	153	137	B ₂
900	154	149	139	135	544	763	654	548	767	743	747	169	141	B ₂
1200	165	162	146	137	641	754	709	660	793	810	771	185	147	L
1500	176	174	153	142	684	822	725	701	809	831	781	201	155	L
1800	188	188	162	148	710	799	720	708	809	813	767	220	164	M
2100	197	200	172	155	628	536	569	688	549	569	574	233	174	K
2700	206	211	190	169	479	262	359	415	324	328	328	237	192	K
3300	210	215	201	181	383	181	266	304	243	244	249	233	204	K
3900	210	217	208	192	318	144	214	241	200	202	207	230	212	B ₂
4500	212	218	214	201	270	122	178	192	167	167	175	236	217	B ₂
5100	212	219	217	208	234	108	155	164	147	148	153	240	220	B ₂
5400	211	219	218	211	219	104	146	155	140	140	145	241	221	B ₂
5700	212	219	219	214	206	101	139	148	133	133	138	242	222	B ₂
6300	211	219	221	217	185	95	126	133	122	122	126	243	223	B ₂
6900	211	219	221	220	168	91	118	122	114	114	118	243	223	B ₂
7500	210	218	222	222	155	87	111	113	106	106	107	243	223	B ₂
8000	210	218	221	221	144	86	107	108	102	101	102	242	222	B ₂



Graph 7: Accident 3 temperatures.



Graph 8: Accident 3 temperatures.



Graph 9: Accident 3 temperatures.

Table 7: Temperatures at locations D' and E' for accident 3.

location	temperature [C]	peak [s]
D'	227	5700
E'	225	5400

6 References

- [1] Work Specification WS7021/3 Thermal Analysis of the R7021 Transport Package, issue 1, 23 January 2008.
- [2] ANSYS CFX 11.0, Ansys, Inc., Canonsburg, 2007.
- [3] Superwool 607 Blanket, Morgan Thermal Ceramics, 11-1-01 E2/02, Augusta, Georgia.
- [4] The Carborundum Company, Niagara Falls, New York.
- [5] Heat Transfer: J.P Holman, 6th Edition, 1986.

Appendix 1: Figures

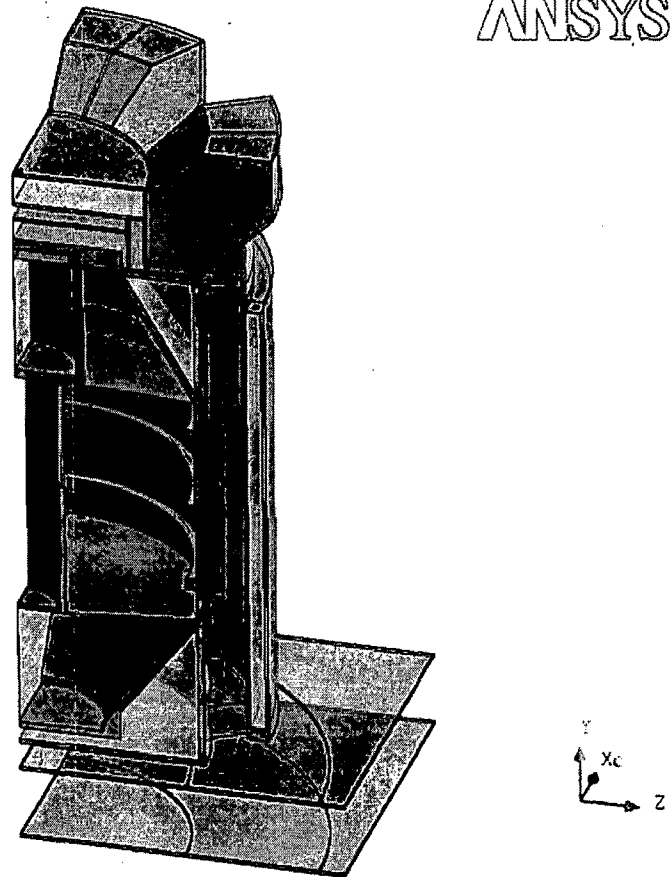


Figure A1.1: Quarter section of the container assembly.

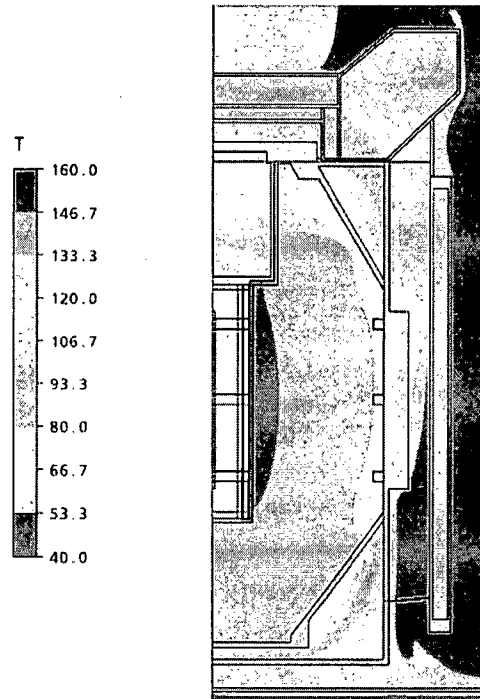


Figure A1.2: Temperature distribution at normal conditions with insolation [°C]

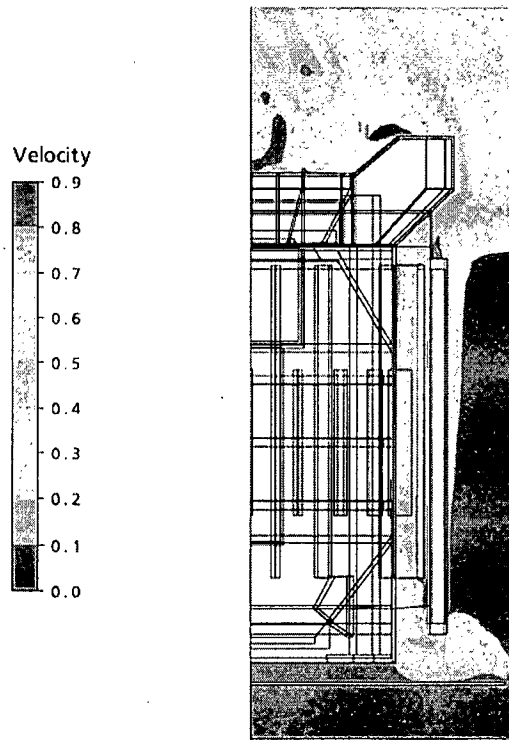


Figure A1.3: Typical flow distribution at normal conditions with insolation [m/s]

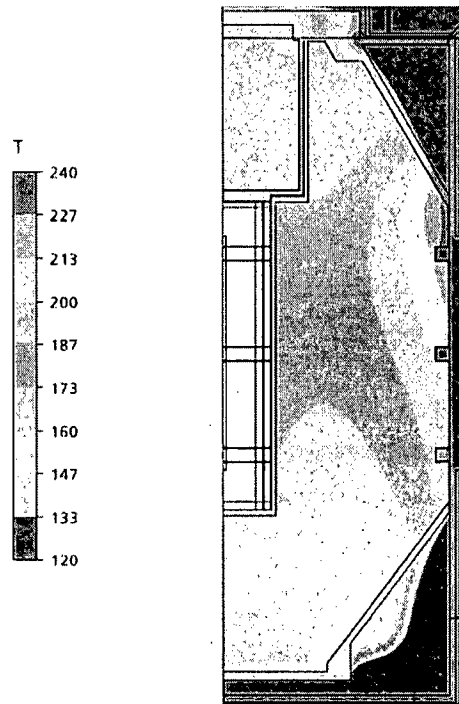


Figure A1.4: Accident 1: Flask core temperature distribution at 1800s [°C]

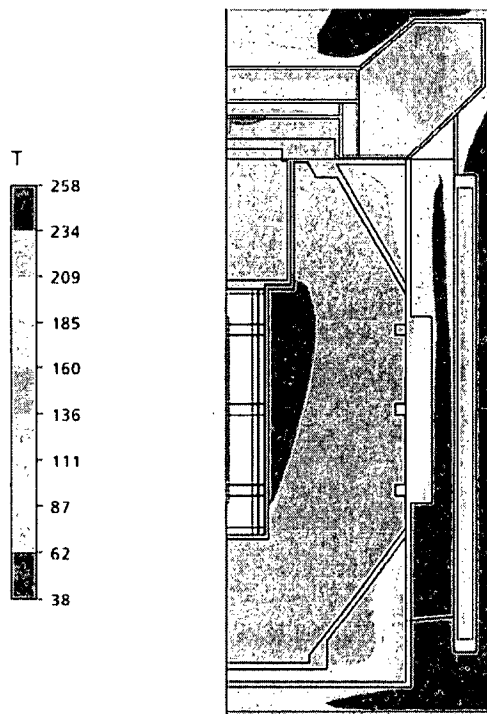


Figure A1.5: Accident 1: Flask core temperature distribution at 6600s [°C]

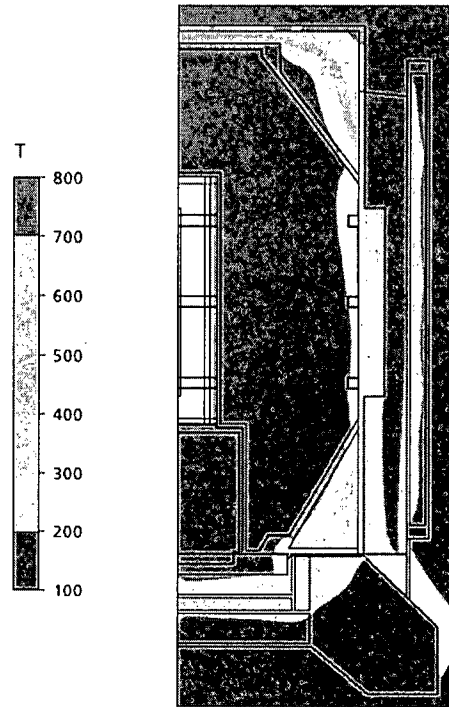


Figure A1.6: Accident 2: Temperature distribution at 1800s [°C]

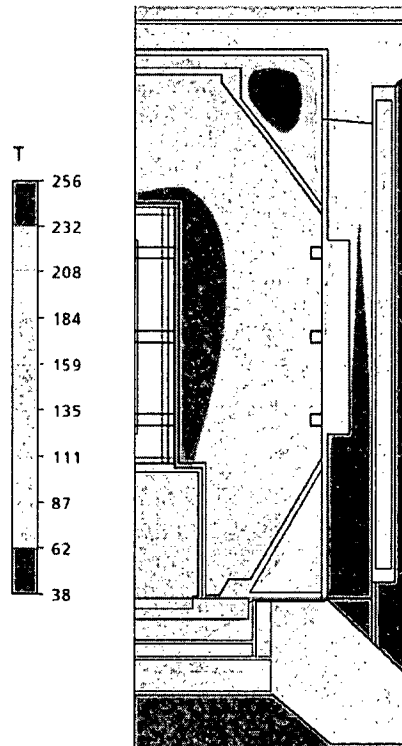


Figure A1.7: Accident 2: Temperature distribution at 6700s [°C]

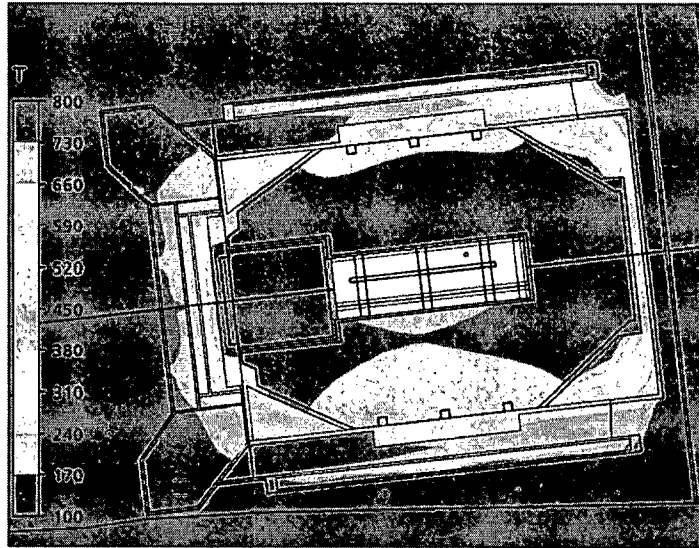


Figure A1.8: Accident 3: Temperature distribution at 1800s [°C]

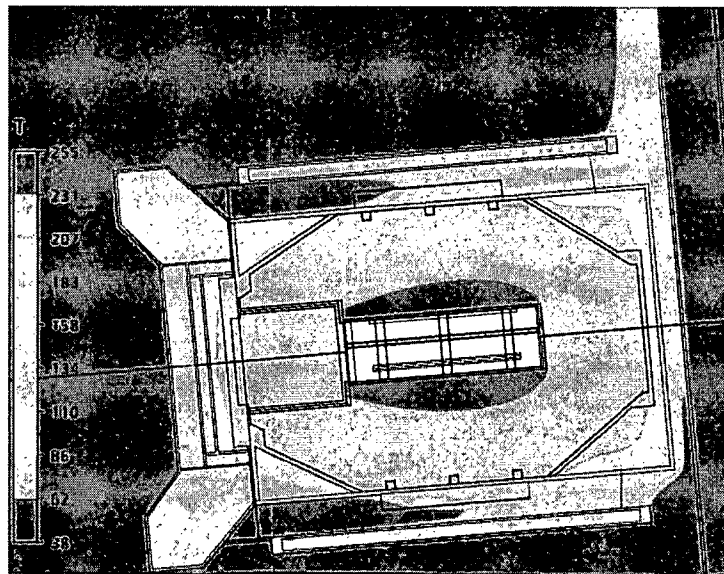


Figure A1.9: Accident 3: Temperature distribution at 6200s [°C]

Appendix 2: Grill Characterization

Pressure loss characteristics were evaluated at air flow rates in the range of 0.25m/s to 1.5m/s for (1) a flat screen similar to the screen incorporated in the design and (2) the corresponding porous model used in the main studies. The typical pressure drop across the screen using the different models is shown in Figure A2.1.

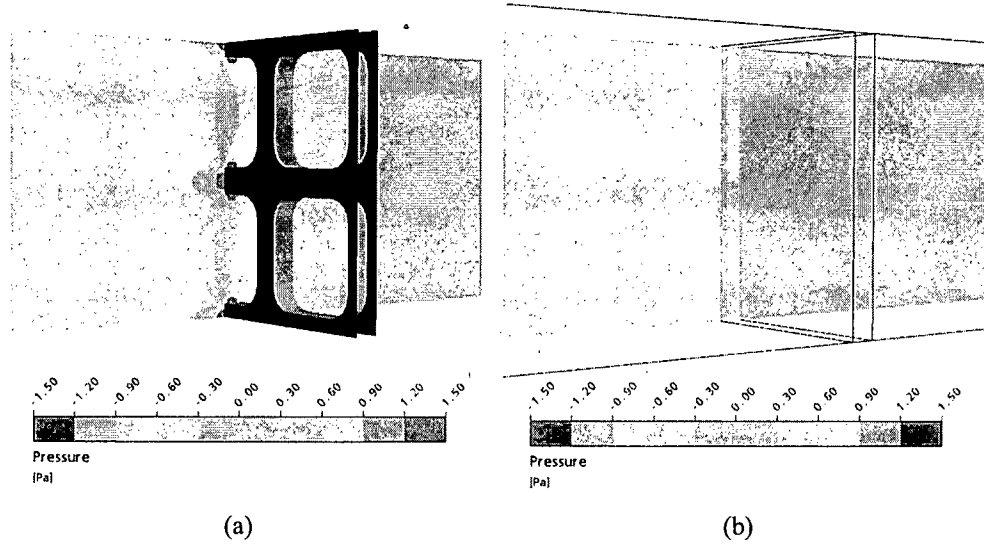


Figure A2.1: (a) Screen pressure loss at $Re=617$ and (b) corresponding pressure loss across porous screen.

The pressure loss coefficient, defined as

$$K_{loss} = \Delta p_t (0.5 \rho V^2)^{-1},$$

is shown in Figure A2.2, where

$$Re = \rho V d / \beta \mu$$

ρ = air density

V = gas velocity

d = equivalent wire diameter (6mm)

β = frontal area of holes / total frontal area

μ = dynamic viscosity

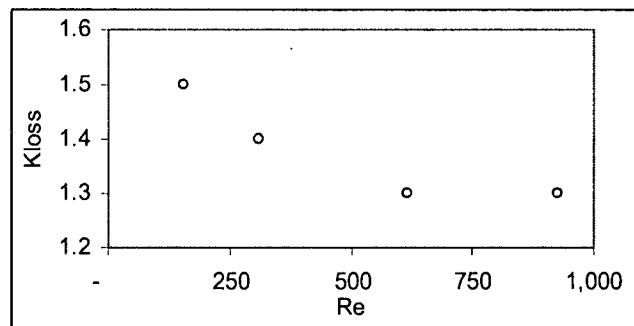


Figure A2.2: Screen pressure loss coefficient.

Thermal Analysis of the R7021 Radioactive Materials Transport Container

Report R7110/1.1

July 2010

Thermal Analysis of the R7021 Radioactive Materials Transport Container

prepared for
REVISS Services (UK) Ltd

Dr M. Beiler
FTT Technology CC

Summary

This report presents a thermal performance analysis of the R7021 transport container under test, IAEA normal and accident conditions of transport, with an internal heat load of 2362W at test conditions and 2460W at transport conditions, respectively. Ambient temperature of 38°C and solar radiation from the top and sides was modelled for normal conditions of transport. The accident analyses modelled an environment simulating an 800°C furnace test with forced updraft around the package in three different flask orientations, namely upright orientation, inverted orientation and the package on its side. The heating phase lasted for thirty minutes, followed by cooling at normal conditions environment. Test results from free drop and punch tests as well as results from computational analyses were used to model the damage.

Contents

Summary	2
1 Purpose and Scope	4
2 R7021 Description and Specifications	4
3 Modelling	4
3.1 Benchmarking	5
3.2 Sensitivity Study	6
3.3 Normal Conditions Analysis	7
3.4 Accident Conditions Analysis	7
4 Results	9
4.1 Benchmarking	9
4.2 Sensitivity Study	10
4.3 Normal Conditions	16
4.4 Accident Conditions	17
4.4.1 Accident 1: Package in Upright Orientation, Undamaged	17
4.4.2 Accident 1: Package in Upright Orientation, Damaged	18
4.4.3 Accident 2: Package in Inverted Orientation, Undamaged	21
4.4.4 Accident 2: Package in Inverted Orientation, Damaged	23
4.4.5 Accident 3: Package on its Side, Undamaged	25
4.4.6 Accident 3: Package on its Side, Damaged	27
4.4.7 Accident Source Temperatures	29
5 Conclusions	30
6 References	31
Appendix 1: Figures	32
Appendix 2: Specifications	43
A2.1 Model	43
A2.2 Material Properties	44
A2.3 Grill Characterization	45

1 Purpose and Scope

The purpose of this report is to benchmark the R7021 transport container and contents at test conditions and to establish the thermal performance of the container under IAEA normal and accident conditions of transport.

2 R7021 Description and Specifications

The R7021 transport container comprises an upright, cylindrical stainless steel flask mounted on a carbon steel pallet^[1]. The flask has a central cavity holding the source capsules and a removable closure plug at the top. Lead surrounds the cavity. Voids in the flask corners and at the base are filled with ceramic fibre insulation. A cylindrical shield surrounds the flask. A second shield is mounted onto the top of the flask. The cylindrical and parts of the top shield are filled with ceramic fibre insulation. Vertical fins are fitted to the cylindrical flask surface. A grill is mounted above the cylindrical shield. The package comprises the following materials:

Flask and closure:	304L stainless steel
Lead:	pure lead
Insulation:	Superwool 607 blanket (64kg/m ³)
Pallet, jacket and top shield:	grey painted carbon steel
Bottom surface of top shield:	304L stainless steel

3 Modelling

The CFD code Ansys CFD was used to model the heat transfer and gas flow processes involved. Ansys CFD is a leading, general purpose CFD code suitable to solve fluid flow, thermal radiation and heat transfer problems.

The model comprises different types of zones. The flask and shields comprise solid heat conducting regions and solid heat conducting and heat generating regions. Regions surrounding the transport package were modelled as gas flow regions with thermal radiation. The voids of the top shield were modelled as gas regions with radiation heat transfer. Natural convection inside the voids was neglected. The grill was modelled as an isotropic porous region with similar pressure loss characteristics (see Appendix 2). The energy equation was solved for solid regions. Continuity, momentum, turbulence and energy equations were solved for the fluid flow domain. A Monte Carlo radiation model was used to calculate thermal radiation between free surfaces emitting, absorbing and reflecting long wavelength radiation.

Test condition and normal conditions steady state temperatures depend mainly on free convection cooling. A flow domain encloses the package to facilitate flow around the package. The package was placed on a solid floor and exposed to natural convection cooling at the prevailing ambient air temperature, either at test conditions or at normal conditions. An insolation heat flux was applied for normal conditions with insolation. Free air flow was allowed across the flow domain so that the floor is free to dissipate received insolation by convection. For the heating phase the container was tested in a furnace model at forced flow

across the transport package. The analysis modelled the furnace test with air at 800°C blown into the domain continuously to simulate the air movement associated with a fire. Salient modelling parameters are presented in Appendix 2.

Continuous heat production was modelled in the cavity wall and lead shielding. Heat from the package contents was modelled as a heat flux applied to the cavity wall. The rate of heat production in each component or region is shown in the following table, with Q_i the total heat production.

Table 1: Specified package heat load distribution.

Location	Energy deposition [W]
Cavity wall heat flux	$0.258Q_i$
Cavity wall	$0.11Q_i$
First 12mm radial lead	$0.397Q_i$
Remaining radial lead	$0.235Q_i$
Total	$1.0Q_i$

A thermal contact resistance was specified between lead and stainless steel surfaces. The appropriate value was obtained from benchmarking simulations. The pallet is in thermal contact with the flask. The top shield rests on the flask, but to model the intermittent contact between the adjacent surfaces of the top shield and flask, a contact resistance equivalent to a 0.1mm gap was modelled. The thin volume between the side and base of the closure and the flask was specified as a non-convective air layer.

The package model does not include the cavity contents; a separate model was used to model the transport processes inside the cavity. The package model provided the cavity wall temperature, which is required to define the cavity model. The cavity model comprises the sources and basket.

Peak source temperatures at transient accident conditions were calculated for the peak cavity wall temperature reached during the accident. The package simulation provided the cavity wall temperature.

3.1 Benchmarking

Two designs were involved. The first design was the prototype and was used to determine package benchmark temperatures at given load conditions. The second design included a few minor design changes.

Both packages were modelled. A model of the prototype was used to benchmark the flask. The contact coefficient between lead and stainless steel surfaces was adjusted until measured and calculated cavity wall and source temperatures correlated well. The source emissivity was then amended iteratively until the best agreement between calculated and measured source temperature was found.

Benchmark conditions were recalculated with the model of the second design. The same parameter settings, as used for the prototype, were specified. Results from both models were

compared to demonstrate to which extent the design changes affect the thermal performance. The second design model has been used for the subsequent work.

The benchmark model incorporates a 3mm gap between closure and flask to model the gap provided for the thermocouple leads to exit. The total heat load of $Q_t=2362\text{W}$ was applied as shown in Table 1. The cavity was filled with air at 1atm.

3.2 Sensitivity Study

The purpose of the sensitivity study is to determine the sensitivity of the design to any assumed modelling values. The total heat load was increased to $Q_t=2460\text{W}$, which is the specified design value used for the subsequent studies described in the following sections. Normal conditions with insolation were predicted for the conditions specified in Table 2, using the reference model of the second design, which was set up in section 3.1. The directional insolation fluxes are given in Appendix 2. The sources were evenly distributed around the outer basket ring.

The emissivity of flask external surfaces corresponds to emissivity values of stainless steel, while the emissivity of carbon steel surfaces corresponds to emissivity values of painted surfaces.

Two complete transient accident simulations were performed for case 11 and 12. The flask was undamaged and the modelling approach is described in section 3.4.

Table 2: Cavity modelling parameters.

Case	Number of sources	Cavity gas	Cavity gas pressure [atm]
1	16	Neon	1
2	12	Neon	1
3	18	Neon	1
4	16	Helium	1
5	16	Air	1
6	16	Neon	2

Table 3: Package modelling parameters.

Case	Emissivity of flask external surfaces	Emissivity of carbon steel surfaces	Insulation conductivity
7	0.2	0.90	k_{ref}
8	0.4	0.90	k_{ref}
9	0.6	0.90	k_{ref}
10	0.4	0.80	k_{ref}
11	0.4	0.98	k_{ref}
12	0.4	0.90	$2k_{ref}$

3.3 Normal Conditions Analysis

The normal conditions analyses determine equilibrium temperature distribution throughout the package and contents under IAEA normal conditions of transport. The model described in section 3.1 was employed to predict temperatures at normal conditions, but the emissivity of external surfaces (stainless steel and painted carbon steel) and the insulation conductivity were adjusted to those values from the sensitivity study which resulted in the highest temperatures. Package temperatures were calculated with and without solar insolation. Insolation heat fluxes are included in Appendix 2. An ambient air temperature of 38°C was specified.

3.4 Accident Conditions Analysis

The model of section 3.3 was used to predict package temperatures during the transient period simulating a fire under IAEA accident conditions of transport. The package was placed in a furnace at temperature of 800°C for thirty minutes. An upward air flow, which resulted in peak flow velocity surrounding the package of not less than 10m/s, was applied to the enclosing flow domain. The temperature of both inflow and surrounding vertical walls was 800°C. The emissivity of external surfaces was changed to a value of 0.8 to represent blackened surfaces. The wall emissivity was specified as 0.9. Insolation heat fluxes were excluded. The steady state solution for normal transport conditions provided the initial condition temperatures of the package. A cooling period at normal conditions followed the heating phase. The package was placed in air, allowing for free convection cooling at an ambient air temperature of 38°C. Insolation heat fluxes, as described in section 3.3, were applied during the cooling phase.

Three package orientations were considered:

- Accident 1: Package in upright orientation
- Accident 2: Package in inverted orientation
- Accident 3: Package placed on its side

Package temperatures for each orientation were calculated for undamaged and damaged conditions.

Damage to the package in the upright, inverted and side orientation was modelled according to information provided in [17-24]. Drop test and punch test damage from each orientation were combined into a single model. The punch and impact damage to the package in upright orientation deformed the upper pallet plate, while a hole was cut into the lower pallet plate. This damage was modeled as shown in Figure A1.4. The hole in the centre of the pallet was modelled as a 150mm x 150mm square hole.

Damage to the package in inverted orientation was modelled as a 150mm x 150mm square hole in the center of the top shield outer plate. The cones were completely crushed and were therefore removed.

The package with side impact damage is shown in Figure A1.6. The pallet, top shield and jacket were deformed, in order to resemble the actual package damage.

The following measurement location references are used throughout this report:

A1	Cavity wall (50mm below top)
A2	Lead adjacent to A1
B1	Cavity wall (mid-height)
B2	Lead adjacent to B1
C1	Cavity wall (50mm above base)
C2	Lead adjacent to C1
D	Lead (closure base centre)
E	Lead (closure top centre)
F	Closure O-ring flange fixings and vent plug (20mm below upper surface, 50mm from outer edge)
G	Lifting fin (100mm from top edge, 75mm from outer edge)
H	Lifting fin (40mm from top edge, 55mm from outer edge)
I	Lifting fin (135mm from top edge, 35mm from outer edge)
J	Lead (top chamfer top corner)
K	Lead (top chamfer bottom corner)
L	Flask wall (mid-height, midway between fins)
M	Lead (bottom chamfer top corner)
N ₁	Drain point (centre of cylinder, outer surface)
N ₂	Drain plug O-ring (centre of cylinder, 70mm from outer surface for the prototype, 80mm for the new design)
O	Lead (bottom chamfer bottom corner)
P	Flask foot (top surface, 30mm from outer edge)
Q	Jacket (mid height outer surface)
R	Jacket (top edge)
S	Jacket (inner surface, 40mm from top edge)
T	Top shield (mid height vertical face)
U	Top shield (half way across horizontal face)
V	Top shield (top surface centre)
W	Maximum lead temperature
X	Mean lead temperature
Y	Maximum lead temperature location

4 Results

4.1 Benchmarking

The measured temperatures [12] were used to validate the model. The external flask temperatures depend on the heat transfer processes, while the cavity temperature is also affected by the contact coefficients between lead and stainless steel surfaces. Flask surface emissivity was set to a nominal value of 0.45 then the lead/stainless steel contact resistance was adjusted until measured and predicted cavity wall temperatures were in agreement. A contact coefficient of $400\text{W/m}^2\text{K}$ resulted in good agreement of temperatures at the cavity wall and was used for subsequent analyses.

Table 4 shows calculated and measured package temperatures at various locations. Temperatures, except G and N1, deviate not more than 7°C from measured temperatures. Measurement G was a single measurement and it is possible that the thermocouple was faulty. The calculated temperature N1 is best explained by the fact that the drain plug was not separated from the drain point in the computational model and therefore would be less readily cooled. Comparing column four and five shows that the design changes have no significant effect on package temperatures.

A nominal cavity wall emissivity was specified (0.40) and the source emissivity was adjusted until a good overall correlation between the sources and measured temperatures was reached. Table 5 presents measured and calculated temperatures for the source arrangement. The source temperatures are taken 280mm from the cavity base. The measured values are in the range of 311°C to 342°C as compared to the calculated values of 332°C to 337°C . The larger measured temperature differences between individual sources could not exactly be reproduced. An emissivity of 0.6 was selected to match the higher temperatures.

Table 4: Measured and predicted package temperatures at benchmark conditions ^[6].

Identity	Location	Temperature [$^\circ\text{C}$]		
		Measurement	Prediction Prototype	Prediction 2 nd Design
A1	Cavity wall (50mm below top)	151 / 196*	152	153
B1	Cavity wall (mid-height)	155 / 155 / 154 / 270*	155	156
C1	Cavity wall (50mm above base)	149	151	152
F	Closure and vent seal	112 / 116	110	114
G	Lifting fin (100mm from top edge, 75mm from outer edge)	49	65	67
H	Lifting fin (40mm from top edge, 55mm from outer edge)	55	57	60
I	Lifting fin (135mm from top edge, 35mm from outer edge)	61 / 59	66	68
L	Flask wall (mid-height, midway between fins)	112 / 111 / 112 / 113	119	120
N1	Drain point (centre of cylinder, outer surface)	83	101	101
P	Flask foot (top surface, 30mm from outer edge)	27 / 27	32	33
R	Jacket (top edge)	36 / 36	39	39

Identity	Location	Temperature [°C]		
		Measurement	Prediction Prototype	Prediction 2 nd Design
S	Jacket (inner surface, 40mm from top edge)	43 / 40	45	46
T	Top shield (mid height vertical face)	35 / 36	42	39
U	Top shield (half way across horizontal face)	35 / 35	41	38
V	Top shield (top surface centre)	40	49	37
T _a	Ambient	21	21	21

* Measurements A1 and B1 were ignored due to inconsistency with the remaining measurements.

Table 5: Measured and predicted source temperatures 280mm from bottom of cavity ^[6].

Position	Temperature [°C]	
	Measured	Predicted
2	342 / 341 / 342	337
10	311 / 312 / 312	332
18	333 / 333 / 330	335

4.2 Sensitivity Study

The reference case in Table 6, column 2, was calculated using an emissivity for the external flask stainless steel surfaces (SS) of 0.4 and an emissivity for painted carbon steel surfaces (CS) of 0.9. The following columns show the effect of different emissivity values and insulation conductivity. The package temperatures increase if the emissivity of external flask surfaces is reduced to 0.20.

Painted surfaces are found on the top shield, pallet and jacket. A higher emissivity affects flask temperatures insignificantly, since the thermal connection between these components and the flask is limited. A temperature increase of about 4°C can be observed on the top shield top surface. The temperature rise is attributed to the larger emissivity value and higher absorption of incident insolation.

Increasing the insulation conductivity by a factor of two does not show any effect on the normal conditions temperatures. The insulation inside the surrounding jacket protects the flask during accident from high radiation. This is reflected in Graph 1.1 to 1.3 and 2.1 to 2.3, which show a larger temperature rise, if the insulation conductivity increases.

Considering the temperature curves in Graph 1.1 to 2.3, it can be observed that all temperatures begin to fall, or are already in decline, except the lead closure temperatures D and E. A small air gap separates the closure lead from the flask body. The flask and closure are in contact at the closure flange, where the closure is bolted to the flask body. As no heat is generated within the closure and no heat flux is applied to the cavity base, the heat flow path to the closure is restricted. Consequently, temperatures D and E are lagging behind the higher temperature of the main lead body. Consider the main body lead temperature at the closure and at the same height as D and E. These locations are referred to as D2 and E2 and are shown in Graph 1.4. Temperatures D and E are following the higher lead temperatures

D2 and E2, respectively. Temperatures D and E are 6°C to 12°C lower than D2 and E2, respectively, at the end of the transient. As temperatures D and E cannot exceed D2 and E2, the peak of D and E will be lower than D2 and E2 at the end of the transient. Closure lead temperatures will also always be lower than the flask lead temperatures.

Table 7 compares the peak temperatures, which were predicted for accident conditions. Flask temperatures rise if the insulation conductivity is raised. The mean cavity wall temperature rise is about 7°C.

The highest source temperatures were predicted for a cavity filling gas of air and 12 sources arranged uniformly in the basket (Table 8). Increasing the cavity pressure to 2atm had a negligible effect on source temperature.

The results indicate that an emissivity of 0.2 for external surfaces and the doubled insulation conductivity will produce the highest normal conditions flask temperatures. An increase of the emissivity for painted surfaces raises the external surfaces temperature, while flask temperatures remain almost unchanged. Therefore, an emissivity for flask surfaces of 0.2, an emissivity of 0.98 for painted surfaces and the larger insulation conductivity were selected to predict normal conditions temperatures. The cavity was filled with air for a twelve-source arrangement. The cavity air pressure for subsequent simulations was 1atm abs.

Table 6: Effect of input parameter variations on normal condition package temperatures.

Location	Temperature [°C]					
	Reference	Emissivity of SS =0.20	Emissivity of SS =0.60	Emissivity of CS =0.80	Emissivity of CS=0.98	Insulation conductivity $2 \cdot k_{ins}$
A1	175	181	173	176	176	175
A2	165	171	162	166	165	164
B1	178	184	176	179	178	178
B2	167	174	165	168	168	167
C1	173	179	171	174	173	172
C2	162	169	160	164	163	162
D	143	149	140	143	143	142
E	140	146	137	141	140	139
F	136	142	133	137	137	136
G	94	96	92	95	93	94
H	87	88	85	88	85	85
I	94	96	91	95	94	94
J	141	147	139	142	142	141
K	142	148	140	143	142	141
L	139	146	137	141	140	139
M	138	144	137	140	139	138
N1	120	125	117	121	120	120
N2	138	144	135	139	138	137
O	146	152	144	147	146	144
P	62	62	64	64	62	63
Q	65	68	58	66	59	61
R	70	61	71	71	72	67
S	74	67	77	74	74	72

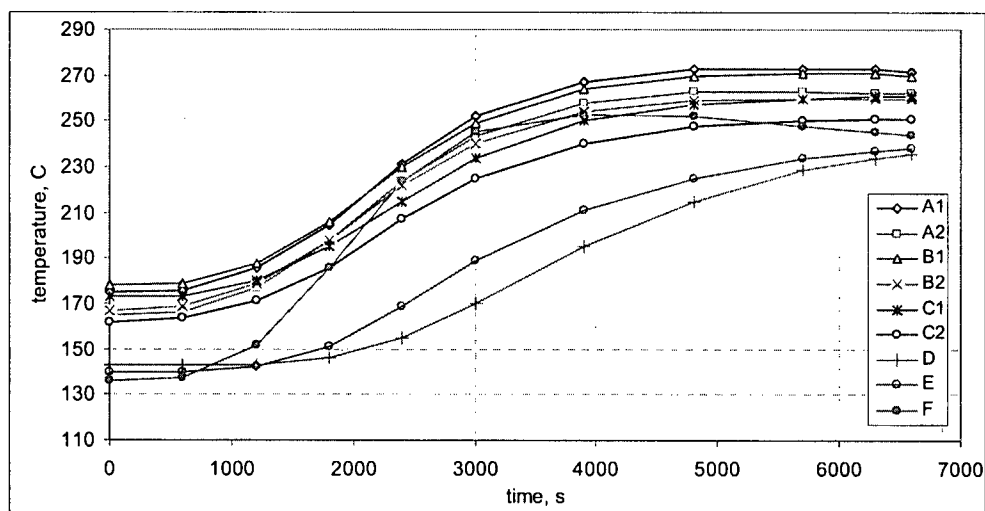
Location	Temperature [°C]					
	Reference	Emissivity of SS =0.20	Emissivity of SS =0.60	Emissivity of CS =0.80	Emissivity of CS=0.98	Insulation conductivity $2 \cdot k_{ins}$
T	79	77	76	80	79	78
U	82	81	80	83	86	82
V	95	83	87	92	99	91
W	168	175	166	169	169	168
X	147	154	145	148	148	147
T _a	38	38	38	38	38	38

Table 7: Effect of a variation in insulation conductivity on peak package temperatures at accident conditions.

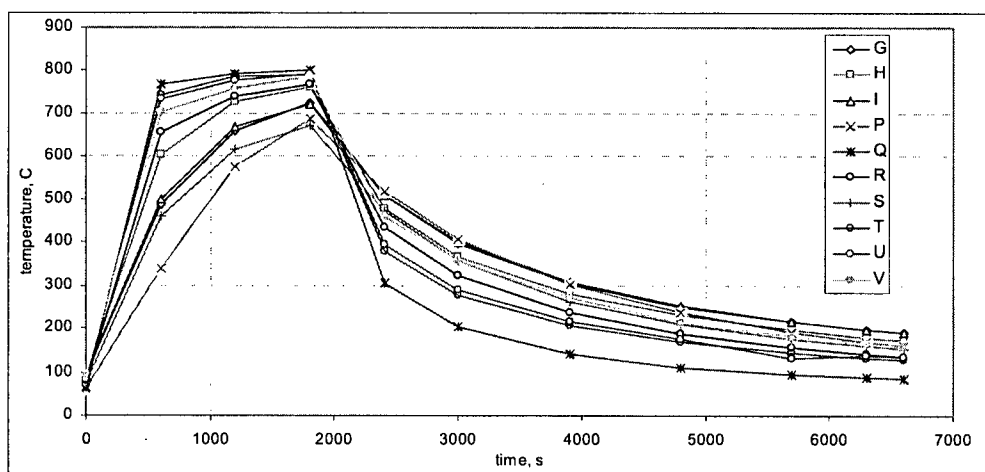
Location	$k_{ins,ref}$	$2 \cdot k_{ins,ref}$
A1	273	280
A2	263	270
B1	271	278
B2	260	267
C1	261	268
C2	251	258
D	236	241
E	238	243
F	253	258
G	723	721
H	761	756
I	721	723
J	250	255
K	257	264
L	254	264
M	226	235
N1	298	314
N2	224	231
O	229	237
P	687	684
Q	802	770
R	769	775
S	671	679
T	790	789
U	791	802
V	787	767
W	268	271
X	240	246

Table 8: Effect of cavity parameter variations on source temperatures.

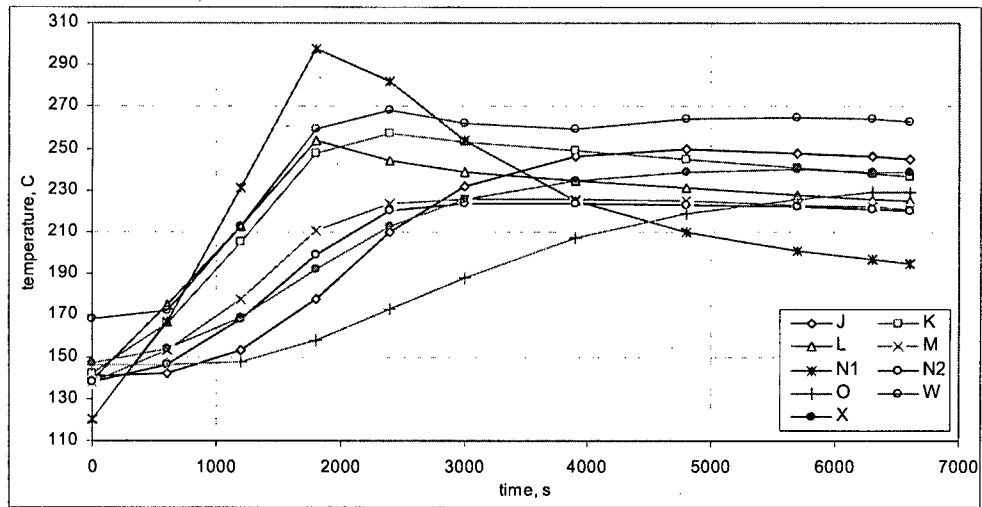
Location	Reference Case	Case 2	Case 3	Case 4	Case 5	Case 6
Source emissivity	0.60	0.60	0.60	0.60	0.60	0.60
Cavity wall emissivity	0.40	0.40	0.40	0.40	0.40	0.40
Sources	16	12	18	16	16	16
Cavity pressure [atm]	1	1	1	1	1	2
Cavity gas	Neon	Neon	Neon	Helium	Air	Neon
$T_{src,max}$ [°C]	334	348	325	265	360	332



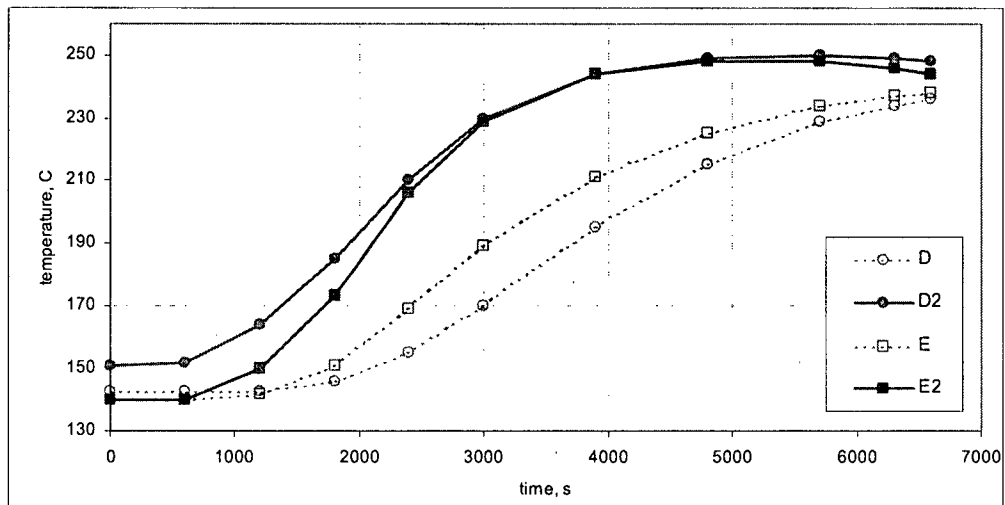
Graph 1.1: Accident temperatures for undamaged flask (upright orientation) at reference insulation conductivity $k_{ins,ref}$ [°C]



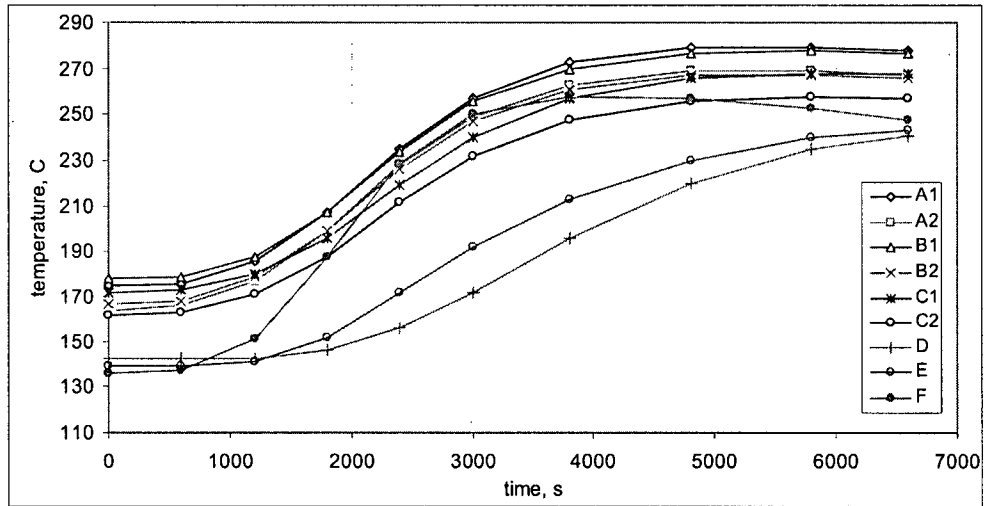
Graph 1.2: Accident temperatures for undamaged flask (upright orientation) at reference insulation conductivity $k_{ins,ref}$ [°C]



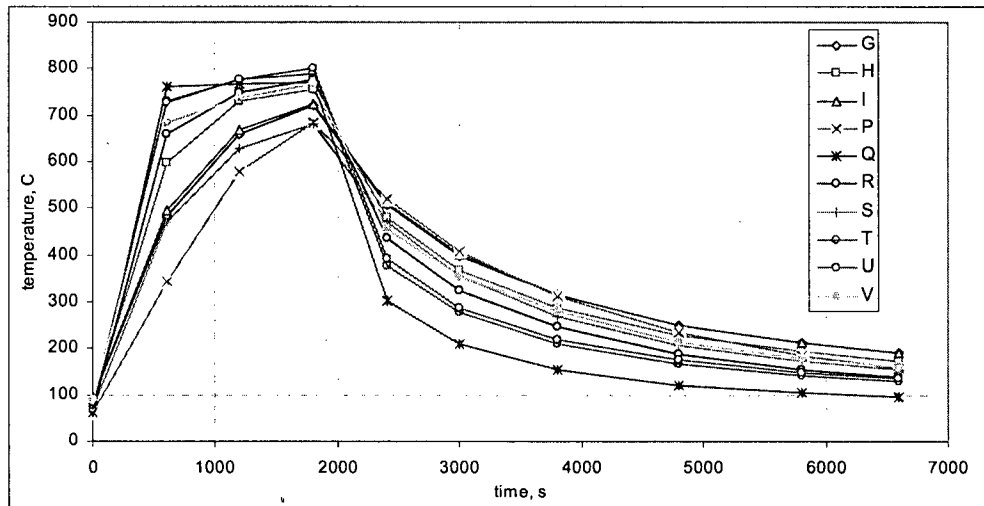
Graph 1.3: Accident temperatures for undamaged flask (upright orientation) at reference insulation conductivity $k_{ins,ref}$ [°C]



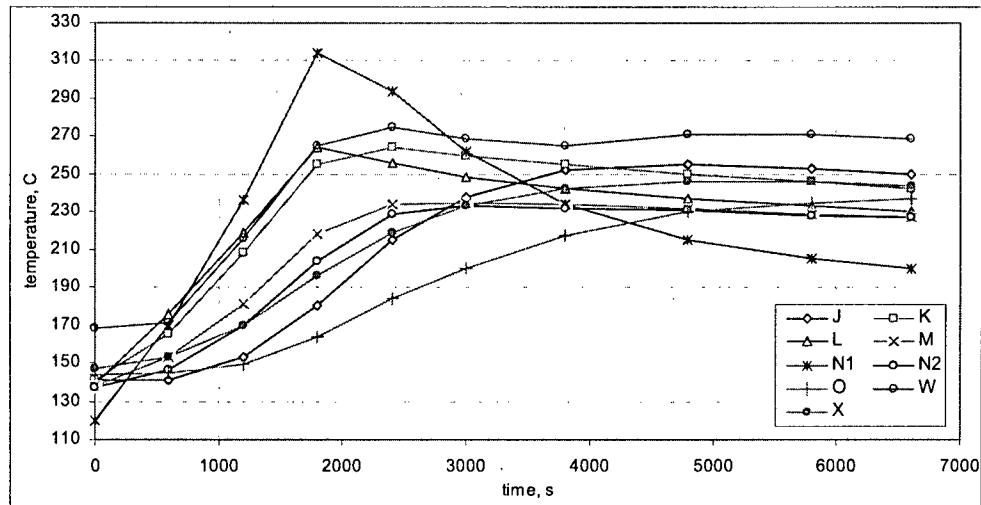
Graph 1.4: Lead temperatures at the closure for undamaged flask (upright orientation) at reference insulation conductivity $k_{ins,ref}$ [°C]



Graph 2.1: Accident temperatures for undamaged flask (upright orientation) at insulation conductivity $k_{ins}^* = 2 k_{ins,ref}$ [°C]



Graph 2.2: Accident temperatures for undamaged flask (upright orientation) at insulation conductivity $k_{ins}^* = 2 k_{ins,ref}$ [°C]



Graph 2.3: Accident temperatures for undamaged flask (upright orientation) at insulation conductivity $k_{ins}^* = 2 k_{ins,ref}$ [°C]

4.3 Normal Conditions

Table 9 presents steady state temperatures for normal conditions without and with insolation. Temperature and flow distributions on a vertical section are shown in Figure A1.7 and A1.8.

Table 9: Normal conditions temperatures [°C].

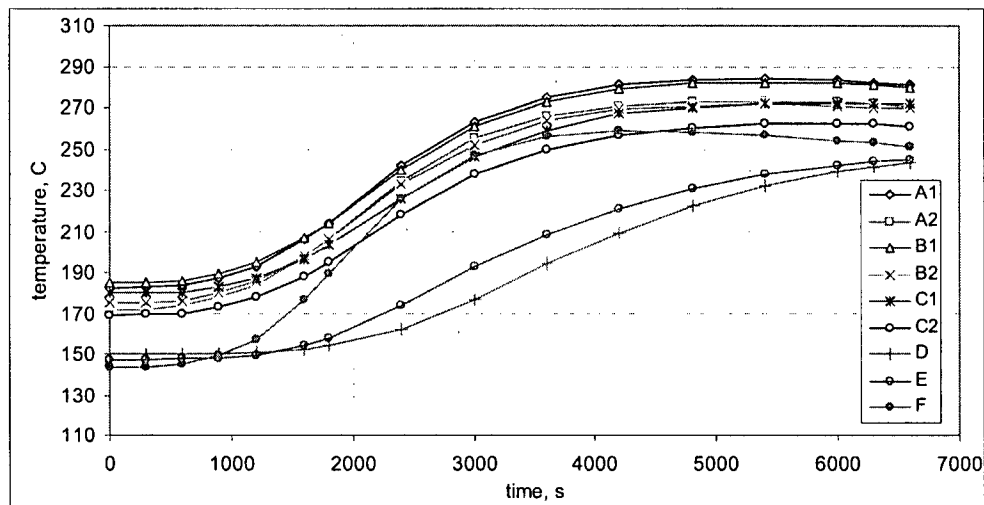
Location	Without insolation	With insolation
A1	176	181
A2	166	171
B1	180	184
B2	169	174
C1	174	179
C2	164	169
D	142	149
E	139	146
F	135	142
G	87	96
H	79	87
I	88	96
J	141	147
K	143	148
L	141	146
M	140	145
N1	122	126
N2	139	144
O	146	151
P	51	68
Q	43	63
R	50	63
S	55	66
T	55	76

Location	Without insolation	With insolation
U	55	83
V	53	103
W	170	175
X	149	153
T _a	38	38
T _{source,max}	377	379

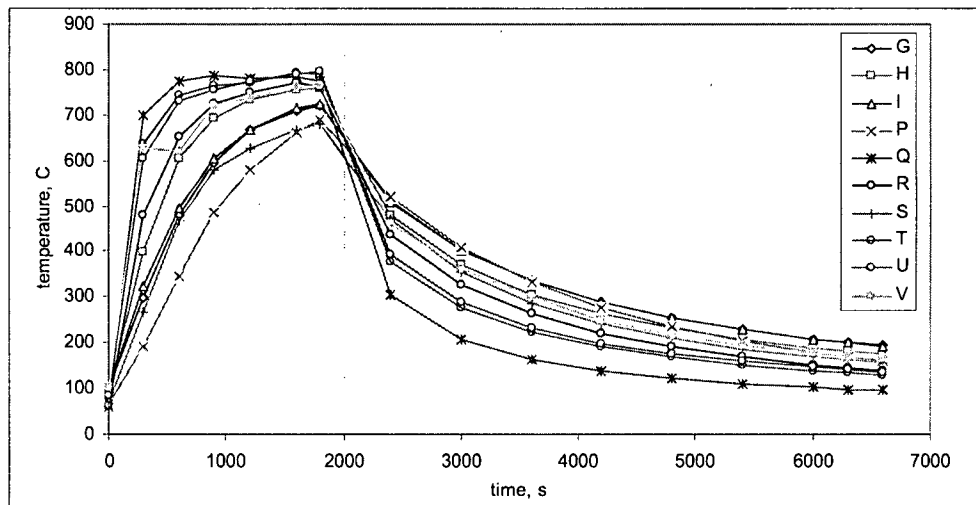
4.4 Accident Conditions

4.4.1 Accident 1: Package in Upright Orientation, Undamaged

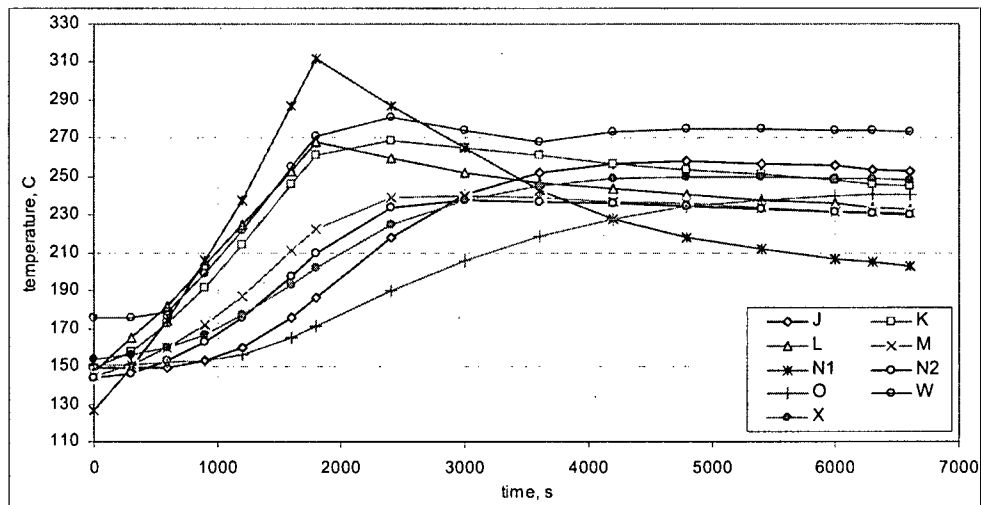
Temperatures histories during heating and subsequent cooling at various locations for the undamaged package in upright orientation are plotted in Graph 3.1 to 3.3. The maximum lead temperature occurs at t=2400s and is found at the vertical finned flask wall.



Graph 3.1: Accident temperatures for upright package orientation, undamaged [°C]



Graph 3.2: Accident temperatures for upright package orientation, undamaged [°C]



Graph 3.3: Accident temperatures for upright package orientation, undamaged [°C]

4.4.2 Accident 1: Package in Upright Orientation, Damaged

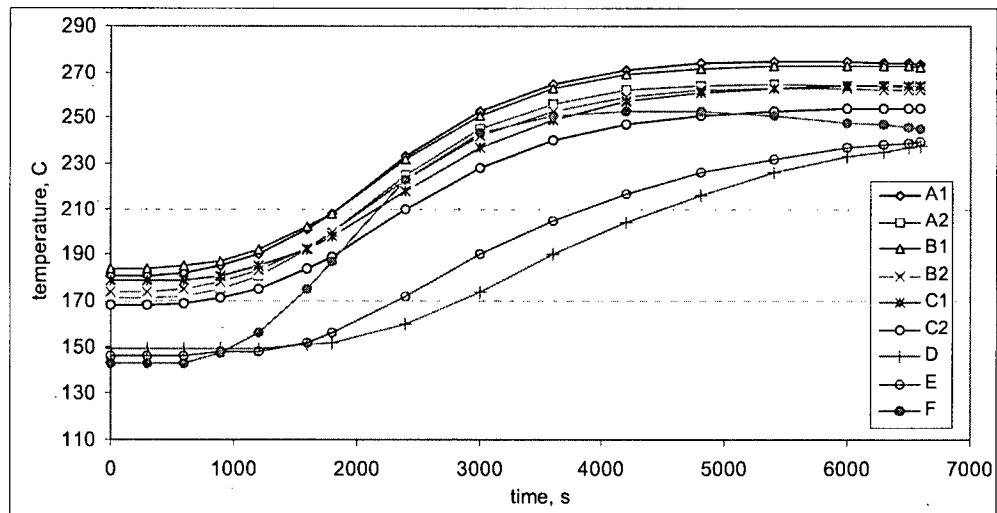
The temperatures histories for the damaged upright package, during heating and subsequent cooling at various locations, are plotted in Graph 4.1 to 4.3. Table 10 shows the peak temperatures that were reached and compares the results with the undamaged package. Lower peak temperatures were predicted for the damaged package. The likely reason for this is the deformed pallet, which obstructs the flow and thereby reduces the heat input to the flask during the heating phase.

The maximum lead temperature occurs at $t=2400s$ and is found at the vertical finned flask wall. Typical temperature distributions at 1800s and 6600s after onset of the accident are shown in Figures A1.9 and A1.10.

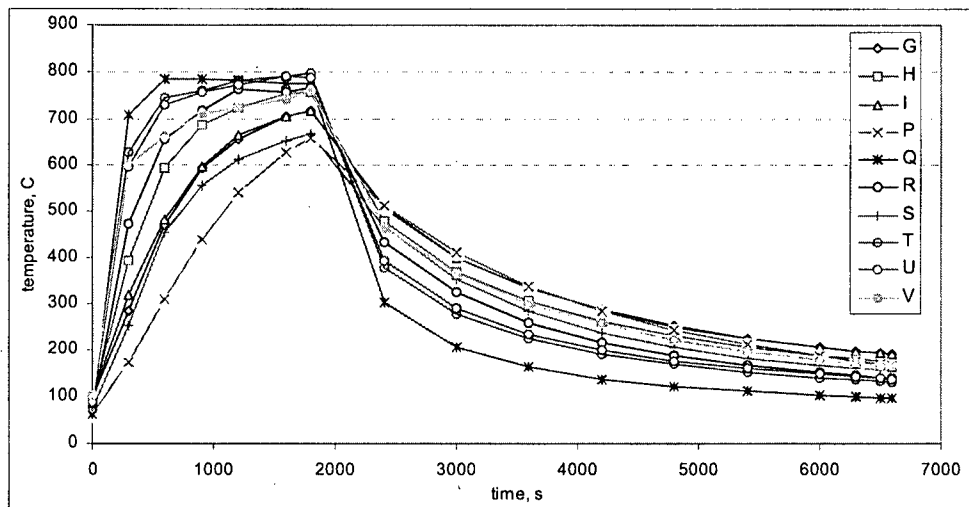
In all cases accident conditions models were run until flask lead temperatures had clearly peaked. Although closure lead temperatures tended to be still rising marginally, this was because the closure has a large thermal capacity, is in poor thermal contact with the flask, and as there was no internal heat generation. As discussed in section 4.2, the closure lead temperatures D and E cannot rise more than about $10^{\circ}C$ and cannot exceed the flask lead temperature W.

Table 10: Peak temperatures accident 1, damaged

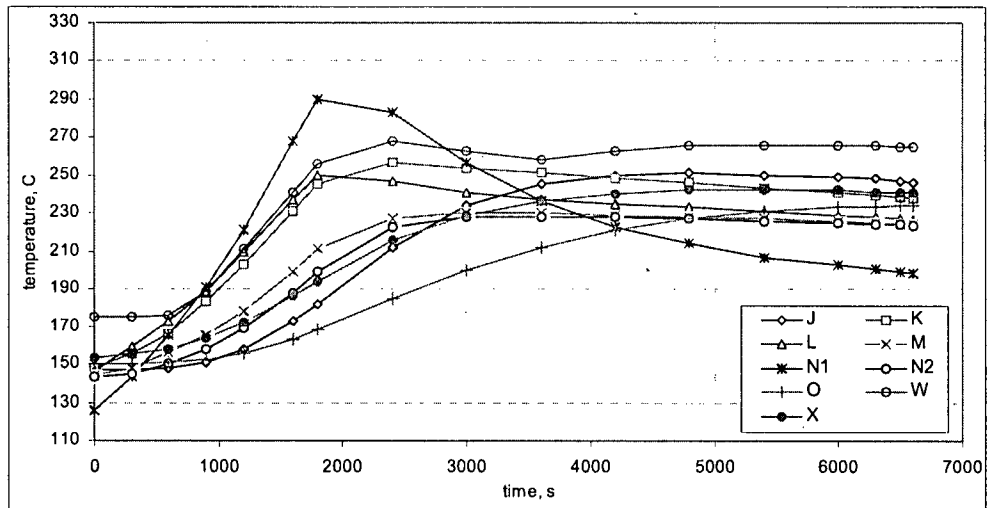
	Location	Temperature [C]	
		Undamaged	Damaged
A1	Cavity wall (50mm below top)	284	275
A2	Lead adjacent to A1	273	265
B1	Cavity wall (mid-height)	282	273
B2	Lead adjacent to B1	272	263
C1	Cavity wall (50mm above base)	272	264
C2	Lead adjacent to C1	262	254
D	Lead (closure base centre)	243	237
E	Lead (closure top centre)	245	239
F	Closure and vent seal	259	253
H	Lifting fin (40mm from top edge, 55mm from outer edge)	760	760
J	Lead (top chamfer top corner)	258	251
K	Lead (top chamfer bottom corner)	269	261
L	Flask wall (mid-height, midway between fins)	268	268
M	Lead (bottom chamfer top corner)	240	230
N2	Drain point seal	236	228
O	Lead (bottom chamfer bottom corner)	241	234
P	Flask foot (top surface, 30mm from outer edge)	689	689
Q	Jacket (mid height outer surface)	788	788
V	Top shield (top surface centre)	764	764
W	Maximum lead temperature	281	268
X	Mean lead temperature	250	242



Graph 4.1: Accident temperatures for upright package orientation, damaged [°C]



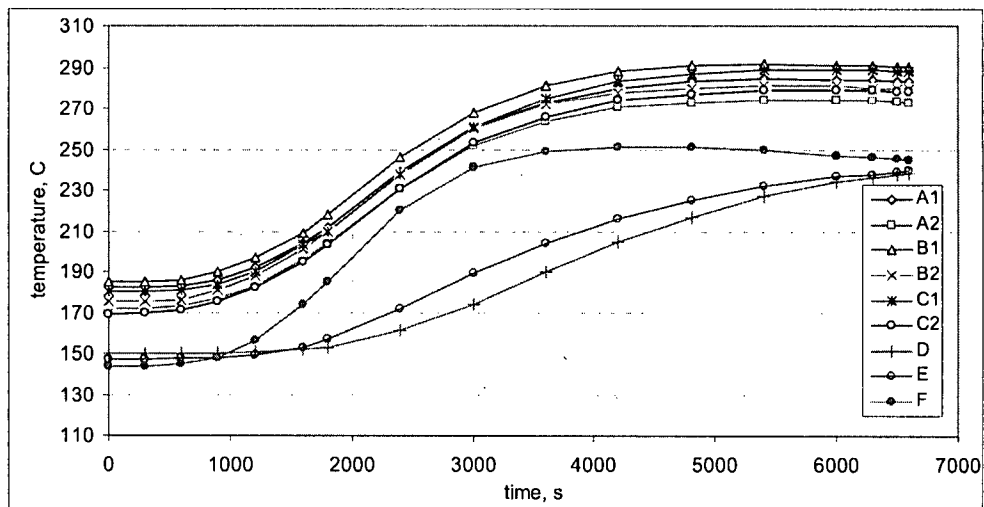
Graph 4.2: Accident temperatures for upright package orientation, damaged [°C]



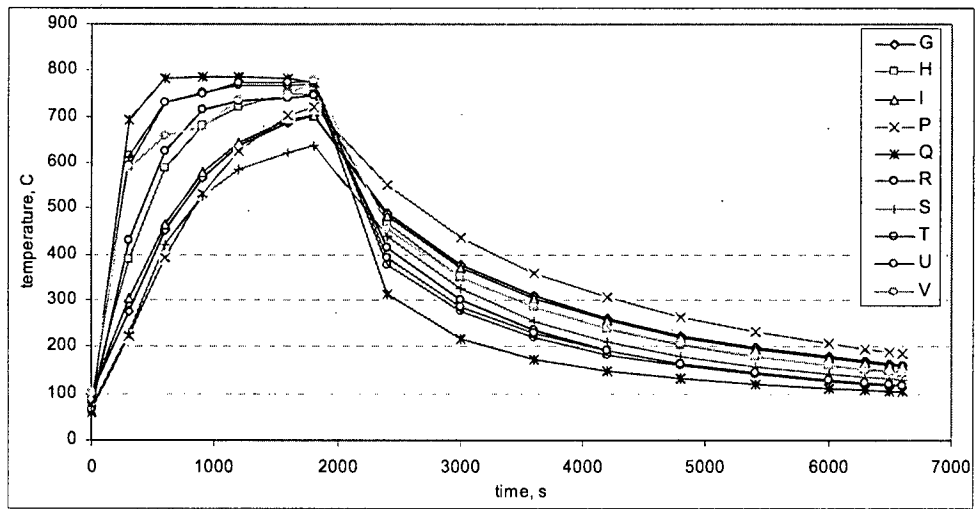
Graph 4.3: Accident temperatures for upright package orientation, damaged [°C]

4.4.3 Accident 2: Package in Inverted Orientation, Undamaged

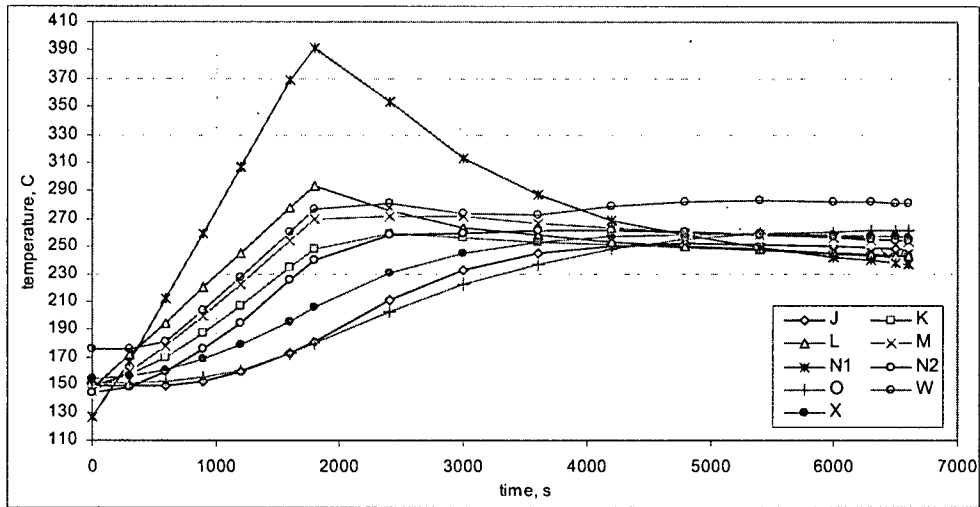
The temperatures histories during heating and subsequent cooling at various locations are plotted in Graph 5.1 to 5.3.



Graph 5.1: Accident temperatures for inverted package orientation, undamaged [°C]



Graph 5.2. Accident temperatures for inverted package orientation, undamaged [°C]



Graph 5.3 Accident temperatures for inverted package orientation, undamaged [°C]

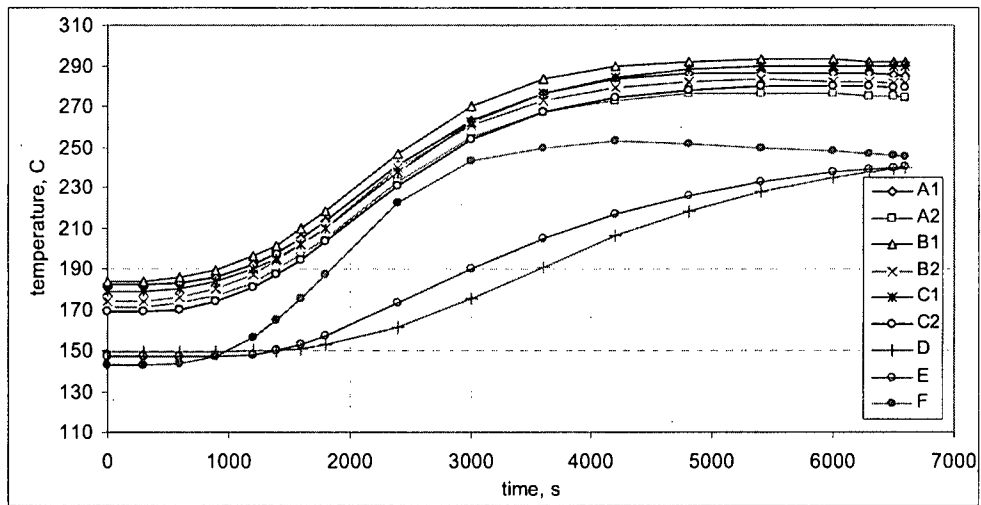
4.4.4 Accident 2: Package in Inverted Orientation, Damaged

The temperatures histories during heating and subsequent cooling for accident 2 at various locations are listed in Table 11 and plotted in Graph 6.1 to 6.3. The results indicate minor changes of temperature for the damaged and undamaged package.

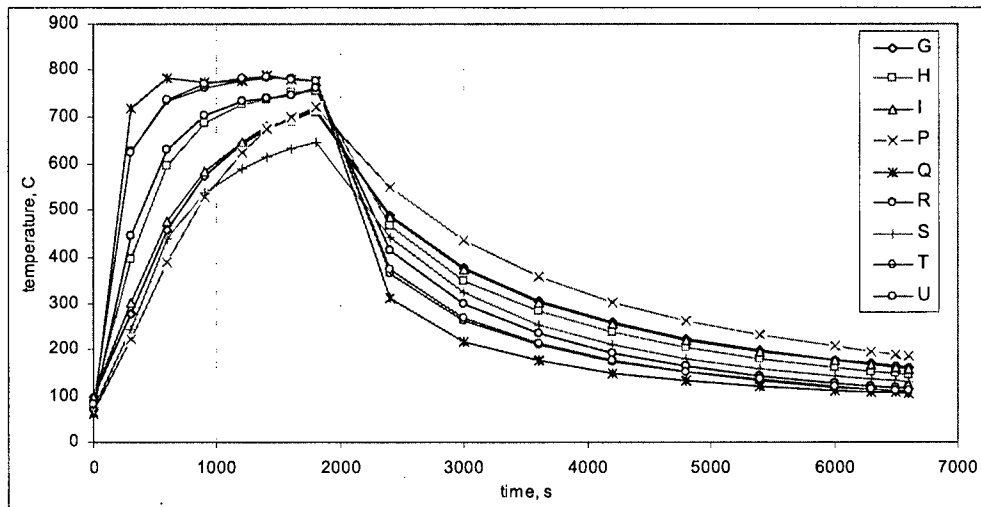
The peak lead temperature occurs at $t = 5400$ s at the vertical cavity wall. Typical temperature distributions at 1800s and 6600s after onset are shown in Figures A1.11 and A1.12.

Table 11: Peak temperatures accident 2, damaged

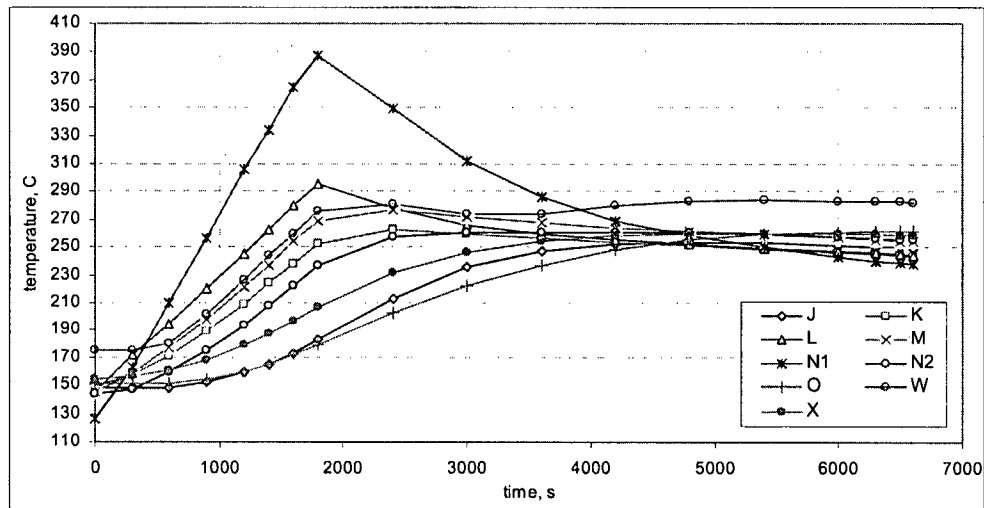
	Location	Temperature [C]	
		Undamaged	Damaged
A1	Cavity wall (50mm below top)	285	286
A2	Lead adjacent to A1	274	276
B1	Cavity wall (mid-height)	292	293
B2	Lead adjacent to B1	281	283
C1	Cavity wall (50mm above base)	289	290
C2	Lead adjacent to C1	279	280
D	Lead (closure base centre)	239	240
E	Lead (closure top centre)	240	240
F	Closure and vent seal	251	253
H	Lifting fin (40mm from top edge, 55mm from outer edge)	750	756
J	Lead (top chamfer top corner)	252	253
K	Lead (top chamfer bottom corner)	259	263
L	Flask wall (mid-height, midway between fins)	294	296
M	Lead (bottom chamfer top corner)	272	277
N2	Drain point seal	262	261
O	Lead (bottom chamfer bottom corner)	262	262
p	Flask foot (top surface, 30mm from outer edge)	721	721
Q	Jacket (mid height outer surface)	787	788
V	Top shield (top surface centre)	780	-
W	Maximum lead temperature	283	284
X	Mean lead temperature	259	260



Graph 6.1: Accident temperatures for inverted package orientation, damaged [°C]



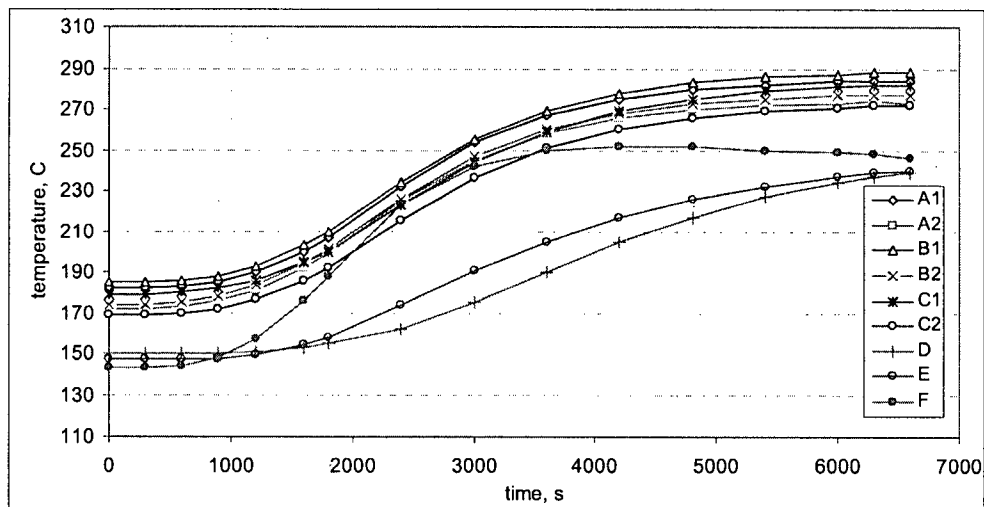
Graph 6.2: Accident temperatures for inverted package orientation, damaged [°C]



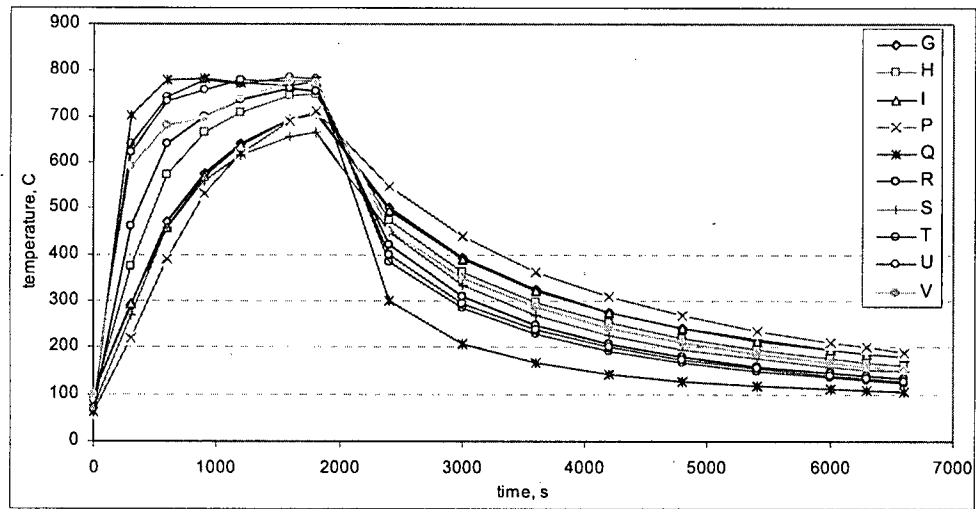
Graph 6.3 Accident temperatures for inverted package orientation, damaged [°C]

4.4.5 Accident 3: Package on its Side, Undamaged

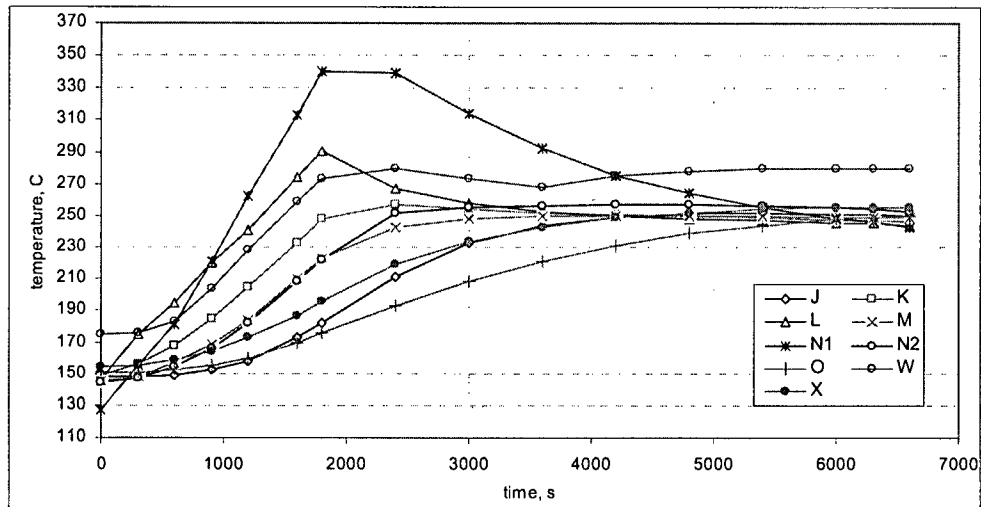
The temperature curves during heating and subsequent cooling at various locations for the undamaged flask placed on its side are plotted in Graph 7.1 to 7.3.



Graph 7.1: Accident temperatures for package on its side, undamaged [°C]



Graph 7.2. Accident temperatures for package on its side, undamaged [°C]



Graph 7.3 Accident temperatures for package on its side, undamaged [°C]

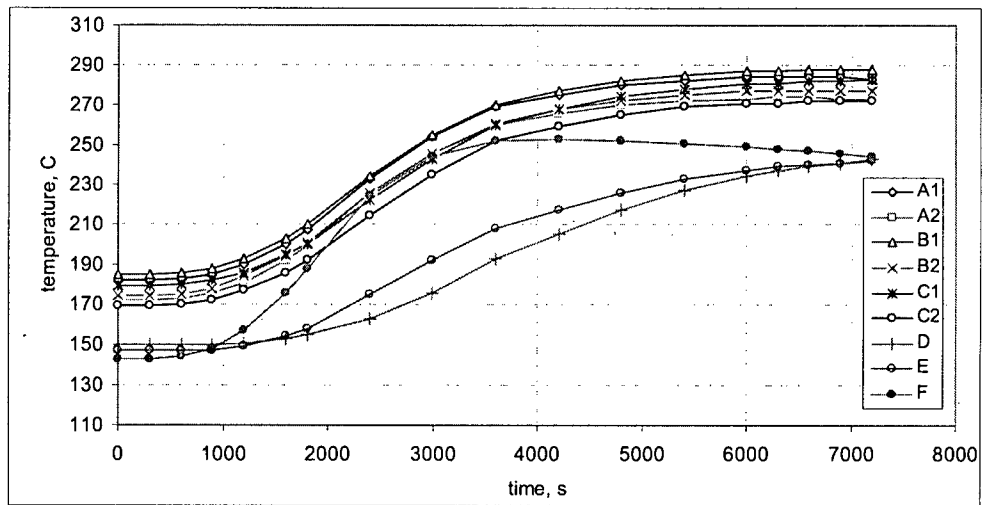
4.4.6 Accident 3: Package on its Side, Damaged

Table 12 presents the peak temperatures for damaged and undamaged package conditions, when the package is on its side and exposed to accident conditions. The temperature difference is negligible, as can be seen from the table. The corresponding temperature profiles are plotted in Graph 8.1 to 8.3.

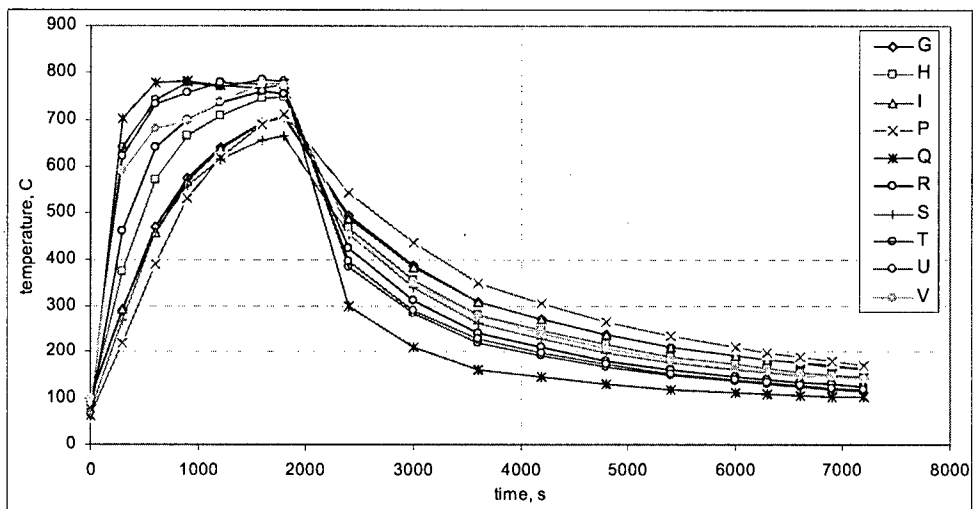
The peak lead temperature is to be found at $t = 5400\text{s}$ at the cavity wall. Typical temperature distributions at 1800s and 6600s after onset are shown in Figures A1.13 and A1.14.

Table 12: Peak temperatures accident 3, damaged.

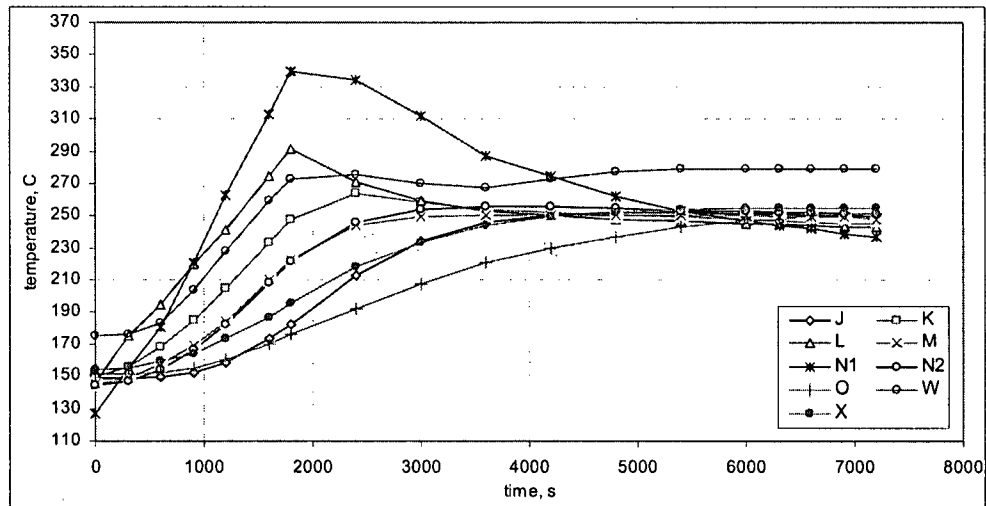
	Location	Temperature [C]	
		Undamaged	Damaged
A1	Cavity wall (50mm below top)	284	284
A2	Lead adjacent to A1	274	274
B1	Cavity wall (mid-height)	288	288
B2	Lead adjacent to B1	277	277
C1	Cavity wall (50mm above base)	282	283
C2	Lead adjacent to C1	272	272
D	Lead (closure base centre)	239	243
E	Lead (closure top centre)	240	242
F	Closure and vent seal	252	253
H	Lifting fin (40mm from top edge, 55mm from outer edge)	750	750
J	Lead (top chamfer top corner)	252	252
K	Lead (top chamfer bottom corner)	257	264
L	Flask wall (mid-height, midway between fins)	291	291
M	Lead (bottom chamfer top corner)	250	250
N2	Drain point seal	257	256
O	Lead (bottom chamfer bottom corner)	250	251
p	Flask foot (top surface, 30mm from outer edge)	711	711
Q	Jacket (mid height outer surface)	782	782
V	Top shield (top surface centre)	776	776
W	Maximum lead temperature	280	279
X	Mean lead temperature	255	255



Graph 8.1: Accident temperatures for package on its side, damaged [°C]



Graph 8.2: Accident temperatures for package on its side, damaged [°C]



Graph 8.3 Accident temperatures for package on its side, damaged [°C]

4.4.7 Accident Source Temperatures

Steady state source temperatures were calculated for the contents exposed to the cavity peak wall temperatures for each of the three undamaged packages. The case, which resulted in the highest source temperatures, was then recalculated for damaged package conditions. Table 13 presents the maximum source temperatures. The small difference between the inverted undamaged and damaged flask orientation is attributed to cavity wall temperatures differing insignificantly (Table 11). Figure A1.15 depicts the peak accident source temperature distribution.

Table 13: Peak source temperatures during accident conditions.

Case	Temperature [°C]
Upright, undamaged	433
Inverted, undamaged	437
Side, undamaged	435
Inverted, damaged	437

5 Conclusions

1. The difference between the predicted temperatures for the prototype and design is insignificant. The best correlation between measurement and prediction was reached for a source emissivity of 0.60 and a contact resistance of $400\text{W/m}^2\text{K}$.
2. The sensitivity study concluded that the source temperature is sensitive to the cavity gas and also to the number of sources used, but not to cavity pressure. Highest source temperatures were reached when the cavity was filled with air and twelve sources were used. The design was not particularly sensitive to the emissivity of painted carbon steel surfaces. A low emissivity of flask external surfaces (0.20) and an insulation conductivity of twice the actual value resulted in the highest flask temperatures.
3. The R7021 transport package temperatures, as calculated under IAEA TS-R-1 normal and accident conditions of transport with an internal heat load equivalent to 2460W , are summarized in the following table.

Location	Temperature [$^{\circ}\text{C}$]		
	Normal conditions		Accident conditions with damage
	without insulation	with insulation	
Source surface	377	379	437
Cavity wall B ₁	180	184	293
Closure and vent seal location F	135	142	253
Lifting fin H	79	87	760
Drain plug seal location N ₂	139	144	261
Flask wall at mid-height L	141	146	296
Flask foot P	51	68	721
Top shield to surface V	53	103	776
Lead shielding (max) W	170	175	284
Lead shielding (mean) X	149	153	260

4. Package temperatures are not particularly sensitive to damage.

6 References

- [1] Work Specification WS7021/14, Thermal Analysis of the R7021 Transport Package, Reviss Services.
- [2] ANSYS V12, Ansys, Inc., Canonsburg, 2009.
- [3] Superwool 607 Blanket, Morgan Thermal Ceramics, 11-1-01 E2/02, Augusta, Georgia.
- [4] The Carborundum Company, Niagara Falls, New York.
- [5] Heat Transfer: J.P Holman, 6th Edition, 1986.
- [6] R7021 Thermal Survey Record OP215, TSR 7021/04, Reviss Services.
- [7] Superwool 607 Blanket, Morgan Thermal Ceramics, 11-1-01 E2/02, Augusta, Georgia.
- [8] The Carborundum Company, Niagara Falls, New York.
- [9] Viscous Fluid Flow, F. White, Mc-Graw-Hill, 1974.
- [10] The Properties of Gases and Liquids, Reid, Prausnitz, Sherwood, McGraw-Hill, 1977.
- [11] R. B. Bird, R. W.E. Stewart, E.N. Lightfoot, Transport Phenomena, John Wiley, 1960.
- [12] RTR 225, R7021 Thermal Survey Record on 3981/01, Reviss Services, 2008.
- [13] QS 7021 issue 2: R7021 Transport Container Drawings List and Drawings (Prototype), Reviss Services.
- [14] QS 7021 issue 4: R7021 Transport Container Drawings List and Drawings (Design), Reviss Services.
- [15] QS 8064 issue 2: R8064 Basket Drawings List and Drawings, Reviss Services.
- [16] QS 2089 issue 10: R2089 Source Drawings List and Drawings, Reviss Services.
- [17] RTR 239, 3981/01 1.0m Punch Test – Angled Upright, Reviss Services, 2009.
- [18] RTR 240, 3981/01 9.0m Free Drop Test – Upright, Reviss Services, 2009.
- [19] RTR 242, 3981/01 1.0m Punch Test – Angled Inverted, Reviss Services, 2009.
- [20] RTR 243 3981/01 9.0m Free Drop Test – Vertical Inverted, Reviss Services, 2009.
- [21] RTR 248 3981/01 1.0m Punch Test – Angled Side, Reviss Services, 2009.
- [22] RTR 249 3981/01 9.0m Free Drop Test – Side Horizontal, Reviss Services, 2009.
- [23] IR 0675 issue 1, Reviss Services, 2009.
- [24] Impact Assessment of the Reviss R7021 Package, Issue 2, C15578/TR/0001, 2010, AMEC.

Appendix 1: Figures

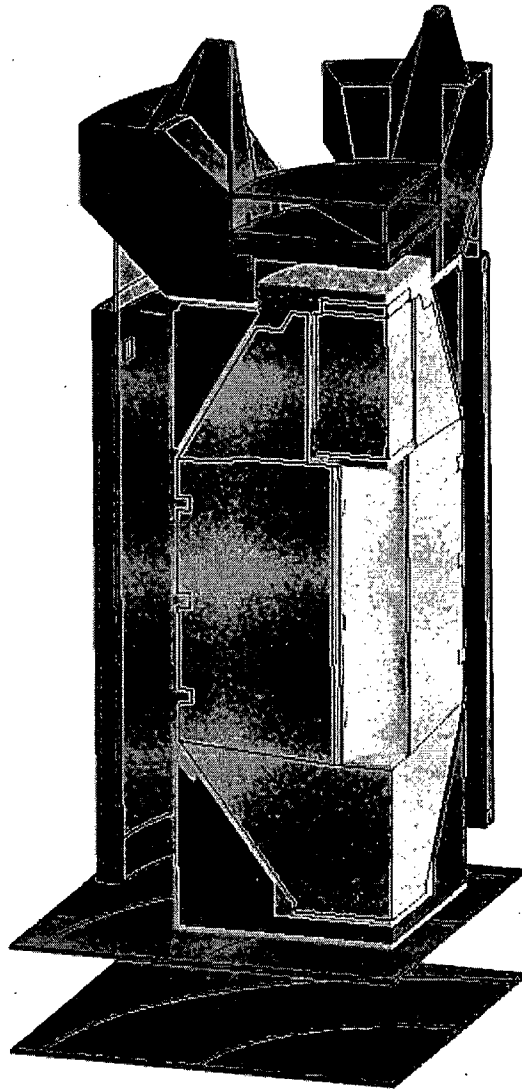


Figure A1.1: Sectional view of the prototype transport package assembly.

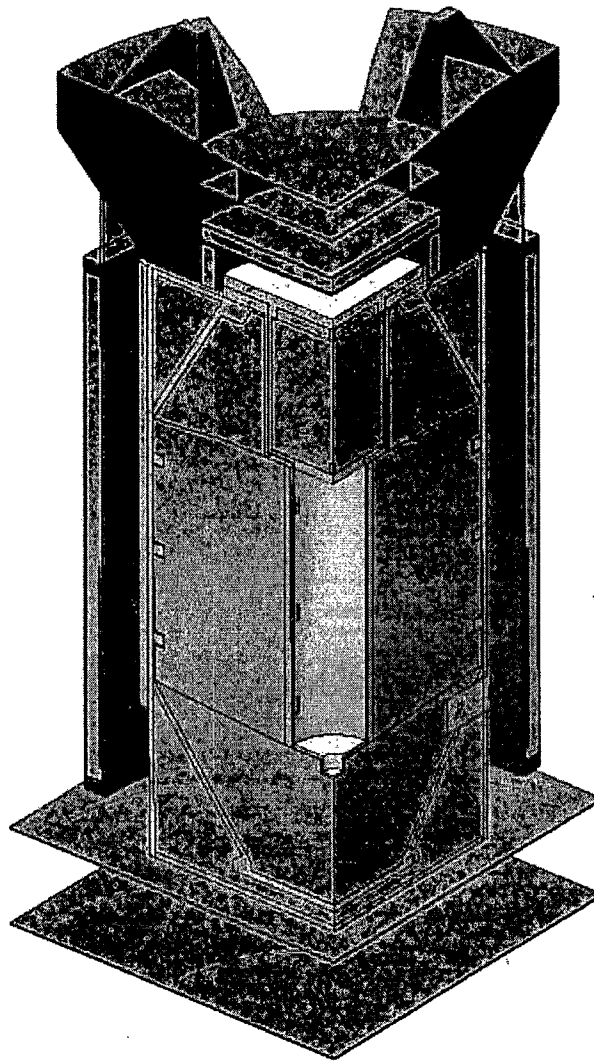
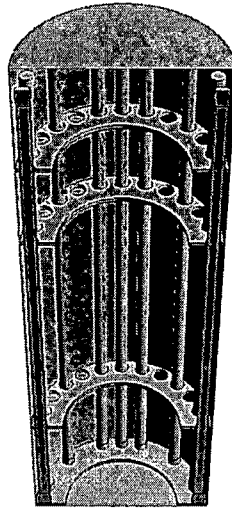
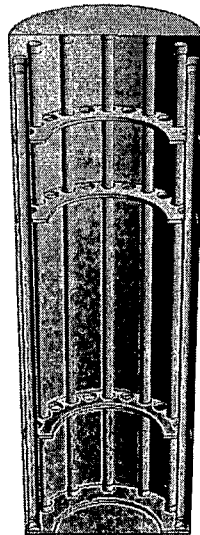


Figure A1.2: Sectional view of the transport package assembly (production design).



(a)



(b)

Figure A1.3: Sectional view of the cavity and contents: (a) benchmark configuration and (b) 12 source configuration.

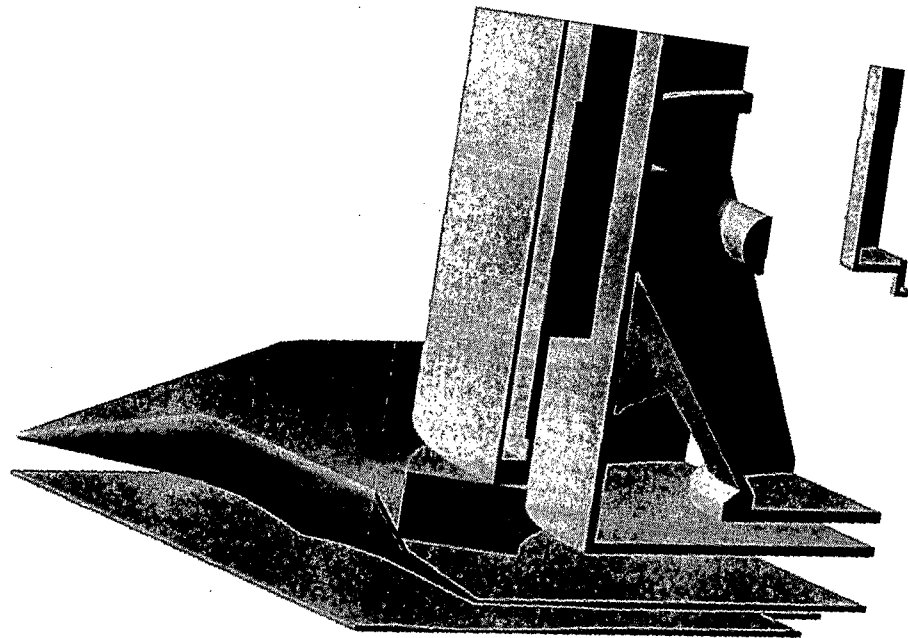
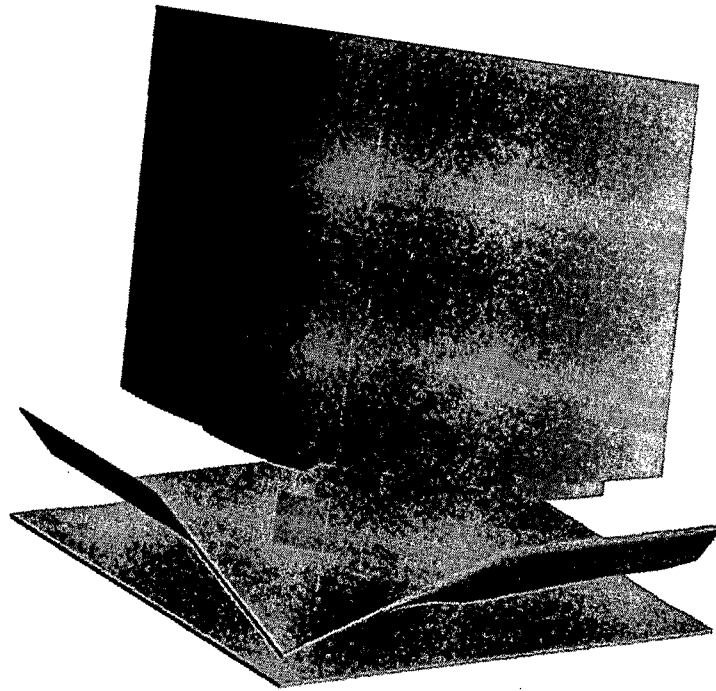


Figure A1.4: Transport package model for damage in upright orientation.

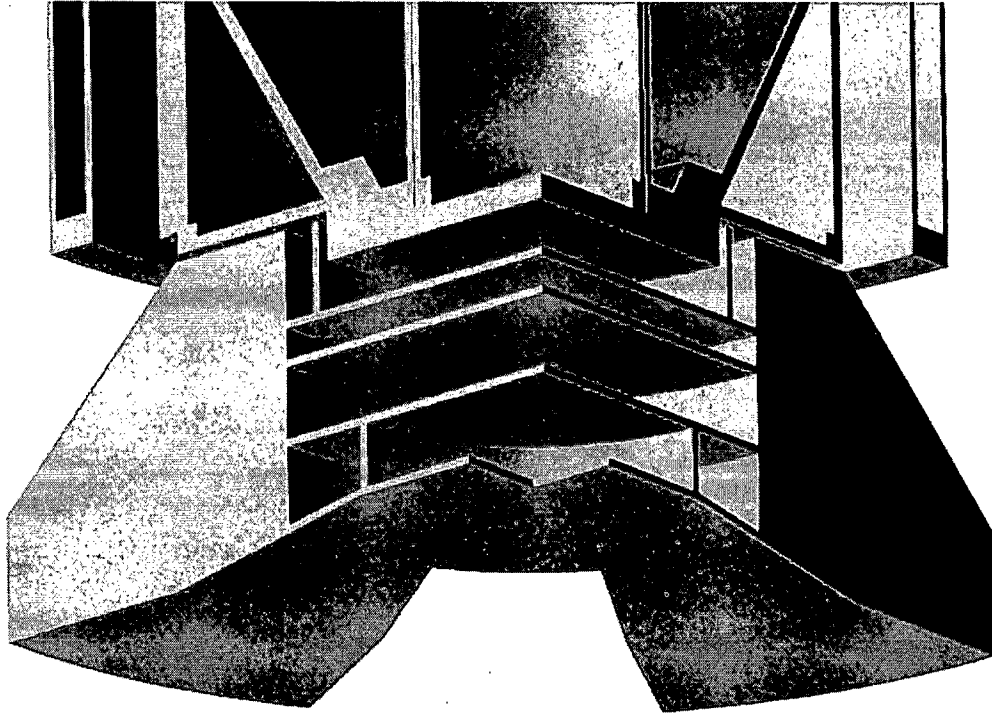


Figure A1.5: Transport package model for damage in inverted orientation.

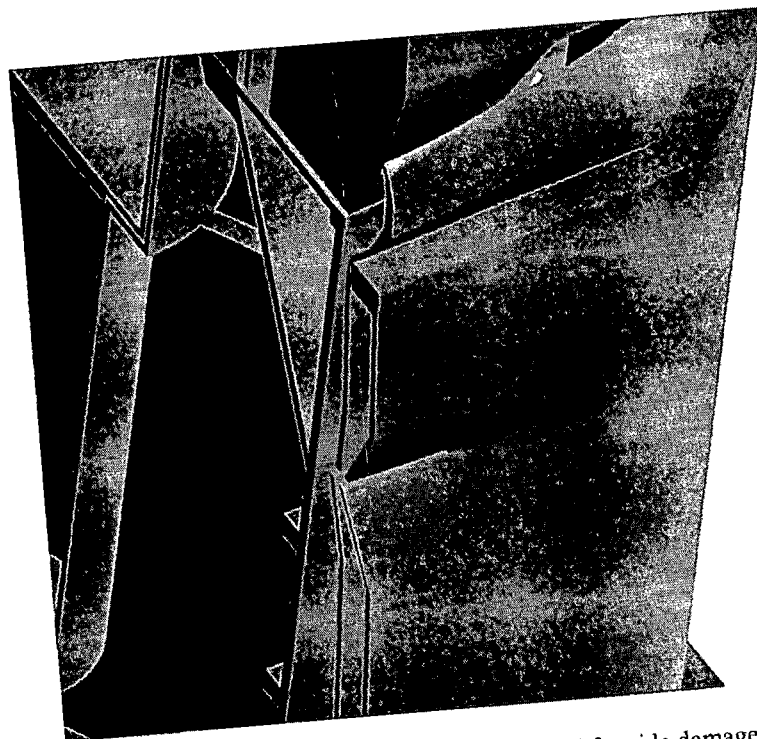
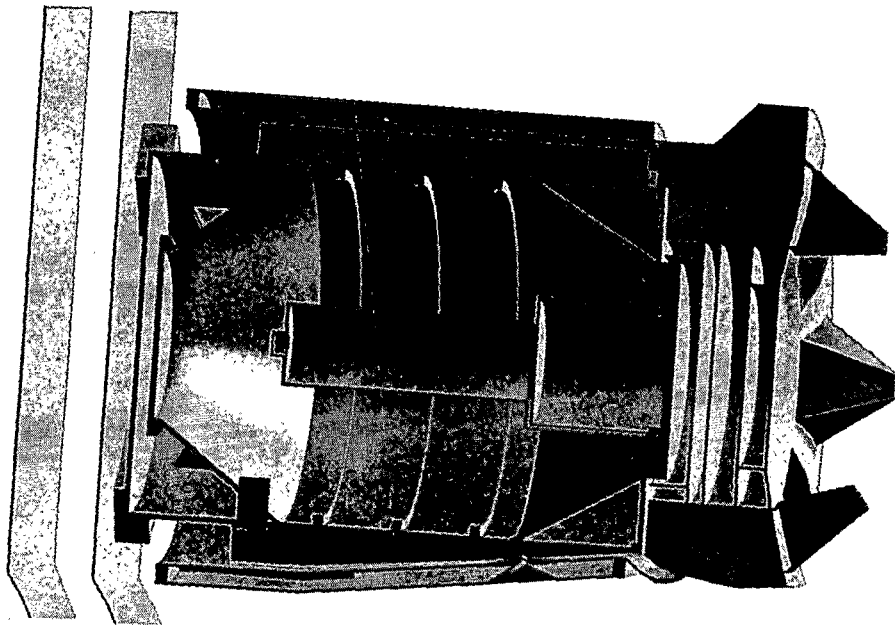


Figure A1.6: Transport package model for side damage.

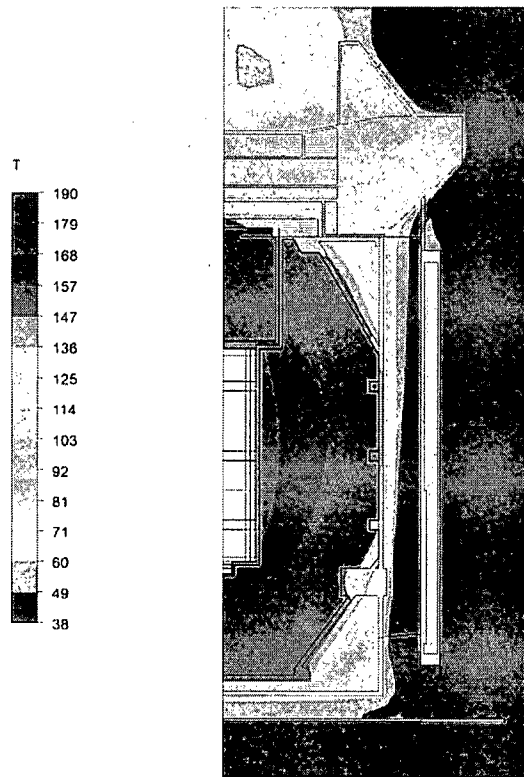


Figure A1.7: Temperature distribution at normal conditions with insolation [°C]

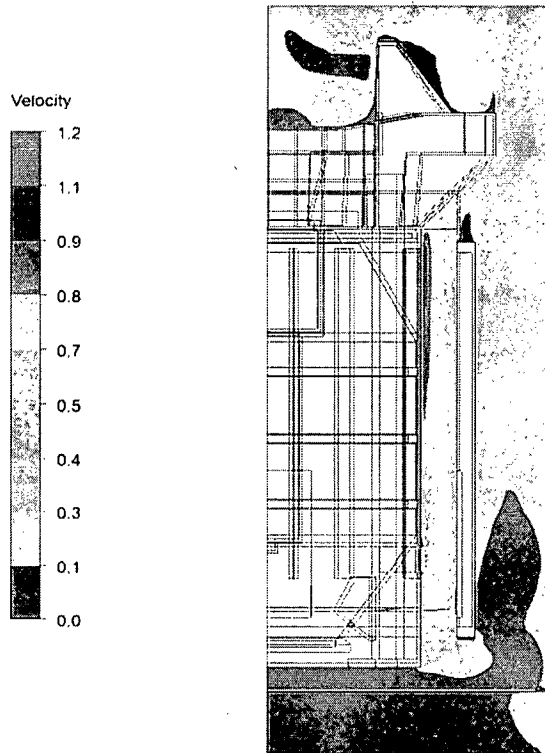


Figure A1.8: Typical flow distribution at normal conditions with insolation [m/s]

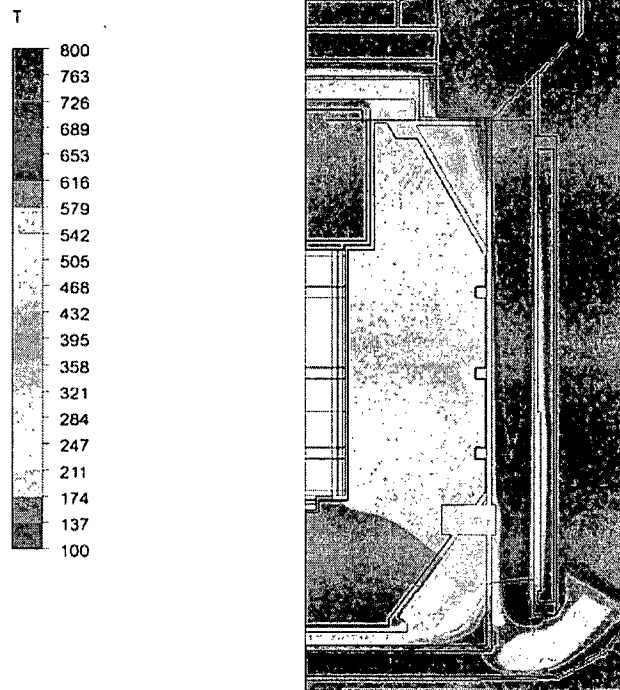


Figure A1.9: Accident 1: Flask core temperature distribution at 1800s [°C]

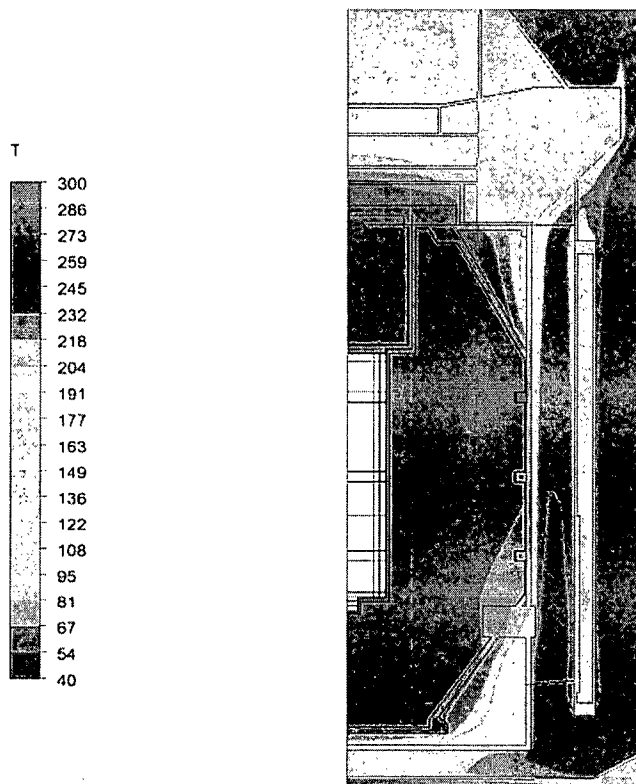


Figure A1.10: Accident 1: Flask core temperature distribution at 6600s [°C]

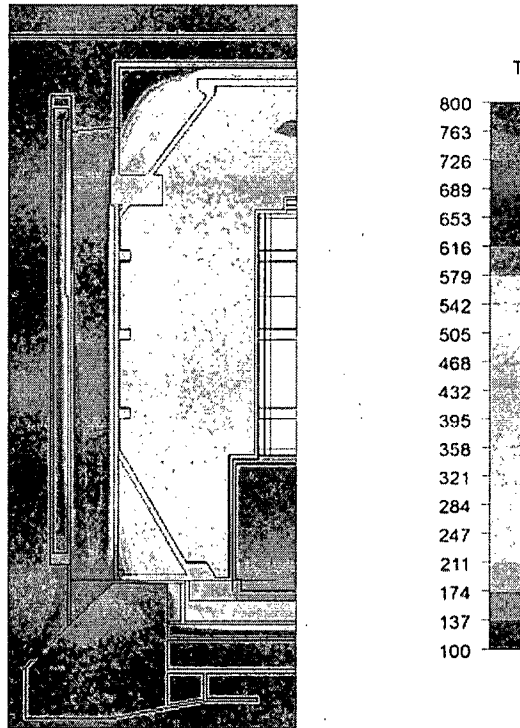


Figure A1.11: Accident 2: Temperature distribution at 1800s [°C]

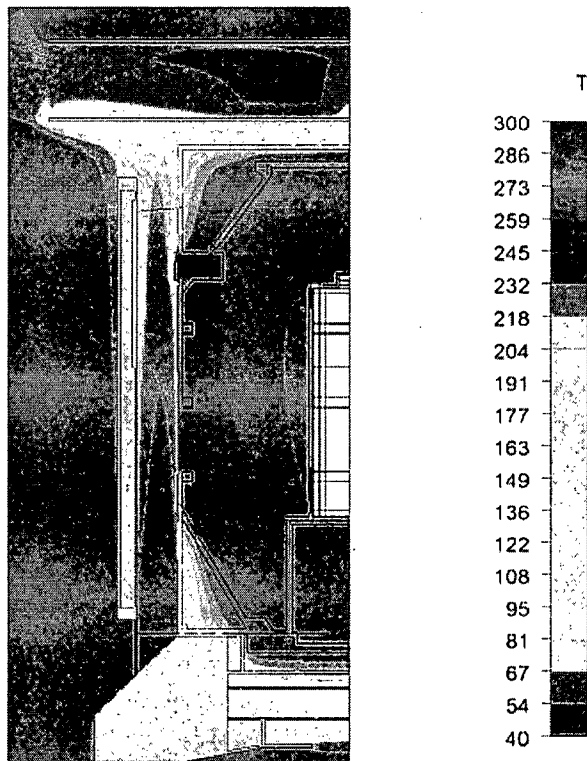


Figure A1.12: Accident 2: Temperature distribution at 6600s [°C]

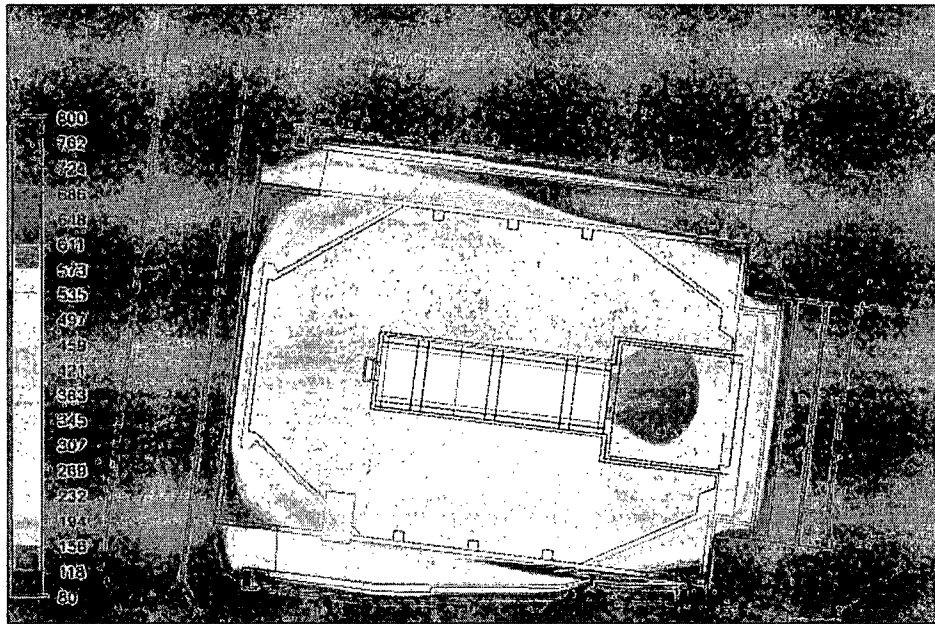


Figure A1.13: Accident 3: Temperature distribution at 1800s [°C]

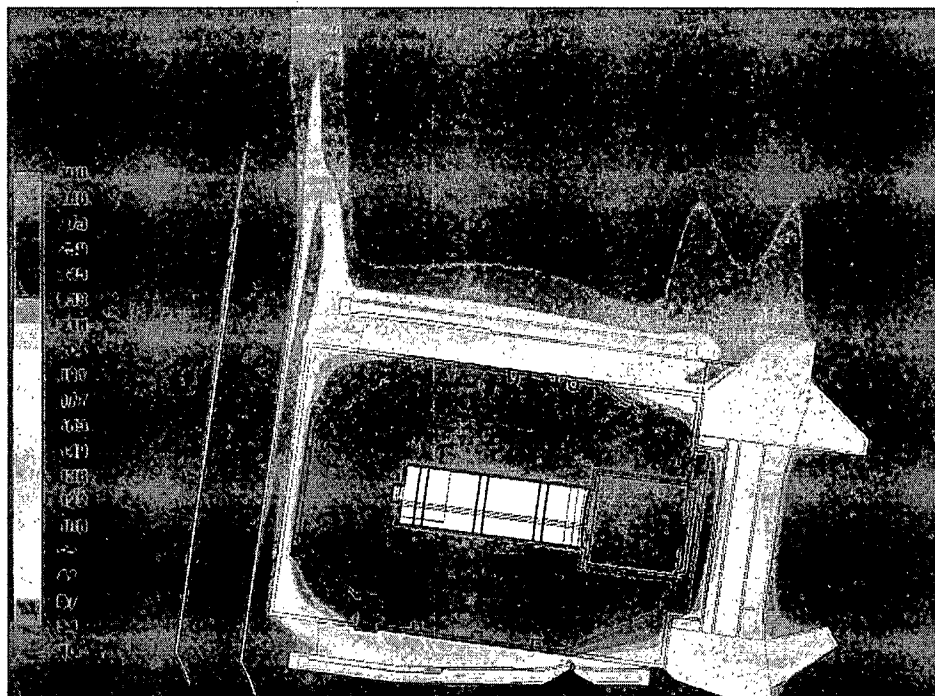


Figure A1.14: Accident 3: Temperature distribution at 6600s [°C]

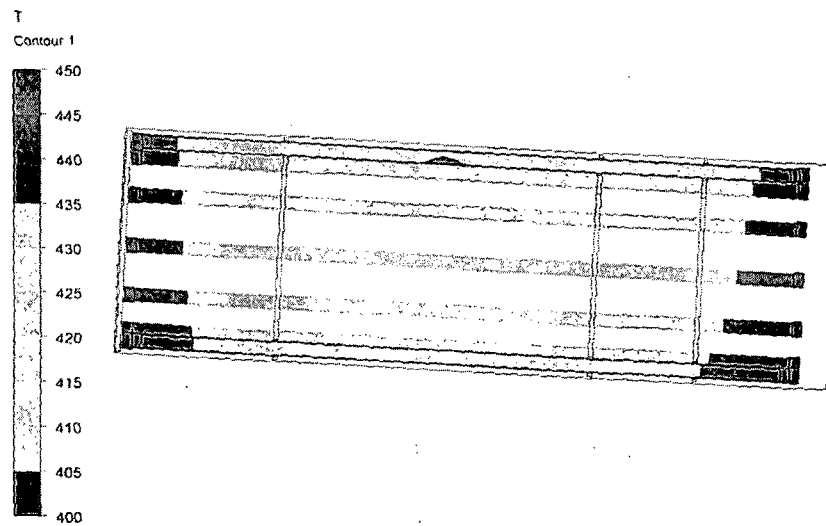


Figure A1.15: Accident 3: Peak accident conditions source temperature distribution [$^{\circ}\text{C}$]

Appendix 2: Specifications

A2.1 Model

General

Domain overall height	6m
Domain height above pallet base	3.5m
Domain width / depth (complete model)	5.5m
Heat load at benchmark conditions	2362W
Heat load at transport conditions	2460W

Emissivities:

Benchmark:

External flask surfaces emissivity	0.45
Unpainted carbon steel surfaces emissivity	0.90
Painted carbon steel surfaces emissivity	0.90
Cavity wall emissivity	0.40

Normal conditions:

External flask surfaces emissivity	0.20
Unpainted carbon steel surfaces emissivity	0.98
Painted carbon steel surfaces emissivity	0.98
Cavity wall emissivity	0.40

Thermal test and cooling period:

Flask surface covered by top shield emissivity	0.20
Unpainted carbon steel surfaces emissivity	0.98
Blackened external surfaces emissivity	0.80
Furnace walls emissivity	0.90
Cavity wall emissivity	0.40

Domain conditions

Insolation:

Downward heat flux (-y direction):	800W/m ²
Horizontal direction (-x direction):	200W/m ²
Horizontal direction (+x direction):	200W/m ²
Horizontal direction (-z direction):	200W/m ²
Horizontal direction (+z direction):	200W/m ²

Normal conditions:

Ambient air temperature:	38°C
Sides and top:	Open flow boundaries
Floor:	Solid base
Flow:	Turbulent, free convection flow

Thermal test:

Ambient air temperature:	800°C
Base:	8m/s inflow at domain base (package suspended)
Sides:	Wall
Top:	Opening
Flow:	Turbulent, free and forced convection flow

Cooling period:

Ambient air temperature:	38°C
Base:	Wall (package suspended)
Sides and top:	Open flow boundaries
Flow:	Turbulent, free convection flow

A2.2 Material Properties

1. Lead: ^[5]

Density: $\rho = 11370 \text{ kg/m}^3$
Conductivity: $k(T) = 35.51 + 16.62(T/1000) - 84.60(T/1000)^2 + 66.67(T/1000)^3 \text{ W/m.K}$
Specific heat: $c_p = 130 \text{ J/kg.K}$

2. Stainless steel: ^[5]

Density: $\rho = 7817 \text{ kg/m}^3$
Conductivity: $k(T) = 17.36 - 8.170(T/1000) + 18.60(T/1000)^2 - 2.877(T/1000)^3 \text{ W/m.K}$
Specific heat: $c_p = 460 \text{ J/kg.K}$

3. Carbon steel: ^[5]

Density: $\rho = 7833 \text{ kg/m}^3$
Conductivity: $k(T) = 36.54 + 49.14(T/1000) - 104.04(T/1000)^2 + 48.32(T/1000)^3 \text{ W/m.K}$
Specific heat: $c_p = 465 \text{ J/kg.K}$

4. Superwool: ^[8]

Density: $\rho = 64 \text{ kg/m}^3$
Conductivity [W/mK]: $k(T) = -1.513E-2 + 0.1586(T/1000) - 7.25E-3(T/1000)^2 + 5.769E-2(T/1000)^3$
Specific heat: $c_p = 1050 \text{ J/kg.K}$

5. Air: ^[9]

Density: $\rho = p/(R.T)$
Conductivity [W/mK]: $k(T) = -0.015125 + 0.15859(T/1000) - 7.254E-4(T/1000)^2 + 5.76904E-2(T/1000)^3$
Viscosity: Sutherlands law for viscosity
Specific heat [J/kg.K]: $c_p(T) = R \cdot (3.657 - 1.272(T/1000) + 2.955(T/1000)^2 - 1.365(T/1000)^3)$

6. Helium: ^[5]

Density: Equation of state. $\rho = p/(R.T)$
Conductivity [W/mK]: $k(T) = 0.03885 + 0.45662(T/1000) - 0.34453(T/1000)^2 + 0.178547(T/1000)^3$
Viscosity [kg/m.s]: $\mu(T) = 1.9464E-06 + 7.99E-05(T/1000) - 7.4092E-05(T/1000)^2 + 3.849E-05(T/1000)^3$
Specific heat: $c_p = 5196.3 \text{ J/kg.K}$

7. Neon: ^[10,11]

Density: Equation of state. $\rho = p/(R.T)$
Conductivity [W/mK]: $k(T) = 0.01319 + 0.13562(T/1000) - 0.06271(T/1000)^2 + 0.02058(T/1000)^3$
Viscosity [kg/m.s]: $\mu(T) = 8.539E-06 + 8.779E-05(T/1000) - 4.06E-05(T/1000)^2 + 1.333E-05(T/1000)^3$
Specific heat: $c_p = 1030 \text{ J/kg.K}$

A2.3 Grill Characterization

The grill, which is located at the top of the jacket, was replaced with a simple porous domain. The porous domain was modelled to show a pressure loss equivalent to the pressure loss across the grill. Pressure loss characteristics were evaluated at air flow rates in the range of 0.25m/s to 1.5m/s for (1) a flat grill similar to the grill incorporated in the design and (2) the corresponding porous model used in the analyses. The typical pressure drop across the grill using the actual grill model and an equivalent computational model is shown in Figure A2.1.

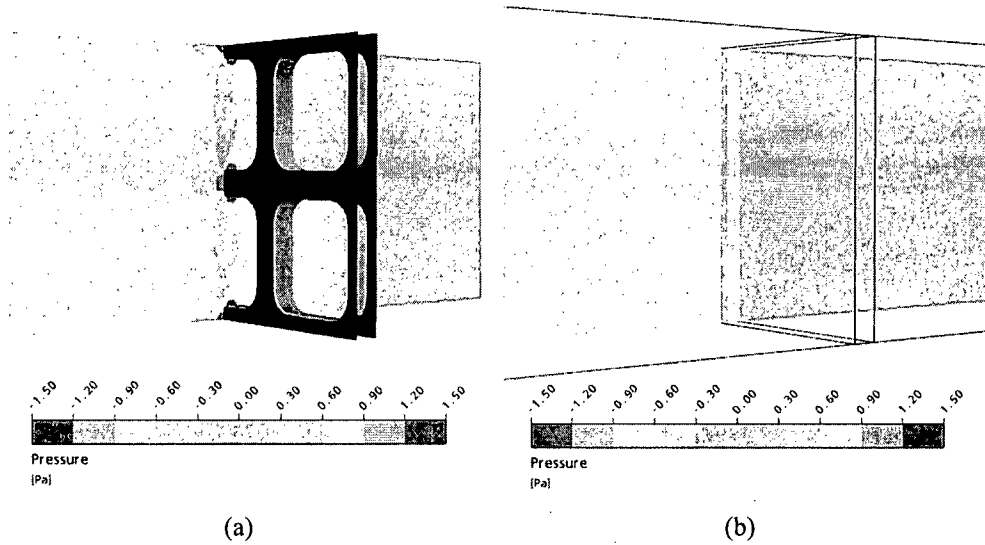


Figure A2.1: (a) Grill pressure loss at $Re=617$ and (b) corresponding pressure loss across porous grill.

The pressure loss coefficient, defined as

$$K_{loss} = \Delta p_t (0.5 \rho V^2)^{-1},$$

is shown in Figure A2.2, where

- $Re = \rho V d / \beta \mu$
- ρ = air density
- V = gas velocity
- d = equivalent wire diameter (6mm)
- β = frontal area of holes / total frontal area
- μ = dynamic viscosity

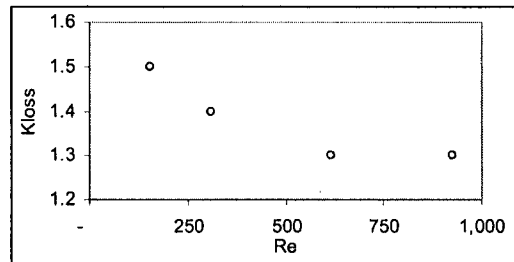
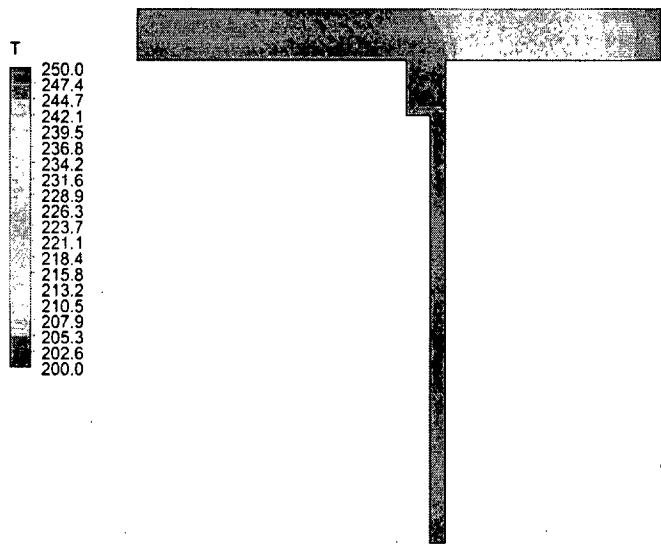


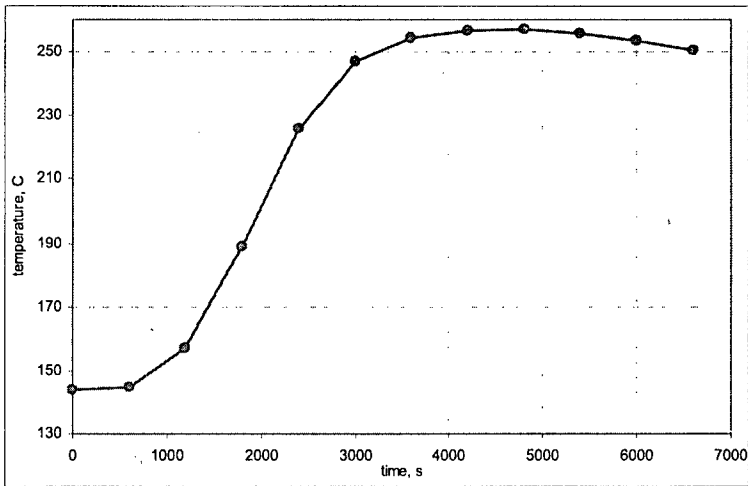
Figure A2.2: Grill pressure loss coefficient.

Appendix 3: Maximum Reverse Temperature Gradient in Closure Flange

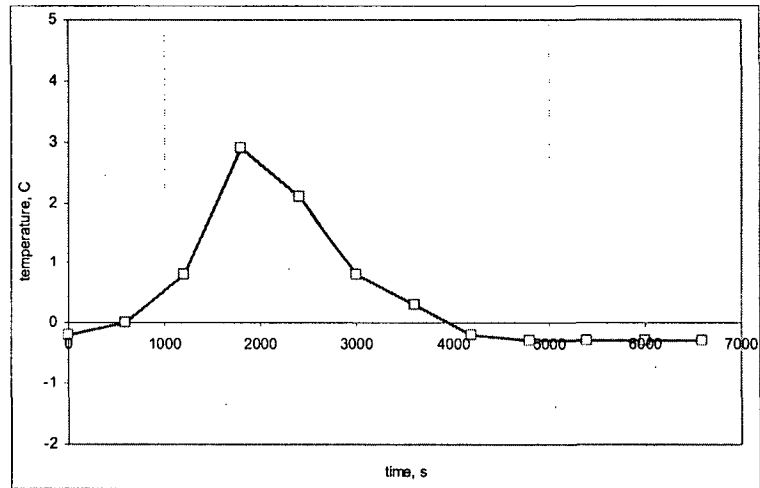
The normal temperature gradient is outwards. The only occasion when this is reversed is during accident conditions. The maximum reverse temperature gradient in the closure flange occurs in the case in which that component attains its highest peak temperature (upright and undamaged) and approximately at the point at which its rate of temperature increase is at its greatest. The following figures illustrate the temperature profile in the closure flange and the temperature difference between its upper and lower surfaces during the transient:



Temperature distribution on a vertical section of the package at peak rate of closure seal temperature rise ($t=2400s$)



Temperature at the top of the closure at seal location



Temperature difference between flange top and flange base at seal location ($\Delta T = T_{top} - T_{bottom}$)

Thermal Analysis of the R7021 Radioactive Materials Transport Container at 3074W Internal Heat Load

Report R7410/1.1

July 2010

Thermal Analysis of the R7021 Radioactive Materials Transport Container at 3074W Internal Heat Load

prepared for
REVISS Services (UK) Ltd

Dr M. Beiler
FTT Technology CC

Summary

This report extends a previous study of the R7021 transport container^[2]. It presents a thermal analysis of the container under IAEA normal and accident conditions of transport with an internal heat load of 3074W. Normal conditions was modelled as an ambient temperature of 38°C and solar radiation from the top and sides. Accident conditions modelled an environment simulating an 800°C furnace test with a forced updraft around the container. This heating phase lasted for thirty minutes and was followed by natural cooling in the normal conditions environment. The container was modelled upright for normal conditions and then inverted, with drop test damage, for accident conditions as that had previously been shown to generate the highest shielding temperature. The radioactive contents were modelled separately in each instance using the maximum cavity wall temperature.

Contents

Summary	2
1 Purpose and Scope	4
2 R7021 Description and Specification	4
3 Modelling.....	4
3.1 Benchmarking	5
3.2 Normal Conditions Analysis.....	6
3.3 Accident Conditions Analysis.....	6
4 Results.....	7
4.1 Benchmarking	7
4.2 Normal Conditions.....	8
4.3 Accident Conditions.....	9
5 Conclusions	11
5.1 Benchmarking	11
5.2 Results.....	11
6 References	11
Appendix 1: Figures	12
Appendix 2: Specifications	18

1 Purpose and Scope

The purpose of this report is to demonstrate the thermal performance of the R7021 container under IAEA normal and accident conditions of transport with an internal heat load of 3074W.

2 R7021 Description and Specification

The R7021 transport container comprises an upright, cylindrical stainless steel flask mounted on a carbon steel pallet^[1]. The flask has a central cavity holding the source capsules and a removable closure plug at the top. Lead surrounds the cavity. Voids in the flask corners and at the base are filled with ceramic fibre insulation. Vertical fins are fitted to the cylindrical flask surface. A cylindrical shield, the jacket, surrounds the flask. A second shield is mounted on top of the flask. The jacket and parts of the top shield are filled with ceramic fibre insulation. A simple screen is mounted between the jacket and the top shield.

3 Modelling

The CFD code Ansys CFD was used to model the heat transfer and gas flow processes involved. Ansys CFD is a leading, general purpose CFD code suitable to solve fluid flow, thermal radiation and heat transfer problems.

The model comprises different types of zones. The flask and shields comprise solid heat conducting regions and solid heat conducting and heat generating regions. Regions surrounding the transport container were modelled as gas flow regions with thermal radiation. The voids of the top shield were modelled as gas regions with radiation heat transfer. Natural convection inside the voids was neglected. The screen was modelled as an isotropic porous region with similar pressure loss characteristics. The energy equation was solved for solid regions. Continuity, momentum, turbulence and energy equations were solved for the fluid flow domain. A Monte Carlo radiation model was used to calculate thermal radiation between free surfaces emitting, absorbing and reflecting long wavelength radiation.

Steady state temperatures depend mainly on natural convection therefore a flow domain enclosed the container. The container was modelled on a solid floor and exposed to natural convection at the required ambient air temperature. A heat flux was applied to simulate insolation. Free air flow was allowed across the flow domain so that the floor was free to dissipate heat from insolation. For accident conditions the container was modelled in an 800°C furnace with an 800°C forced updraught to simulate the air movement associated with a fire. All salient modelling parameters are presented in Appendix 2.

Continuous heat production was modelled in the cavity wall and lead shielding. Heat from the container contents was modelled as a heat flux applied to the cavity wall. The rate of heat production in each component or region is shown in the following table, with Q , the total heat production.

A thermal contact resistance was specified between lead and stainless steel surfaces. The appropriate value was obtained from benchmarking simulations. The pallet is in thermal contact with the flask. The top shield rests on the flask, but to model the intermittent contact between the adjacent surfaces of the top shield and flask, a contact resistance equivalent to a 0.1mm gap was modelled. The thin volume between the side and base of the closure and the flask was specified as a non-convective air layer.

Table 1: Internal Heat Load Distribution.

Location	Energy deposition [W]
Cavity wall heat flux	$0.258Q_i$
Cavity wall	$0.11Q_i$
First 12mm radial lead	$0.397Q_i$
Remaining radial lead	$0.235Q_i$
Total	$1.0Q_i$

The container model does not include the cavity contents; a separate model was used to model the transport processes inside the cavity. The container model provided the cavity wall temperature, which is required to define the cavity model. The cavity model comprises the sources and basket.

Source temperatures at accident conditions were calculated using the peak cavity wall temperature.

3.1 Benchmarking

This study revisited benchmarking as the previously predicted flask surface temperatures were generally higher than the measured values. The benchmark model incorporated a 3mm gap between closure and flask to model the gap provided for the thermocouple leads to exit. The total heat load of $Q_i = 2362\text{W}$ was applied as shown in Table 1.

The following parameter changes were found to give improved results and were adopted:

1. The emissivity of flask external surfaces was increased from 0.45 to 0.55
2. The two-equation $k-\omega$ based shear stress transport turbulence model was replaced with the standard two-equation $k-\omega$ based turbulence model.

The reduction in flask surface temperatures resulted in the contact coefficient at lead-stainless steel interfaces having to be reduced from $400\text{W/m}^2\text{K}$ to $330\text{W/m}^2\text{K}$ to provide the required mid-height cavity wall temperature.

3.2 Normal Conditions Analysis

The normal conditions analyses determine equilibrium temperature distribution throughout the container and contents under IAEA normal conditions of transport. The model described in section 3.1 was employed to predict temperatures at normal conditions, but the emissivity of external painted carbon steel surfaces and the insulation conductivity were adjusted to the values from a previous sensitivity study, which resulted in the highest temperatures^[2]. Container temperatures were calculated with and without solar insolation. An ambient air temperature of 38°C was specified.

The basket was loaded with fourteen capsules, increased from twelve in the previous study in proportion to the increased heat load. The capsules were evenly distributed around the basket (positions 1, 3, 4, 6, 8, 10, 11, 13, 15, 16, 18, 20, 22 & 23) which was then enclosed in an air filled, cylindrical domain representing the cavity wall.

3.3 Accident Conditions Analysis

The model was used to predict container temperatures during the transient period simulating a fire under IAEA accident conditions of transport. The container was modelled in a furnace at a temperature of 800°C for thirty minutes. An upward air flow, which resulted in peak flow velocity surrounding the container of not less than 10m/s, was applied to the enclosing flow domain. The temperature of both inflow and surrounding vertical walls was 800°C. The emissivity of external surfaces was changed to a value of 0.8 to represent blackened surfaces. The wall emissivity was specified as 0.9. Insolation heat fluxes were excluded. The steady state solution for normal transport conditions provided the initial condition temperatures of the container. A cooling period at normal conditions followed the heating phase. The container was modelled in air, allowing for free convection cooling at an ambient air temperature of 38°C. The normal conditions insolation heat fluxes were re-applied during the cooling phase.

The container was modelled inverted throughout and included a representation of the drop test damage from the inverted drop tests as this had been determined by the previous report to generate the highest shielding temperature. Damage, as before, was modelled as a 150mm x 150mm hole in the center of the top shield outer plate and with the cones completely removed.

The basket and contents were modelled inverted in an air filled, cylindrical domain representing the cavity at its peak temperature.

4 Results

4.1 Benchmarking

Table 2 shows the measured temperatures, the previously predicted temperatures and the temperatures of the revised benchmark model. It can be seen that the revised model provides a better correlation. In most locations temperature variance is reduced and nowhere has it increased. The deviation at flask surface mid-height between the fins (L) decreased from 8°C to 4°C. The deviation at the lifting fin (H) decreased from 5°C to 0°C.

Table 2: Measured and Calculated Container Temperatures.

Identity	Location	Temperature [°C]		
		Measurements ^[3]	Previous Results ^[2]	New Results
A1	Cavity wall (50mm below top)	151 / 196*	153	152
B1	Cavity wall (mid-height)	155 / 155 / 154 / 270*	156	155
C1	Cavity wall (50mm above base)	149	152	150
F	Closure and vent seal	112 / 116	114	111
G	Lifting fin (100mm from top edge, 75mm from outer edge)	49	67	64
H	Lifting fin (40mm from top edge, 55mm from outer edge)	55	60	55
I	Lifting fin (135mm from top edge, 35mm from outer edge)	61 / 59	68	65
L	Flask wall (mid-height, midway between fins)	112 / 111 / 112 / 113	120	116
N1	Drain point (centre of cylinder, outer surface)	83	101	97
P	Flask foot (top surface, 30mm from outer edge)	27 / 27	33	32
R	Jacket (top edge)	36 / 36	39	39
S	Jacket (inner surface, 40mm from top edge)	43 / 40	46	46
T	Top shield (mid height vertical face)	35 / 36	39	38
U	Top shield (half way across horizontal face)	35 / 35	38	38
V	Top shield (top surface centre)	40	37	39
T _a	Ambient	21	21	21

*The highest measurement in both A1 and B1 were ignored as they were inconsistent with the other measurements.

4.2 Normal Conditions

Table 3 presents steady state temperatures for normal conditions without and with insolation. The temperature distribution on a vertical section is shown in Figure A1.2, and Figure A1.3. illustrates the source temperature distribution.

Table 3: Normal Conditions Temperatures [°C].

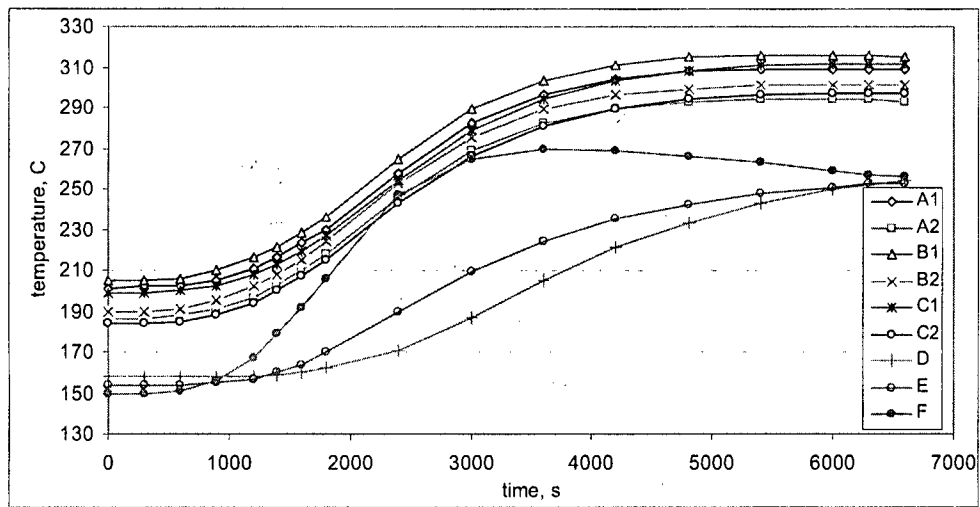
Location	Location	Without insolation	With insolation
T_{Cmax}	Capsule wall	409	411
A1	Cavity wall (50mm below top)	196	201
A2	Lead adjacent to A1	181	186
B1	Cavity wall (mid-height)	201	205
B2	Lead adjacent to B1	185	190
C1	Cavity wall (50mm above base)	194	199
C2	Lead adjacent to C1	179	184
D	Lead (closure base centre)	151	158
E	Lead (closure top centre)	146	154
F	Closure and vent seal	141	150
H	Lifting fin (40mm from top edge, 55mm from outer edge)	79	93
J	Lead (top chamfer top corner)	150	157
K	Lead (top chamfer bottom corner)	153	158
L	Flask wall (mid-height, midway between fins)	149	153
M	Lead (bottom chamfer top corner)	150	154
N2	Drain seal	148	152
O	Lead (bottom chamfer bottom corner)	157	161
P	Flask foot (top surface, 30mm from outer edge)	50	67
Q	Jacket (mid height outer surface)	51	64
V	Top shield (top surface centre)	57	100
W	Maximum lead temperature	186	191
T _a	Ambient	38	38

4.3 Accident Conditions

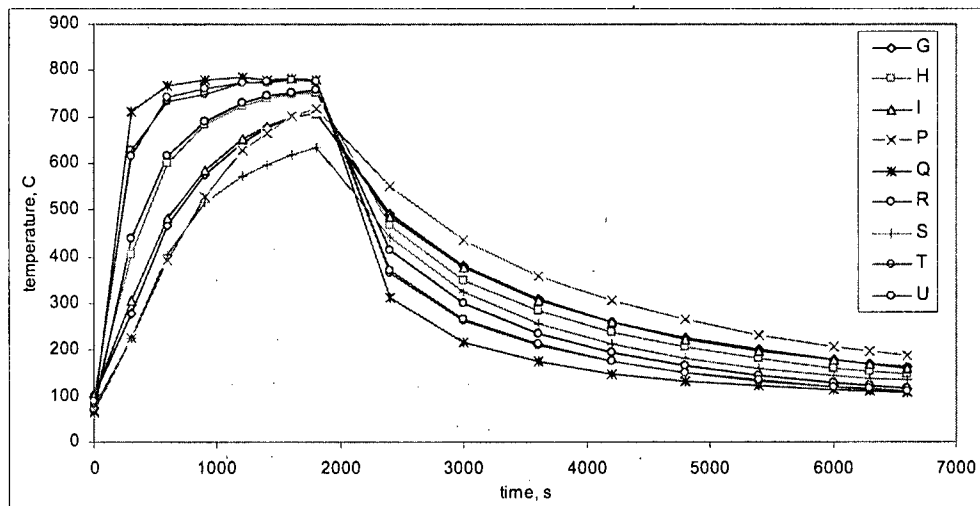
Table 5 shows the calculated peak temperatures for the damaged inverted container. The temperatures histories during heating and subsequent cooling at various locations are shown in Graph 4 to 6. The peak lead temperature is reached at $t=5400s$ at the vertical cavity wall. Typical temperature distributions at 1800s and 6600s after the start of the accident are shown in Figures A1.6 and A1.7. Steady state capsule temperatures were calculated for the contents exposed to the peak cavity wall temperature. Figure A1.8 illustrates the capsule temperature distribution at peak accident conditions.

Table 5: Peak Accident Conditions Temperatures

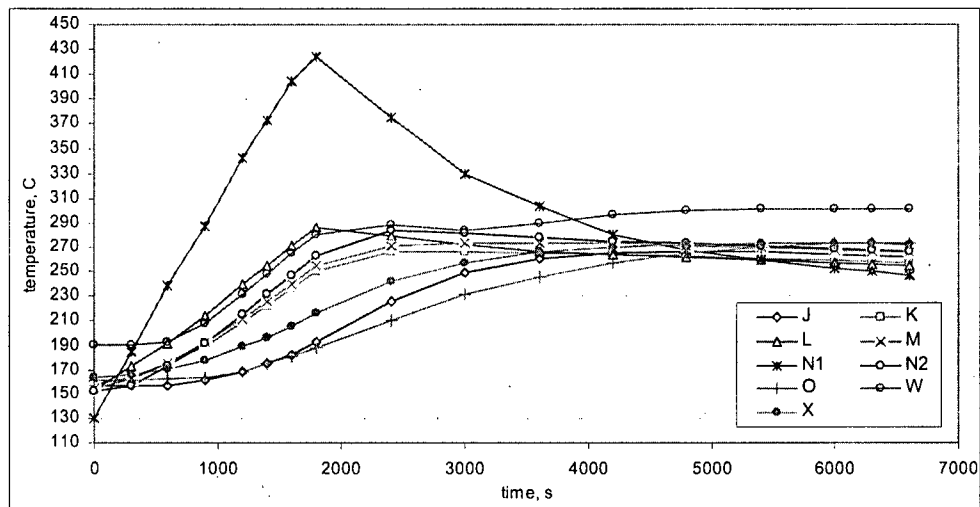
	Location	Temperature [C]
T_{Cmax}	Capsule wall	471
A1	Cavity wall (50mm below top)	309
A2	Lead adjacent to A1	294
B1	Cavity wall (mid-height)	316
B2	Lead adjacent to B1	301
C1	Cavity wall (50mm above base)	312
C2	Lead adjacent to C1	297
D	Lead (closure base centre)	254
E	Lead (closure top centre)	253
F	Closure and vent seal	270
H	Lifting fin (40mm from top edge, 55mm from outer edge)	753
J	Lead (top chamfer top corner)	267
K	Lead (top chamfer bottom corner)	266
L	Flask wall (mid-height, midway between fins)	287
M	Lead (bottom chamfer top corner)	274
N2	Drain point seal	284
O	Lead (bottom chamfer bottom corner)	274
P	Flask foot (top surface, 30mm from outer edge)	718
Q	Jacket (mid height outer surface)	787
V	Top shield (top surface centre)	800
W	Maximum lead temperature	302



Graph 1: Accident temperatures for inverted container orientation, damaged [°C]



Graph 2: Accident temperatures for inverted container orientation, damaged [°C]



Graph 3: Accident temperatures for inverted container orientation, damaged [°C]

5 Conclusions

5.1 Benchmarking

The correlation between predicted and measured temperatures is improved when:

- the emissivity of external flask surfaces is increased from 0.45 to 0.55,
- the two-equation $k-\omega$ based shear stress transport model is replaced with the standard two-equation $k-\omega$ based turbulence model,
- the contact coefficient is reduced from 400W/m²K to 330W/m²K.

5.2 Results

The R7021 transport container temperatures, under IAEA TS-R-1 normal and accident conditions of transport with an internal heat load equivalent to 3074W, are summarized in the following table.

Location	Temperature [°C]		
	Normal conditions		Peak accident conditions with damage
	Without insolation	With insolation	
Capsule wall	409	411	471
Cavity wall	201	205	316
Closure and vent seal	141	150	270
Lifting fin	79	93	753
Drain plug seal	148	152	284
Flask wall at mid-height	149	153	287
Flask foot	50	67	718
Top shield top surface	57	100	800
Lead shielding (max)	186	191	302

6 References

- [1] QS7021 issue 4: R7021 Transport Container Drawings List and associated drawings, Reviss Services (UK) Ltd.
- [2] R7110/1.1: Thermal Analysis of the R7021 Radioactive Materials Transport Container, FTT Technology, July 2010.
- [3] RTR 225: R7021 Thermal Survey Record on 3981/01, Reviss Services (UK) Ltd.

Appendix 1: Figures

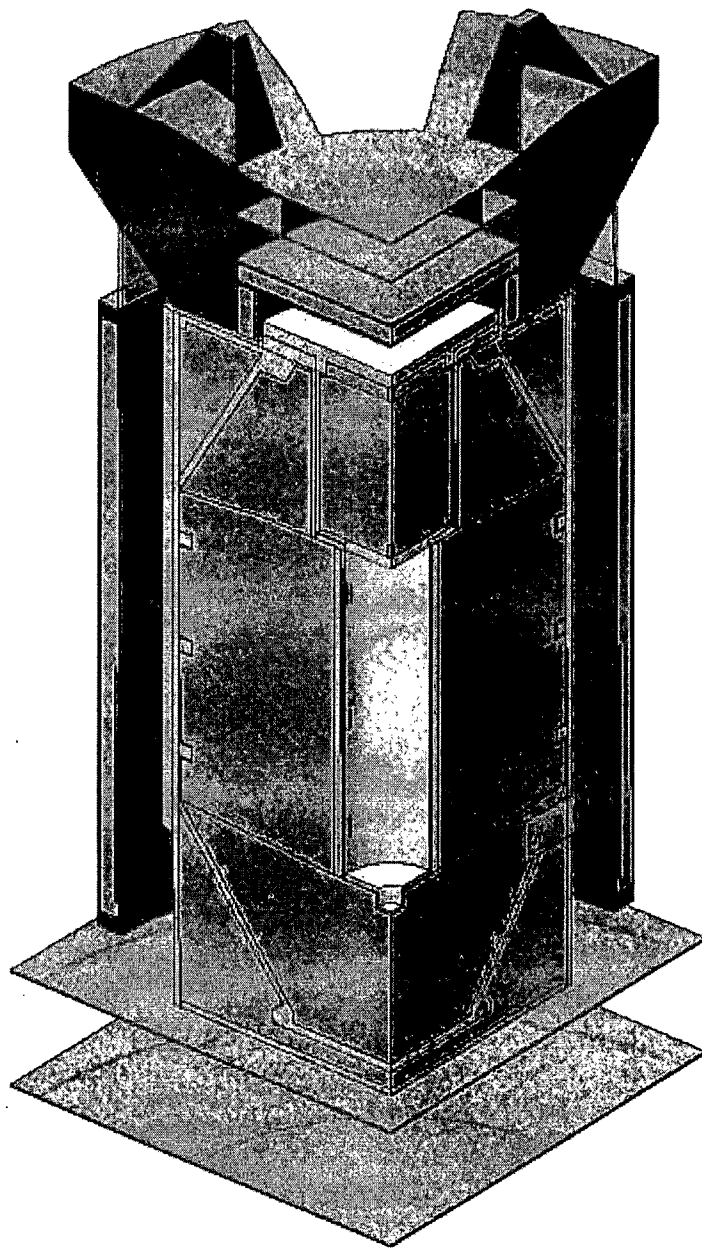


Figure A1.1: Sectional view of the transport container assembly.

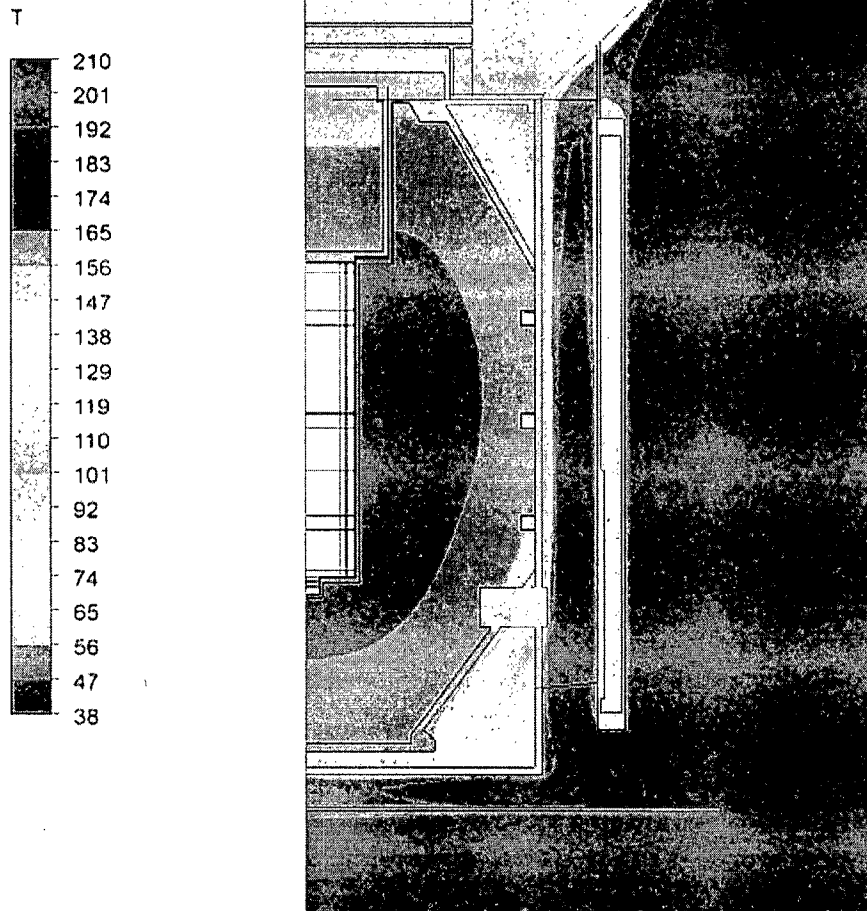


Figure A1.2: Temperature distribution at normal conditions with insolation [°C]

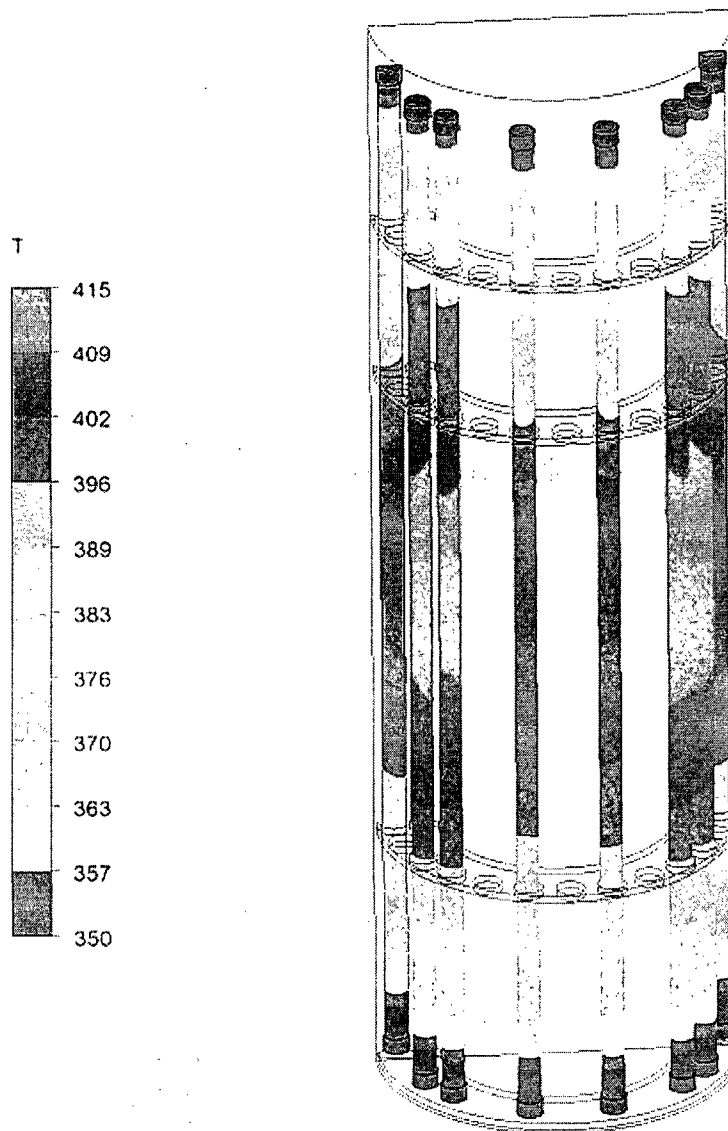


Figure A1.3: Capsule temperatures at normal conditions with insolation [°C]

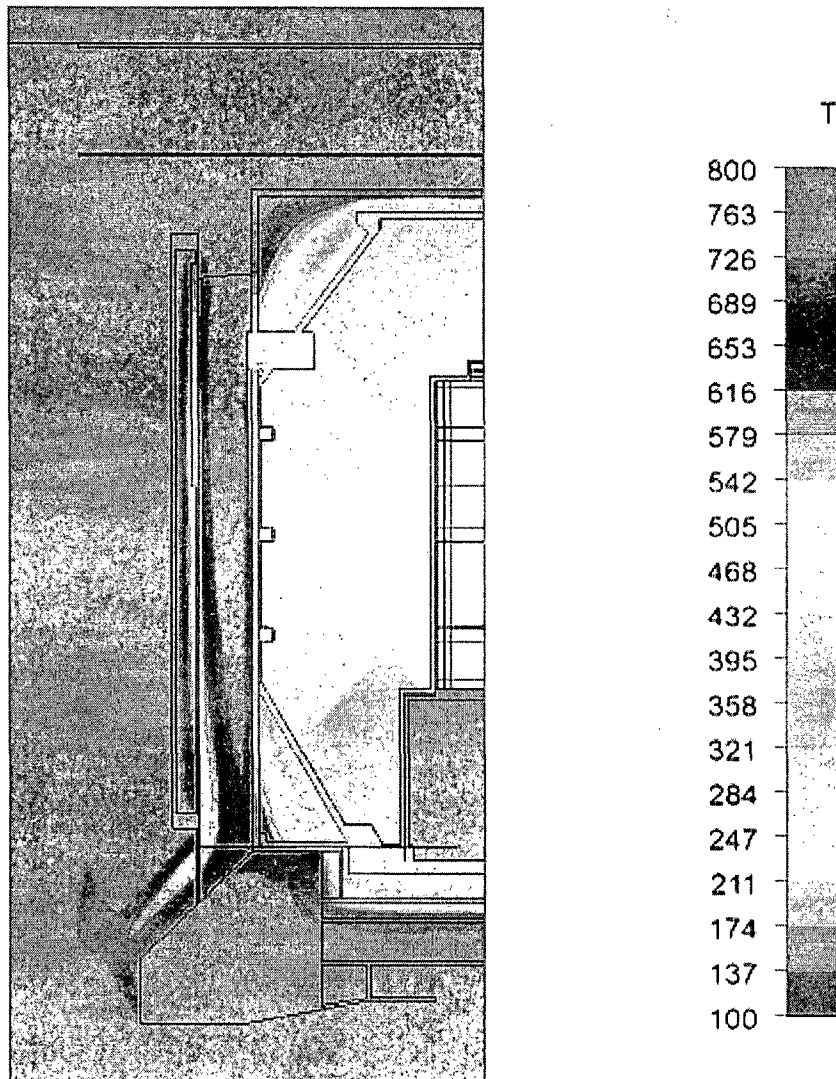


Figure A1.4: Accident conditions temperature distribution at 1800s [°C]

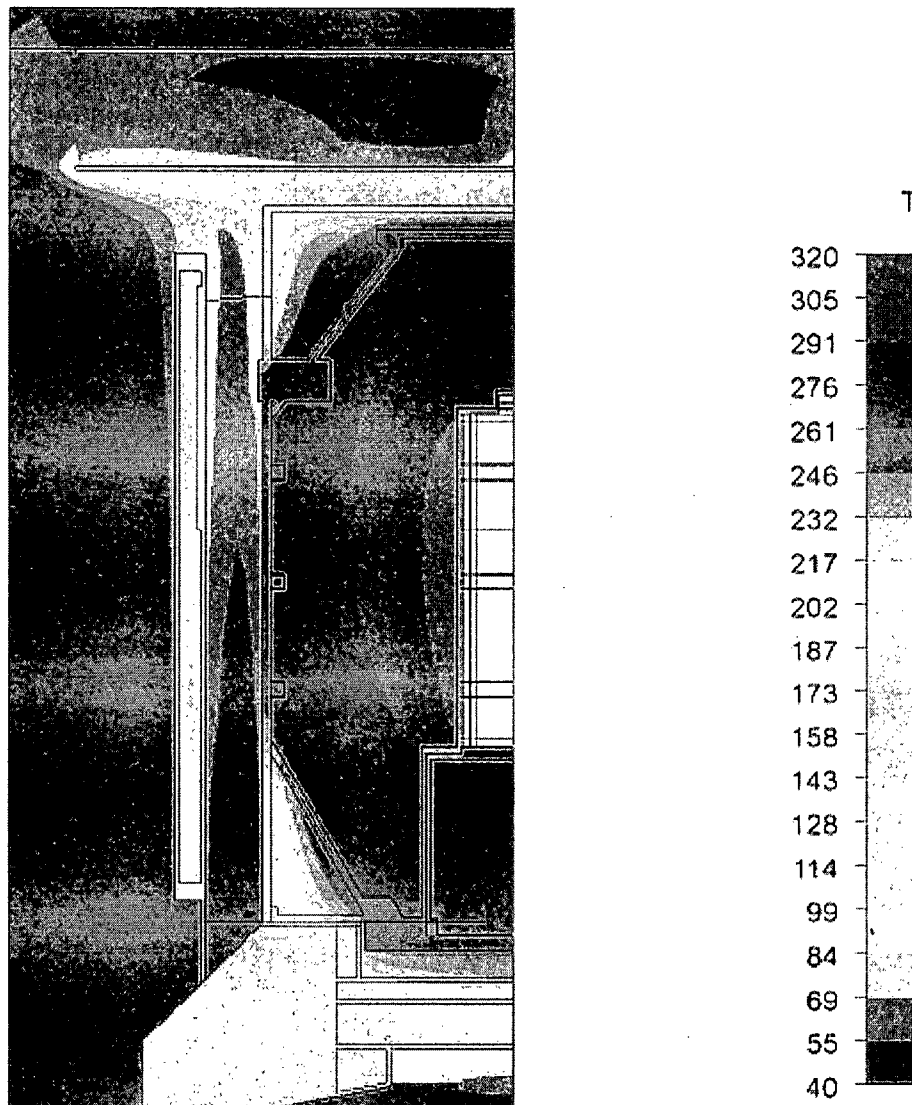


Figure A1.5: Accident conditions temperature distribution at 6600s [°C]

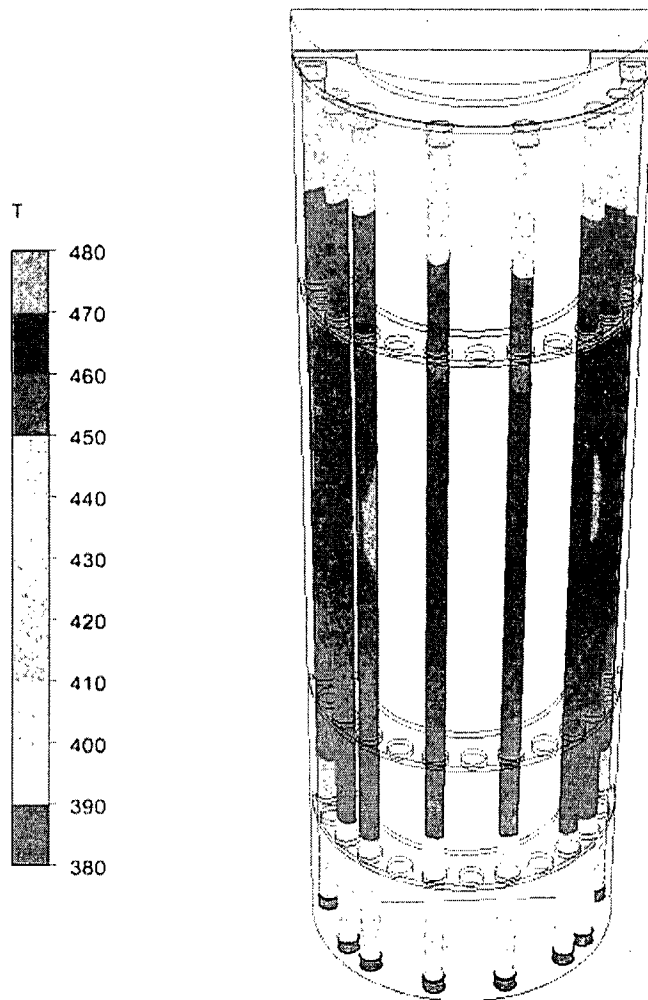


Figure A1.6: Peak accident conditions source temperature distribution [$^{\circ}\text{C}$]

Appendix 2: Specifications

General

Domain overall height	6m
Domain height above pallet base	3.5m
Domain width / depth (complete model)	5.5m
Heat load at benchmark conditions	2362W
Heat load at transport conditions	3074W

Emissivities:

Benchmark:

External flask surfaces emissivity	0.55
Unpainted carbon steel surfaces emissivity	0.90
Painted carbon steel surfaces emissivity	0.90
Cavity wall emissivity	0.40

Normal conditions:

External flask surfaces emissivity	0.55
Unpainted carbon steel surfaces emissivity	0.98
Painted carbon steel surfaces emissivity	0.98
Cavity wall emissivity	0.40

Thermal test and cooling period:

Flask surface covered by top shield emissivity	0.55
Unpainted carbon steel surfaces emissivity	0.98
Blackened external surfaces emissivity	0.80
Furnace walls emissivity	0.90
Cavity wall emissivity	0.40

Domain conditions

Insolation:

Downward heat flux (-y direction):	800W/m ²
Horizontal direction (-x direction):	200W/m ²
Horizontal direction (+x direction):	200W/m ²
Horizontal direction (-z direction):	200W/m ²
Horizontal direction (+z direction):	200W/m ²

Normal conditions:

Ambient air temperature:	38°C
Sides and top:	Open flow boundaries
Floor:	Solid base
Flow:	Turbulent, free convection flow

Thermal test:

Ambient air temperature:	800°C
Base:	8m/s inflow at domain base (container suspended)
Sides:	Wall
Top:	Opening
Flow:	Turbulent, free and forced convection flow

Cooling period:

Ambient air temperature:	38°C
Base:	Wall (container suspended)
Sides and top:	Open flow boundaries
Flow:	Turbulent, free convection flow



Unit 10 Caddsdwn Industrial Park
Clovelly Road Bideford Devon EX39 3DX
Telephone : +44 (0) 1237 421255
Facsimile : +44 (0) 1237 423541
e-mail: info@parcsw.co.uk Website: www.parcsw.co.uk

TEST REPORT

Document No. TR2
Revision C
Customer Confidential

Page 1 of 15

Report No
2209

Requested By
Mr. S. Cheung

Customer Details
REVISS Services (UK) Ltd.
6 Chiltern Court
Asheridge Road
Chesham
Buckinghamshire
HP5 2PX

Date Samples Received
19/11/08

Date Started
20/11/08

Date Finished
24/11/08

Date of Issue
27/11/08

Product Description:

(2x) Stainless Steel Tube
loaded with pellets
(1 off identified with red tape, 1 off identified with black tape)

Tests Performed and Test Specifications:

- Random Vibration – carried out in accordance with Def Stan 00-35 Test M1 Annex A. To simulate 10,000km on road, duration of 2 hours per axis.
- Shock – carried out in accordance with Def Stan 00-35 Test M3. 11ms half sine pulse, carried out at 4g, 5g and 6g.

Disposal of Samples:
Returned to customer

Report Summary:

The samples were subjected to the test outlined above, the details and methodology of which are described in the following report.

No observations were noted during the test programme.

On completion of testing the samples were returned to the customer for further examination.



Distribution: Mr. S. Cheung, PARC File

Test Engineer: M. Woodland

M. Woodland
Approved: D. Pile (Senior Engineer)

Any opinions or interpretations expressed within this report, together with tests marked 'Non UKAS' are not included in the UKAS Accreditation Schedule for this Laboratory.

1. Sample Content

(2x) Stainless Steel Tube
loaded with pellets
(1 off identified with red tape, 1 off identified with black tape)

2. Equipment

<i>Description</i>	<i>PARC ID</i>	<i>Calibration Due</i>
Shaker System	377	Monitored by calibrated equipment
Power Amplifier	378	Monitored by calibrated equipment
Controller	177	18/06/09
Charge Amplifier	332	13/06/09
Accelerometer	350	24/07/09
Controller	194	24/10/09
Shaker System	13	Monitored by calibrated equipment
Power amplifier	14	Monitored by calibrated equipment
Charge Amplifier	205	04/02/09

3. Test Schedule

3.1 Random Vibration

The sample was subjected to the Random Vibration test in accordance with Def Stan 00-35 Test M1 Annex A. The following conditions were applied:

Road Transport – Wheeled Vehicles (On Road)

<i>Frequency (Hz)</i>	<i>PSD(g^2/Hz)</i>
10	0.015
50	0.015
500	0.001

Total grms: 1.42

Duration of test: 2 hours per axis (equivalent to 10,000km On Road)

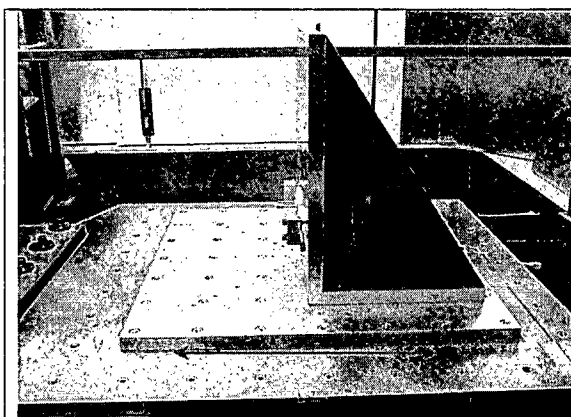
Test carried out in all 3 axes

3.1.1 Sample identification and orientation

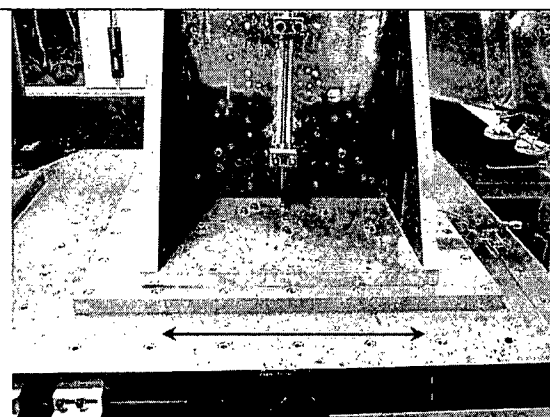
The samples were identified: 1 off with Black insulation tape at end, and
1 off with Red insulation tape at end

The customer specified that the Red ended sample be held in the test jig in a vertical position and the Black ended sample be held in a horizontal position.

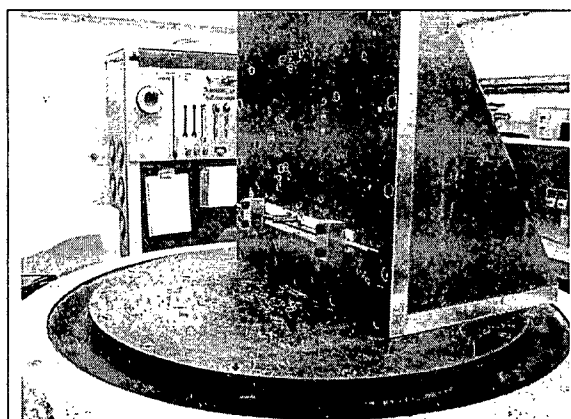
The photographs overleaf demonstrate the test sample orientation and test axes undertaken.



Axis 1

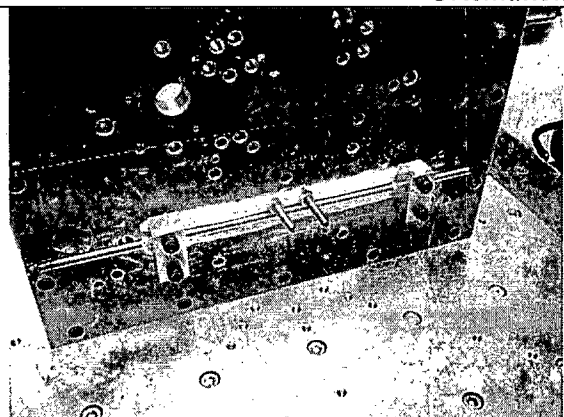


Axis 2

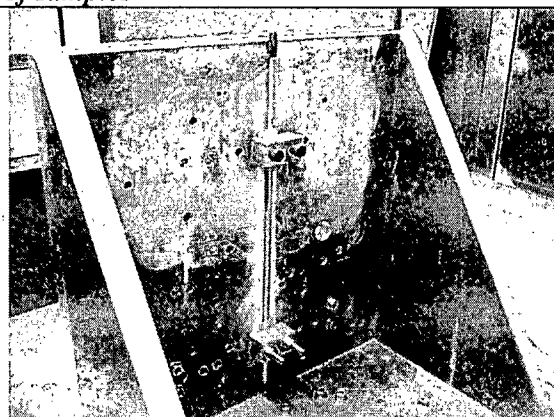


Axis 3

Orientation of samples



Sample with black tape (horizontal on jig)

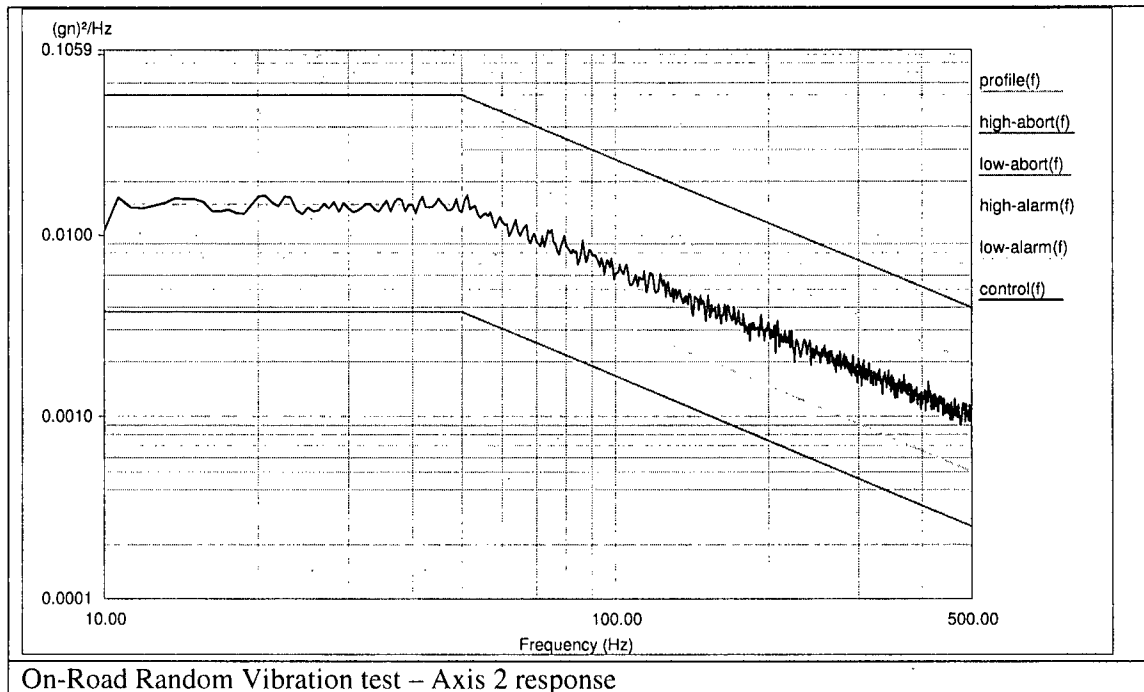
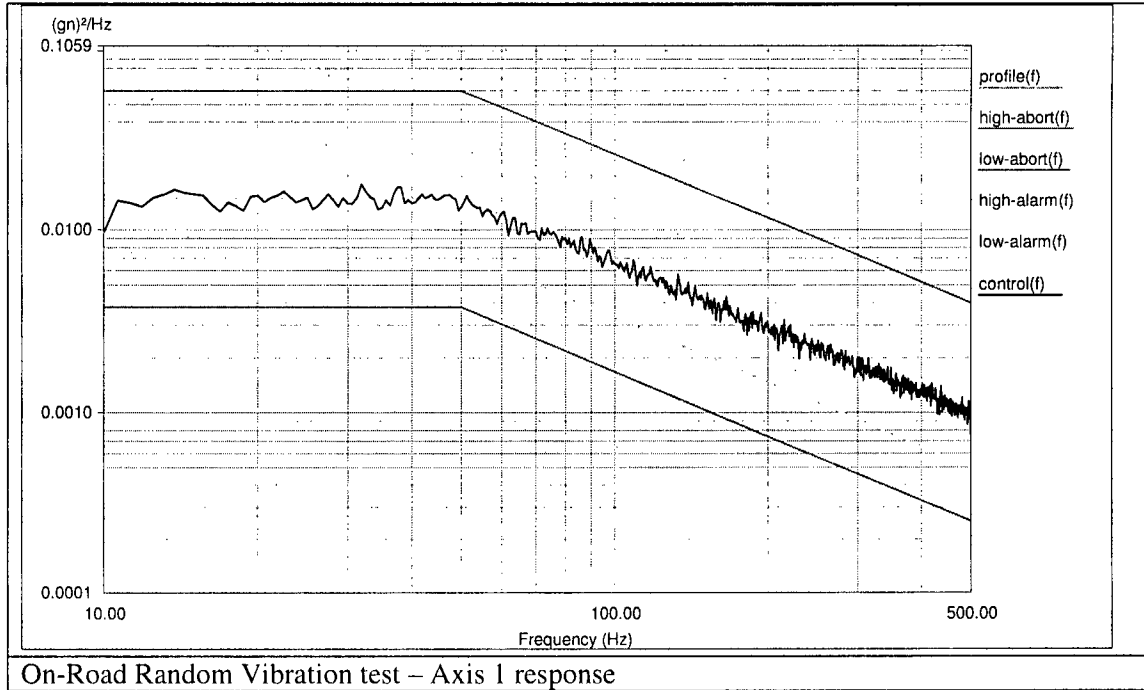


Sample with red tape (Vertical on jig)

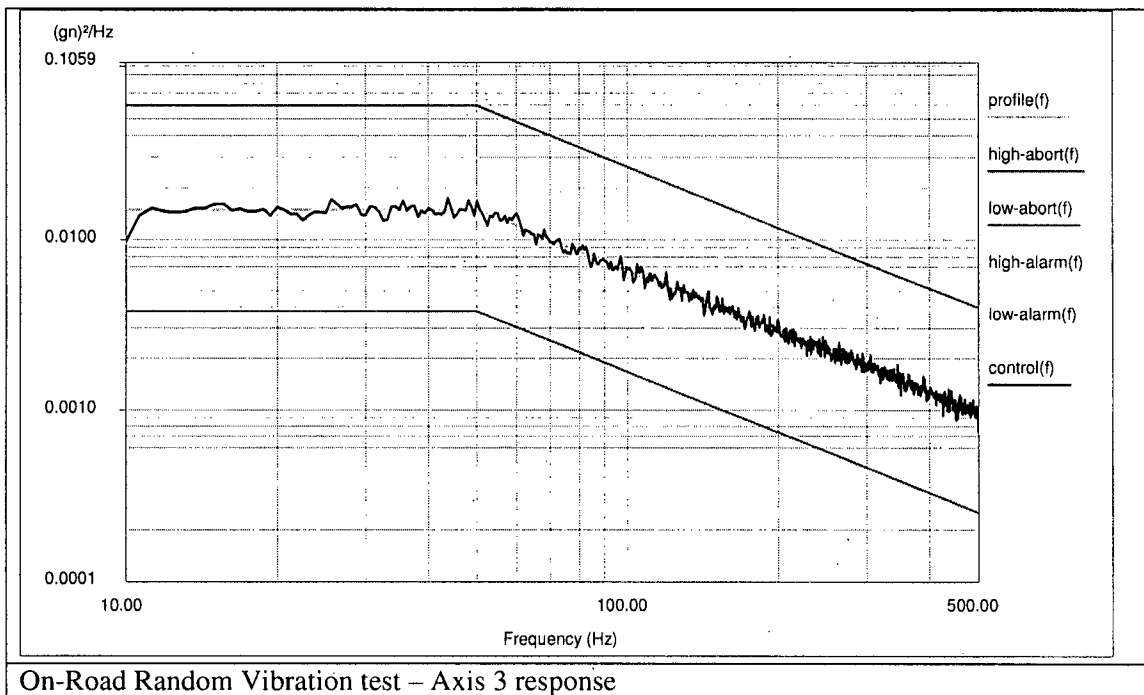
Any opinions or interpretations expressed within this report, together with tests marked 'Non UKAS' are not included in the UKAS Accreditation Schedule for this Laboratory.

3.1.2 Test Responses

The following responses were generated by this test:



Any opinions or interpretations expressed within this report, together with tests marked 'Non UKAS' are not included in the UKAS Accreditation Schedule for this Laboratory.



3.2 Shock tests

The samples were subjected to the shock test in accordance with Def Stan 00-35 Test M3. The following levels and conditions were applied:

Shock Test 1

Half sine shock pulse

11mS duration

Level: 4g

Number of shocks: 84 Shocks in each sense in each axis
(168 Shocks per axis)

Shock Test 2

Half sine shock pulse

11mS duration

Level: 5g

Number of shocks: 42 Shocks in each sense in each axis
(84 Shocks per axis)

Shock Test 3

Half sine shock pulse

11mS duration

Level: 6g

Number of shocks: 6 Shocks in each sense in each axis
(12 Shocks per axis)

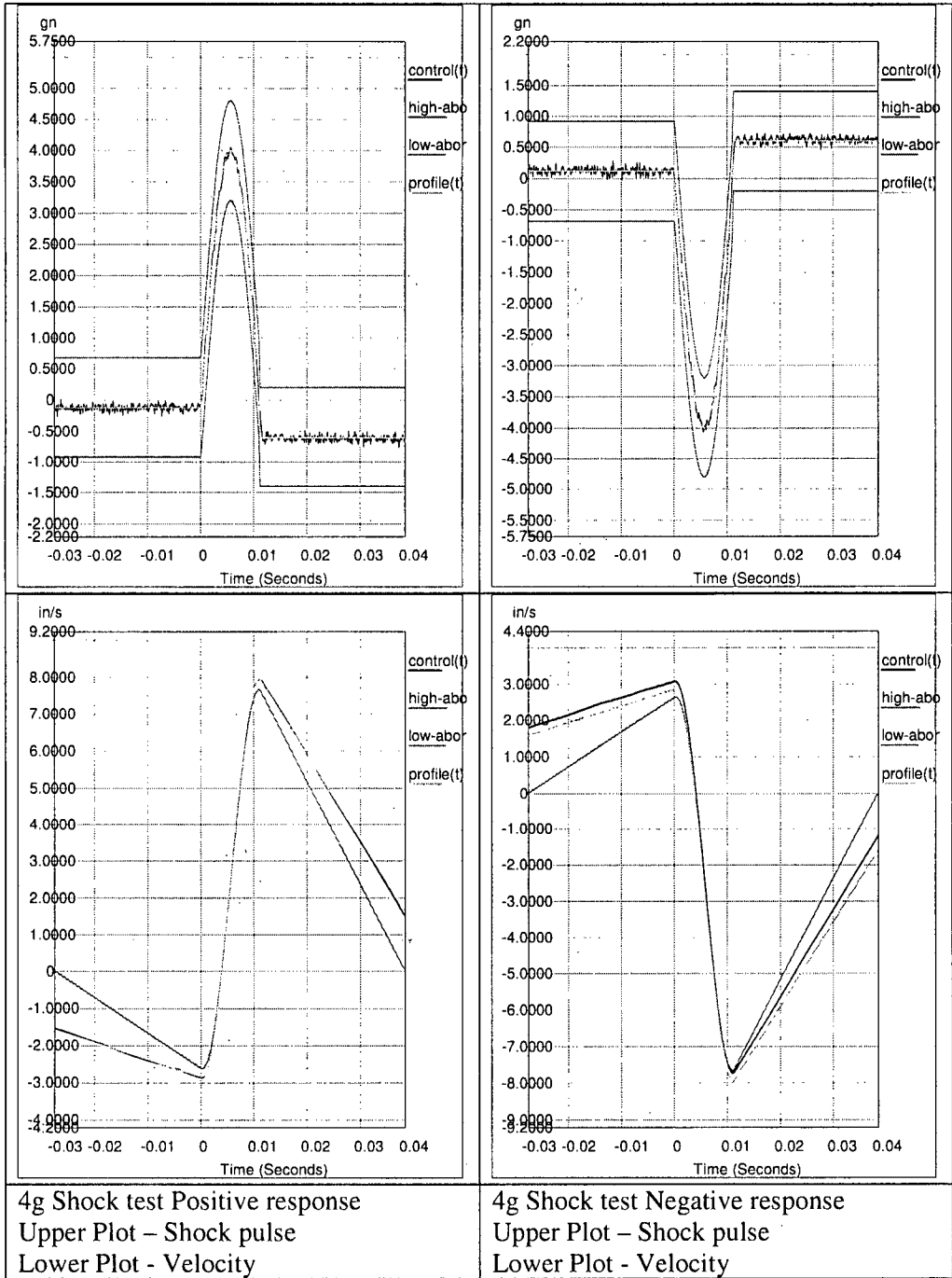
Note: The number of shocks carried out relates to an equivalent of 10,000km (as per Def Stan 0035)

Any opinions or interpretations expressed within this report, together with tests marked 'Non UKAS' are not included in the UKAS Accreditation Schedule for this Laboratory.

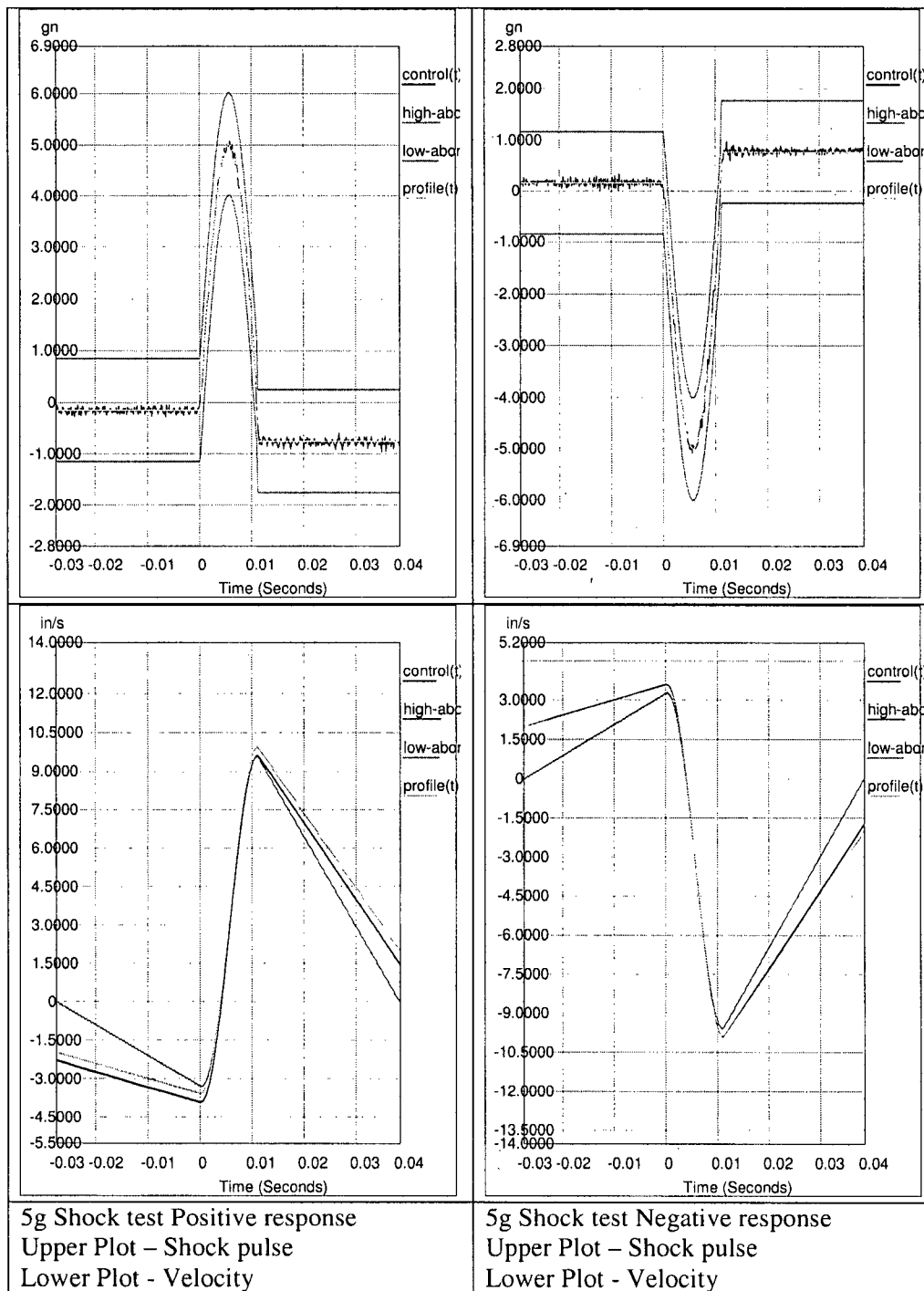
3.2.1 Test Responses

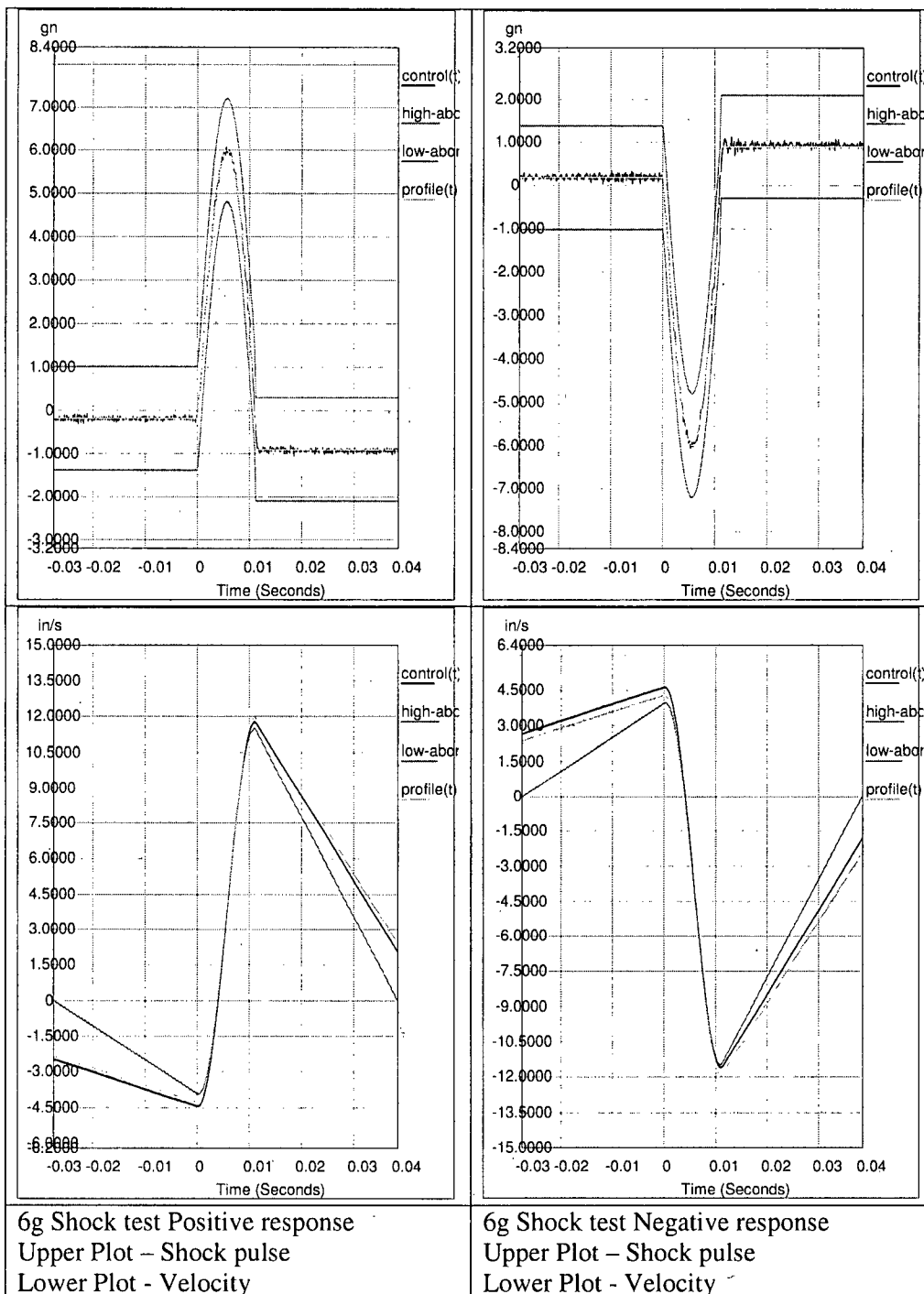
The following responses were generated by the shock tests:

3.2.1.1 Axis 1

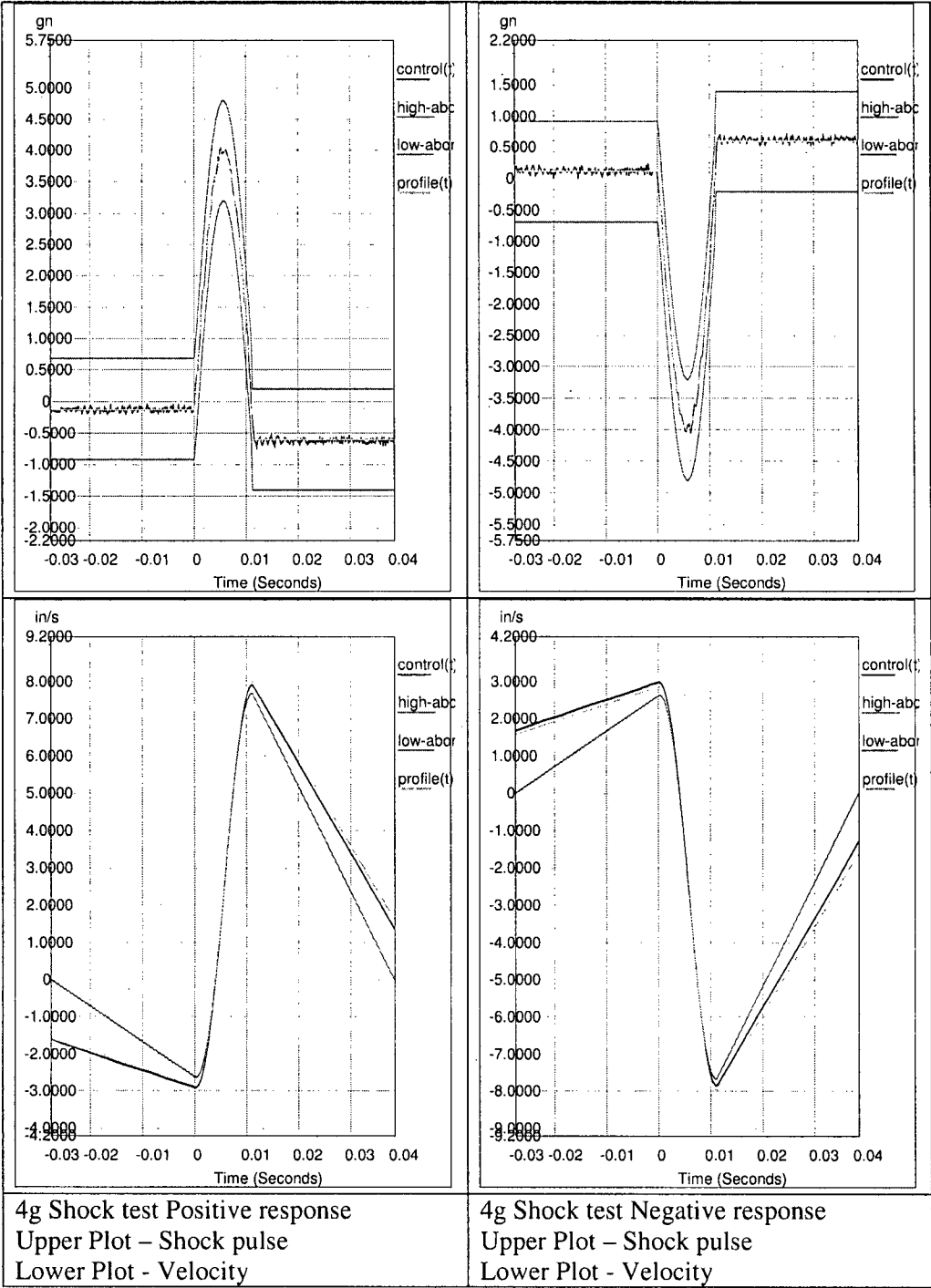


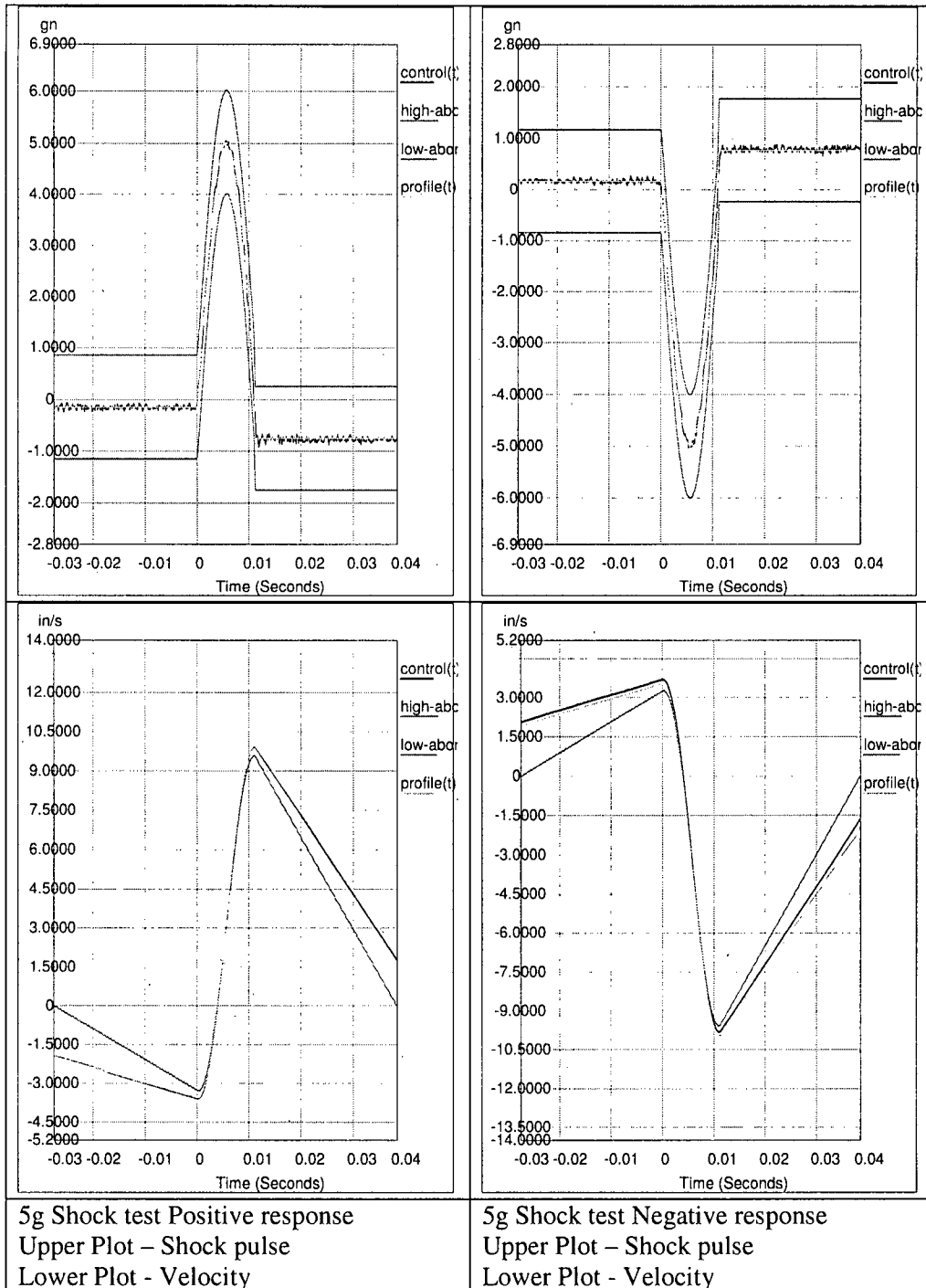
Any opinions or interpretations expressed within this report, together with tests marked 'Non UKAS' are not included in the UKAS Accreditation Schedule for this Laboratory.

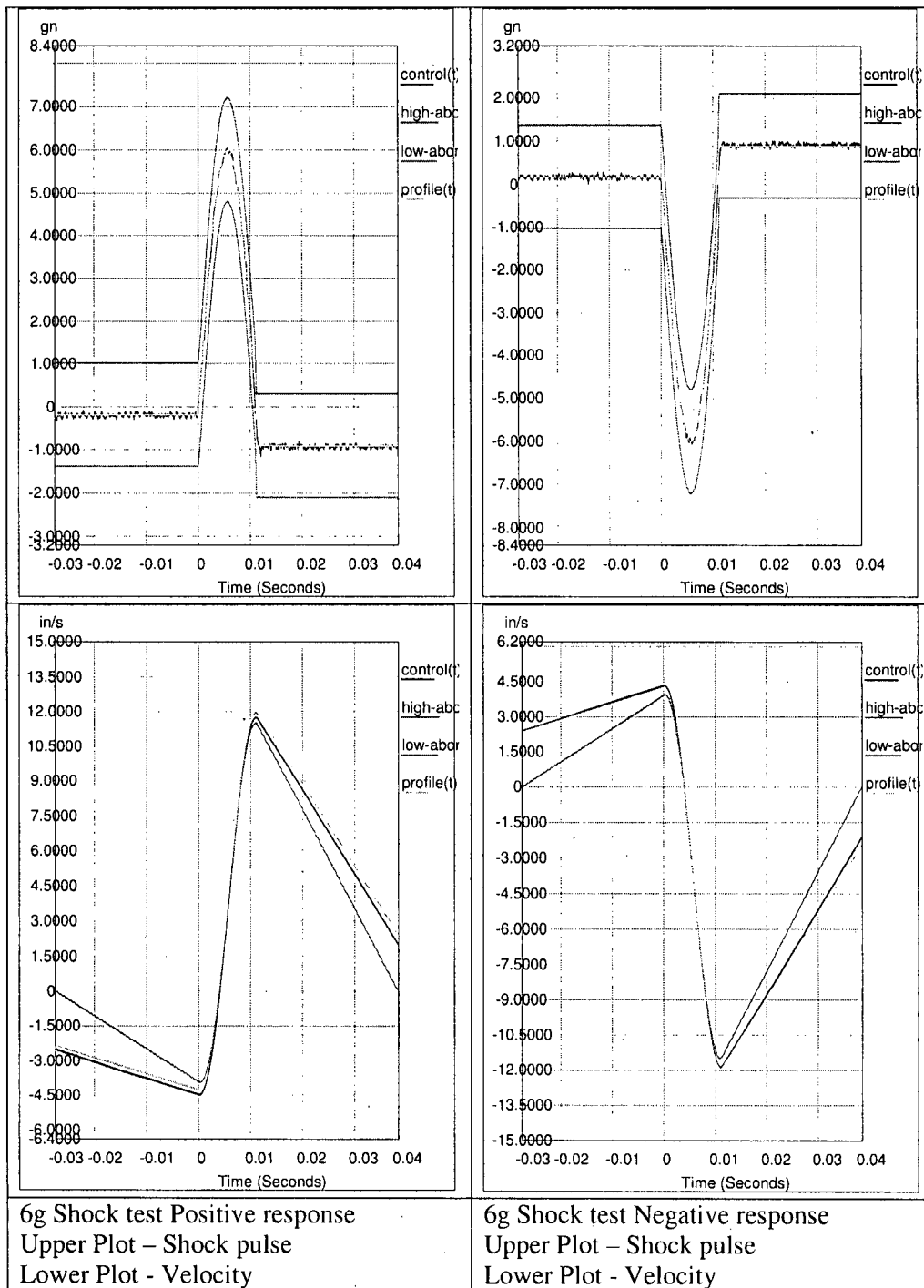




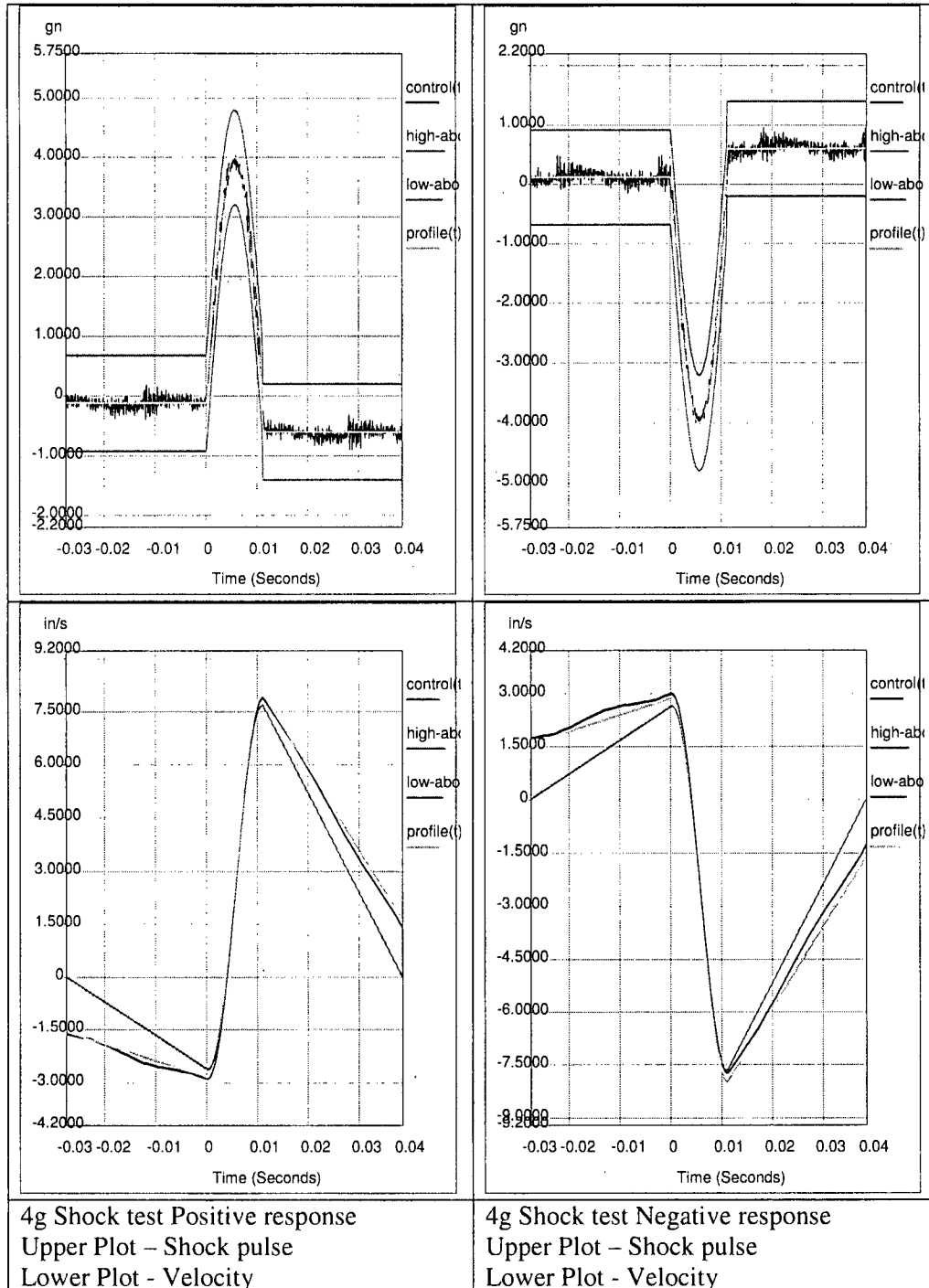
3.2.1.2 Axis 2

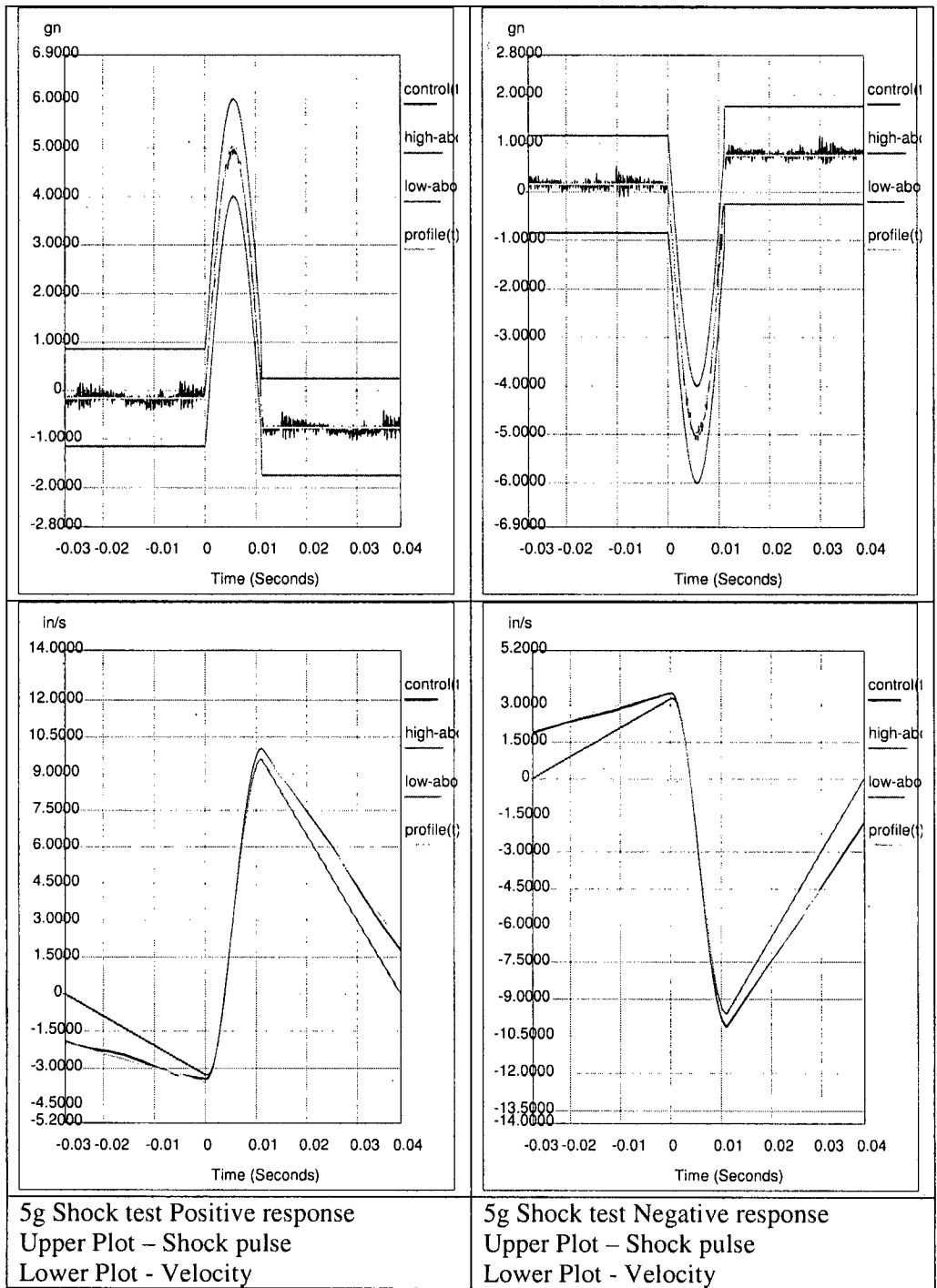


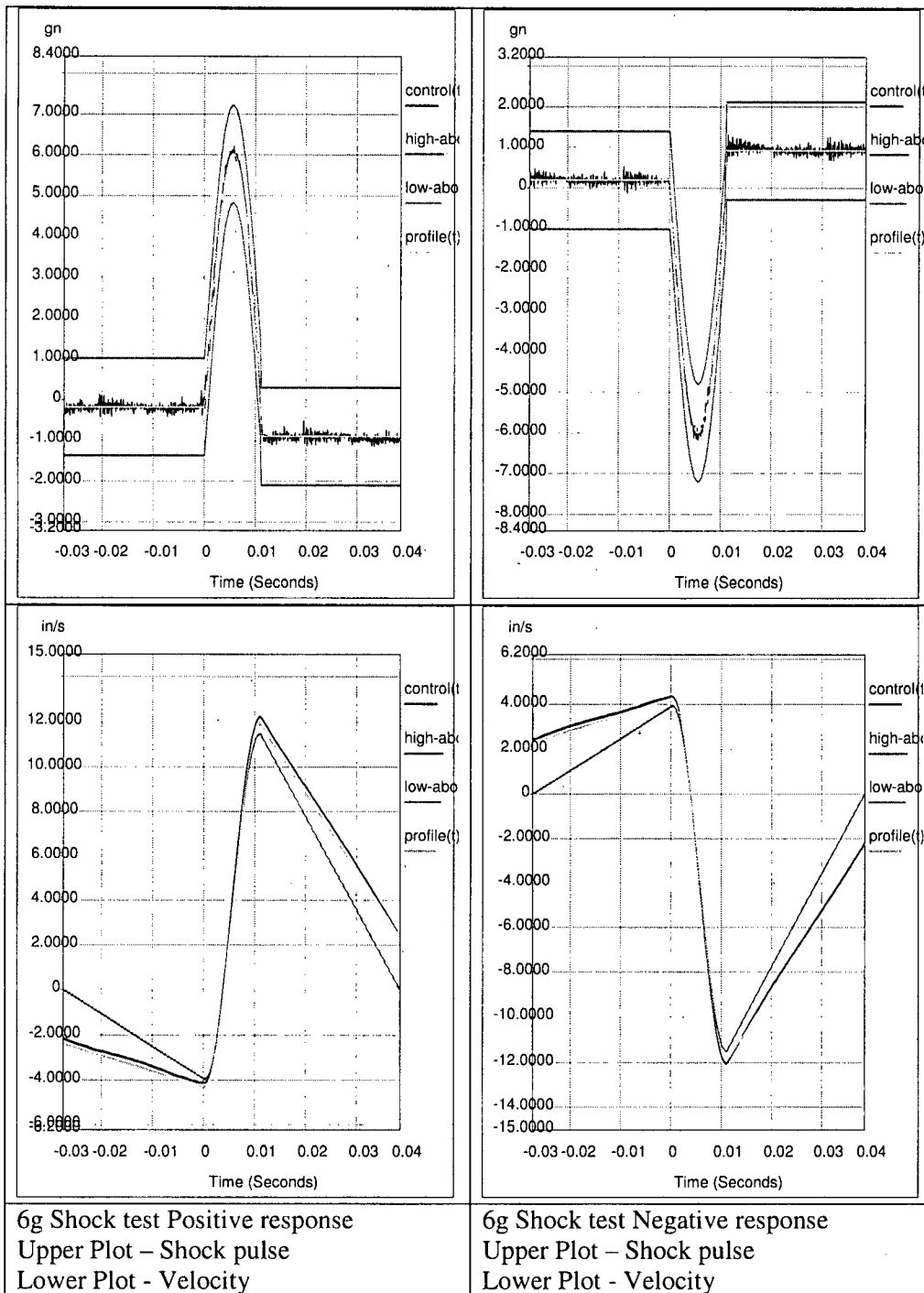




3.2.1.3 Axis 3







4. Report Summary

The samples were subjected to the tests detailed within this report in accordance with all customer instructions and relevant specifications.

No observations were noted during the test programme.

On completion of testing the samples were returned to the customer for further examination.

END OF REPORT



Compression Set testing on V1289-75 compound using Type A Buttons at 260°C and 270°C

Report No: 22550B/C

Materials and Methods.

2 compression set tests were conducted in accordance with ISO 815: 2008 method A. The initial thickness of three compression set buttons was measured for each test. Spacers were selected to give the required 25% compression. The buttons were mounted in the test jig and placed in an ageing oven at the test temperature of 260°C or 270°C dependant on which test was carried out. The jig was removed following an exposure period of two hours. The test pieces were removed from the jig and allowed to cool to standard laboratory temperature (23 +/- 2°C). The thickness of the test pieces was measured 30 minutes following removal from the jig, in accordance with the standard.

All instruments used e.g. digital gauge, temperature sensors were calibrated before use. The digital thickness gauge used to measure the test pieces was calibrated internally. The Instron oven when set at 260 °C gave a reading of 261.3°C on the externally calibrated thermometer and a reading of 261.1 on a separate digital thermometer (internally calibrated).

The readings recorded on setting the oven to a temperature of 270°C were 271.8 and 271.4°C respectively for the externally calibrated and second digital thermometer. (internally calibrated).

The compression set jigs comprise two metal plates of approximate 12mm thickness. For standard tests, at least 24 hours duration, any time lag in heating of the plates would not be an issue and it would be very small in terms of the duration of the test. However the test required in this study was not standard in terms of duration or temperature.

The oven cooled down by no more than 10°C and the temperature recovered to the set-point within 5 minutes of placing the jig in the oven.

The test period of 2 hours was taken from time the oven recovered to the preset temperature.

Test Piece: Cylindrical Type A Button: 29mm +/- 0.5mm diameter and thickness 12.5mm +/- 0.5mm. Oven atmosphere was air



Registered in England No. 2251723

Ceetak Ltd Head Office
Fraser Road, Priory Business Park
Bedford, MK44 3WH
Tel: 01234 832200
Fax: 01234 832299

Web: www.ceetak.com
Email: info@ceetak.com

Ceetak Aberdeen
Block 1, Unit 13
Souterhead Rd
Altens Industrial Estate
Aberdeen, AB12 3LF
Tel: 01224 249690
Fax: 01224 249691



Compression Set test results

The compression set results should be quoted to the nearest whole unit in accordance with the ISO 815:2008 standard.

The ISO standard indicates that no individual test result shall vary from the numerical value of the median compression set by more than 2% or by more than 1/10th of the mean, whichever is higher. If it does, three more test pieces shall be tested and the median value of all results shall be reported, together with the number of test pieces tested.

The compression set results calculated to one decimal place were as follows:

Test : Ref 22550B

Tested to ISO 815-1:2008: Method A

Lab Temp(°C): 23

Compression (%) = 25%

Test duration = 2 hrs

Rest duration = 30 min

Micrometer foot diameter = 4 mm

Sample Identification	Test Temp (°C)	Test Piece 1 (%)	Test Piece 2 (%)	Test Piece 3 (%)	MEDIAN (%)
V1289-75	260	9	8	9	9

Test : Ref 22550C

Tested to ISO 815-1:2008: Method A

Lab Temp(°C): 23

Compression (%) = 25%

Test duration = 2 hrs

Rest duration = 30 min

Micrometer foot diameter = 4 mm

Sample Identification	Test Temp (°C)	Test Piece 1 (%)	Test Piece 2 (%)	Test Piece 3 (%)	MEDIAN (%)
V1289-75	270	12	10	10	10



Registered in England No. 2251723

Ceetak Ltd Head Office
Fraser Road, Priory Business Park
Bedford, MK44 3WH
Tel: 01234 832200
Fax: 01234 832299

Web: www.ceetak.com
Email: info@ceetak.com

Ceetak Aberdeen
Block 1, Unit 13
Souterhead Rd
Altens Industrial Estate
Aberdeen, AB12 3LF
Tel: 01224 249690
Fax: 01224 249691



Test Report No: 22550 B/C

Date: 30th November 09

Signed: Tarsem Sandhu – Application Engineer

Signed: Chris Challis – Quality Manager

CEETAK LTD
Fraser Road
Priory Business Park
Bedford
MK44 3WH

ISO 9001:2000: Certificate No. LRQ 0936916
ISO 14001:2004: Certificate No. GV 16197



Registered in England No. 2251723

Ceetak Ltd Head Office
Fraser Road, Priory Business Park
Bedford, MK44 3WH
Tel: 01234 832200
Fax: 01234 832299

Web: www.ceetak.com
Email: info@ceetak.com

Ceetak Aberdeen
Block 1, Unit 13
Souterhead Rd
Altens Industrial Estate
Aberdeen, AB12 3LF
Tel: 01224 249690
Fax: 01224 249691



SHEFFIELD TESTING LABORATORIES



Date: 29/06/2009

Serial No: 9060433

Page 1 of 1

Test Report

Client: REVISS
6 CHILERN COURT, ASHERIDGE ROAD, CHESHAM,
BUCKINGHAMSHIRE, HP5 2PX

Order No: RSL06797
Test Date: 22/06/09

Material Spec: S355
Sample Description: 6mm Plate

Comments: TENSILES LONGITUDINAL TO GRAIN

Mechanical Properties Tested in accordance with BSEN 10002-1 :2001

All requirements are minimum unless stated.

Test No	ID	Area	Temp °C		Units	0.2% Proof Stress	UTS	Elongation %	Reduction of Area %	Hardness HBW/10/30C0	Izod (ft/lbs) Circular Specimen Striking Energy 120 ft/lbs
		mm ²		Requirements	N/mm ²						
F643		80.37	RT	Results	N/mm ²	393	562	29.5	62*		
F644		79.79	RT		N/mm ²	391	559	29.5	65*		
F645		80.64	RT		N/mm ²	396	561	31.0	64*		

Remarks: *Reduction of Area values are approximate

Authorised Signatory

L Mangham
Test House Manager

END OF RESULTS

This certificate is issued in accordance with the laboratory accreditation requirements of the United Kingdom Accreditation Service. It provides traceability of measurement to recognised national standards, and to units of measurement realised at the National Physical Laboratory or other recognised national standards laboratories. If, upon reproduction, only part of this report is copied, STL will not bear any responsibility for content, purport and conclusions of that reproduction. This report has legal value only when printed on STL paper and furnished with an authorised signature. Digital versions of this report have no legal value. The Terms & Conditions of STL (to be found at www.sheffieldtesting.com) are applicable on all services provided by STL.

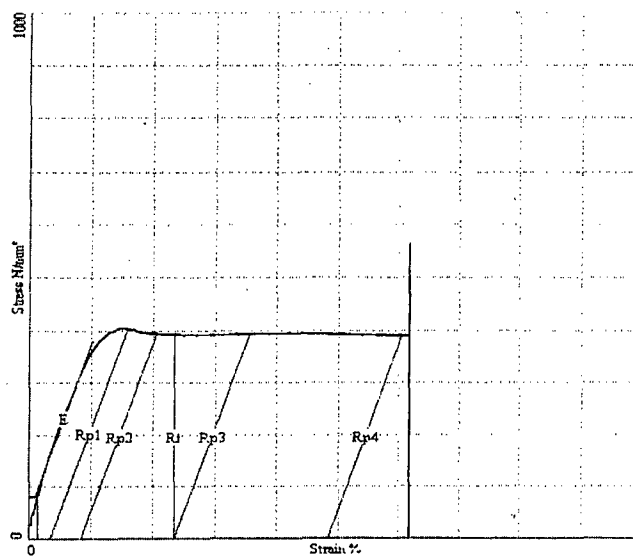
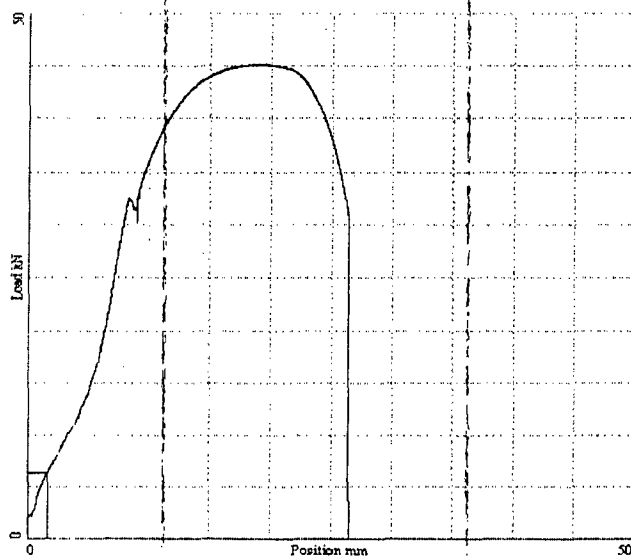


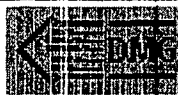
SHEFFIELD TESTING LABORATORIES MATERIAL TESTING SYSTEM

Page: 1

Monday, June 22, 2009 12:53:44

Test Reference.....	5024
Batch Reference #1.....	9060433
Batch Reference #2.....	F643
Specification Id.....	Flat Tensile
Description.....	Flat Tensile
Test Type.....	Tensile
Test Standard.....	BS EN 10 002-1
Date.....	22/06/2009
Time.....	12:48:48
Machine Operator.....	Ben
Cross-Sectional Area.....	80.37 mm ²
Thickness.....	6.44 mm
Width.....	12.48 mm
Specimen Geometry.....	Solid Rectangular Bar
Specimen Gauge Length.....	50 mm
Parallel Length.....	75 mm
Extensometer Gauge Length.....	25 mm
Maximum Load.....	45.18 kN
Ultimate Tensile Strength.....	562.141 N/mm ² (45.18 kN)
Fracture Strength.....	85.6028 N/mm ² (6.88 kN)
Young's Modulus.....	162.5 kN/mm ²
Rt (C.5%).....	392.926 N/mm ² (31.58 kN)
Rp1 (0.1%).....	402.826 N/mm ² (32.3756 kN)
Rp2 (0.2%).....	393.314 N/mm ² (31.6111 kN)
Rp3 (0.5%).....	393.424 N/mm ² (31.62 kN)
Rp4 (1%).....	390.489 N/mm ² (31.3840 kN)
Temperature.....	Ambient
% Elongation.....	29.4
% Reduction in Area.....	100
Load Device.....	Load1
Load Serial No.....	.
Extr Device.....	Extrl
Extr Serial No.....	.



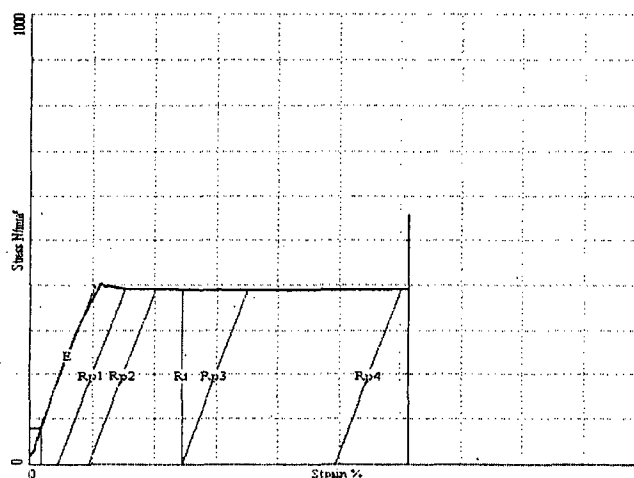
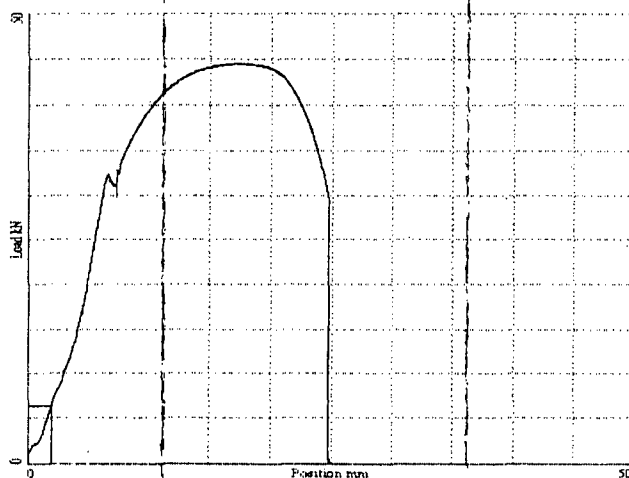


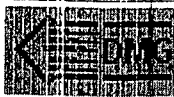
SHEFFIELD TESTING LABORATORIES MATERIAL TESTING SYSTEM

Page: 1

Monday, June 22, 2009 13:06:56

Test Reference.....	5025
Batch Reference #1.....	9060433
Batch Reference #2.....	F644
Specification Id.....	Flat Tensile
Description.....	Flat Tensile
Test Type.....	Tensile
Test Standard.....	BS EN 10 002-1
Date.....	22/06/2009
Time.....	13:00:53
Machine Operator.....	Ben
Cross-Sectional Area.....	79.79 mm ²
Thickness.....	6.44 mm
Width.....	12.39 mm
Specimen Geometry.....	Solid Rectangular Bar
Specimen Gauge Length.....	50 mm
Parallel Length.....	75 mm
Extensometer Gauge Length.....	25 mm
Maximum Load.....	44.56 kN
Ultimate Tensile Strength.....	558.454 N/mm ² (44.56 kN)
Fracture Strength.....	7.01828 N/mm ² (0.56 kN)
Young's Modulus.....	183.1 kN/mm ²
Rt (0.5%).....	390.444 N/mm ² (31.1541 kN)
Rp1 (0.1%).....	392.773 N/mm ² (31.34 kN)
Rp2 (0.2%).....	391.269 N/mm ² (31.22 kN)
Rp3 (0.5%).....	389.881 N/mm ² (31.1092 kN)
Rp4 (1%).....	391.362 N/mm ² (31.2274 kN)
Reh.....	405.055 N/mm ² (32.32 kN)
Rel.....	393.775 N/mm ² (31.42 kN)
Temperature.....	Ambient
% Elongation.....	29.4
% Reduction in Area.....	64.96
Load Device.....	Load1
Load Serial No.....	.
Extr Device.....	Extr1
Extr Serial No.....	.



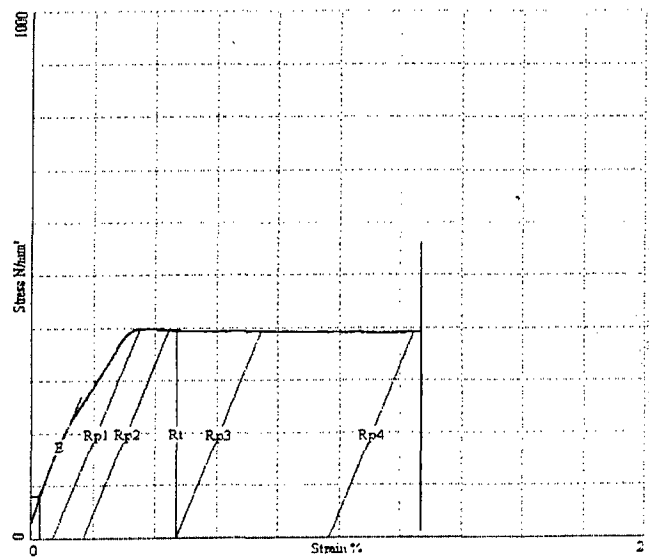
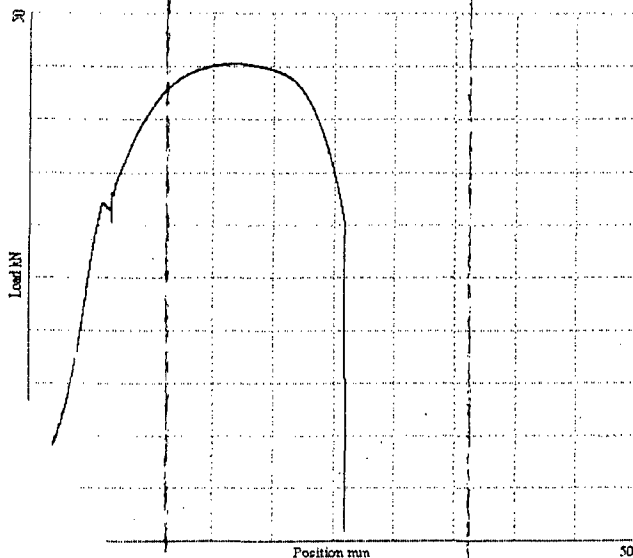


SHEFFIELD TESTING LABORATORIES MATERIAL TESTING SYSTEM

Page: 1

Monday, June 22, 2009 13:16:38

Test Reference.....	5026
Batch Reference #1.....	9060433
Batch Reference #2.....	F645
Specification Id.....	Flat Tensile
Description.....	Flat Tensile
Test Type.....	Tensile
Test Standard.....	BS EN 10 002-1
Date.....	22/06/2009
Time.....	13:10:09
Machine Operator.....	Ben
Cross-Sectional Area.....	80.69 mm ²
Thickness.....	6.44 mm
Width.....	12.53 mm
Specimen Geometry.....	Solid Rectangular Bar
Specimen Gauge Length.....	50 mm
Parallel Length.....	75 mm
Extensometer Gauge Length.....	25 mm
Maximum Load.....	45.28 kN
Ultimate Tensile Strength.....	561.137 N/mm ² (45.28 kN)
Fracture Strength.....	20.5717 N/mm ² (1.66 kN)
Young's Modulus.....	142 kN/mm ²
Rt(0.5%).....	395.324 N/mm ² (31.9 kN)
Rp1(0.1%).....	397.555 N/mm ² (32.08 kN)
Rp2(0.2%).....	395.587 N/mm ² (31.9211 kN)
Rp3(0.5%).....	392.974 N/mm ² (31.7104 kN)
Rp4(1%).....	392.102 N/mm ² (31.64 kN)
Temperature.....	Ambient
% Elongation.....	30.8
% Reduction in Area.....	63.79
Load Device.....	Load1
Load Serial No.....	.
Extr Device.....	Extr1
Extr Serial No.....	.



**Test Report**

Client: REVISS
6 CHILTERN COURT, ASHERIDGE ROAD, CHESHAM,
BUCKINGHAMSHIRE, HP5 2PX

Order No: RSL06797

Test Date: Click here to enter a date.

Material Spec: -

Sample Description: Drain Tube Weld

Mechanical Properties Tested in accordance with MTP 2

All requirements are minimum unless stated.

Test No	ID	Stress Area	Units	Temp °C		Stress at 0.2% Permanent Strain	Max Load	Elongation after Fracture (mm)	Hardness
		-			Requirements	-	-	-	-
F652	-	-	KN	RT	Results	-	50.76	-	-
F653	-	-	KN	RT		-	50.90	-	-
F654	-	-	KN	RT		-	45.06	-	-

Remarks: F652 - Fracture occurred in the weld
F653 - Fracture occurred in the tube section
F654 - Fracture occurred in the weld

Authorised Signatory

L Mangham
Test House Manager

END OF RESULTS

This certificate is issued in accordance with the laboratory accreditation requirements of the United Kingdom Accreditation Service. It provides traceability of measurement to recognised national standards, and to units of measurement realised at the National Physical Laboratory or other recognised national standards laboratories. If, upon reproduction, only part of this report is copied, STL will not bear any responsibility for content, purport and conclusions of that reproduction. This report has legal value only when printed on STL paper and furnished with an authorised signature. Digital versions of this report have no legal value. The Terms & Conditions of STL (to be found at www.sheffieldtesting.com) are applicable on all services provided by STL.

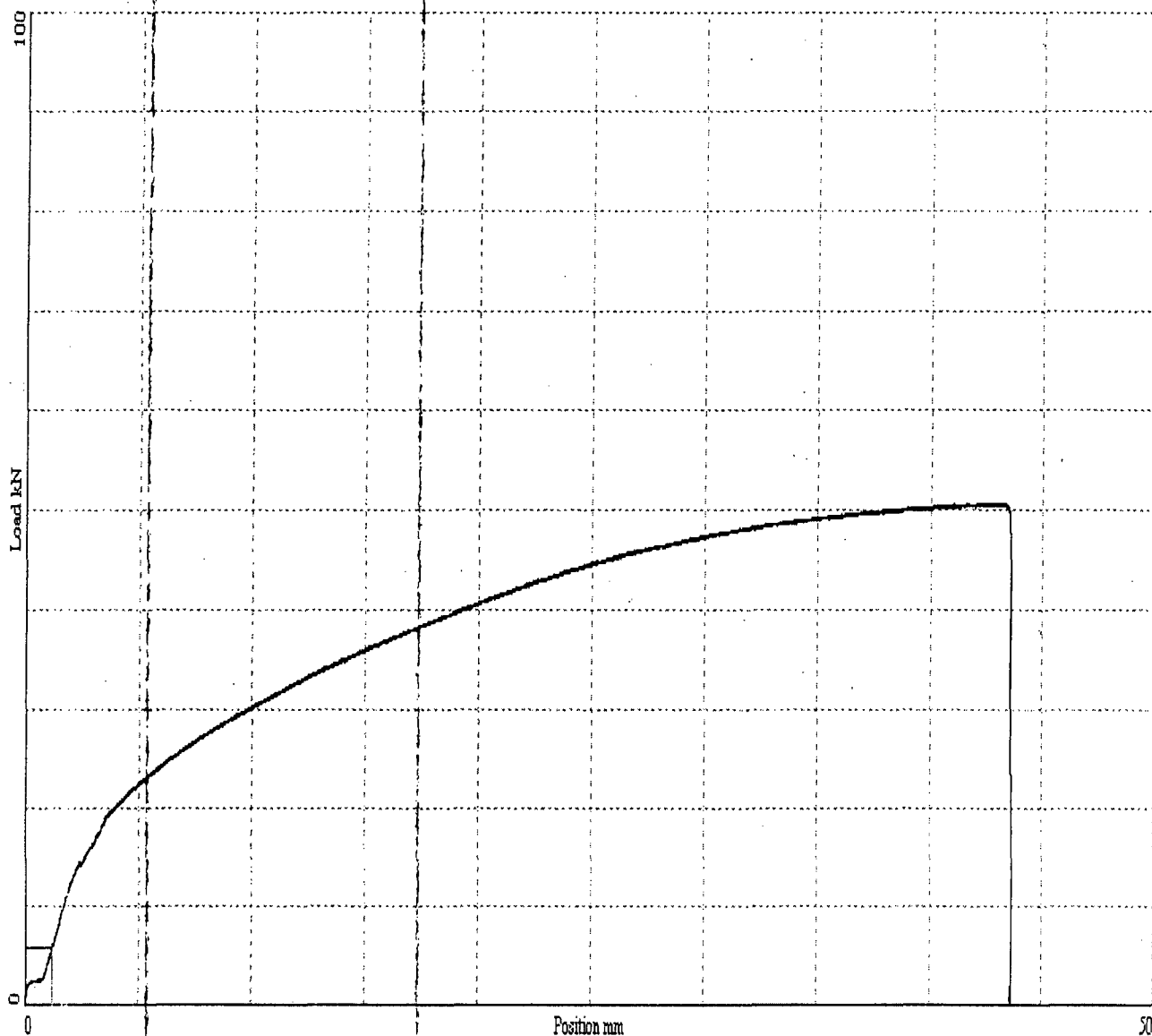


SHEFFIELD TESTING LABORATORIES MATERIAL TESTING SYSTEM

Page: 1

Monday, June 22, 2009 13:49:17

Test Reference.....	: 5027
Batch Reference #1.....	: 9060436
Batch Reference #2.....	: F652
Specification Id.....	: PULL TEST
Test Type.....	: Tensile
Test Standard.....	: BS EN 10 002-1
Batch Reference #3.....	: 1
Date.....	: 22/06/2009
Time.....	: 13:33:50
Machine Operator.....	: Ben
Specimen Geometry.....	: [None]
Maximum Load.....	: 50.76 kN
Temperature.....	: Ambient
Load Device.....	: Load1
Load Serial No.....	: .
Extr Device.....	: Extr1
Extr Serial No.....	: .



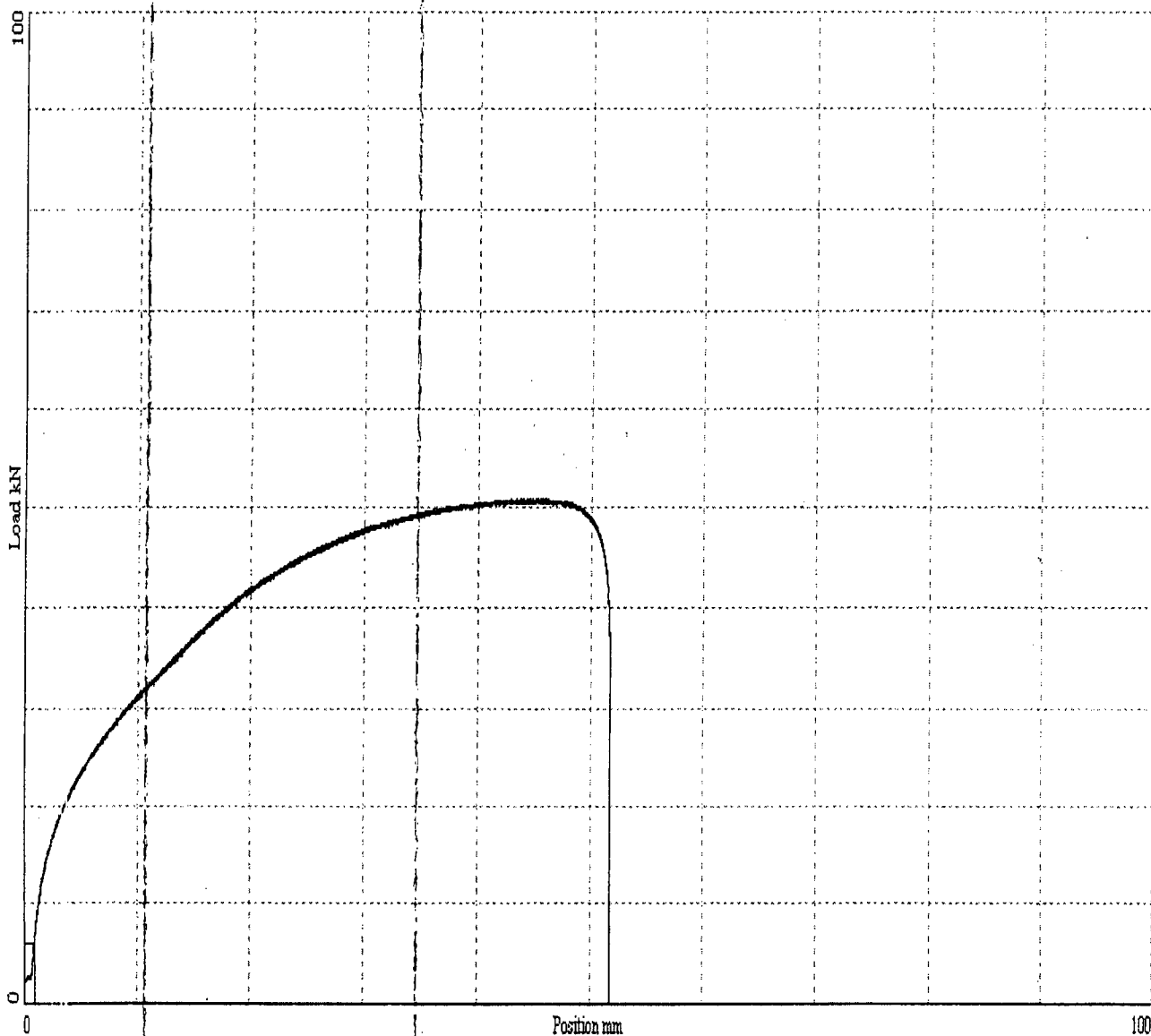


SHEFFIELD TESTING LABORATORIES MATERIAL TESTING SYSTEM

Page: 1

Monday, June 22, 2009 14:19:41

Test Reference.....:	5028
Batch Reference #1.....:	9060436
Batch Reference #2.....:	F653
Specification Id.....:	PULL TEST
Test Type.....:	Tensile
Test Standard.....:	BS EN 10 002-1
Batch Reference #3.....:	2
Date.....:	22/06/2009
Time.....:	13:51:40
Machine Operator.....:	Ben
Specimen Geometry.....:	[None]
Maximum Load.....:	50.9 kN
Temperature.....:	Ambient
Load Device.....:	Load1
Load Serial No.....:	.
Extr Device.....:	Extr1
Extr Serial No.....:	.



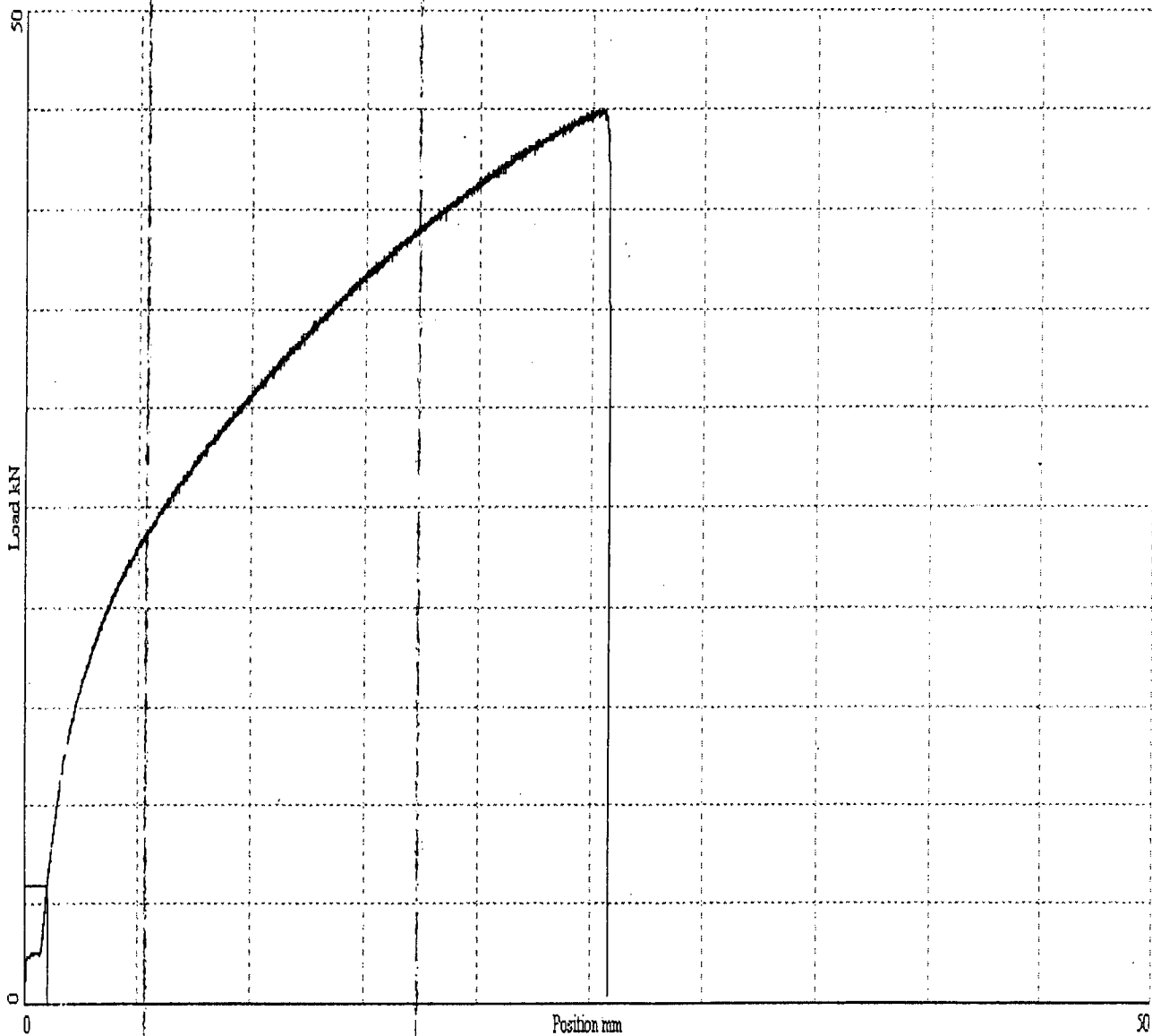


SHEFFIELD TESTING LABORATORIES MATERIAL TESTING SYSTEM

Page: 1

Monday, June 22, 2009 14:39:12

Test Reference.....:	5029
Batch Reference #1.....:	9060436
Batch Reference #2.....:	F654
Specification Id.....:	PULL TEST
Test Type.....:	Tensile
Test Standard.....:	BS EN 10 002-1
Batch Reference #3.....:	3
Date.....:	22/06/2009
Time.....:	14:26:27
Machine Operator.....:	Ben
Specimen Geometry.....:	[None]
Maximum Load.....:	45.06 kN
Temperature.....:	Ambient
Load Device.....:	Load1
Load Serial No.....:	.
Extr Device.....:	Extrl
Extr Serial No.....:	.



**Test Report**

Client: REVISS SERVICES LTD
6 CHILTERN COURT, ASHERIDGE ROAD, CHESHAM,
BUCKINGHAMSHIRE, HP5 2PX

Order No:
Test Date: 02/07/09

Material Spec:
Sample Description: M24 HT Studs

Marks :

Mechanical Properties Tested in accordance with BSEN 10002-1 :2001

All requirements are minimum unless stated.

Test No	ID	Area	Temp °C		Units	0.2% Proof Stress	UTS	Elongation %	Reduction of Area %	Hardness HBW/10/3000	Izod (ft/lbs) Circular Specimen Striking Energy 120 ft/lbs
		mm ²		Requirements	N/mm ²						
F778	-	19.64	RT	Results	N/mm ²	922	995	10.0	61		
F778A		19.64	RT		N/mm ²	900	963	11.0	62		

Remarks:

Authorised Signatory

L Mangham
Test House Manager

END OF RESULTS

This certificate is issued in accordance with the laboratory accreditation requirements of the United Kingdom Accreditation Service. It provides traceability of measurement to recognised national standards, and to units of measurement realised at the National Physical Laboratory or other recognised national standards laboratories. If, upon reproduction, only part of this report is copied, STL will not bear any responsibility for content, purport and conclusions of that reproduction. This report has legal value only when printed on STL paper and furnished with an authorised signature. Digital versions of this report have no legal value. The Terms & Conditions of STL (to be found at www.sheffieldtesting.com) are applicable on all services provided by STL.

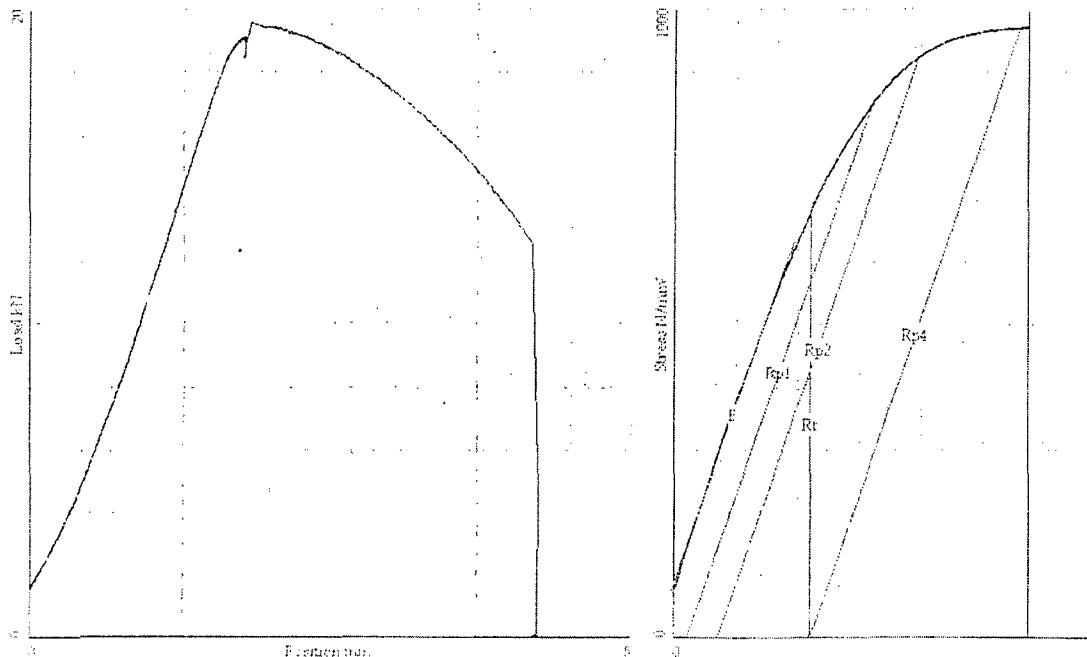


SHEFFIELD TESTING LABORATORIES MATERIAL TESTING SYSTEM

Page: 1

Thursday, July 2, 2009 09:16:36

Reference No.....	4196
Test Serial No.....	9060549
Test No.....	F778
Specification Id.....	BSEN 5.00
Description.....	5.00 Tensile
Test Type.....	Tensile
Test Standard.....	BS EN 10 002-1
Date.....	02/07/2009
Time.....	09:10:12
Machine Operator.....	tom
Cross-Sectional Area.....	19.64 mm ²
Specimen Geometry.....	Solid Circular Bar
Specimen Gauge Length.....	25 mm
Parallel Length.....	30 mm
Extensometer Gauge Length.....	12.5 mm
Maximum Load.....	19.54 kN
Ultimate Tensile Strength.....	994.993 N/mm ² (19.5416 kN)
Fracture Strength.....	279.192 N/mm ² (5.48333 kN)
Young's Modulus.....	141.9 kN/mm ²
Rt(0.5%).....	679.785 N/mm ² (13.3509 kN)
Rp1(0.1%).....	851.486 N/mm ² (16.7231 kN)
Rp2(0.2%).....	922.441 N/mm ² (18.1167 kN)
Rp4(0.5%).....	969.019 N/mm ² (19.0315 kN)
Temperature.....	Ambient
% Elongation.....	10
% Reduction in Area.....	61.32
Load Device.....	Load1
Load Serial No.....	.
Extr Device.....	Extr1
Extr Serial No.....	.



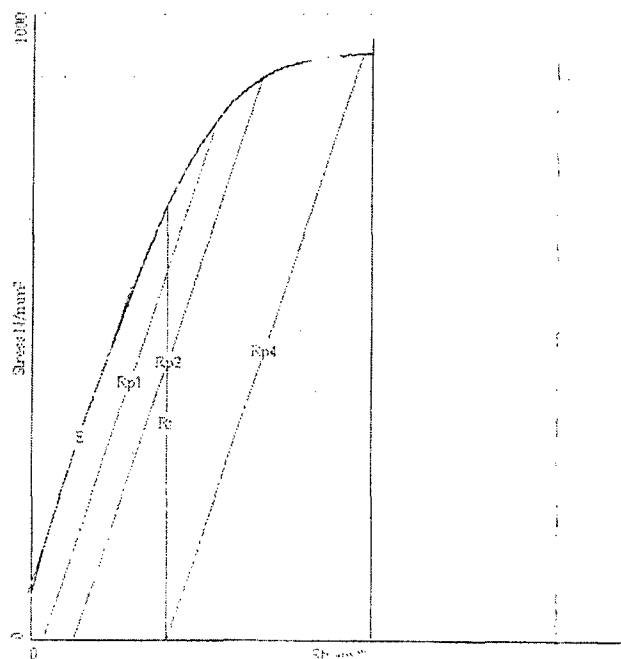
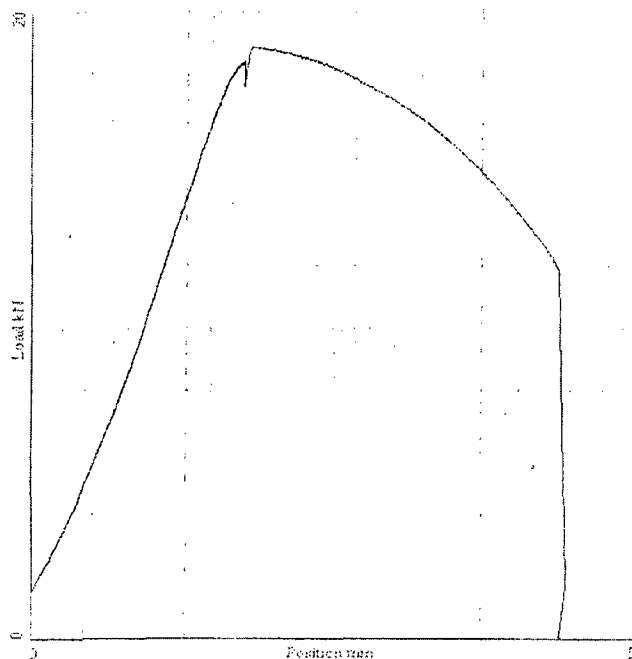


SHEFFIELD TESTING LABORATORIES MATERIAL TESTING SYSTEM

Page: 1

Thursday, July 2, 2009 09:26:45

Reference No.....	4197
Test Serial No.....	9060549
Test No.....	F778A
Specification Id.....	BSEN 5.00
Description.....	5.00 Tensile
Test Type.....	Tensile
Test Standard.....	BS EN 10 002-1
Date.....	02/07/2009
Time.....	09:19:37
Machine Operator.....	tom
Cross-Sectional Area.....	19.64 mm ²
Specimen Geometry.....	Solid Circular Bar
Specimen Gauge Length.....	25 mm
Parallel Length.....	30 mm
Extensometer Gauge Length.....	12.5 mm
Maximum Load.....	18.91 kN
Ultimate Tensile Strength.....	962.746 N/mm ² (18.9083 kN)
Fracture Strength.....	90.8010 N/mm ² (1.78333 kN)
Young's Modulus.....	148.2 kN/mm ²
Rt(0.5%).....	696.706 N/mm ² (13.6833 kN)
Rp1(0.1%).....	834.181 N/mm ² (16.3833 kN)
Rp2(0.2%).....	899.949 N/mm ² (17.675 kN)
Rp4(0.5%).....	937.712 N/mm ² (18.4166 kN)
Temperature.....	Ambient
% Elongation.....	11
% Reduction in Area.....	62.06
Load Device.....	Load1
Load Serial No.....	.
Extr Device.....	Extrl
Extr Serial No.....	.





Intertek MSG
Inorganic & X-Ray Analysis

E224

Tel: 01642 435749

Test Report: No. INORG/W000925RL001

Determination of Cobalt and Nickel contents on filter papers by ICP-OES.

Date: 07/01/2009

For

Sammy Cheung

Reviss Services (UK) Ltd

Tel.:

Prepared by:

Peter Duck

Inorganic Analysis Laboratory



0967

Intertek MSG

The Wilton Centre, Redcar, TS10 4RF, UK

Tel: +44 (0)1642 435788

Fax: +44 (0)1642 435777

Work reported in this document, unless otherwise stated, was carried out under the terms of the UKAS accreditation for UKAS Laboratory No 0967. Opinions and interpretations contained herein are outside the scope of UKAS accreditation.

TEST REPORT

Determination of Cobalt and Nickel contents on filter papers by ICP-OES.

Report Number PS/W000339RL001
Chit Number 11111
Receipt Date 18/12/2008
Lab Book Reference P.G DUCK 20/114
File Reference Location E224
Number of Samples 3
Description of Work Required Co Ni by ICP-OES
Method Reference SOP/IA/2

Samples Submitted

Sample Identifier	Sample Description	Customer Identifier
PS/W000339-1	Filter Paper	Control
PS/W000339-2	Filter Paper	Red Assembly went thro' 106 µm
PS/W000339-3	Filter Paper	Black Assembly went thro' 106 µm

Table of Results

SAMPLE ID	µg Co	µg Ni
Control Filter	0.3	1.3
RED Assembly went thro' 106 µm sieve	106	23
BLACK Assembly went thro' 106 µm sieve	46	25

Statement of Uncertainty

Instrumental uncertainty on above results is 5% relative or better.

Report Authorisation

SCIENTIST'S NAME

Signature of Scientist

P. G DUCK

P. Geoffrey Duck

Date

07/01/2009

Work reported in this document, unless otherwise stated, was carried out under the terms of the UKAS accreditation for UKAS Laboratory No 0967. Opinions and interpretations contained herein are outside the scope of UKAS accreditation.

Revis Services (UK) Limited
6 Chilton Court
Asheridge Road
Chesham
Buckinghamshire
HP5 2PX
Client Contact: David Rogers

Report No. L91805 Issue 1

Order No. RSL06647

Date Tested: 03.03.2009

Date Reported: 06.03.2009

Description: R7021 Transport Package - Jacket and Drain Tube Weld Strength Assessment

1.0 Introduction:

Caparo Testing Technology were requested to conduct a prescribed program (Work specification WS7021/11) of tests to enable the strength of the jacket and drain tube welds to be quantified and the mode of the drain tube's failure identified.

2.0 Findings:

2.1 Jacket Assessment:

A 35mm section of the upper ring with the inner and outer 6mm cladding still attached was supplied for weld and strength assessment.

2.1.1 Macro examination (in-house technical laboratory procedure LTP/101)

Outer cladding Section (refer to figure 1): A smooth weld profile exhibiting a depth of 3.5mm of fused penetration. A lack of side wall fusion measuring 0.8mm was present at the root position due to misalignment of the weld in respect to the joint centreline.

Inner cladding Section (refer to figure 2): A smooth weld profile exhibiting a depth of 4.0mm of fused penetration. A lack of side wall fusion measuring 1.9mm was present at the root position due to misalignment of the weld in respect to the joint centreline.

2.1.2 Tensile Strength

Tensile Test – BS EN 10002-1:2001/BS EN 895:1995			
Position	Length of Weld Section (mm)	UTL (kN)	Comments
Outer Clad Section	32.24	22.19	Position of fracture: T/V Weld Metal (¹ see note below)
Inner Clad Section	32.30	21.48	Position of fracture: T/V Weld Metal (¹ see note below)
¹ Note: Yawning of joint prior to fracture due to partial penetration characteristics of the joint under test Test Equipment S/No 29193 Calibrated in accordance with BS EN ISO 7500-1 Class 1 by a UKAS accredited calibration laboratory Cert No. 23071 and 23072 refers			

Revisss Services (UK) Limited

Report No. L91805 Issue 1

2.2 Drain Tube Assessment

2.2.1 Fractured Drain Tube Sample

An initial examination of the supplied sample showed complete transverse fracture of the fillet weld which joined the tube to the assembly section. The tube and its associated assembly were sectioned longitudinally. The internal counter bore revealed circumferential witness marks approximately 6.5mm from the end face (refer to figure 3). These marks appeared to coincide with the end of the tube, indicating possible partial insertion of the tube at least to this depth (refer to figure 4). Note: the end of the tube section had been sealed by welding by a client after failure prior to supplying the items for examination).

A macroscopic examination of the weld deposited, from the fractured ligaments, showed the fillet weld to exhibit a relatively smooth weld profile, free from undercutting, with complete sidewall fusion and penetration (refer to figure 3). No obvious injurious weld related volumetric defects were apparent within the section examined.

Weld dimensions:

Leg Lengths = 2.5/3.4mm with a throat thickness of 1.9mm. The depth of penetration into the tube = 1.1mm

An examination of the fractured surface was performed using a Cambridge Stereo-scan Scanning Electron Microscope. The following observations were made: Evidence of Laminar tearing with the direction of the fracture opening being orientated away from the bore surface (refer to figure 5). The general surface showed exhibited micro ductile dimpling fractures, the orientation of which was again away from the bore surface (refer to figure 6). The general fracture morphology was typical of a ductile tensile overload.

2.2.2 Fabrication Test Drain Tube Samples

Five fabricated test drain tube samples were submitted for comparative testing, one for macro-examination (sample 1A) and two samples for tensile testing and fracture surface evaluation (sample 1 -105Amp and Sample 2 – 115Amp). An addition two further samples (sample 3 -105Amp and Sample 4 – 115Amp) were supplied for compression testing and subsequent evaluation. It should be noted that the tubes within the compression test pieces supplied were only partially inserted into the assembly blocks (6-7mm of insertion) compared with the samples for supplied tensile testing which were fully inserted.

2.2.2a Sample 1A

A macro weld examination was conducted on a longitudinal section taken through the sample (refer to figure 7). The drain tube was noted to have been fully inserted within the counter-bore. The fillet weld present was noted to exhibited a relatively smooth weld profile, free from undercutting, with complete sidewall fusion and penetration (refer to figure 8 and 9). No obvious injurious weld related volumetric defects were apparent within the section examined.

Weld dimensions:

Position 0°: Leg Lengths = 2.6/4.2mm with a throat thickness of 2.0mm. The depth of penetration into the tube = 1.1mm

Position 180°: Leg Lengths = 2.5/4.0mm with a throat thickness of 1.8mm. The depth of penetration into the tube = 1.1mm

Revisss Services (UK) Limited

Report No. L91805 Issue 1

2.2.3 Tensile Testing - Fabrication Test Drain Tube Samples

Two of the fabricated drain tube samples were subject to axial loading in full section to determine the load to fracture and for subsequent evaluation of the fractured surfaces. In addition a tensile test was performed on the parent tube (in full section) for comparative purposes.

Tensile Test – BS EN 10002-1:2001/BS EN 895:1995		
Sample Ref:	Max Load UTL (kN)	Comments
Sample 1 – 105Amp	50.4	Position of fracture – Weld metal. Note length of tube insertion 14.4mm refer to figure 10
Sample 2 – 115Amp	51.0	Position of fracture – Weld metal. Note length of tube insertion 14.4mm refer to figure 11
Parent Tube	51.6	UTS = 608MPa based upon a CSA of 84.8mm ²
Test Equipment S/No 29193 Calibrated in accordance with BS EN ISO 7500-1 Class 1 by a UKAS accredited calibration laboratory Cert No. 23071 and 23072 refers		

An examination of the fractured surfaces was performed after tensile testing on both of the fabricated samples, using a Cambridge Stereo-scan Scanning Electron Microscope. The following observations were made:

Both fracture surfaces exhibited essential similar morphologies being that of slightly elongated micro ductile dimpling, the orientation of which was from their respective bore surfaces (refer to figures 12-15). The general fracture morphologies were typical of those produced by tensile overloading within ductile materials.

2.2.4 Compression Testing - Fabrication Test Drain Tube Samples

The length of the tube section was reduced to 12mm to minimise the effect of buckling due to the aspect ratio of tube length to diameter during compression testing

Compression Test – In-house laboratory Test Procedure LTP/002		
Sample Ref:	Max Load (kN)	Comments
Sample 3 – 105Amp	125+	Test terminated: Severe deformation of the weld and tube - Weld remained intact
Sample 4 – 115Amp	125+	Test terminated: Severe deformation of the weld and tube - Weld remained intact
Test Equipment S/No 29193 Calibrated in accordance with BS EN ISO 7500-1 Class 1 by a UKAS accredited calibration laboratory Cert No. 23071 and 23072 refers		

After compression testing longitudinal sections were taken through the samples (refer to figure 16 and 17) to evaluation the welds present. In both of the welded samples examined the fillet weld applied had fully penetrated the drain tube walls. As a consequence the welds were heavily deformed but the fused joint remained intact and showing no evidence of fracture/rupture (refer to figures 18 to 21).

Reviss Services (UK) Limited

Report No. L91805 Issue 1

3.0 Summary Remarks

1. The welds attaching the inner and outer 6mm cladding on the upper ring Jacket exhibited partial penetration of their respective joints due to slight misalignment of the weld centreline in respect to the joint line.
2. The failed fracture drain tube sample appeared to exhibit only partial insertion into the counter-bore within the block assembly
3. The tensile strength of the fabricated fillet weld samples was within 2.5% of the strength of the parent tube.
4. The welds present on the fabricated samples were fully inserted into their respective counter-bores. No injurious volumetric weld related defects were apparent within the section examined.
5. The results of the comparative fractographic examination conducted on the fractured drain tube and the fabricated sample test pieces after tensile testing would indicate that the mode of fracture was essentially similar.
6. It was not possible to replicate the failure by compression testing using the supplied test pieces. The welds within these test pieces had fully penetrated the drain tube wall.

Opinions and interpretations expressed herein are outside the scope of our UKAS accreditation.

-----End of Certificate Comments -----

CTT
WITNEY TESTING
RUSSELL OWEN
OPERATIONS MANAGER

Tested By: R.J.Owen

Authorised Signatory:

*This certificate should not be reproduced other than in full without the written permission of Materials Testing Services.
The results quoted refer only to the item(s) tested as sampled by the client unless otherwise stated.*

Report No.	L91805 Issue 1
Customer	Reviss Services (UK) Limited
Description	R7021 Transport Package -Jacket and Drain Tube Weld Strength Assessment

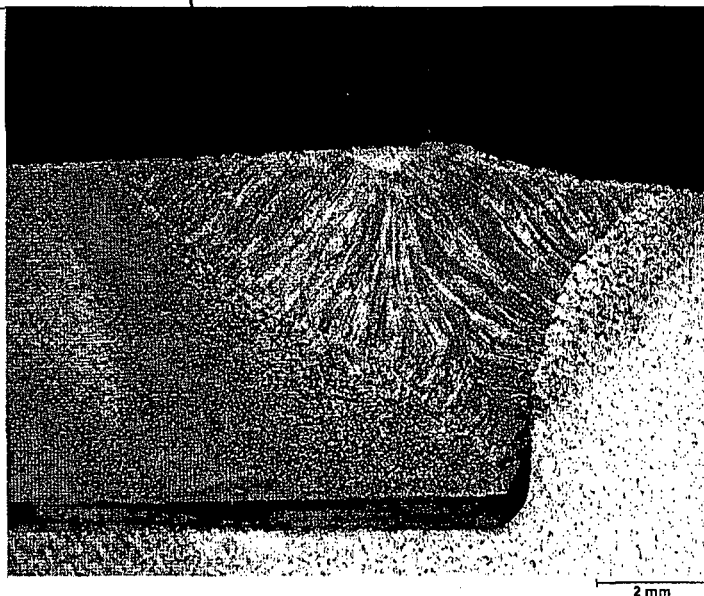


Figure: 1

Magnification: 8.5

Etchant: 10% Nital

Macrosection: Outer Clad Layer Weld

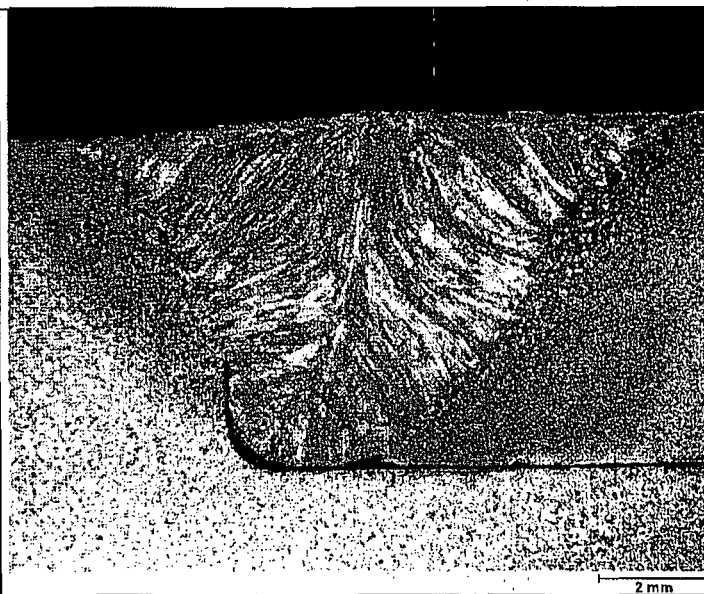


Figure: 2

Magnification: 8.5

Etchant: 10% Nital

Macrosection: Inner Clad Layer Weld

Report No.	L91805 Issue 1
Customer	Reviss Services (UK) Limited
Description	R7021 Transport Package -Jacket and Drain Tube Weld Strength Assessment

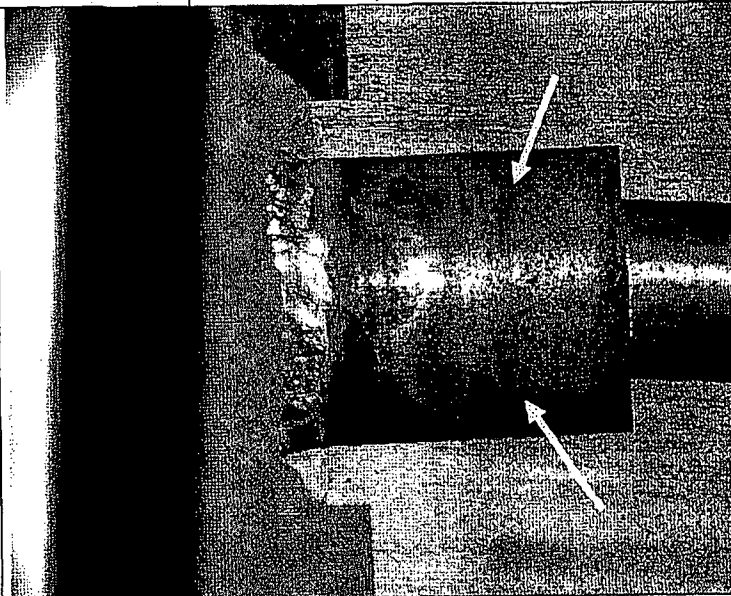


Figure: 3

Magnification: 5

Fracture Drain Tube sample: Showing a section through the fractured Drain tube sample. Note the circumferential witness mark approximately 6.5mm from end of the counter-bore (highlighted)

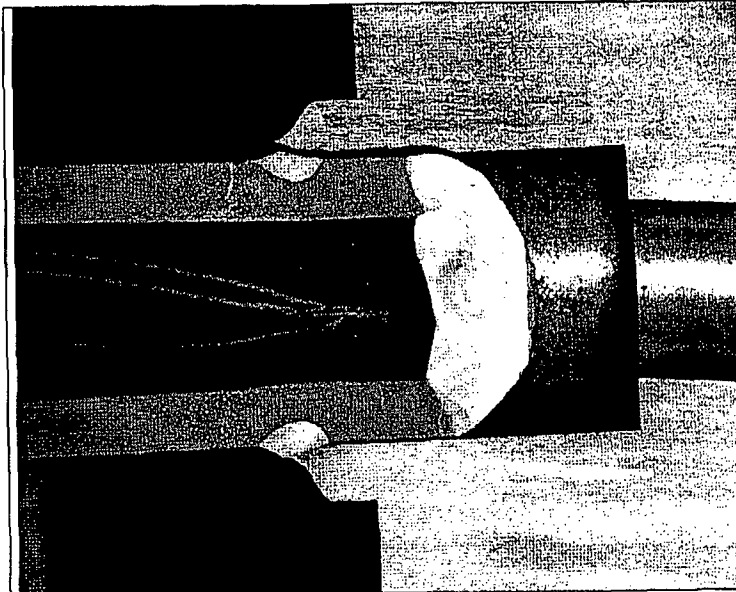


Figure: 4

Magnification: 5

*Sections etched using Marbles
Reagent to reveal the
macrostructure present*

Fracture Drain Tube sample: Showing the drain tube sample section with the associated tube inserted. Note the tube section indicates only partial insertion (coincide with the witness marks – refer to figure 4).

Report No.	L91805 Issue 1
Customer	Reviss Services (UK) Limited
Description	R7021 Transport Package -Jacket and Drain Tube Weld Strength Assessment

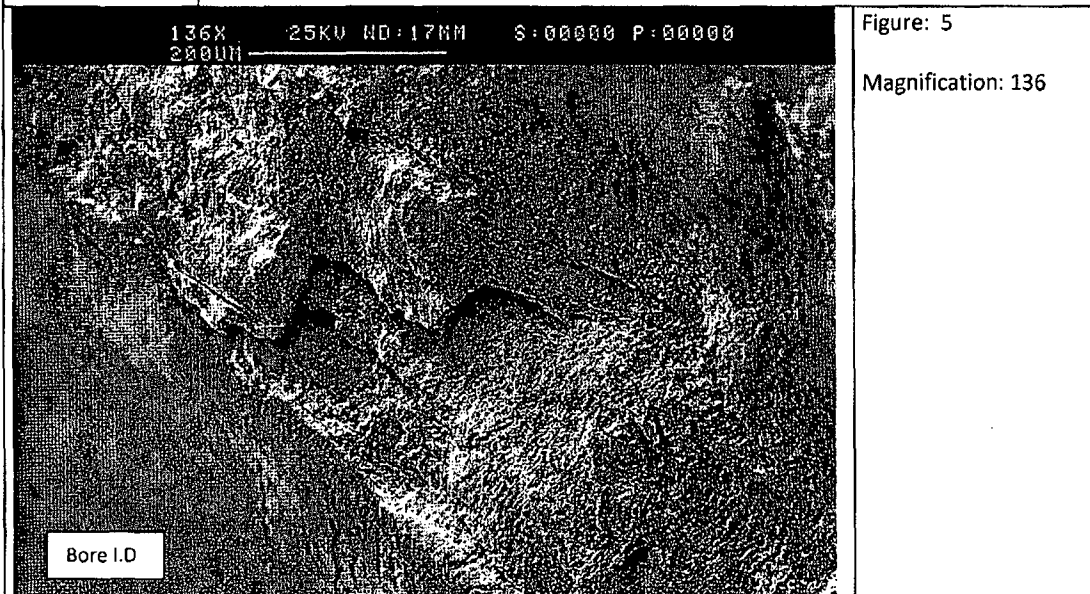


Figure: 5

Magnification: 136

Fracture Drain Tube sample: Showing lamellar tearing of the weld metal the crack growth is indicated

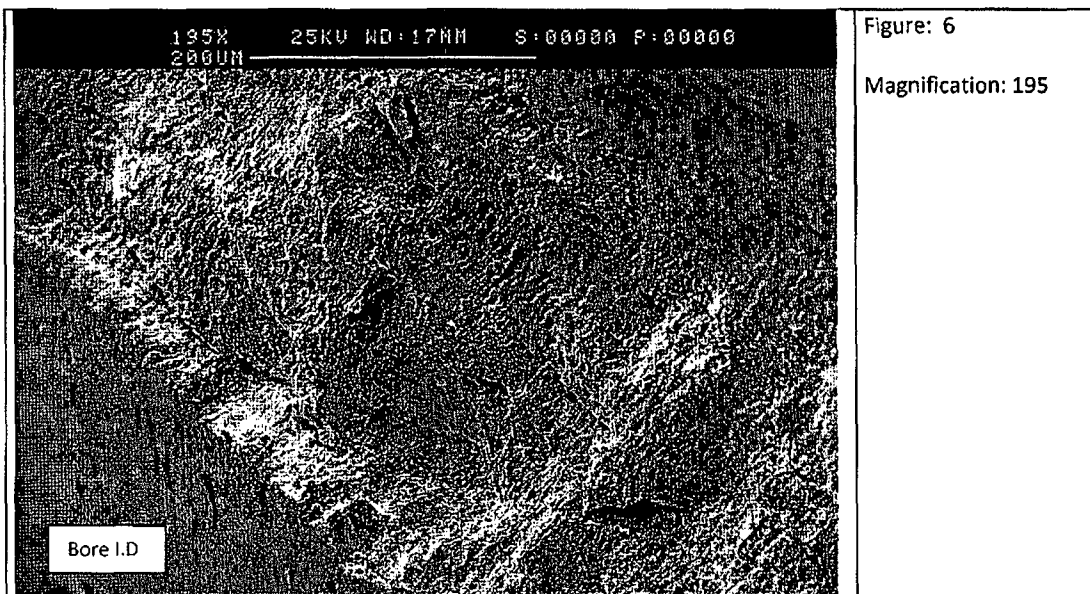


Figure: 6

Magnification: 195

Fracture Drain Tube sample: Showing the generalised ductile dimpling typical of a tensile overload

Report No.	L91805 Issue 1
Customer	Revis Services (UK) Limited
Description	R7021 Transport Package -Jacket and Drain Tube Weld Strength Assessment

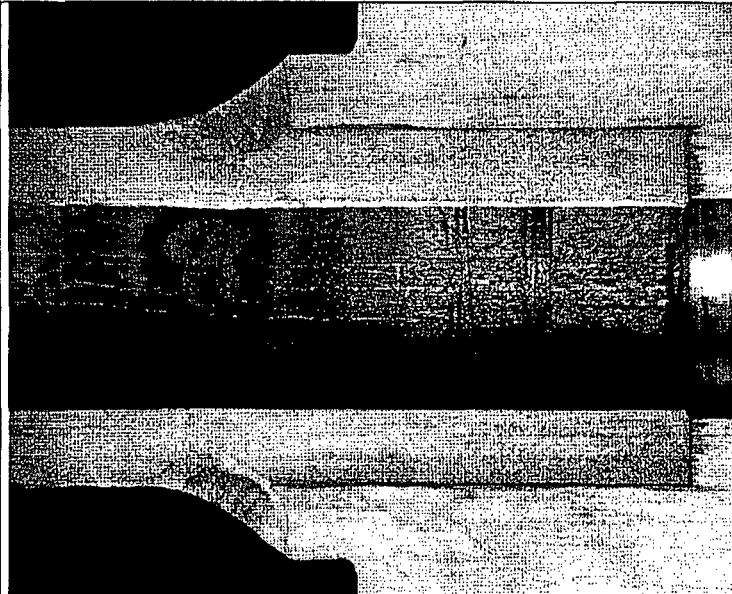


Figure: 7

Magnification: 5

Etch: Marbles Reagent

Fabricated Sample 1A: Showing a general Macrosection taken longitudinally through the sample

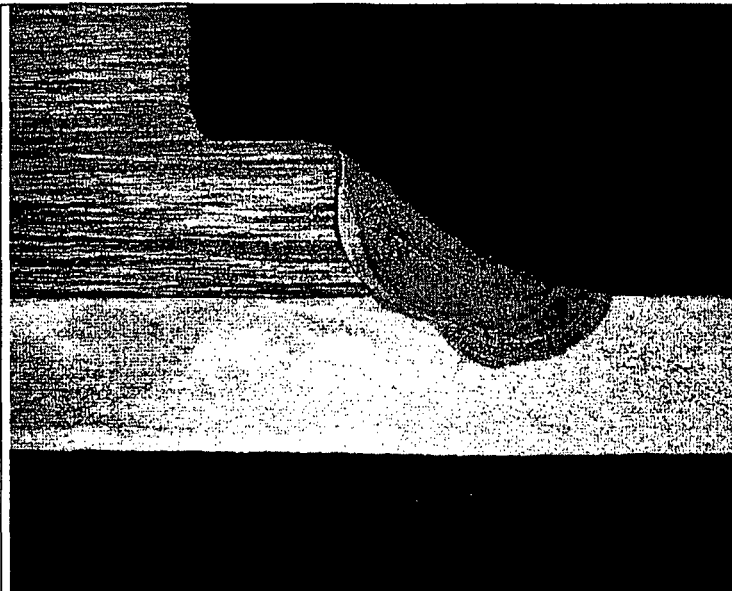
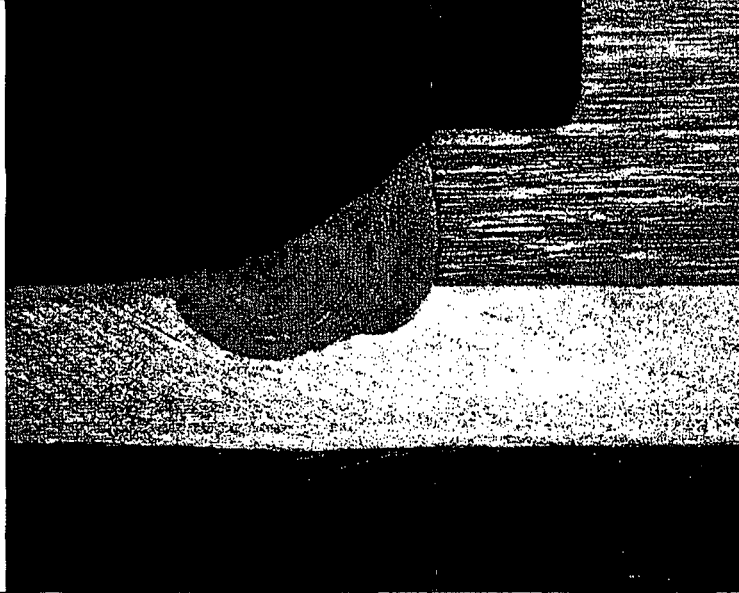


Figure: 8

Magnification: 8

Etch: Marbles Reagent

Fabricated Sample 1A: Showing a view of the weld present (Position 0°)

Report No.	L91805 Issue 1
Customer	Revis Services (UK) Limited
Description	R7021 Transport Package -Jacket and Drain Tube Weld Strength Assessment
<div>  <div> <p>Figure: 9</p> <p>Magnification: 5</p> <p>Etch: Marbles Reagent</p> </div> </div>	
Fabricated Sample 1A: Showing a view of the weld present (Position 180°)	

Report No.	L91805 Issue 1
Customer	Revis Services (UK) Limited
Description	R7021 Transport Package -Jacket and Drain Tube Weld Strength Assessment

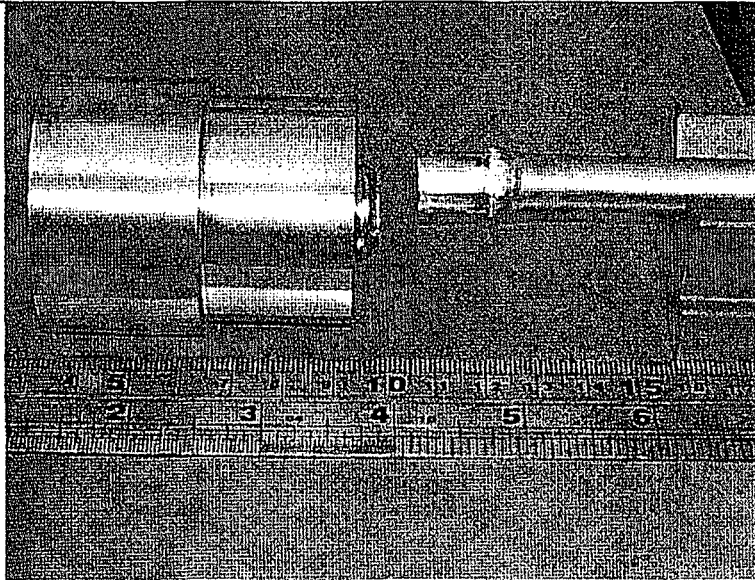


Figure: 10

Fabricated Sample 1 – 105Amp: General view of the sample after tensile testing

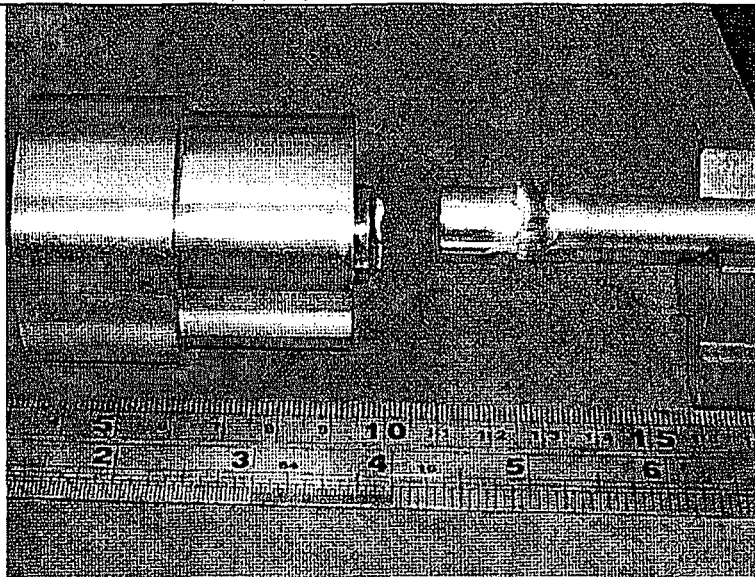


Fig 11

Fabricated Sample 2 – 115 Amp: General view of the sample after tensile testing

Report No.	L91805 Issue 1
Customer	Reviss Services (UK) Limited.
Description	R7021 Transport Package -Jacket and Drain Tube Weld Strength Assessment

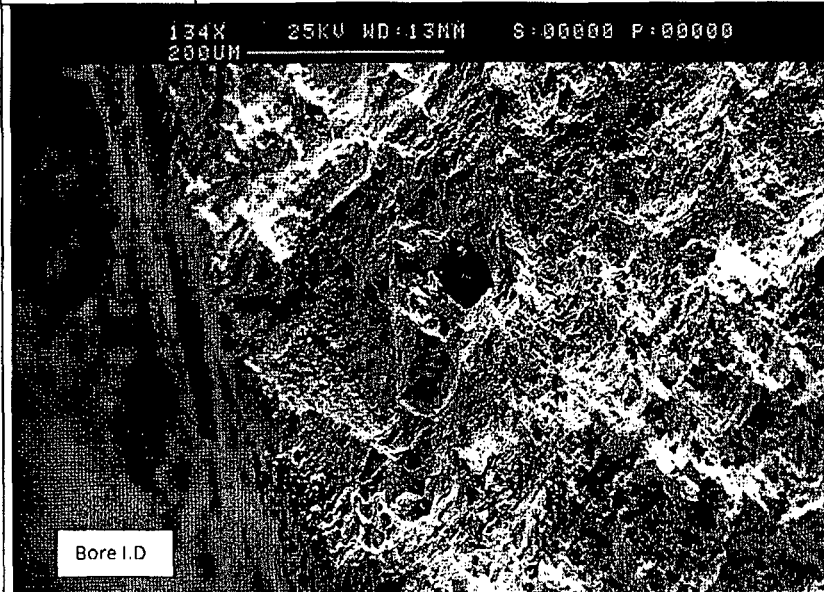


Figure: 12

Magnification: 134

Fabricated Sample 1 – 105Amp: Showing the general orientation of fracture away from the bore I.D
Note: crack growth is indicated

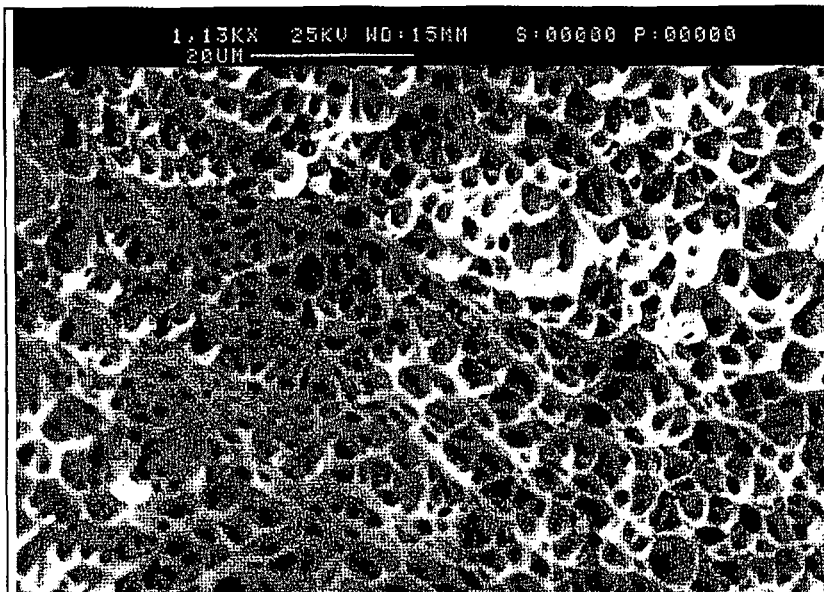
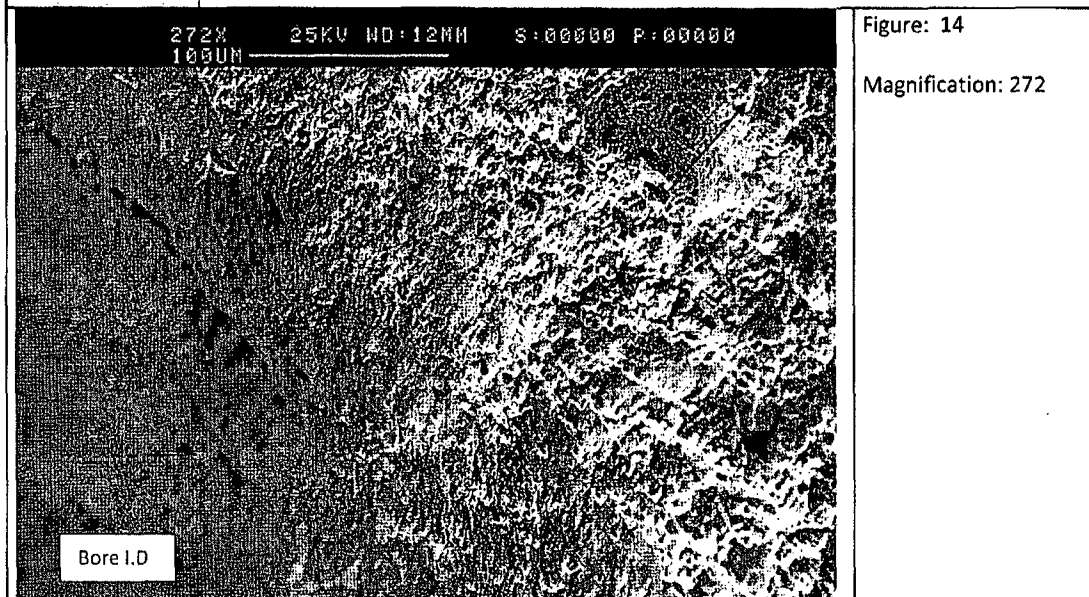


Figure: 13

Magnification: 1130

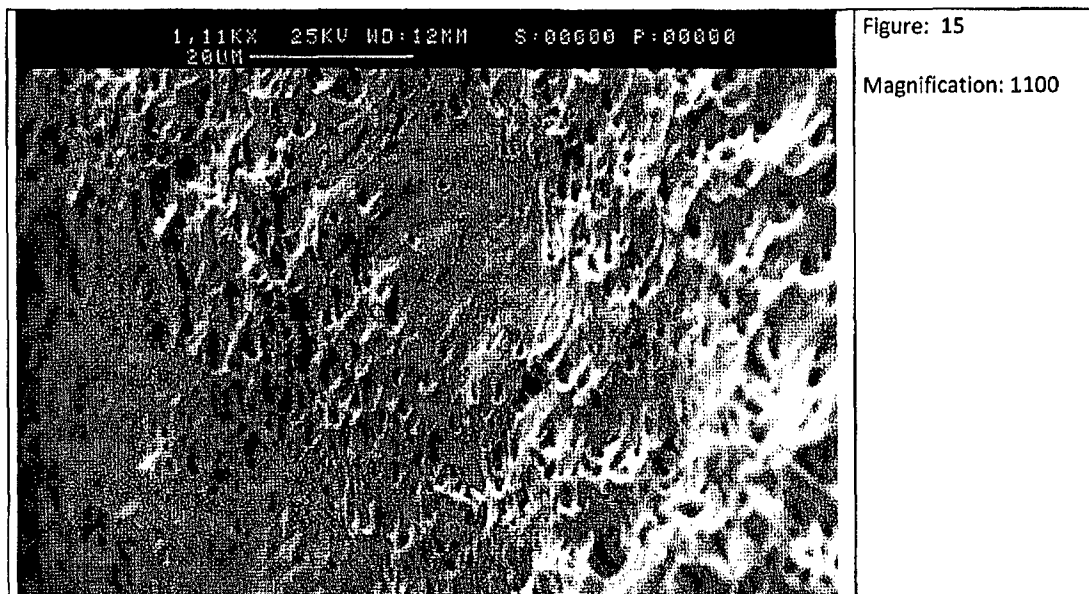
Fabricated Sample 1 – 105Amp: Showing the ductile dimpling typical of a tensile overload

Report No.	L91805 Issue 1
Customer	Reviss Services (UK) Limited
Description	R7021 Transport Package -Jacket and Drain Tube Weld Strength Assessment



Fabricated Sample 2 – 115Amp: Showing the general orientation of fracture away from the bore I.D

Note: crack growth is indicated



Fabricated Sample 2 – 115Amp: Showing the ductile dimpling typical of a tensile overload

Report No.	L91805 Issue 1
Customer	Revis Services (UK) Limited
Description	R7021 Transport Package -Jacket and Drain Tube Weld Strength Assessment



Figure: 16

Magnification: 5

Etch: Marbles Reagent

Fabricated 'compression' Sample 3: 105Amp -After Compression Test

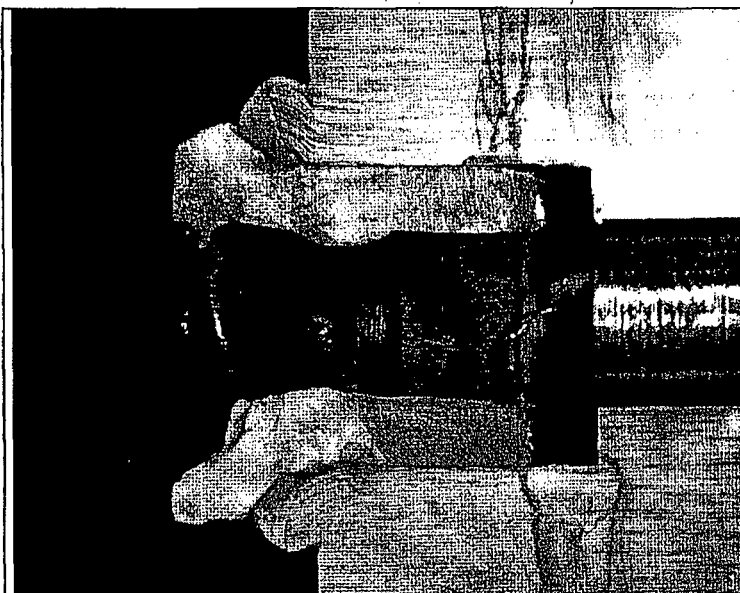


Figure: 17

Magnification: 5

Etch: Marbles Reagent

Fabricated 'compression' Sample 4: 115Amp -After Compression Test

Report No.	L91805 Issue 1
Customer	Reviss Services (UK) Limited
Description	R7021 Transport Package -Jacket and Drain Tube Weld Strength Assessment

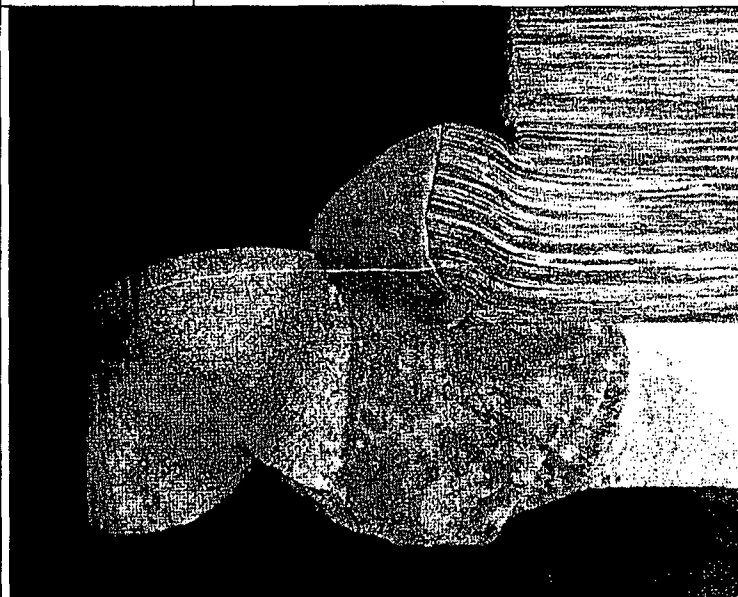


Figure: 18

Magnification: 8

Etch: Marbles Reagent

Fabricated 'compression' Sample 3- 105Amp -After Compression Test (Position 0°)
Note the weld is heavily deformed but the joint is 'intact'

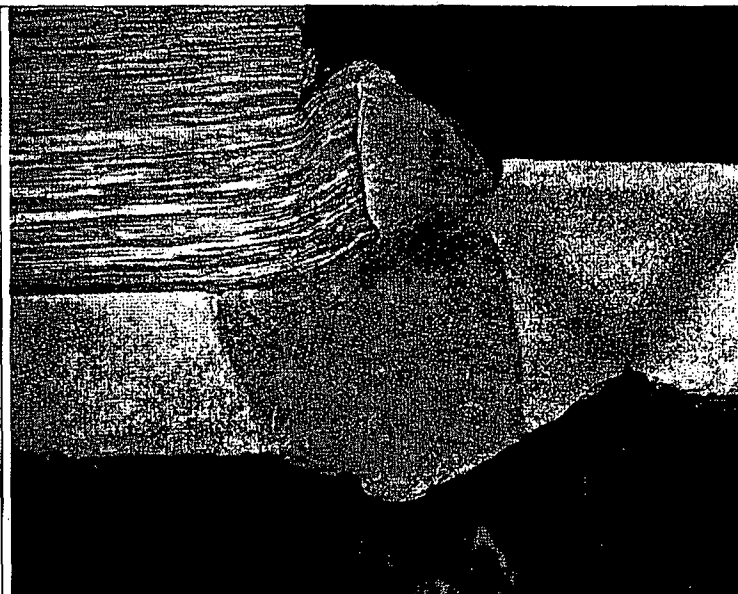


Figure: 19

Magnification: 8

Etch: Marbles Reagent

Fabricated 'compression' Sample 3- 105Amp -After Compression Test (Position 180°)
Note the weld is heavily deformed but the joint is 'intact'

Report No.	L91805 Issue 1
Customer	Revis Services (UK) Limited
Description	R7021 Transport Package -Jacket and Drain Tube Weld Strength Assessment

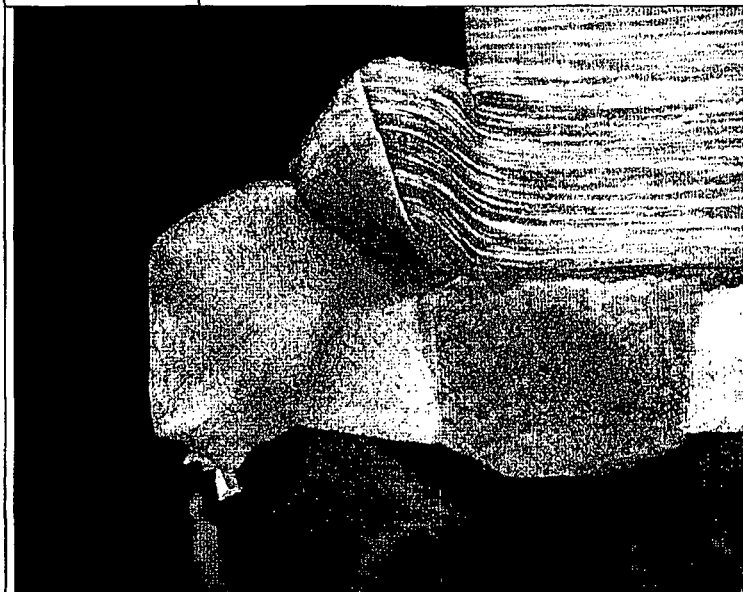


Figure: 20

Magnification: 8

Etch: Marbles Reagent

Fabricated 'compression' Sample 4 - 115Amp -After Compression Test (Position 0°)
Note the weld is heavily deformed but the joint is 'intact'

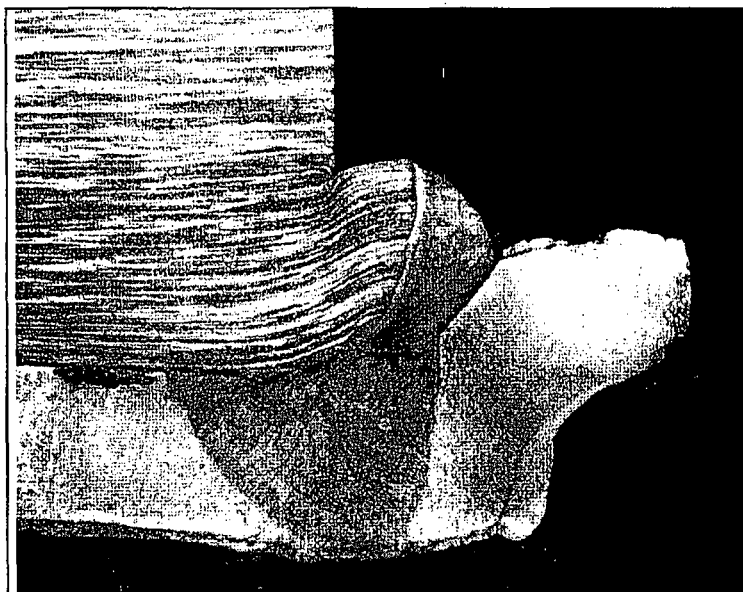


Figure: 21

Magnification: 8

Etch: Marbles Reagent

Fabricated 'compression' Sample 4 - 115Amp -After Compression Test (Position 180°)
Note the weld is heavily deformed but the joint is 'intact'

Intertek

Intertek MSG

Microscopy

C135

Tel: 01642 435704

Test Report: No. PS/W000339RL001

Isolation and chemical analysis of fragments of metal particles produced during the vibration testing of cobalt pellets

Date: 12/01/2009

For

Sammy Cheung

Reviss Services (UK) Ltd

6 Chiltern Court

Asheridge Road

CHESHAM

Bucks

HP5 2PX

Tel.: 01494 777444

Prepared by:

Bill Meredith

Particle Sizing Laboratory

TEST REPORT
Isolation and chemical analysis of fragments of metal particles produced during the vibration testing of cobalt pellets

Report Number	PS/W000339RL001
Chit Number	
Receipt Date	10/11/2008
Lab Book Reference	Lab Notebook INT0014
File Reference Location	
Number of Samples	2
Description of Work Required	(1) Cleaning and weighing of pellets and tubes (2) isolation by filtration of any metal fragments produced after vibration (3) chemical analysis (Co and Ni) of any fragments retained on filter papers using ICP-OES (performed by another Intertek section)
Method Reference	Sieving methodology

Samples Submitted

<u>Sample Identifier</u>	<u>Sample Description</u>	<u>Customer Identifier</u>
PS/W000339-1	Tube closed with Red tape plus cobalt pellets	
PS/W000339-2	Tube closed with Black tape plus cobalt pellets	

Experimental

Small, metal (nickel-coated cobalt) pellets and two stainless steel tubes with stainless steel end-closings were received from Revis Services (UK) Ltd. A procedure had previously been agreed with Revis as to how to deal with these articles before and after vibration testing. In summary the following was performed in Intertek MSG laboratories:

1. The as-received pellets and the tubes were washed vigorously with distilled water and then washed twice more with isopropanol (IPA). Finally the pellets were washed in IPA whilst they were agitated in an ultrasonic bath for 5 minutes to remove any loosely adhered particles that might be present on the pellets. All items were finally dried thoroughly in an oven and then allowed to fully cool in the air.
2. Approximately 78 grams of the pellets were weighed into one tube and approximately 46 grams of pellets were weighed into the other. Both tubes were closed with the clean metal closures (slight tapping proved necessary in both cases) and these closures were then taped in place with heavy duty red and black tape respectively. The tubes were seen to be firmly closed in both cases.
3. The tubes were placed in an expandable plastic covering and then placed in plastic bubble wrap. They were finally placed inside cardboard tubes and sent by courier to a second company (Parc - Product Assessment and Reliability Ltd) where specific vibration conditions were applied to the metal tubes. The samples were then returned unopened to Intertek MSG.

4. On return, the tubes were opened carefully and the pellets were poured directly into a 850 micron sieve which had been previously been thoroughly cleaned (water and IPA) and dried. This sieve caught the large pellets but allowed the washings and any fragments present to pass through. IPA was poured onto the pellets whilst they were very gently stirred (to facilitate the passage of any fragments).
5. IPA was poured into each tube a number of times and the contents poured into the sieve so that any particles present were washed out. Underneath the 850 micron sieve was a 106 micron sieve and below that a solid capture tray. The closure piece of each tube was also washed with IPA and all washings were put into the top sieve.
6. When the pellets had been washed they were removed from the sieve and the empty sieve was washed with more IPA. Some gentle brushing of the sieve was carried out to facilitate passage of any fragments and at the same time washing with IPA to ensure that no fragments were trapped in the brush.
7. The material passing through the final 106 micron metal sieve was captured and analysed. This was done by filtering the IPA that was in the bottom metal tray (under gravity and overnight). Whatman 542 hardened, ashless filter paper was employed. This paper is acid hardened (which reduces the ash produced to an extremely low level) and its tough surface makes it suitable for a wide range of critical analytical filtration operations*.
8. The two filter papers (for the RED and the BLACK tubes) were then dried and were then passed to the chemical analysis section of Intertek MSG where the Co and Ni levels were established.

Results

Table: Mass of the Nickel coated Cobalt pellets

SAMPLE ID	Mass
RED Assembly	76.709±0.001g
BLACK Assembly	47.768±0.001g

The following data is taken from Intertek report no. INORG/W000925RL001 entitled: "Determination of Cobalt and Nickel contents on filter papers by ICP-OES" which has been submitted separately to Reviss since it was carried out by a different section of Intertek (not by Bill Meredith). It is included in this report for completion only.

Table: Co and Ni Analysis of Filter Papers

SAMPLE ID	µg Co	µg Ni
Control Filter Paper	0.3	1.3
RED Assembly went thro' 106 µm sieve	106	23
BLACK Assembly went thro' 106 µm sieve	46	25

Statement of Uncertainty

Instrumental uncertainty on above ICP-OES results is 5% relative or better.

Report Authorisation

SCIENTIST'S NAME

Signature of Scientist

Bill Meredith

Bill Meredith

Date

04/02/2009

Footnote

- * According to the Whatman website this paper has a pore size of 2.7 microns and is described in the following way: The paper gives "high retention of fine particles under demanding conditions. Slow flow rate. Very hard and strong with excellent chemical resistance. Often used in gravimetric metal determinations.



Low Temperature testing of Parker V1289-75 O-rings

Summary

A sample of 3 V1289-75 O-rings were fitted to the pressure rig supplied and subjected to a cooling cycle to determine the temperature at which seal integrity was lost. For one of the three O-rings, the temperature was subsequently increased in order to determine the temperature at which an effective seal was restored. The results indicate that V1289 O-rings, runs 1 and 2, lost seal integrity at a temperature of approximately -50°C. The O-ring for run 3 lost seal integrity at around -54°C and re-sealed at around -52°C.

Materials and methods

Pressure test rig was supplied by our customer. Ref details as follows:

Test Rig drawing No. R8097-200/201 (Issue A), Vent Plug drawing No. R8097-203 (Issue A)

The reference details of the V1289-75 O-rings were as follows: Ceetak ref. 42870, Batch No. 80082263, Product code P2-117 V1289-75, Description 20.29 x 2.62, cure date 1Q08.

The reference details of the silicone O-rings were as follows: Ceetak ref. 42870, Batch No. 31002469, Product code P2-126 S383-70, Description 34.59 x 2.62 Silicone 70, cure date 1Q09.

All o-rings conformed to ISO 3601/1 tolerances and ISO 3601/3 Surface Imperfection control.

All instruments used e.g. pressure gauge, temperature sensors and torque wrench were calibrated before use.

A thermocouple was inserted down the centre of the test plug (marked P for pressure testing) and positioned with the thermocouple tip located within the vent port; as illustrated in Figure 1. The thermocouple was in close proximity to the inner o-ring.

A V1289-75 O-ring (black) was fitted in the inner groove and a Silicone 70 O-ring (red) was fitted in the outer groove, as illustrated in Figure 1. The plug was screwed into the test rig and tightened to a torque of 2kg.m.

The nominal section of the O-ring, in combination with the nominal depth of the vessel groove, resulted in a squeeze of 24%. This is deemed typical and conforms to typical sealing design guidelines.

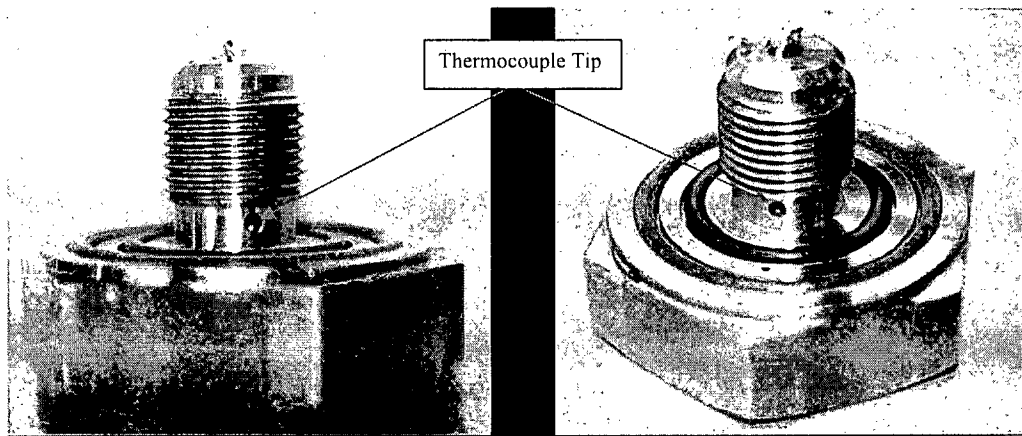


Figure 1 Position of thermocouple within plug fixture

Fittings were attached to enable the test rig to be pressurised and connected to a digital pressure meter. These are illustrated in Figure 2. The rig was placed within the test chamber (a modified Instron environmental test chamber) as illustrated in Figure 3. Gaseous CO₂ was used as the cooling medium and the chamber was connected to a CO₂ cylinder, as illustrated in Figure 4. The thermocouple was attached to a data-logging unit. The thermocouple, located within the test rig, was calibrated together with the data-logging unit prior to conducting studies with a pressurised system.

The digital pressure meter was attached to a T piece as illustrated in Figure 2. The system was pressurised to approximately 1 Bar using a hand pump attached to a section of rubber hose. The system was sealed with a clamp. The system was typically left for a period of at least 5 to 10 minutes, to check for system integrity, prior to chilling the test rig.

The target temperature of the control chamber was set to -55°C for the first run. The first run was used to provide an indication of the temperature range associated with loss of seal integrity. The second and third runs were more carefully controlled. They were intended to give more detailed information in the critical temperature range associated with loss of seal integrity.

The target temperature was initially set to -50°C for the second and third runs. This resulted in rapid cooling of the test rig. The target temperature was altered as the test proceeded, to reduce the rate of cooling of the rig as the temperature approached that associated with loss of seal integrity. The aim was to maintain the temperature at close to -45°C for a period of at least 20 minutes and to monitor for seal integrity at this temperature. The temperature was then lowered slowly to determine when seal integrity was lost. The temperature of the chamber was subsequently increased, following loss of seal integrity (for run 3), in order to determine the temperature at which an effective seal was restored.

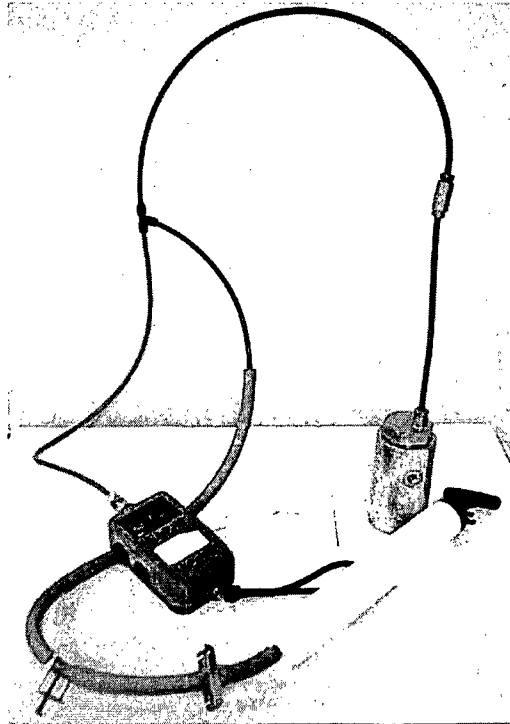
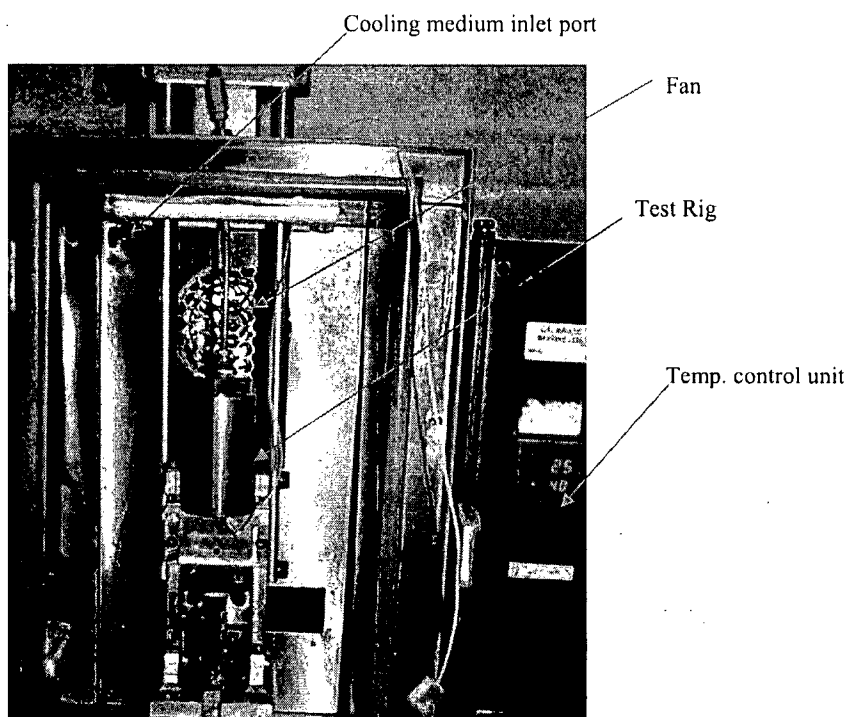


Figure 2 Test rig, pressurising system and digital pressure monitor

Figure 3 Close up of environmental test chamber



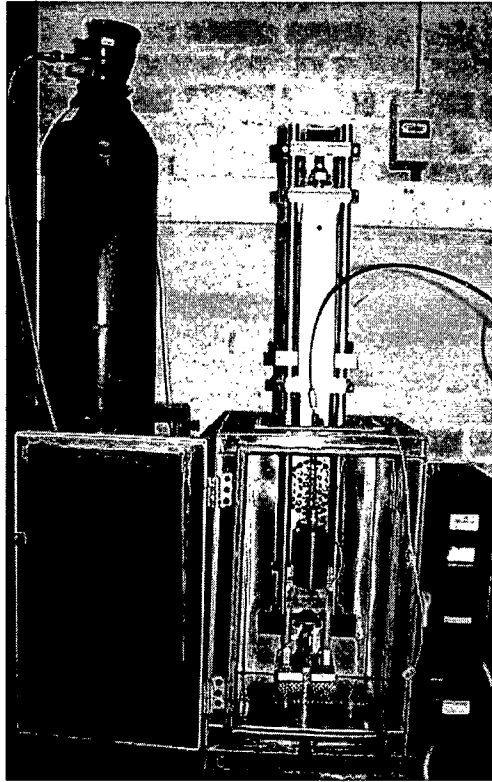


Figure 4 Test Chamber with CO₂ cylinder attached

Results

The results show that the V1289-75 O-rings lost seal integrity at temperature of -50 to -54°C . A sharp decrease in pressure, as illustrated in Figure 5, was recorded. On subsequently increasing the temperature, run 3, the temperature at which seal integrity was restored was -52°C .

A shallow decrease in pressure was noted during the initial cooling cycle, prior to loss of seal integrity. This was attributed to the air, within the pressurised system, obeying the gas laws; pressure decreasing with decreasing temperature. The small increase in pressure recorded for run 3, from 0.68 to 0.72 Bar, on heating the system would tend to support this.

The temperature and pressure profiles for the O-rings are included. These have been plotted as a function of elapsed time and are illustrated in figure 6 to 8. In addition to showing a sharp decrease in pressure at around -50°C , figures 6 and 7 also indicate that there was no loss in pressure over a 20 minute period at a temperature of around -45°C . The loss recorded for run 3 over the same region of the profile, 0.01 Bar was not significant.

Effect of temperature on seal integrity of V1289-75 o-ring

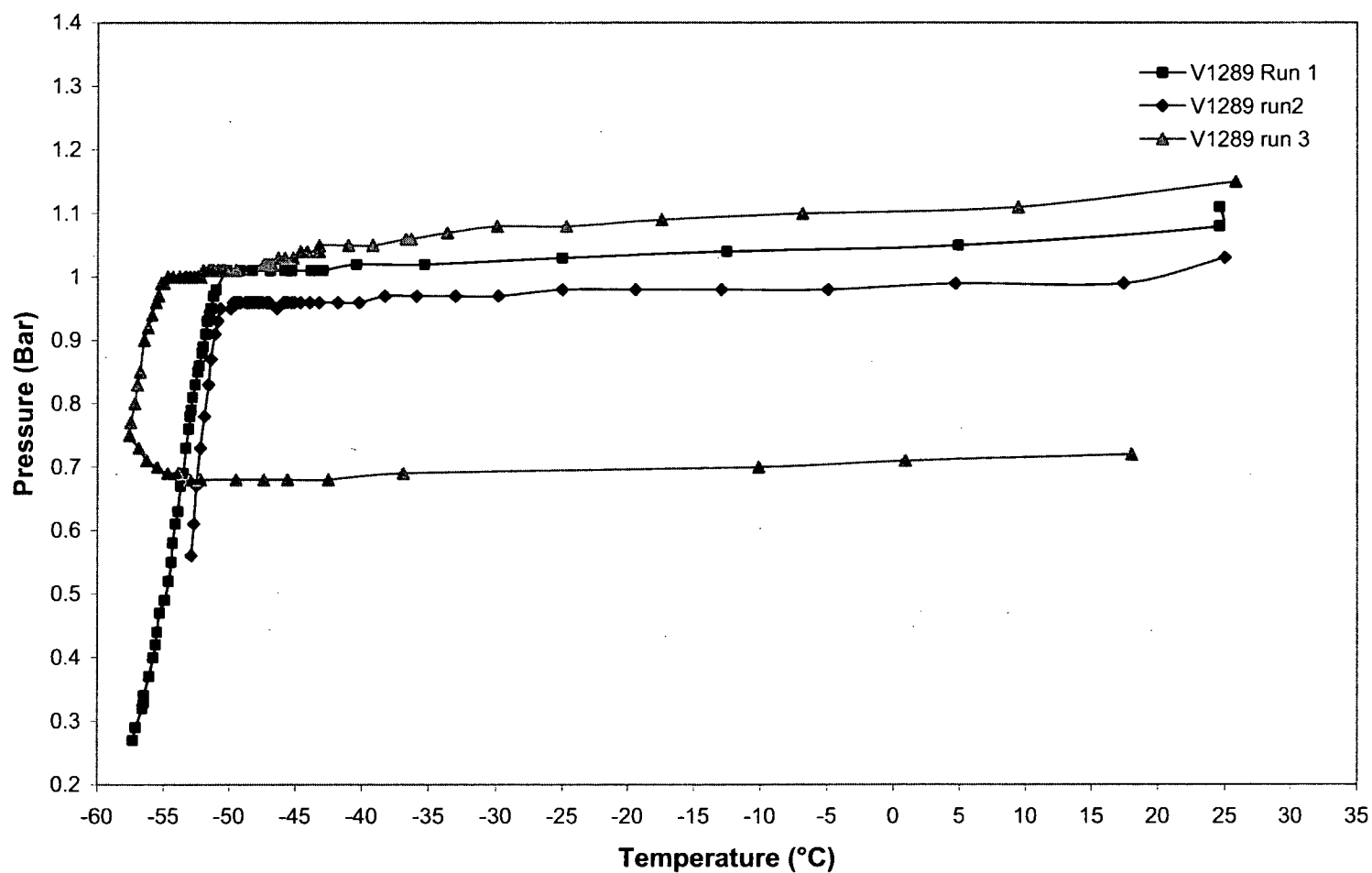


Figure 5 Effect of temperature on seal integrity of V1289-75 O-rings



V1289-75 run 1

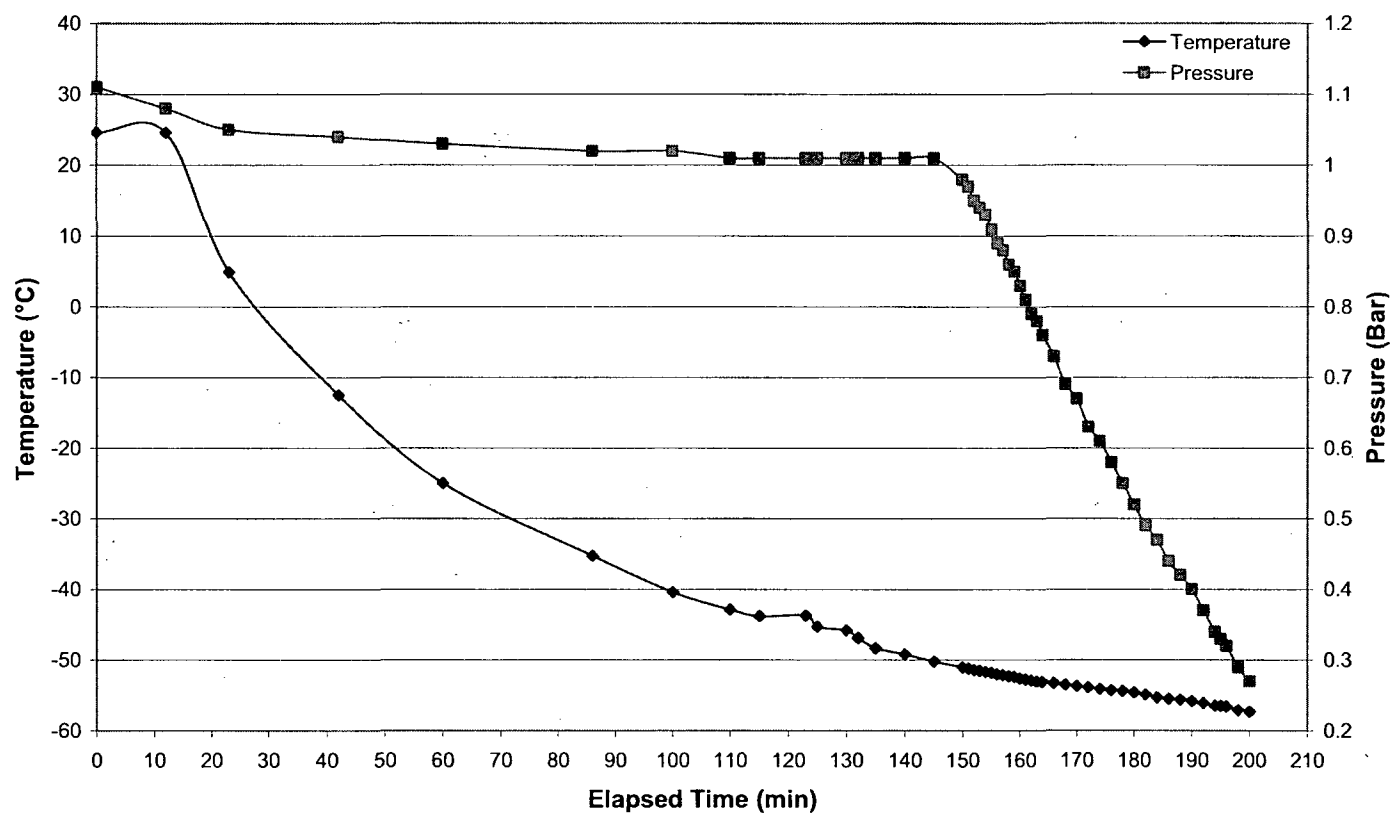


Figure 6 Temperature – Pressure profile for V1289-75 O-ring (Run 1)



V1289-75 run 2

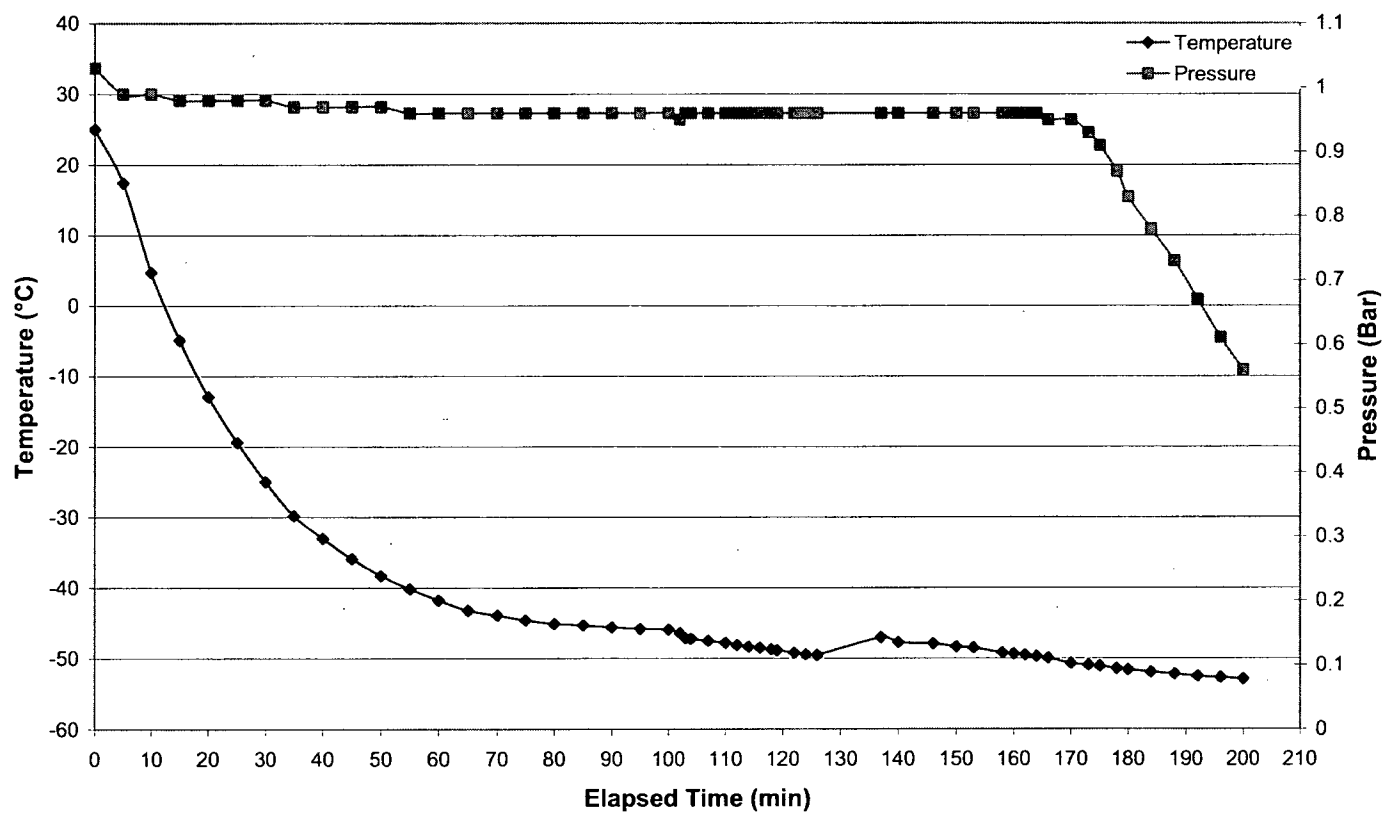


Figure 7 Temperature – Pressure profile for V1289-75 O-ring (Run 2)



V1289-75 run 3

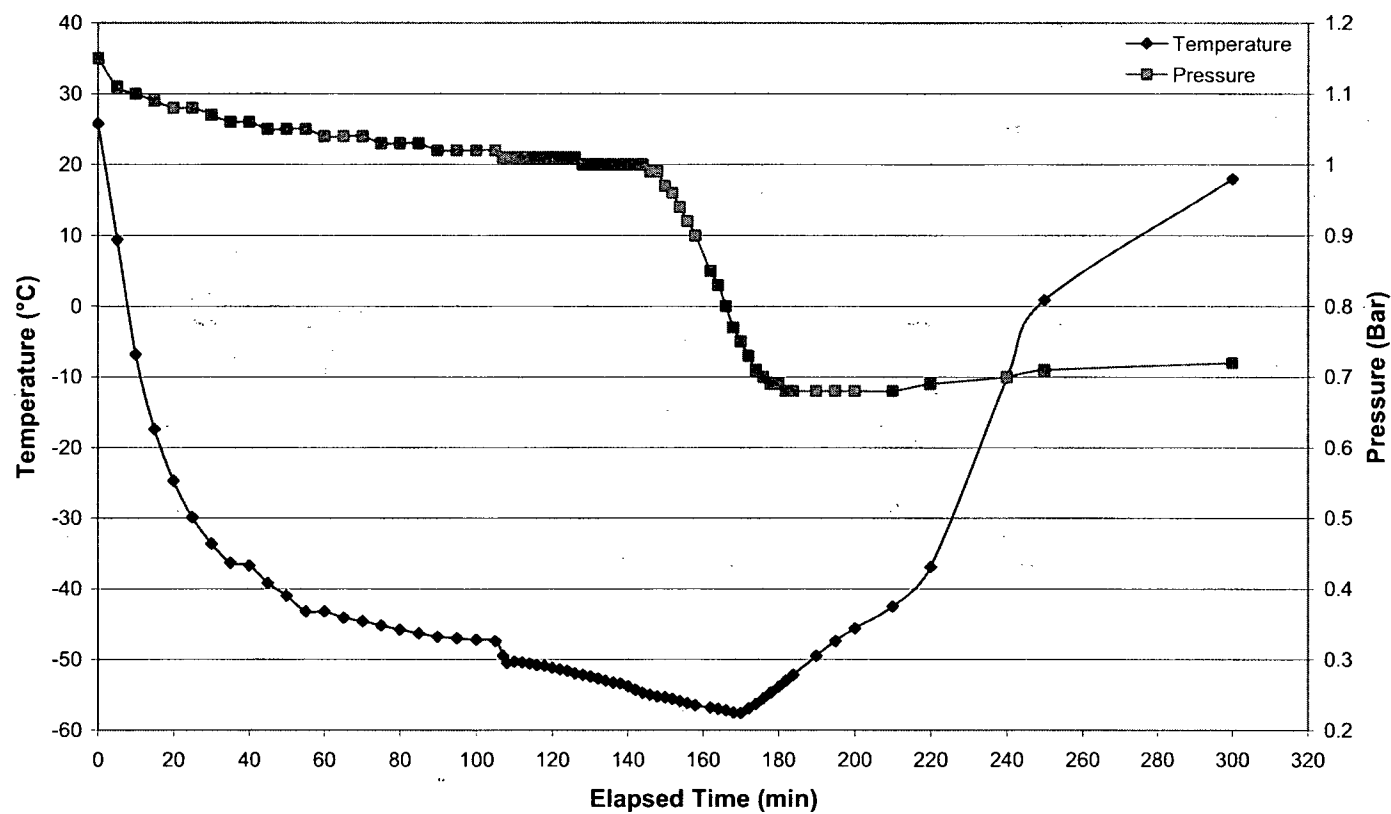


Figure 8 Temperature – Pressure profile for V1289-75 O-ring (Run 3)



Test Report No: RC 19356A

Date: 2nd September 09

Signed: Tarsem Sandhu – Application Engineer

A handwritten signature in black ink, appearing to read "T. Sandhu", written over a horizontal line.

Signed: Chris Challis – Quality Manager

A handwritten signature in black ink, appearing to read "C. Challis", written over a horizontal line.

CEETAK LTD

Fraser Road

Priory Business Park

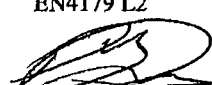
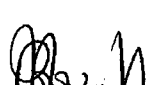
Bedford

MK44 3WH

ISO 9001:2000: Certificate No. LRQ 0936916

ISO 14001:2004: Certificate No. GV 16197

CERTIFICATE OF INSPECTION (ULTRASONIC)

CLIENT - NAME AND ADDRESS: REVISS Services (UK) Ltd 6 Chiltern Court Asheridge Road Chesham Buckinghamshire HP5 2PX				SHEET 1 OF 2 SHEET JOB No: 91018 (Aerospace) REPORT No: REV/011/0609 UT WORKS ORDER No: TBA PURCHASE ORDER No: RSL06814 DATE OF TEST: 23 Jun 09			
PLACE OF TEST: Colston, Brunel Park, Bumpers Farm, Chippenham, Wiltshire SN14 6NQ							
DESCRIPTION OF ITEMS INSPECTED (INCLUDE DRAWING / PART No. WHEN POSSIBLE)		QUANTITY	MATERIAL	ITEM IDENT OR SERIAL No.	STAGE OF PRODUCTION OR HEAT TREATMENT		
Isotope Transportation Flask		1 off	Stainless Steel (Grade unknown). H ₂ O	-	As manufactured		
INSPECTION STANDARD: Nil Supplied			ACCEPTANCE STANDARD: To estimate average gap between Inner Surface of Steel Outer Casing and the Lead Shield Material				
INSPECTION TECHNIQUE: Nil Supplied							
Surface: Plate		Access: Good		Weld Process: N/A		Joint Type: N/A	
Instrument Type: Krautkramer USN 58L		Serial No: 01D4YP		Couplant: Sonagel/H ₂ O		PCP Ults 13 Completed:	
Probe Type	Crystal Size	Frequency	Serial No.	Sensitivity	Timebase	Reject	Cal. Block
0 Deg.	0.5" DIA	5MHz	01XRFD		See Below	0	Nil
INSPECTION DETAILS AND RESULTS:							
Ref Block: A flat topped lead block was submerged in a water bath. 2 off 1.00mm Spacers were placed on top of the lead block. A 10mm Stainless Steel Plate was placed on top of the spacers. (Spacers of 0.50mm, 1.00mm, 1.50mm and 2.00mm were available for use).							
Instrument Setup: The following parameters were set into the Instrument.							
Range: 3.00mm Probe Delay: 3.4106µS Velocity: 1501 M/S Display Delay: Zero Frequency: 5 MHz Rectify: RF Gain: 66dB An acetate cover was placed on to the Instrument Display window							
Method: Area of Interest is the gap between the backwall of the Stainless Steel Casing and the Lead Block. The probe was placed on the Steel surface and the first and second returns from the Steel/H ₂ O interface were marked on the acetate with chinagraph pencil. The return from the Lead Block was marked on the Acetate with a second colour chinagraph. The 1.00 mm spacers were replaced with 2.00mm spacers. The return from the Lead block was again marked on the acetate. This operation was repeated for 0.50 and 1.50mm spacers. Displays were rechecked for the different spacers.							
REMARKS:							
TESTED BY: P Davies S.N.T. EN4179 L2 SIGNED:  DATE: 23 Jun 09				APPROVED BY: SIGNED:  DATE: 23 Jun 09 For and on behalf of Caparo Testing Technologies.			



CERTIFICATE OF INSPECTION

SERIAL No.: 91018 (Aerospace) REV/011/0609 UT

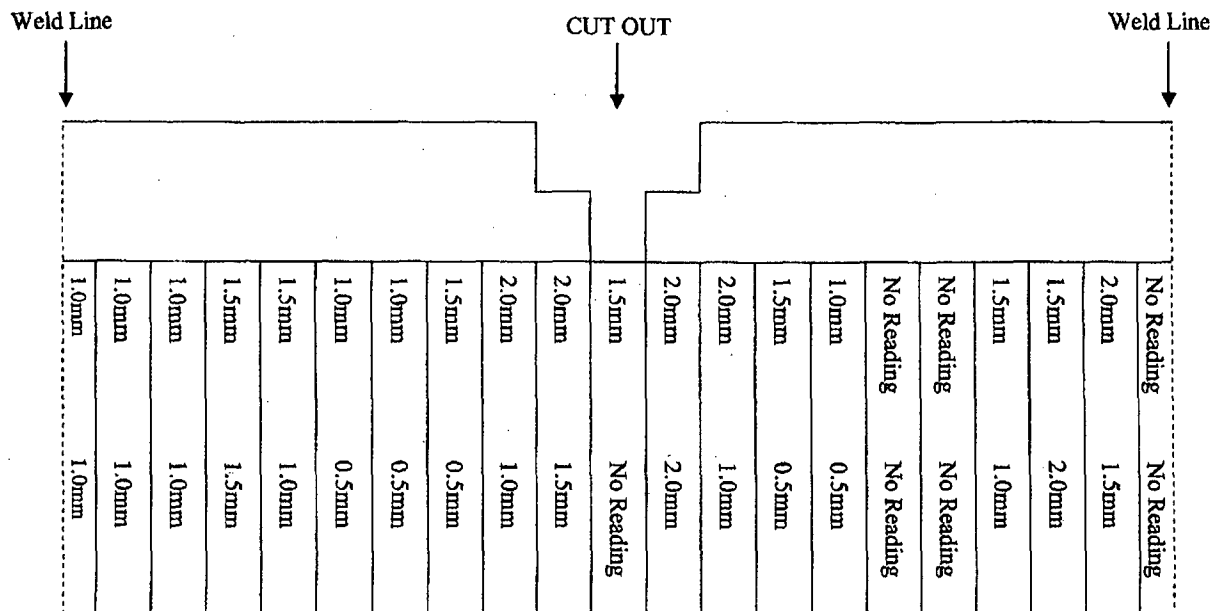
SHEET 2 OF 2 SHEETS

RESULTS

Ultrasonic readings were taken on the Steel Casing between the vanes around the flask. Vertically between the Intrnal Top and Centre Steel Bands and between the Centre and Lower Steel Bands. 42 off Readings.

Each Reading that had an ultrasonic return has been included on Fig. 1 below. Where no return was indicated, a value of 'No Reading' has been inserted.

ALL MEASUREMENTS ARE APPROXIMATE.



Kipper Diagram of Transportation Flask.

Fig. 1

TESTED BY: P Davies
S.N.T. EN4179 L2

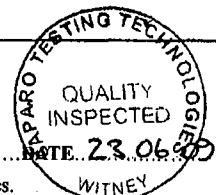
SIGNED: DATE: 23 Jun 09



APPROVED BY:

SIGNED: DATE: 23.06.09

For and on behalf of Caparo Testing Technologies.



All business is undertaken by the Company on the terms of the Company's Conditions of Business available on request.

Official Doc.No.30 Iss.3

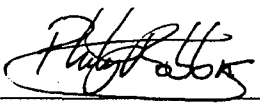





**REVISS Services
Quality and Regulatory Group**

Technical Memorandum

**Internal Stresses in the
R7021 Transport Container**

Author:		Reviewer:	
Name	P J G Robbins	Name	D W Rogers
Signature		Signature	
Date	28/07/10	Date	28/07/2010

1. PURPOSE AND SCOPE

The R7021 is a Type B transport package designed to transport both Special Form and non-SF solid radioactive material. This document analyses the thermal and mechanical stresses and strains generated in the principal structural elements of the R7021 flask under various extremes of regulatory environmental conditions. Internal pressures and the resultant stresses are functions of the design and its heat generating contents. Environmental conditions include maximum ambient temperature, insolation, reduced ambient pressure and immersion. The resulting stresses are quantified and compared with the material design limits (certain stress combinations are considered for worst-case conditions). The risk of fatigue failure in the flask and closure fixings is also assessed.

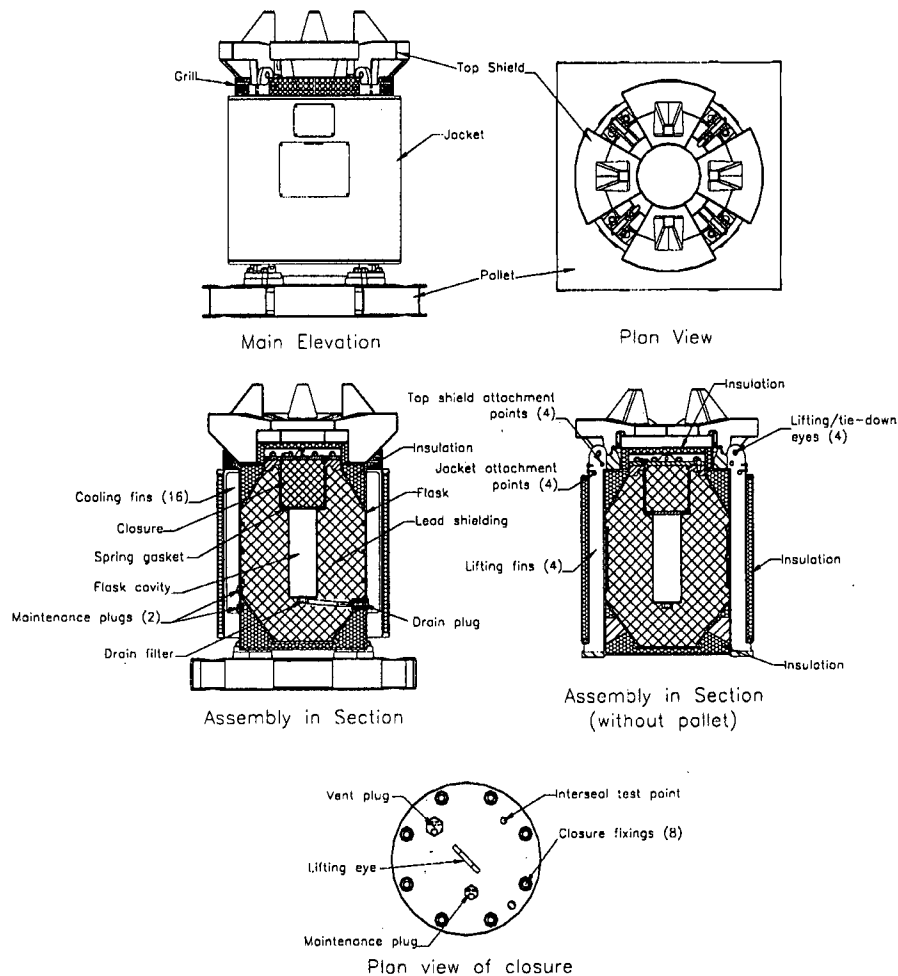


Figure 1: R7021 Assembly

2. DESCRIPTION

The design consists of a shielded, stainless steel flask mounted on a pallet and protected from heat and impact by a jacket and top shield (Figure 1). The flask is an upright, cylindrical fabrication closed with a removable shield plug, the closure, at the top. As it is designed to ship non-Special Form material the closure, vent and drain plugs are sealed with elastomer O-

rings and therefore the potential exists for the contents to heat the internal atmosphere and create a pressure differential to its environment.

3. CRITERIA

- Maximum Normal Operating Pressure (MNOP), i.e. at equilibrium loaded with 200 kCi (7.40 PBq) ^{60}Co in an ambient of 38°C with full insolation, shall not exceed 700 kPa gauge (para 662, TS-R-1).
- Stresses in the closure fixings or flask inner wall shall not exceed 10% of the design strength (yield) at the maximum normal conditions temperature as a result of:
 - internal pressure, or
 - a reduction in external pressure to 5 kPa (para 619, TS-R-1) or
 - the combination of the above.
- Stresses in the closure fixings or flask inner or outer walls resulting from internal pressures shall not exceed 10% of the design strength (yield) at the maximum accident conditions temperature.
- Compressive stresses in the flask outer wall shall not exceed the yield strength when a flask is immersed to a depth of 15m (para 729, TS-R-1).
- Stress levels shall be such that fatigue failure is not credible during the design life of 50 years.

4. ANALYSIS

This analysis calculates the stresses generated in the R7021 flask and closure fixings under a variety of regulatory conditions. It also examines the likelihood of fatigue failure from thermal cycling or repeated tightening during its design life.

4.1 ASSUMPTIONS

- Gas temperature within the containment system is taken to be the capsule temperature, i.e. the pressure in the cavity is the same as in the capsule.
- Gas temperature within the flask shielding volume is taken to be the cavity wall temperature.
- The flask is assumed closed at normal room temperature, though in practice this would be impossible to achieve given the significant time necessary to load the flask, fit the closure and purge the interior.
- Fixings strength at elevated temperature is reduced in the same proportion as the material into which they are screwed as that is the weaker of the two.
- The load on the closure fixings exerted by cavity pressure will be counteracted by the weight of the closure. The analysis will ignore this effect and consider the closure weightless.
- The pressure in the shielding space will counteract the pressure in the cavity. The analysis will ignore this effect.
- At 15m immersion depth the external pressure will be 0.150 N/mm² and the flask is assumed to be at the water temperature, i.e. with no internal pressure to counteract the external pressure.
- Stresses in the vent and drain plugs from the pressure differentials are ignored due to the very small area encompassed within the O-ring.
- For simplicity, the yield strength in compression is taken to be the same as in tension.

4.2 DATA

4.2.1 Temperature Maxima (RTM 120)

Component	Prior To Transport	Normal Conditions (MNOP)	Accident Conditions
Capsules	409	411	471
Closure fixings	141	150	270
Cavity wall	201	205	316
Flask wall	149	153	287

4.2.2 Design Stresses

These are taken from the pressure vessel standard, PD 5500:

Maximum Design Stress (N/mm ²)						
Temperature (°C)	20	141-150	153	201-205	270-287	316
304S11 *	200	155	141	133	126	120
Closure studs **	600	466	-	-	379	-

* Yield strength data is taken from BS EN 10088-2 for 1.4307 (304L) plate and reduced, by proportion, using the reduction in design strength cited in PD 5500 for a similar grade steel (304-S11).

** A4-80, BS EN ISO 3506-1, reduced as for 304S11.

4.2.3 Internal Pressures

- Prior to shipment: The gas inside the flask cavity expands as it is heated and exerts a pressure on the underside of the closure. According to the gas laws the flask cavity pressure, P_{cv1} , is:

$$P_{cv1} = \left(\left(\frac{273 + T_{c1}}{273 + T_a} \right) - 1 \right) \times P_a$$

where

T_{c1} = capsule temperature prior to shipment = 409°C

P_a = atmospheric pressure at time of closing = 0.101 MPa

T_a = ambient temperature at time of closing = 20°C

thus

$$P_{cv1} = \left(\left(\frac{273 + 409}{273 + 20} \right) - 1 \right) \times 0.101 = 0.134 \text{ MPa (gauge).}$$

The gas inside the shielding volume also expands as it is heated and exerts a pressure on the flask outer wall. The shielding pressure, P_{s1} , therefore is:

$$P_{s_1} = \left(\left(\frac{273 + T_{cv_1}}{273 + T_a} \right) - 1 \right) \times \text{Pa}$$

where

T_{cv_1} = cavity wall temperature prior to shipment = 201°C

thus

$$P_{s_1} = \left(\left(\frac{273 + 201}{273 + 20} \right) - 1 \right) \times 0.101 = 0.062 \text{ N/mm}^2 \equiv 0.062 \text{ MPa (gauge)}.$$

- MNOP (as above but including insolation):

$$P_{cv_2} = \left(\left(\frac{273 + T_{c_2}}{273 + T_a} \right) - 1 \right) \times \text{Pa}$$

where

T_{c_2} = capsule temperature = 411°C

thus

$$P_{cv_2} = \left(\left(\frac{273 + 411}{273 + 20} \right) - 1 \right) \times 0.101 = 0.135 \text{ MPa (gauge)}.$$

and

$$P_{s_2} = \left(\left(\frac{273 + T_{cv_2}}{273 + T_a} \right) - 1 \right) \times \text{Pa}$$

where

T_{cv_2} = cavity wall temperature = 205°C

thus

$$P_{s_2} = \left(\left(\frac{273 + 205}{273 + 20} \right) - 1 \right) \times 0.101 = 0.064 \text{ N/mm}^2 \equiv 0.064 \text{ MPa (gauge)}.$$

- Accident conditions:

$$P_{cv_3} = \left(\left(\frac{273 + T_{c_3}}{273 + T_a} \right) - 1 \right) \times \text{Pa}$$

where

T_{c_3} = capsule temperature = 471°C

thus

$$P_{cv_3} = \left(\left(\frac{273 + 471}{273 + 20} \right) - 1 \right) \times 0.101 = 0.155 \text{ MPa (gauge)}.$$

and

$$P_{s_3} = \left(\left(\frac{273 + T_{cv_3}}{273 + T_a} \right) - 1 \right) \times P_a$$

where

T_{cv_3} = cavity wall temperature = 316°C

thus

$$P_{s_3} = \left(\left(\frac{273 + 316}{273 + 20} \right) - 1 \right) \times 0.101 = 0.102 \text{ N/mm}^2 \equiv 0.102 \text{ MPa (gauge)}.$$

Internal Pressures Summary (MPa)			
Component	Prior To Transport	Normal Conditions (MNOP)	Accident Conditions
Cavity (Pcv)	0.134	0.135	0.155
Shielding space (Ps)	0.062	0.064	0.102

4.3 STRESS CALCULATIONS

4.3.1 Internal Pressure

- Closure Fixings Tensile Stress (Sf_1)

The weight of the closure, which would normally counteract any pressure in the cavity, is ignored here.

$$Sf_1 = \frac{D^2 \cdot P_{cv}}{N \cdot d^2}$$

where

D = O-ring internal diameter = 279 mm

Pcv = cavity pressure (see 4.2.3).

N = number of fixings = 8

d = fixings effective tensile diameter = 17.7 mm (M20, BS 3643)

Environment	Prior To Transport	Normal Conditions (MNOP)	Accident Conditions
Pressure, Pcv (MPa)	0.134	0.135	0.155
Fixings Stress, Sf_1 (N/mm ²)	4.16	4.19	4.81

- Cavity Wall Hoop Stress (Scv_h)

The pressure in the shielding space, which would normally counteract any pressure in the cavity, is ignored here.

$$Scv_h = \frac{P_{cv} \cdot R}{t} \quad (\text{Table 13.1, Case No 1c, Roark})$$

where

R = internal wall radius = 75 mm

t = wall thickness = 6.2 mm
thus

Environment	Prior To Transport	Normal Conditions (MNOP)	Accident Conditions
Pressure, P_{cv} (MPa)	0.134	0.135	0.155
Hoop Stress, Scv_h (N/mm ²)	1.62	1.63	1.88

- Cavity Wall Axial Stress (Scv_a)
 $Scv_a = \frac{P_{cv} \cdot R}{2t}$ (Table 13.1, Case No 1c, Roark)

thus

Environment	Prior To Transport	Normal Conditions (MNOP)	Accident Conditions
Pressure, P_{cv} (MPa)	0.134	0.135	0.155
Axial Stress, Scv_a (N/mm ²)	0.810	0.817	0.938

- Outer Wall Hoop Stress
 R = mean radius = 352 mm
 t = wall thickness = 10 mm

thus the hoop stress, Ss_{hl} , is as follows:

Environment	Prior To Transport	Normal Conditions (MNOP)	Accident Conditions
Pressure, P_s (MPa)	0.062	0.064	0.102
Hoop Stress, Ss_{hl} (N/mm ²)	2.18	2.25	3.59

- Outer Wall Axial Stress
The axial stress, Ss_{al} , is as follows:

Environment	Prior To Transport	Normal Conditions (MNOP)	Accident Conditions
Pressure, P_s (MPa)	0.062	0.064	0.102
Axial Stress, Ss_{al} (N/mm ²)	1.09	1.13	1.80

4.3.2 Reduced External Pressure

- Closure Fixings Tensile Stress (Sf_2)
 $Sf_2 = \frac{D^2 \cdot p}{N \cdot d^2}$

where

p = pressure differential (95 kPa) = 0.095 N/mm²

thus

$$S_{f2} = \frac{279^2 \times 0.095}{8 \times 17.7^2} = 2.95 \text{ N/mm}^2$$

- Outer Wall Hoop Stress, S_{sh2} :

$$S_{sh2} = \frac{p.R}{t} \quad (\text{Table 13.1, Case No 1c, Roark})$$

where

R = mean wall radius = 352 mm
 t = wall thickness = 10 mm

thus

$$S_{sh2} = \frac{0.095 \times 352}{10} = 3.34 \text{ N/mm}^2$$

- Outer Wall Axial Stress

$$S_{sa2} = \frac{p.R}{2t}$$

thus

$$S_{sa2} = \frac{0.095 \times 352}{2 \times 10} = 1.67 \text{ N/mm}^2$$

Note: there are no stresses in the containment boundary because the flask wall is leak-tight.
 See OP381 for leak-testing requirements.

4.3.3 15m Immersion

- Flask Wall Hoop Stress

$$S_{sh3} = \frac{p.R}{t} \quad (\text{Table 13.1, Case No 1c, Roark})$$

where

p = pressure = -0.150 N/mm^2 (external)
 R = mean wall radius = 352 mm
 t = wall thickness = 10 mm

thus

$$S_{sh3} = \frac{-0.150 \times 352}{10} = -5.28 \text{ N/mm}^2 \text{ (compressive)}$$

- Flask Wall Axial Stress

$$S_{sa3} = \frac{p.R}{2t}$$

thus

$$S_{sa3} = \frac{-0.150 \times 352}{2 \times 10} = -2.64 \text{ N/mm}^2 \text{ (compressive)}$$

Note: there are no stresses in the containment boundary because the flask wall is leak-tight.
 See OP381 for leak-testing requirements.

4.4 RESULTS SUMMARY

4.4.1 Prior to Transport

	Stress (N/mm ²)				
Location	Closure Fixings	Cavity Wall		Outer Wall	
Stress Type	Tensile	Hoop	Axial	Hoop	Axial
Internal pressure	4.16	1.62	0.810	2.18	1.09
Design Stress	466	133		155	
Proportion (%)	0.893	1.22	0.609	1.41	0.703

4.4.2 Normal Conditions

- Individual load conditions

	Stress (N/mm ²)				
Location	Closure Fixings	Cavity Wall		Outer Wall	
Internal pressure	4.19	1.63	0.817	2.25	1.13
5 kPa pressure	2.95	-	-	3.34	1.67
Maximum	4.19	1.63	0.817	3.34	1.67
Design Stress	466	133		141	
Proportion (%)	0.899	1.23	0.614	2.37	1.18

- Load combination

	Stress (N/mm ²)				
Location	Closure Fixings	Cavity Wall		Outer Wall	
Internal pressure	4.19	1.63	0.817	2.25	1.13
5 kPa pressure	2.95	-	-	3.34	1.67
Total	7.14	1.63	0.817	5.59	2.80
Design Stress	466	133		141	
Proportion (%)	1.53	1.23	0.614	3.96	1.99

4.4.3 Accident Conditions

	Stress (N/mm ²)				
Location	Closure Fixings	Cavity Wall		Outer Wall	
Internal pressure	4.81	1.88	0.938	3.59	1.80
Design Stress	379	120		126	
Proportion (%)	1.27	1.57	0.782	2.85	1.43
15m immersion	-	-	-	-5.28	-2.64
Design Stress	-	-		-126	
Proportion (%)	-	-	-	4.19	2.10
Maximum (%)	1.27	1.57	0.782	4.19	2.10

5. FATIGUE

5.1 THERMAL FATIGUE

Thermal stresses are determined by the temperature difference and the coefficient of thermal expansion. The temperature difference is determined by the heat flux, the conductivity of the material and its thickness. Heat flow is predominantly in the radial direction and therefore the highest temperature differences are across the inner and outer flask walls.

5.1.1 Thermal stress in outer flask wall

For thin-walled cylinders (inner radius/wall thickness > 10) with a temperature difference across the wall:

$$\text{Max. stress} = \frac{\Delta T \cdot \gamma \cdot E}{2(1-\nu)} \quad (\text{Roark, p762})$$

where:

$$\begin{aligned}\gamma &= \text{coefficient of thermal expansion} = 8.55 \times 10^{-6} \text{ }^{\circ}\text{F}^{-1} \text{ (Table TE-1, ASME II, Part D)} \\ &= 1.54 \times 10^{-5} \text{ }^{\circ}\text{C}^{-1} \\ E &= \text{Young's modulus} = 200 \text{ GPa} = 200 \times 10^3 \text{ N/mm}^2 \text{ (PD 5500, Table 3.6-3)} \\ \Delta T &= \text{temperature difference} \\ \nu &= \text{Poisson's ratio} = 0.285\end{aligned}$$

From Heat Transfer:

$$q = \frac{-kA}{\Delta x} (T_2 - T_1)$$

where:

$$\begin{aligned}q &= \text{heat} = 3,074 \text{ W (RTM 120)} \\ k &= \text{thermal conductivity} = 9.4 \text{ Btu/h.ft.}^{\circ}\text{F} = 16.3 \text{ W/m.}^{\circ}\text{C} \text{ (Machinery's Handbook, p378, S30400)} \\ A &= \text{surface area of wall} = \pi \times d \times l = \pi \times 0.693 \times 1.02 = 2.22 \text{ m}^2 \\ \Delta x &= \text{thickness of wall} = 0.010 \text{ m} \\ T_2 - T_1 &= \text{temperature difference across wall} = \Delta T\end{aligned}$$

rearranging gives:

$$\Delta T = \frac{q \Delta x}{kA} = \frac{3,074 \times 0.010}{16.3 \times 2.22} = 0.849^{\circ}\text{C}$$

therefore:

$$\text{Max. stress} = \frac{0.849 \times 1.54 \times 10^{-5} \times 200 \times 10^3}{2(1 - 0.285)} = 1.83 \text{ N/mm}^2$$

5.1.2 Thermal stress in cavity wall

As before, assuming all the heat flows through the cavity wall (worst case):

$$\Delta T = \frac{q \Delta x}{kA}$$

where:

$$A = \text{surface area of wall} = \pi \times 0.150 \times 0.476 = 0.224 \text{ m}^2$$

$$\Delta x = \text{thickness of wall} = 0.0062 \text{ m}$$

therefore:

$$\Delta T = \frac{3.074 \times 0.0062}{16.3 \times 0.224} = 5.22^\circ\text{C}$$

therefore:

$$\text{Max. stress} = \frac{4.18 \times 1.54 \times 10^{-5} \times 200 \times 10^3}{2(1 - 0.285)} = 11.2 \text{ N/mm}^2$$

5.1.3 Thermal fatigue

An R7021 is unlikely to be used more than twelve times in a year, which represents a maximum of twenty-four heating and cooling cycles. With a nominal design life of fifty years the flask will be subject to a maximum of 1,200 thermal cycles. Using equation C-5 in PD 5500, Annex C, paragraph 3.1.2, the stress range for 1,200 cycles is 509 N/mm^2 . It is evident therefore that the flask is not at risk from thermal fatigue failure during the design life.

5.2 FASTENERS

The key R7021 fixings are those retaining the closure to the flask (M20, st/st), the jacket and top shield to the flask (M16, c/st) and the flask to the pallet (M24, c/st). As the safe fatigue life is determined by the tensile stress level it can be seen that, as all the fixings are tightened to the same torque (OP 381), the smallest fixings (M20, st/st and M16, c/st) will have the highest tensile stress. The stress, S_t , from the preload is obtained from Machinery's Handbook, p178, as follows:

$$F = Q \times \frac{p + 6.2832\mu r}{6.2832r - \mu p} \times \frac{r}{R}$$

rearranging gives:

$$Q = \frac{F.R}{r} \times \frac{6.2832r - \mu p}{p + 6.2832\mu r}$$

where:

$$Q = \text{load (kgf)}$$

$$F.R = \text{torque (kgf.m)}$$

$$r = \text{pitch radius of screw (m)}$$

$$p = \text{thread pitch (m)}$$

$$\mu = \text{coefficient of friction}$$

5.2.1 Stainless Steel Fasteners

$$\begin{aligned} \text{F.R} &= 15 \text{ kgf.m (OP 381)} \\ r &= 0.0092 \text{ m (BS 3643)} \\ p &= 0.0025 \text{ m (BS 3643)} \\ \mu &= 0.16 \text{ (for lubricated threads, Machinery's Handbook, p173)} \end{aligned}$$

thus:

$$Q = \frac{15}{0.0092} \times \frac{6.2832 \times 0.0092^2 - 0.16 \times 0.0025}{0.0025 + 6.2832 \times 0.16 \times 0.0092} = 7,970 \text{ kg} = 78,200 \text{ N}$$

The tensile stress area of an M20 thread is 245 mm² (BS 3643). The tensile stress, S_t , in the bolt is therefore:

$$S_t = \frac{Q}{A} = \frac{78,200}{245} = 319 \text{ N/mm}^2$$

Section C.3.1.3 of Appendix C in PD 5500 uses the fatigue design curve of Fig. C4 to determine the number of cycles to failure for a given stress range in bolting materials where,

$$S_r = \frac{S_t \times E \times n}{2.09 \times 10^5}$$

Using the default fatigue strength reduction factor, n , of 4 (para. C.3.3.4, PD 5500) and a Young's modulus, E , of $200 \times 10^3 \text{ N/mm}^2$ (PD 5500, Table 3.6-3) the stress range S_r is given by:

$$S_r = \frac{319 \times 200 \times 10^3 \times 4}{2.09 \times 10^5} = 1,220 \text{ N/mm}^2$$

Stainless steel is an inherently ductile material. Therefore, in the stainless steel studs, any localised stress concentration (in this case in the thread roots) exceeding yield will therefore deform plastically until the stress is reduced to approximately the yield value (p28.10, Standard Handbook of Machine Design). From the fatigue design curve, the maximum allowable number of operating cycles for a stress range of yield (600 N/mm^2 , section 4.2.2) is not less than 3,000 cycles.

5.2.2 Carbon Steel Fasteners

5.2.2.1 M16 Shoulder Bolts

$$\begin{aligned} \text{F.R} &= 6 \text{ kgf.m (OP 381)} \\ r &= 0.0074 \text{ m (BS 3643)} \\ p &= 0.0020 \text{ m (BS 3643)} \\ \mu &= 0.16 \text{ (for lubricated threads, Machinery's Handbook, p173)} \end{aligned}$$

thus:

$$Q = \frac{6}{0.0074} \times \frac{6.2832 \times 0.0074^2 - 0.16 \times 0.0020}{0.0020 + 6.2832 \times 0.16 \times 0.0074} = 3,970 \text{ kg} = 38,900 \text{ N}$$

The tensile stress area of an M16 thread is 157 mm² (BS 3643). The tensile stress, S_t , in the

bolt is therefore:

$$S_t = \frac{Q}{A} = \frac{38,900}{157} = 248 \text{ N/mm}^2$$

Section C.3.1.3 of Appendix C in PD 5500 uses the fatigue design curve of Fig. C4 to determine the number of cycles to failure for a given stress range in bolting materials where,

$$S_r = \frac{S_t \times E \times n}{2.09 \times 10^5}$$

Using the default fatigue strength reduction factor, n, of 4 (para. C.3.3.4, PD 5500) and a Young's modulus, E, of $209 \times 10^3 \text{ N/mm}^2$ (PD 5500, Table 3.6-3) the stress range S_r is given by:

$$S_r = \frac{248 \times 209 \times 10^3 \times 4}{2.09 \times 10^5} = 992 \text{ N/mm}^2$$

From the fatigue design curve, the maximum allowable number of operating cycles for a stress range of 992 N/mm^2 (section 4.2.2) is not less than 1,500 cycles.

5.2.2.2 M24 Studs

$$\begin{aligned} \text{F.R} &= 15 \text{ kgf.m (OP 381)} \\ r &= 0.0110 \text{ m (BS 3643)} \\ p &= 0.0030 \text{ m (BS 3643)} \\ \mu &= 0.16 \text{ (for lubricated threads, Machinery's Handbook, p173)} \end{aligned}$$

thus:

$$Q = \frac{15}{0.0110} \times \frac{6.2832 \times 0.0110 - 0.16 \times 0.0030}{0.0030 + 6.2832 \times 0.16 \times 0.0110} = 6,660 \text{ kg} = 65,300 \text{ N}$$

The tensile stress area of an M24 thread is 353 mm^2 (BS 3643). The tensile stress, S_t , in the bolt is therefore:

$$S_t = \frac{Q}{A} = \frac{65,300}{353} = 185 \text{ N/mm}^2$$

Section C.3.1.3 of Appendix C in PD 5500 uses the fatigue design curve of Fig. C4 to determine the number of cycles to failure for a given stress range in bolting materials where,

$$S_r = \frac{S_t \times E \times n}{2.09 \times 10^5}$$

Using the default fatigue strength reduction factor, n, of 4 (para. C.3.3.4, PD 5500) and a Young's modulus, E, of $209 \times 10^3 \text{ N/mm}^2$ (PD 5500, Table 3.6-3) the stress range S_r is given by:

$$S_r = \frac{185 \times 209 \times 10^3 \times 4}{2.09 \times 10^5} = 740 \text{ N/mm}^2$$

From the fatigue design curve, the maximum allowable number of operating cycles for a stress range of 740 N/mm^2 (section 4.2.2) is not less than 2,500 cycles.

5.2.3 Fatigue

An R7021 is unlikely to be used more than twelve times in a year, which represents twenty-four tightening operations. With a nominal design life of fifty years the fasteners will be subject to a maximum of 1,200 tightening cycles. It is evident that the fasteners are not at risk from fatigue failure during the design life.

6. CONCLUSIONS

- Maximum Normal Operating Pressure (MNOP) does not exceed 700 kPa (gauge).
- Stresses in the R7021 flask cavity and outer walls and closure fixings do not exceed 10% of the design stress at MNOP, as a result of:
 - internal pressure, or
 - a reduction in external pressure to 5 kPa, or
 - the combination of the above.
- Stresses in the R7021 flask cavity and outer walls and closure fixings as a result of internal pressure do not exceed 10% of the design stress under accident conditions of transport.
- Stresses from immersion to a depth of 15m do not exceed the levels above.
- No component is at risk of fatigue failure during the design life.

7. REFERENCES

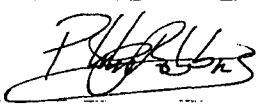

- BS 3643-1: 2007: ISO metric screw threads. Principles and basic data. British Standards Institution.
- BS EN ISO 3506-1: 1998: Mechanical properties of corrosion-resistant stainless-steel fasteners. Bolts, screws and studs. British Standards Institution.
- Heat Transfer, Holman, 8th Edition, McGraw-Hill, 1997.
- OP 381: R7021 Operating and Maintenance Instructions, REVISS Services (UK) Ltd.
- PD 5500: 2009: Specification for unfired fusion welded pressure vessels. British Standards Institution.
- Roark's Formulas for stress and strain, 7th Edition, WC Young, McGraw-Hill, 2002.
- RTM 120 issue 2: Thermal performance of the R7021 transport container, REVISS Services (UK) Ltd.
- Standard Handbook of Machine Design, Shigley, 3rd Edition, McGraw-Hill, 2004.
- TS-G-1.1 (Rev. 1): Advisory Material for the IAEA Regulations for the Safe Transport of Radioactive Material, IAEA, Vienna, 2008.
- TS-R-1: Regulations for the Safe Transport of Radioactive Material, 2005 Edition, IAEA, Vienna.

REVISS

**REVISS Services
Quality and Regulatory Group**

Technical Memorandum

**Thermal Performance
of the R7021 Transport Container**

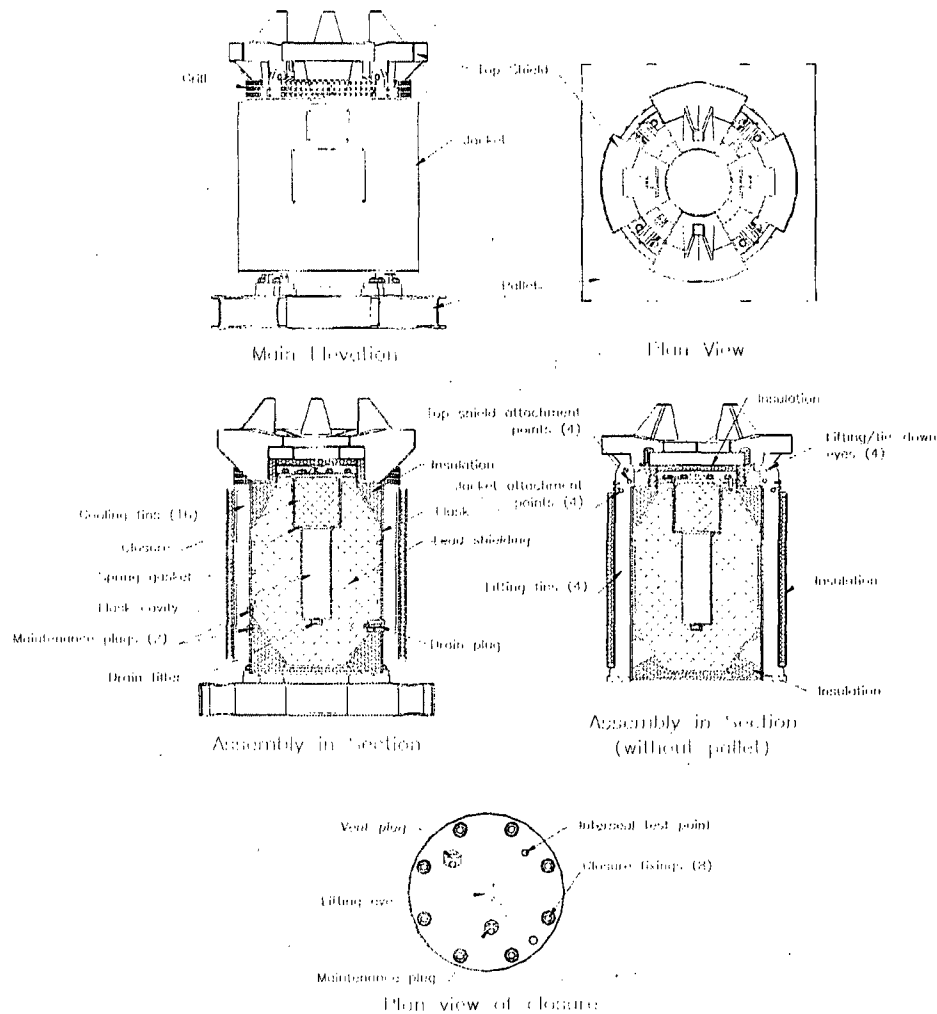
Author:		Reviewer:	
Name	P J G Robbins	Name	D W Rogers
Signature		Signature	
Date	28/07/10	Date	28/07/2010

1. PURPOSE AND SCOPE

This document details the thermal performance of the key features of the R7021 transport container under normal and accident conditions of transport as specified in TS-R-1 for Type B(U) packaging. It also examines the sensitivity of the design to key design features. The results, which are worst-case temperatures at various points in and around the structure, provide reference data for documents that demonstrate various aspects of regulatory compliance.

2. DESCRIPTION

The design consists of a lead shielded, stainless steel flask mounted on a pallet and protected from heat by a jacket and top shield (figure 1). The jacket and top shield are double-skinned fabrications with integral thermal insulation. The flask also contains insulation in its top and bottom corners. The flask is designed to be pond operated and therefore the cavity is equipped with a drain tube at its base and a venting hole through the closure. As it is also designed to transport non-Special Form material the closure, drain and vent plugs are each equipped with an O-ring seal.



3. CRITERIA

1. The thermal performance shall not be sensitive to damage sustained during either normal or accident conditions mechanical testing.
2. No accessible surface shall exceed 50°C under normal conditions of transport in the shade, unless the shipment is made under "Exclusive Use" conditions (TS-R-1, paras. 617 & 652).
3. No accessible surface shall exceed 85°C under normal conditions of transport in the shade (TS-R-1, para. 653).
4. Package ventilation shall not be restricted by adjacent cargo.
5. There shall be no significant difference in the thermal performance of packages manufactured to the current issue of the drawings to that modelled and justified below.

4. ANALYSIS

4.1 GENERAL

4.1.1 Contents

The R7021 is designed to transport up to 5.92 PBq of normal form ^{60}Co which generates an internal heat load of 2,460 watts (RTM 025). It is also designed to transport up to 7.40 PBq of Special Form ^{60}Co which generates an internal heat load of 3,074 watts.

4.1.2 Modelling Software

The thermal performance of the R7021 in the various regulatory conditions has been characterised using the ANSYS CFD finite element computational fluid dynamics program. Its handling of natural and forced convection as well as thermal radiation shadowing and re-emission makes it particularly appropriate for the R7021. CFD was previously known as CFX which has a satisfactory history of being used for IAEA Type B package analysis.

CFD modelling is based on computational modelling of gas flow. The mesh includes the gas regions and at all points in the mesh the key properties of the gas (temperature, viscosity, density, heat capacity and buoyancy) are calculated. It is able therefore to assign accurately calculated heat transfer coefficients to all mesh points for solid surfaces. Unlike conventional finite element analysis (FEA) it does not rely on assumed heat transfer coefficients and therefore is not dependent on comparing calculated results with measured values and adjusting the heat transfer coefficients to obtain the best match.

4.1.3 Modelling

The normal form contents (see R7110/1.1) heat load was modelled as follows:

1. Models of the prototype R7021 (see Fig 2 (QS7021 issue 2 details the manufacturing drawings and issue levels)) and the contents were created to enable them to be benchmarked against temperature measurements taken with a near maximum contents load. This established an appropriate contact resistance for the lead stainless steel interfaces and an emissivity for the contents.
2. A model of the production design (see Fig 3 and QS 7021 issue 4) was created using the same contact resistance to confirm its thermal performance was not affected by the design changes (see RTM 151 for details).
3. A sensitivity study was conducted on the production and contents models under normal and accident conditions of transport thermal environments to assess the significance of various assumed values and attributes.

4. Using the values that gave the highest temperatures, the model was subjected to the normal conditions thermal environment (in its normal orientation).
5. Starting with that temperature profile the container model was subjected to the accident condition thermal test in three different orientations.
6. The contents were modelled in each orientation using the peak cavity wall temperature.
7. To assess the effect of mechanical damage, three new models, incorporating the damage sustained in each orientation, were subjected to the thermal test.
8. The maximum reverse temperature gradient in the closure flange was calculated from the case giving the highest peak temperature at that point.
9. The contents were re-modelled in the orientation that previously gave the highest capsule temperature using the peak cavity wall temperature.

The Special Form contents (see R7410/1.1) heat load was modelled as follows:

1. Benchmarking was revised to establish a more accurate emissivity for the flask surface (in the previous study it had been set to a nominal value).
2. The container and contents models were modified to incorporate the higher heat load and increased number of capsules.
3. The container model was subjected to the normal conditions environment and the contents model to the maximum cavity wall temperature.
4. The container model was subjected the thermal test in the orientation that gave the highest lead temperatures in the previous study.
5. The contents were modelled in the same orientation using the peak cavity wall temperature.

4.1.4 Contents

The contents were simulated using a separate model comprising capsules, basket and cavity wall. Capsules were modelled as solid stainless steel cylinders of the same dimensions as the R2089 capsule. The basket spacer rings were modelled, to capture their effect on air flow, but not the vertical tie-rods. Cavity wall temperatures were taken from the flask model. Accident conditions contents temperatures were modelled using the peak cavity wall temperature with the cavity and contents in the drop test orientation.

4.1.5 Internal heat load

Heat is generated when radiation is absorbed. Monte Carlo analysis of similar containers and contents has shown that the total heat load is proportioned primarily between the contents (by self shielding), the cavity wall, the first radial 12mm of the shielding and the rest of the radial shielding. The container model, which does not include the capsules, distributes their heat evenly over the surface of the cavity wall as a heat flux. The contents model distributes capsule heat evenly through their volume.

Location	Energy deposition [%]
Capsule/cavity wall heat flux	25.8
Cavity wall	11.0
First 12mm radial lead	39.7
Remaining radial lead	23.5
Total	100

4.1.6 Grill Model

The pressure loss characteristics of the grill were evaluated at air flow rates in the range of 0.25m/s to 1.5m/s and then applied to a porous surface representing the grill.

4.1.7 Normal conditions

In normal conditions the model was given the maximum contents heat load, stood upright on a solid flat surface, with an emissivity of 0.90, in 38°C still air and subjected to the insolation specified in TS-R-1.

4.1.8 Accident conditions

In the thermal test the model, in each orientation, was enclosed in an 800°C environment with an emissivity of 0.9, i.e. as in a furnace, but with a forced updraft of 8 m/s producing peak gas flow rates not less than 10 m/s around the package. This complied with the IAEA recommendations, TS-G-1.1. After thirty minutes the environment was replaced by normal conditions, i.e. still air at 38°C with full insolation, until temperatures in all critical areas had stopped rising.

4.2 BENCHMARKING

Once all external temperatures were in agreement with the test results the thermal contact resistance between the lead and stainless steel interfaces was adjusted until the mid-height cavity wall temperature was correct. The value obtained for the normal form model was 400 W/m².°C when the external flask emissivity was set to 0.45. This was changed to 330 W/m².°C when the Special Form study identified an emissivity of 0.55 as giving a better match with the measurements. The results are summarised as follows:

Measured and Modelled Temperatures [°C]				
Location	Measured	Modelled		
		R7110/1.1		R7410/1.1
		Prototype	Production Design	Revised Benchmark
Cavity wall (50mm below top)	151	152	153	152
Cavity wall (mid-height)	155 / 155 / 154	155	156	155
Cavity wall (50mm above base)	149	151	152	150
Closure flange (20mm below upper surface, 50mm from outer edge)	112 / 116	110	114	111
Drain point (centre of cylinder, outer surface)	83 ^{*1}	101	101	97
Flask wall (mid-height, midway between fins)	112 / 111 / 112 / 113	119	120	116
Lifting fin (100mm from top edge, 75mm from outer edge)	49 ^{*2}	65	67	64
Lifting fin (40mm from top edge, 55mm from outer edge)	55	57	60	55
Lifting fin (135mm from top edge, 35mm from outer edge)	61 / 59	66	68	65
Flask foot (top surface, 30mm from outer edge)	27 / 27	32	33	32
Jacket (top edge)	36 / 36	39	39	39

Measured and Modelled Temperatures [°C]				
Location	Measured	Modelled		
		R7110/1.1		R7410/1.1
		Prototype	Production Design	Revised Benchmark
Jacket (inner surface, 40mm from top edge)	43 / 40	45	46	46
Top shield (mid height vertical face)	35 / 36	42	39	38
Top shield (half way across horizontal face)	35 / 35	41	38	38
Top shield (top surface centre)	40	49	37	39
Ambient	21	21	21	21

Notes:

*1: These measurements have been ignored as they are obviously due to malfunctioning thermocouples.

*2: The drain plug head was not explicitly modelled as it has no safety significance. The nearest point was the flask surface which gave a higher calculated value due to the lack of a contact resistance.

In the contents model the emissivity of the stainless steel capsules was adjusted until their mid-height temperatures gave the best match. The value obtained was 0.60. The results are summarised as follows:

Measured and Modelled Source Temperatures [°C]		
Capsule	Measured	Modelled (R7110/1.1)
X	342 / 341 / 342	337
Y	311 / 312 / 312	332
Z	333 / 333 / 330	335

The results demonstrate good agreement with the test results and validate the models and input parameters for IAEA transport conditions modelling.

4.3 THERMAL PERFORMANCE OF THE PROTOTYPE VS THE PRODUCTION DESIGN

When the same internal heat load and contact resistance were applied to the production model all key temperatures remained essentially unchanged (the only significant area of difference being the surface of the top shield which had acquired an additional top plate and therefore ran a little cooler). This confirmed the changes made no significant difference to steady state thermal performance which allowed the contact resistance and capsule emissivity to be carried through without further benchmarking.

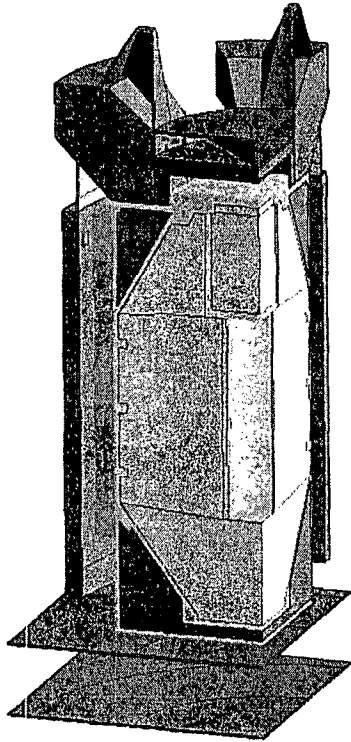


Figure 2: Prototype Thermal Model

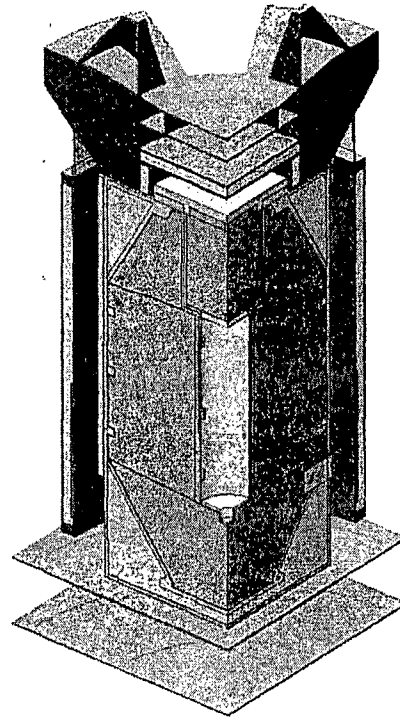


Figure 3: Modified Design Thermal Model

4.4 SENSITIVITY STUDY

The thermal analysis investigated the sensitivity of the design to various assumed values or attributes including those of its contents. The key design and modelling parameters are as follows:

- The emissivity of flask external surfaces.
- The emissivity of carbon steel surfaces.
- The thermal conductivity of the flask, jacket and top shield insulation.
- The number of capsules (total activity remaining constant) in the cavity.
- The gas in the cavity.
- The cavity gas pressure.

The reference case contents consisted of sixteen R2089 sources in a neon filled cavity at 1 atm. The emissivity of the flask external surfaces was 0.4, the emissivity of the carbon steel surfaces was 0.9 and the conductivity of the insulation was the manufacturer's stated value. The contents heat load was the maximum permitted and the environment was normal conditions in all cases except for the insulation conductivity which was also run in accident conditions. The results are summarised as follows:

Effect of Various Parameters on Normal Conditions Package Temperatures [°C]						
Location	Reference Case	Emissivity of S/S		Emissivity of C/S		Ins cond $2 \cdot k_{ins}$
		0.20	0.60	0.80	0.98	
Cavity wall (mid-height)	178	184	176	179	178	178
Maximum lead temperature	168	175	166	169	169	168
Closure flange (20mm below upper surface, 50mm from outer edge)	136	142	133	137	137	136
Drain point (centre of cylinder, 80mm from outer surface)	138	144	135	139	138	137
Flask wall (mid-height, midway between fins)	139	146	137	141	140	139
Flask foot (top surface, 30mm from outer edge)	62	62	64	64	62	63
Top shield (top surface centre)	95	83	87	92	99	91
Ambient	38	38	38	38	38	38

Effect of Variation in Insulation Conductivity on Accident Condition Package Temperatures [°C]		
Location	Reference Case	Conductivity Doubled
Cavity wall (mid-height)	271	278
Maximum lead temperature	268	271
Closure flange (20mm below upper surface, 50mm from outer edge)	253	258
Drain point (centre of cylinder, 80mm from outer surface)	224	231
Flask wall (mid-height, midway between fins)	254	264

Effect of Various Contents Parameters on Source Temperature [°C]					
Reference Case	Number of Capsules		Cavity Gas		Pressure [atm]
16/neon/1 atm	12	18	Helium	Air	2
334	348	325	265	360	332

The sensitivity study demonstrated:

- Flask temperatures are not particularly sensitive to the stainless steel emissivity in normal conditions of transport though a lower value does give slightly higher results.
- Flask temperatures are not sensitive to the carbon steel emissivity or the insulation conductivity in normal conditions of transport.
- Flask temperatures are not particularly sensitive to the insulation conductivity in accident conditions though a higher value does give slightly higher results.
- Contents temperature is sensitive to capsule activity (the higher the activity the higher the temperature) and cavity gas (air being worse than either neon or helium) but is not sensitive to the gas pressure.

4.5 NORMAL CONDITIONS

4.5.1 Drop test damage

The prototype R7021 was subjected to three 1.2m drop tests (RTR 233-235) and one 1m penetration test (RTR 236) causing only superficial damage. Normal conditions of transport tests did not cause any damage that might affect its thermal performance.

4.5.2 Results

Normal conditions for normal form contents was modelled with the maximum activity (5.92 PBq), twelve capsules (the activity per capsule being the normal maximum), air in the cavity at 1 atm, a flask emissivity of 0.20 and a carbon steel emissivity of 0.98. The results are summarised as follows:

Normal Conditions Temperatures [°C]		
Location	Equilibrium in the shade (@ 38°C)	Equilibrium in the sun (@ 38°C)
Capsule wall	377	379
Cavity wall (mid-height)	180	184
Maximum lead temperature	170	175
Closure flange (20mm below upper surface, 50mm from outer edge)	135	142
Drain point (centre of cylinder, 80mm from outer surface)	139	144
Flask wall (mid-height, midway between fins)	141	146
Lifting fin (40mm from top edge, 55mm from outer edge)	79	87
Flask foot (top surface, 30mm from outer edge)	51	68
Top shield (top surface centre)	53	103
Ambient	38	38

Normal conditions for Special Form contents was modelled with the maximum activity (7.40 PBq), fourteen capsules (the activity per capsule being the normal maximum), air in the cavity at 1 atm, a flask emissivity of 0.55 and a carbon steel emissivity of 0.98. The results are summarised as follows:

Normal Conditions Temperatures [°C]		
Location	Equilibrium in the shade (@ 38°C)	Equilibrium in the sun (@ 38°C)
Capsule wall	409	411
Cavity wall (mid-height)	201	205
Maximum lead temperature	186	191
Closure flange (20mm below upper surface, 50mm from outer edge)	141	150
Drain point (centre of cylinder, 80mm from outer surface)	148	152
Flask wall (mid-height, midway between fins)	149	153
Lifting fin (40mm from top edge, 55mm from outer edge)	79	93
Flask foot (top surface, 30mm from outer edge)	50	67
Top shield (top surface centre)	57	100
Ambient	38	38

4.6 ACCIDENT CONDITIONS (WITHOUT DROP TEST DAMAGE)

Accident conditions were modelled with the starting condition above and the carbon steel emissivity set to 0.8, as recommended by TS-G-1.1. The results are summarised as follows:

Normal Form Contents - Peak Accident Conditions Temperatures [°C]				
Location	Normal Form			Special Form
	Upright	Inverted	Side	Upright
Cavity wall (mid-height)	282	292	288	305
Maximum lead temperature	281	283	280	294
Closure flange (20mm below upper surface, 50mm from outer edge)	259	251	252	275
Drain point (centre of cylinder, 80mm from outer surface)	236	262	257	248

4.7 ACCIDENT CONDITIONS (WITH DROP TEST DAMAGE)

In each orientation the nature and extent of the 9m drop test damage was taken from the numerical impact analysis (C15788/IR/0001) and the 1m puncture damage from the prototype test results. See below for more detail.

4.7.1 Upright

Drop test damage (see Figs 4 & 5) consisted primarily of deformation of the upper pallet plate and crushing of the webs under the flask. The top plate was modelled realistically (see Fig 6). The webs were not represented in the model so no change was required.

Vertical upright - 000x000 (Dr

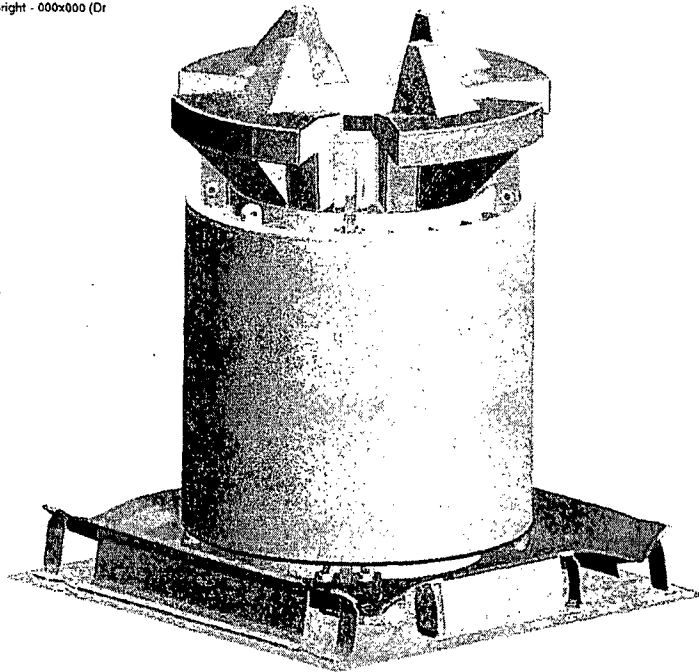


Figure 4: R7021 after 9m upright drop (modelled)

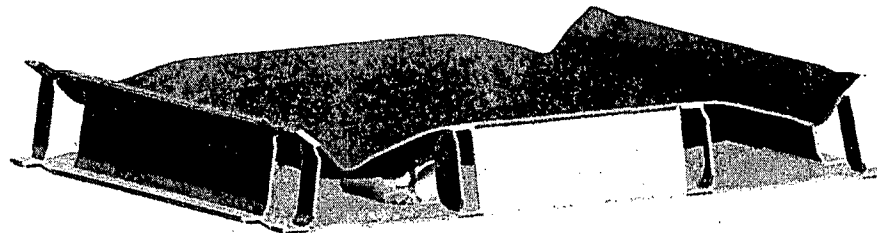


Figure 5: Pallet after 9m upright drop (modelled)

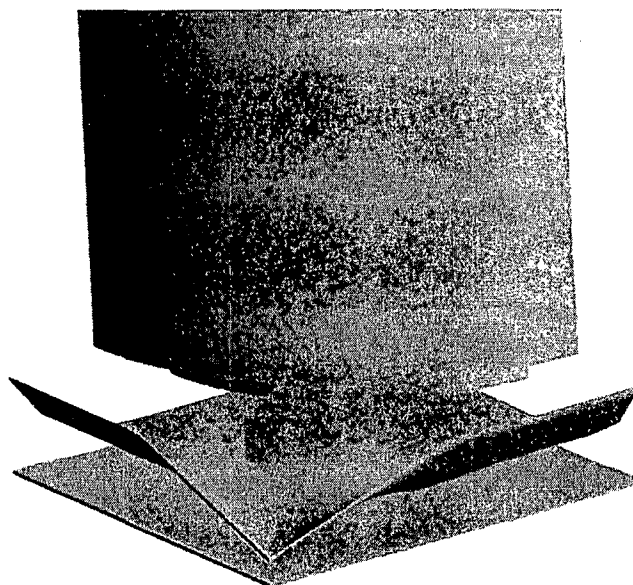


Figure 6: Thermal model (quarter section) showing pallet damage

Punch damage (see Figs 7-9) consisted primarily of partial penetration of the lower plate on a 150mm diameter (see RTR 239). The damage was modelled by completely removing a 150mm square section (see Fig 10). This not only increased heat input in that area as it is a larger area but also permitted free radiation energy and hot gas penetration. The hole was moved to the centre to take advantage of symmetry for ease of modelling.



Figure 7: Pallet after two 1m punch tests

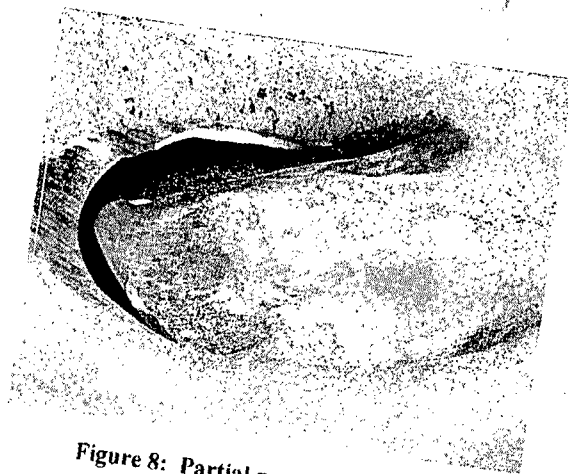


Figure 8: Partial punch penetration



Figure 9: Partial punch penetration

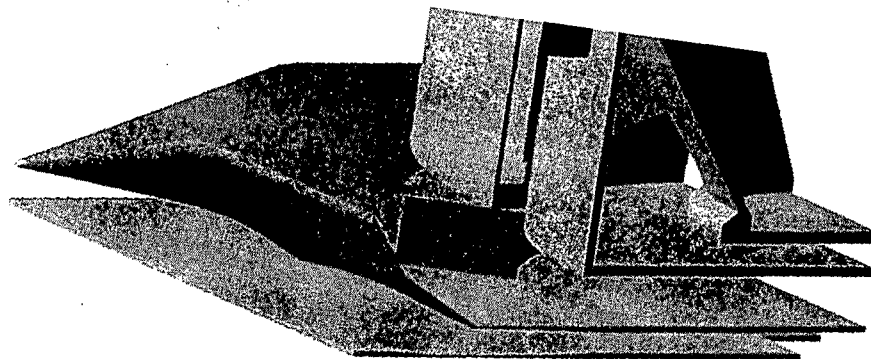


Figure 10: Thermal model (quarter section) showing punch hole

4.7.2 Inverted

Drop test damage (see Figs 11 & 12) consisted primarily of crushing of the top shield cones. For ease of modelling this was modelled by removing the cones (see Fig 13). This removed their shadowing effect on the top shield surfaces immediately below and around them which would only increase heat input to the top shield.

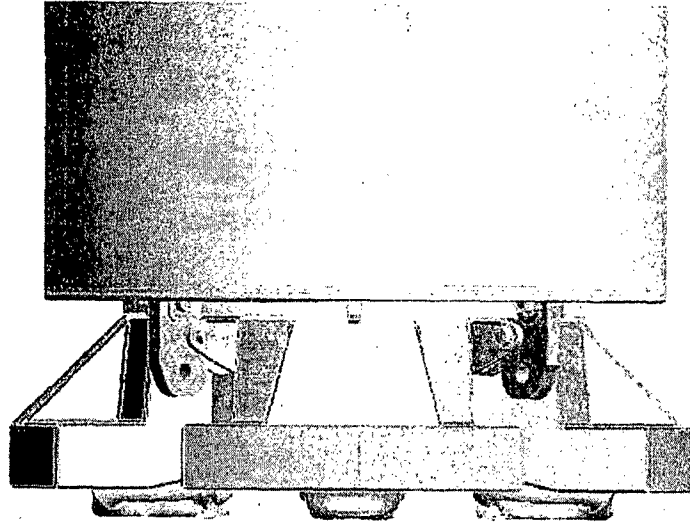


Figure 11: R7021 after 9m inverted drop test (modelled)

QASYS DISPLAY: Run 05 - Vertical inverted - 180x000 ID

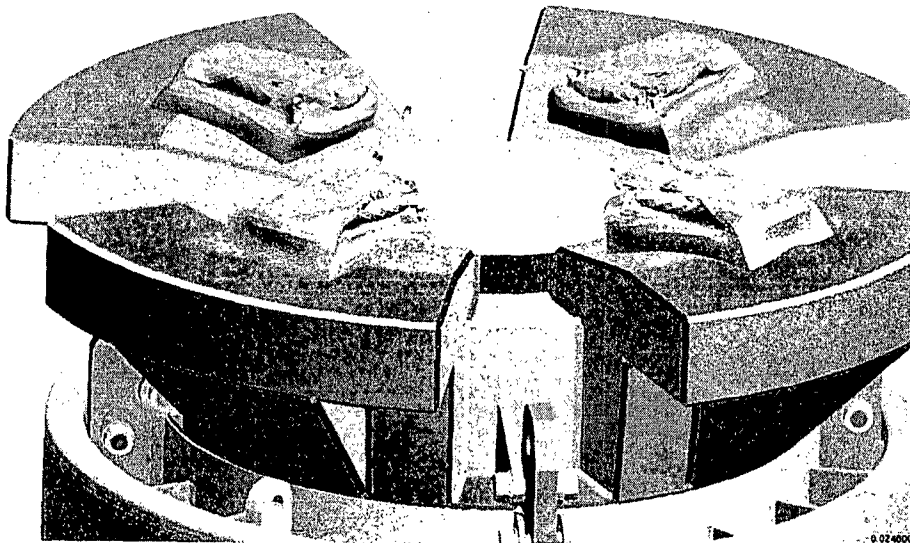


Figure 12: Top shield cones crushed

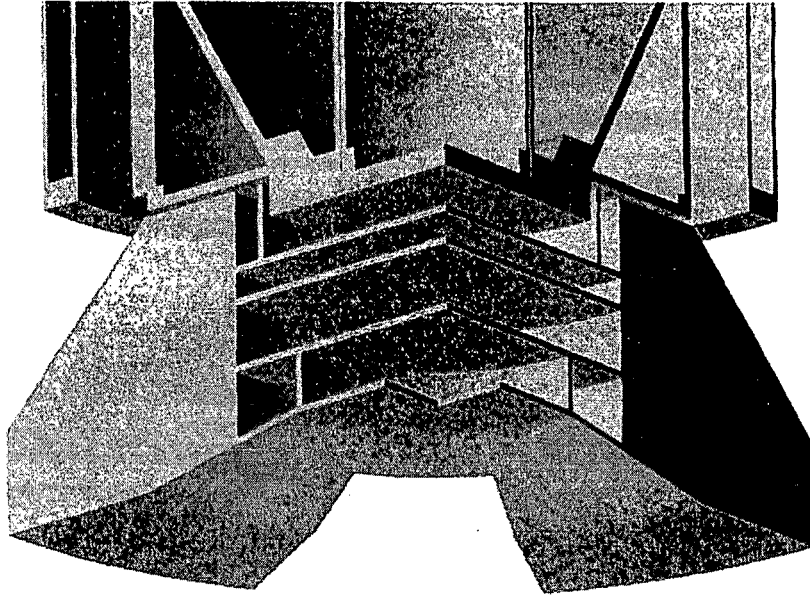


Figure 13: Thermal model (quarter section) without cones

Punch damage (see Figs 14 & 15) consisted primarily of partial penetration of the centre plate on a 150mm diameter (see RTR 242). The modified top shield incorporated greater protection in this area which eliminated the shearing (Fig 16) however, for conservatism, the damage was modelled by completely removing a 150mm square section (see Fig 17). This increased heat input in that area as it is not only a larger area but it also permits free radiation energy and hot gas penetration. The hole was moved to the centre to take advantage of symmetry for ease of modelling.

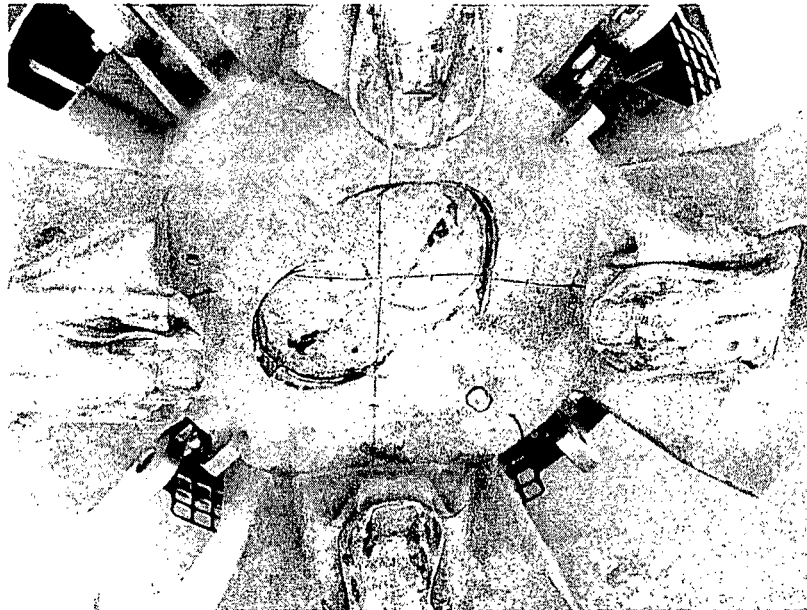


Figure 14: Top shield after two 1m punch tests

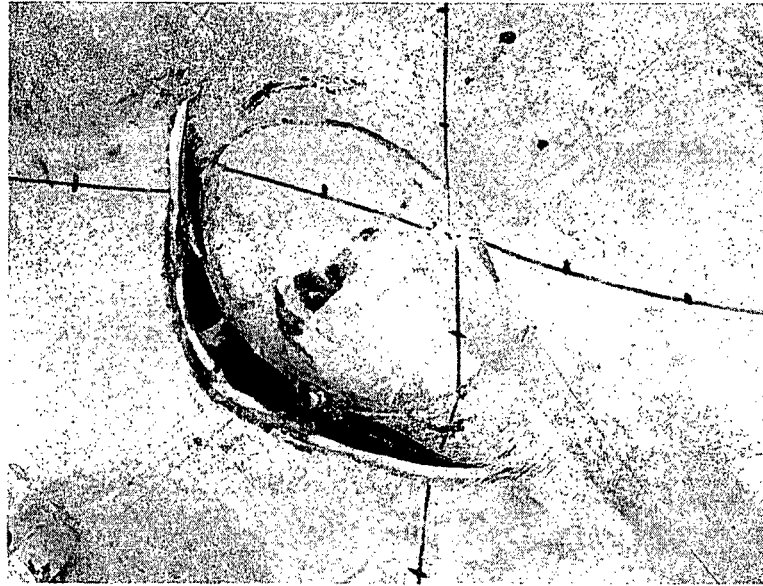


Figure 15: Detail of punch damage

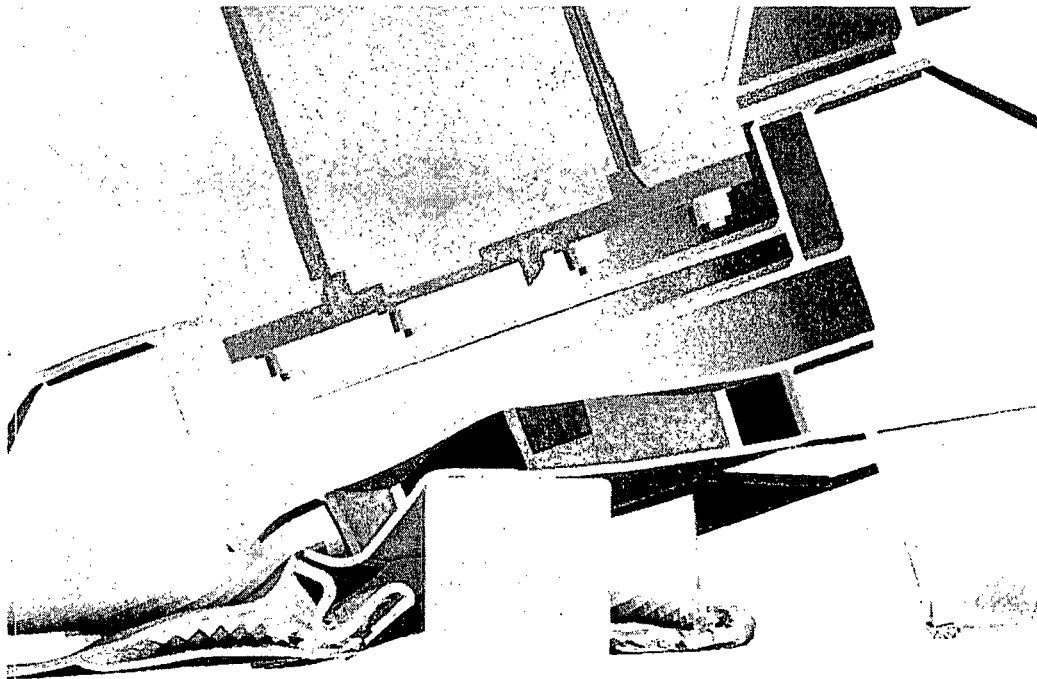


Figure 16: Punch damage to modified top shield (modelled)

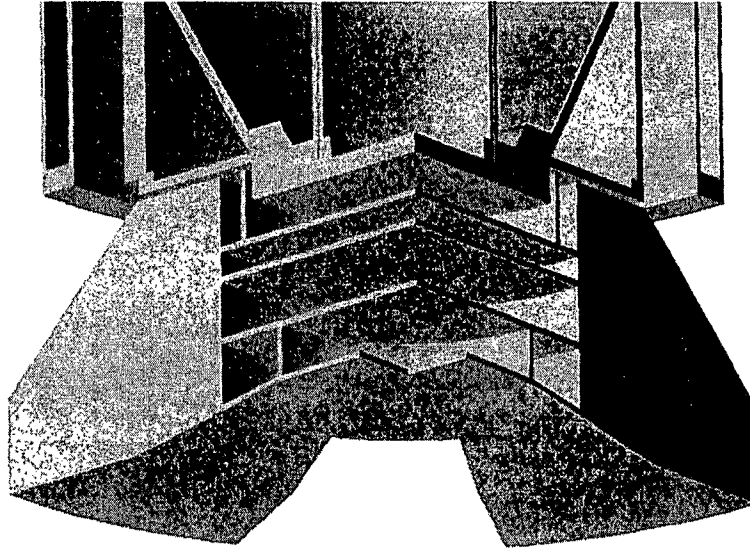


Figure 17: Thermal model (quarter section) showing punch hole

4.7.3 Side

Drop test damage (see Figs 18-22) consisted primarily of partial crushing of one side of the pallet, one of the top shield quadrants and one side of the jacket. The damage was modelled as realistically as possible (Fig 23) by bending up the pallet plates (that being the direction having most effect on gas flow around the container), creating a new outer quadrant surface that best matched the crushed profile and creating a flat in the jacket that best matched the crush damage.

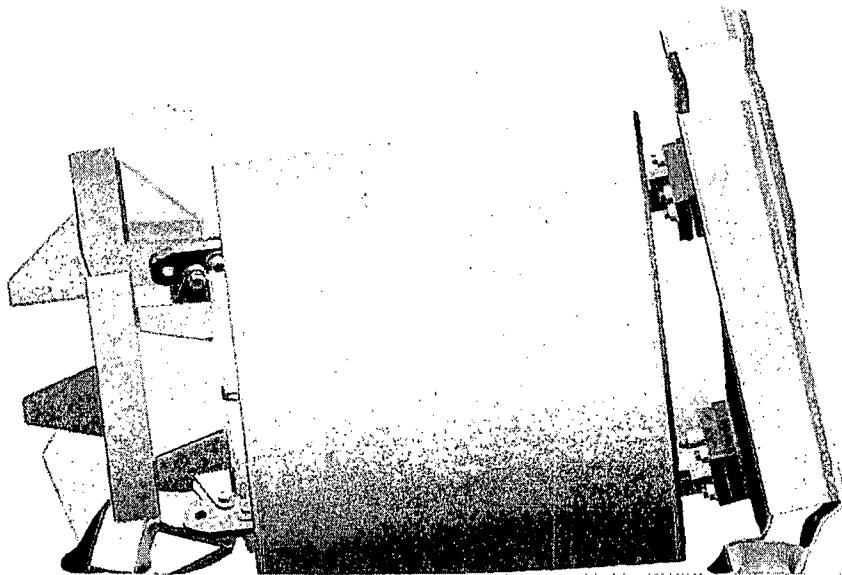


Figure 18: R7021 after 9m side drop (modelled)

090x000 (Drop 15)

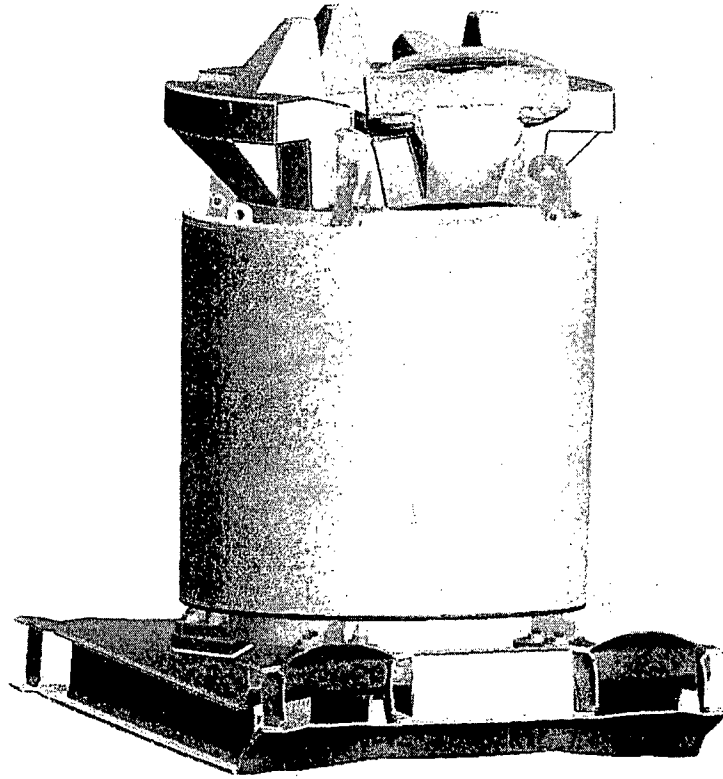


Figure 19: R7021 after 9m side drop (modelled)

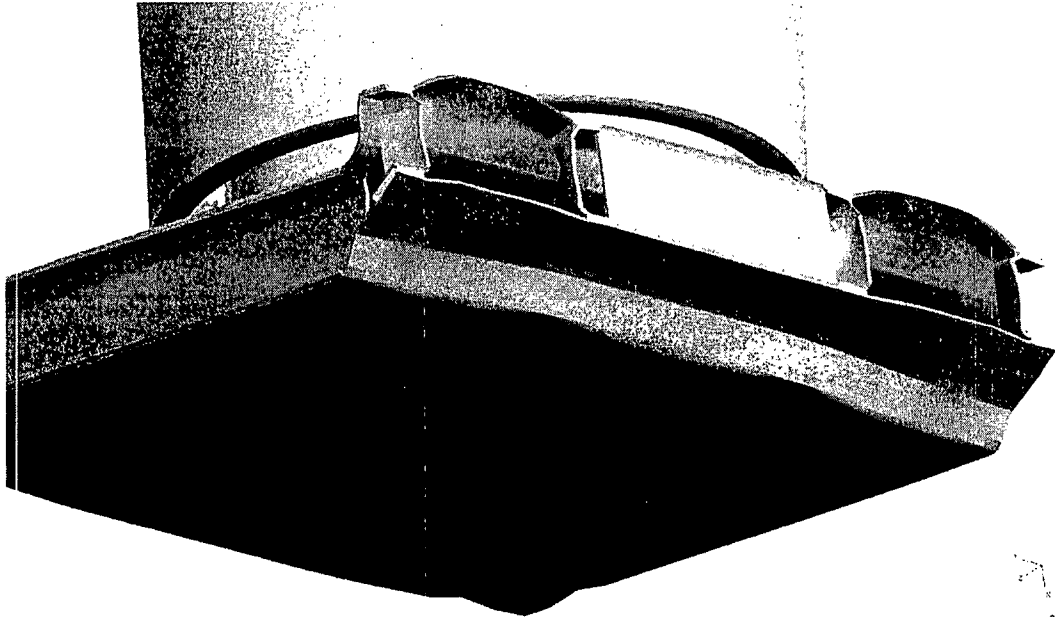
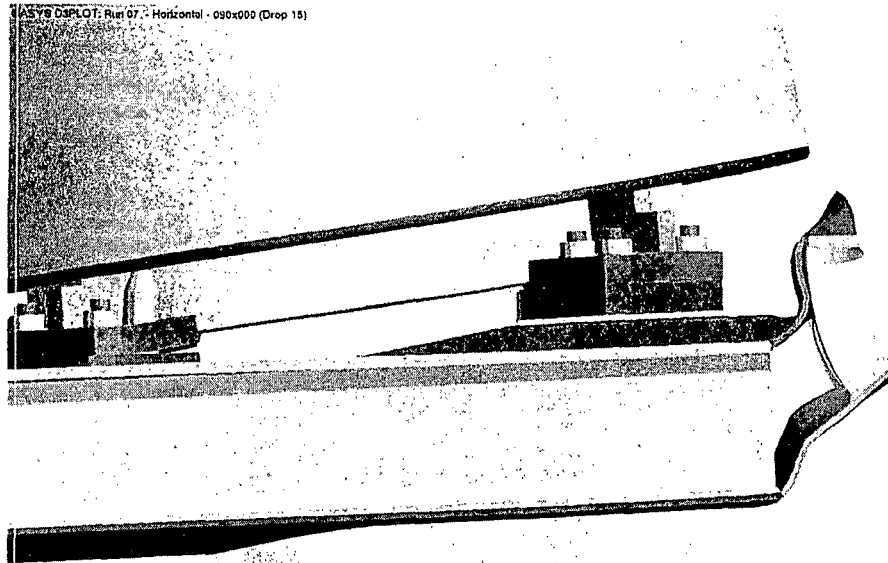


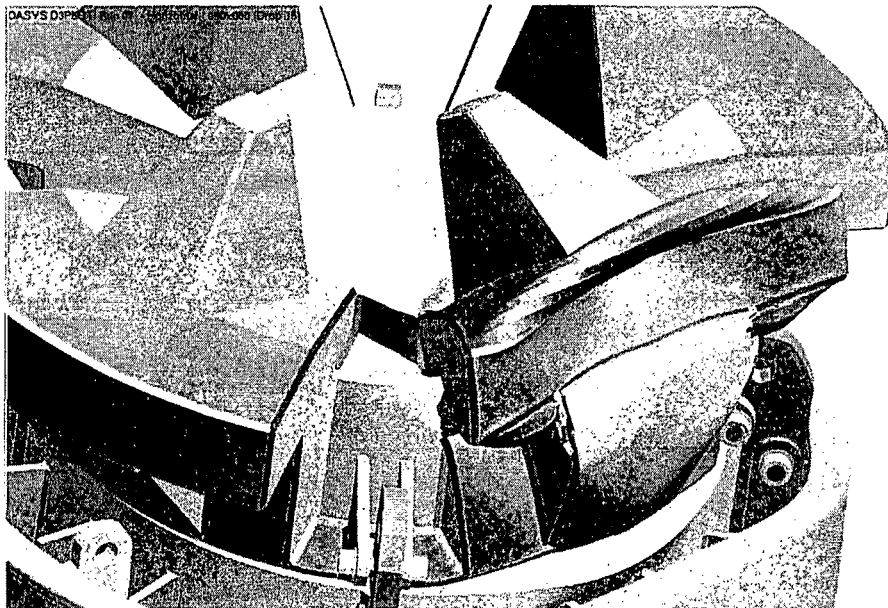
Figure 20: Pallet after 9m side drop (modelled)

0.024275



0.024275

Figure 21: Pallet after 9m side drop (modelled)



0.024275

Figure 22: Top shield after 9m side drop (modelled)

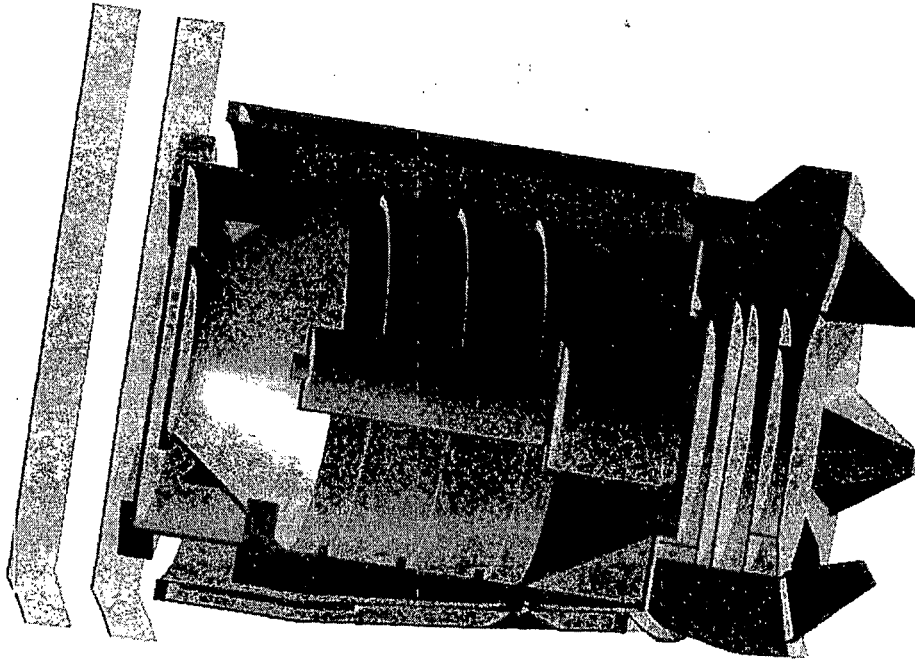


Figure 23: Thermal model (half section) showing 9m side drop damage

Punch damage (see Figs 24-27) consisted primarily of partial penetration of both jacket plates on a 150mm diameter (see RTR 248 & IR 0675). The new jacket design incorporates reinforcement in the area around the drain plug to prevent penetration so the damage was therefore modelled in an unreinforced area where it could still affect the drain plug, i.e. in the same fin channel and still aimed at the centre gravity but angled 25 degrees above the horizontal instead of 25 degrees below it. The actual deformation was modelled as realistically as possible (Fig 28).

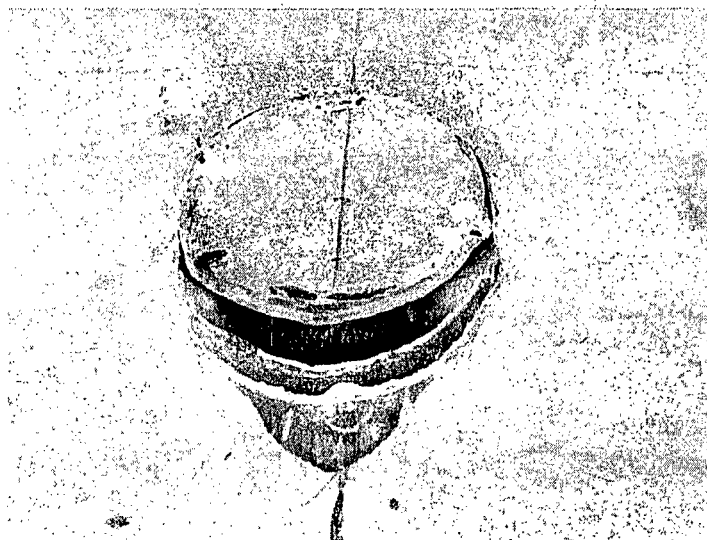


Figure 24: Partial penetration of jacket after 1m punch

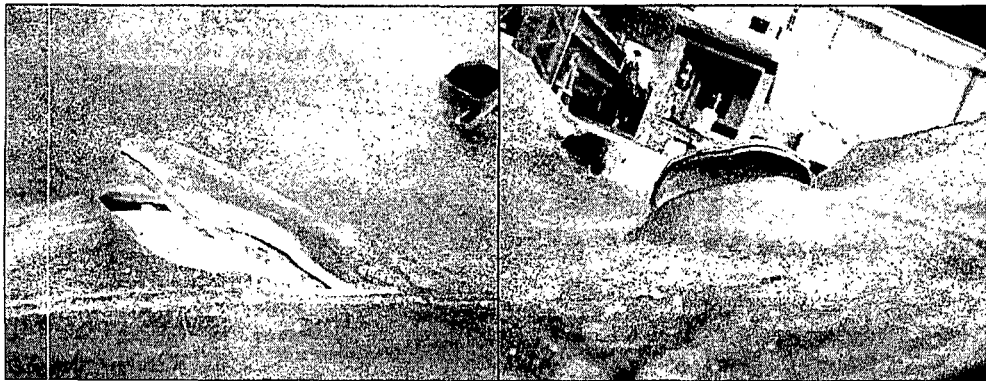


Figure 25: Shearing of jacket outer and inner skins from angled side punch

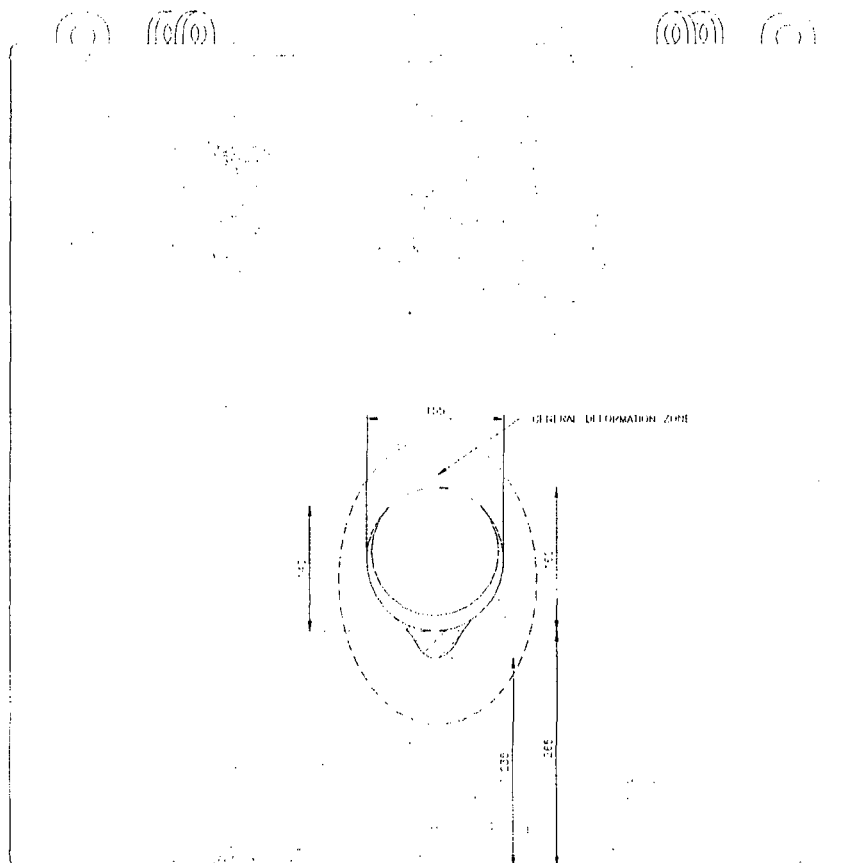


Figure 26: Punch penetration

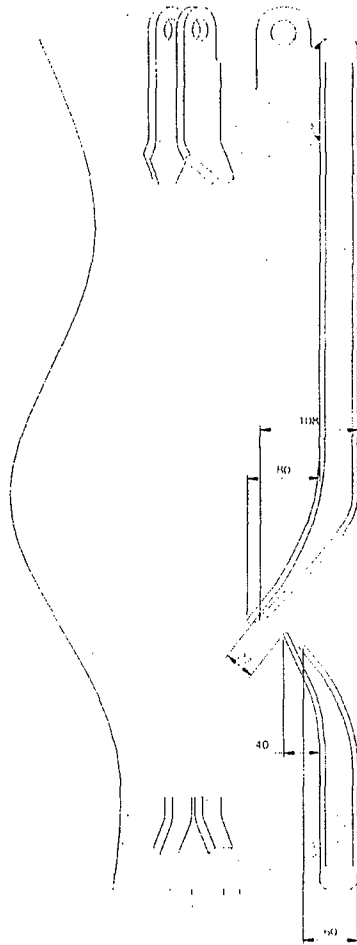


Figure 27: Section through jacket damage

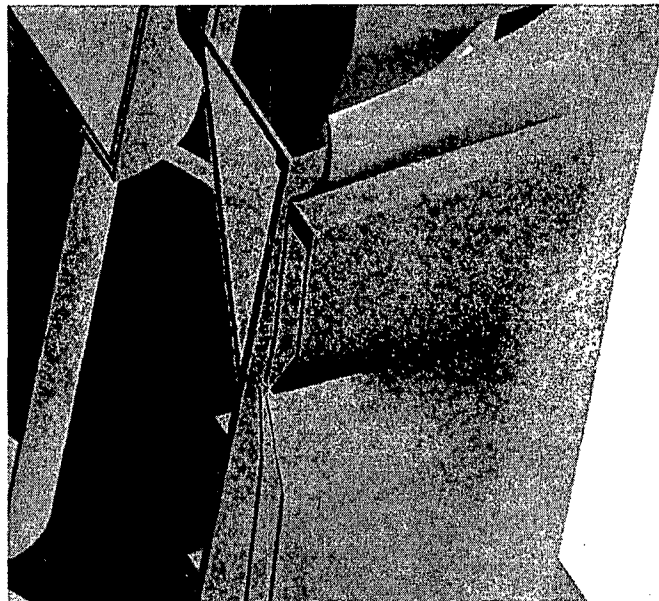


Figure 28: Thermal model (half section) showing punch hole

4.7.4 Package Results

Location	Peak A/C Temperatures (with damage) [°C]			
	Normal Form			Special Form
	Upright	Inverted	Side	Inverted
Cavity wall (mid-height)	273	293	288	316
Maximum lead temperature	271	284	279	302
Closure flange (20mm below upper surface, 50mm from outer edge)	253	253	253	-
Drain point (centre of cylinder, 80mm from outer surface)	228	261	256	-

The maximum peak closure flange temperature was 259°C (Section 4.6, upright and undamaged case). The maximum reverse temperature gradient was 3°C (Appendix 3, R7110/1.1).

4.8 CONTENTS RESULTS

The maximum cavity wall temperature in each orientation was used to model the contents in each orientation:

Orientation and Condition	Temperature [°C]	
	Normal Form	Special Form
Upright, undamaged	433	-
Inverted, undamaged	437	-
Inverted, damaged	437	471
Side, undamaged	435	-

4.9 SURFACE TEMPERATURE IN THE SHADE

The maximum temperature of any normally accessible surface in the shade in a 38°C ambient and with the maximum internal heat load is 79°C (see above). Taking the temperature difference (41°C) as proportional to the heat load, i.e. activity, the temperature reduces to 49.5°C when the contents activity is reduced to 2.08 PBq.

4.10 ADJACENT CARGO

The design of the package is such that adjacent cargo cannot affect its temperature. The pallet prevents other cargo from coming close to the jacket and restricting the free movement of air around the package.

5. CONCLUSIONS

5.1 NORMAL AND ACCIDENT CONDITIONS SUMMARY

Location	Normal Form - Peak Temperatures [°C]		
	Equilibrium in the shade (@ 38°C)	Equilibrium in the sun (@ 38°C)	Thermal Test (maximum with or without drop test damage)
Closure flange (50mm from outer edge)	135	142	259
Drain point (centre of cylinder, 80mm from outer surface)	139	144	262
Maximum reverse gradient in closure flange	-	-	3
	Special Form - Peak Temperatures [°C]		
Capsule wall	409	411	471
Cavity wall (mid-height)	201	205	316
Maximum lead temperature	186	191	302
Closure flange (50mm from outer edge)	141	150	270
Flask wall (mid-height, midway between fins)	149	153	287
Lifting fin (40mm from top edge, 55mm from outer edge)	79	93	-
Flask foot (top surface, 30mm from outer edge)	50	67	-
Top shield (top surface centre)	57	100	-

5.2 NOTES

1. The thermal performance of the R7021 is not sensitive to IAEA normal or accident conditions mechanical testing.
2. The R7021 should be transported under "Exclusive Use" conditions when carrying more than 2.08 PBq of Co⁶⁰.
3. No accessible surface exceeds 85°C under normal conditions of transport in the shade.
4. The thermal performance of the R7021 is not significantly affected by adjacent cargo.
5. The current issue of the manufacturing drawings is detailed in QS7021 issue 5. RTM 151 details all the changes made to the design from QS7021 issue 4. None have any thermal significance therefore the results and conclusions from this document remain valid.

6. REFERENCES

- ANSYS CFD V12, ANSYS Inc., Canonsburg, 2009.
- C15788/TR/0001 issue 2: Impact assessment of the Reviss R7021 package, AMEC Ltd.
- IR 0675 issue 1: 3981/01 inspection after accident conditions testing, REVISS Services (UK) Ltd.
- QS 7021 issue 2: R7021 Transport container drawings List and drawings, REVISS Services (UK) Ltd.
- QS 7021 issue 4: R7021 Transport container drawings List and drawings, REVISS Services (UK) Ltd.
- QS 7021 issue 5: R7021 Transport container drawings List and drawings, REVISS Services (UK) Ltd.
- R7110/1.1: Thermal Analysis of the R7021 Radioactive Materials Transport Container, FTT Technology, July 2010.
- R7410/1.1: Thermal Analysis of the R7021 Radioactive Materials Transport Container at 3074W Internal Heat Load, FTT Technology, July 2010.
- RTM 025: Nuclide Heating, REVISS Services (UK) Ltd.
- RTM 151 issue 1: R7021 Transport Container Design Justification, REVISS Services (UK) Ltd.
- RTR 233 issue 1: 3981/01, 1.2m Free Drop Test- Upright, REVISS Services (UK) Ltd.
- RTR 234 issue 1: 3981/01, 1.2m Free Drop Test- Side Horizontal, REVISS Services (UK) Ltd.
- RTR 235 issue 1: 3981/01, 1.2m Free Drop Test- Vertical Inverted, REVISS Services (UK) Ltd.
- RTR 236 issue 1: 3981/01, 1.0m Penetration Bar onto Jacket, REVISS Services (UK) Ltd.
- RTR 239 issue 1: 3981/01, 1.0m Punch Test- Angled Upright, REVISS Services (UK) Ltd.
- RTR 242 issue 1: 3981/01, 1.0m Punch Test- Angled Inverted, REVISS Services (UK) Ltd.
- RTR 248 issue 1: 3981/01, 1.0m Punch Test- Angled Side, REVISS Services (UK) Ltd.
- TS-G-1.1 (Rev. 1): Advisory Material for the IAEA Regulations for the Safe Transport of Radioactive Material, IAEA, Vienna, 2008.
- TS-R-1: Regulations for the Safe Transport of Radioactive Material, 2005 Edition, IAEA, Vienna.

10 CFR 72, Subpart K, "General License for Storage of Spent Fuel at Power Reactor Sites,"
Regulatory Issues

BACKGROUND

There are several long standing 10 CFR Part 72, Subpart K issues that have created significant confusion to internal and external NRC stakeholders. Background is provided below.

1. 10 CFR 72.212 - Conditions of general license issued under § 72.210.

(a)(1) The general license is limited to that spent fuel which the general licensee is authorized to possess at the site under the specific license for the site.

(2) This general license is limited to storage of spent fuel in casks approved under the provisions of this part.

§ 72.3 Definitions

Spent fuel storage cask or cask means all the components and systems associated with the container in which spent fuel or other radioactive materials associated with spent fuel are stored in an ISFSI.

2. 10 CFR 72.214 List of approved spent fuel storage casks.

§ 72.244 Application for amendment of a certificate of compliance.

Whenever a certificate holder desires to amend the CoC (including a change to the terms, conditions or specifications of the CoC), an application for an amendment shall be filed with the Commission fully describing the changes desired and the reasons for such changes, and following as far as applicable the form prescribed for original applications.

§ 72.246 Issuance of amendment to a certificate of compliance.

In determining whether an amendment to a CoC will be issued to the applicant, the Commission will be guided by the considerations that govern the issuance of an initial CoC.

ISSUES REQUESTING OGC GUIDANCE AND RESOLUTION

1. Despite the definition of *cask* provided in § 72.3, there is still general confusion regarding the specific bounds of systems, structures, and components that are to be considered part of the CoC or its amendments. Clarification is requested regarding the extent of changes that should be allowed to be considered as an amendment to an existing certificate, versus requiring assignment as a new cask system CoC.
2. The current guidance is to treat CoC amendments as stand-alone systems. General licensees are required to comply with the provisions of the CoC amendment and supporting Final Safety Analysis Report revision that supports the amendment that they initially identified as using. They must have an approved exemption request in order to adopt the provisions of a different amendment other than the original one identified they identified as using. CoC holders may submit amendment requests, and these are evaluated through the

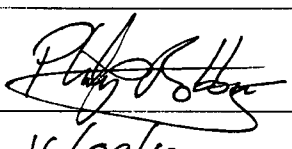
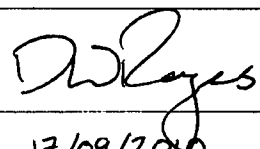
rule making process, and if approved added to the approved cask systems in § 72.214. This process, however, does not provide a regulatory mechanism to allow revising or correcting CoC Technical Specifications identified by either the NRC or the COC holder. Corrections can be made in later CoC amendments, but those changes would only apply to general licensees using the later amendments. OGC guidance is requested regarding the regulatory process currently allowed by the regulations that would allow the NRC to make these types of revisions / corrections to existing approved CoCs and their amendments.



**REVISS Services
Quality and Regulatory Group**

Technical Memorandum

**Performance of the R7021 (GB 3981) Transport
Container under IAEA Tie-Down Loads**

Author:		Reviewer:	
Name	P J G Robbins	Name	D W Rogers
Signature		Signature	
Date	16/09/10	Date	17/09/2010

1. PURPOSE AND SCOPE

This document analyses the tie-down load paths in the R7021 transport container. It calculates stresses under worst-case accelerations and compares them and the associated fatigue life against the design criteria.

2. DESCRIPTION

The design consists of a shielded, stainless steel flask mounted on a pallet and protected from heat and impact by a jacket and top shield (Figure 1). The maximum gross weight of the design and key sub-assembly are tabulated below.

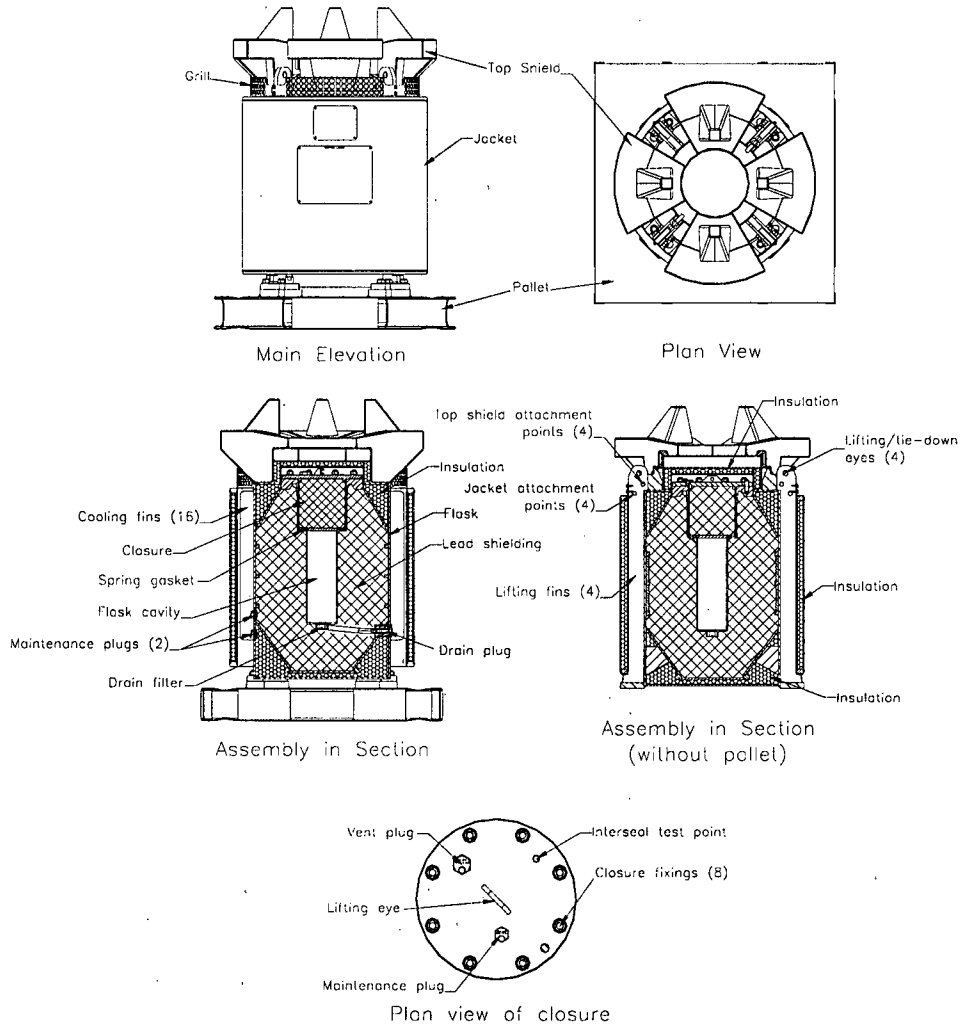


Figure 1: R7021 Assembly

Maximum Gross Assembly Weights (kg)	
Assembly (maximum gross weight)	4,600
Assembly minus pallet (maximum gross weight)	4,350

3. ASSESSMENT

3.1 CRITERIA

- The design strength (yield) shall not be exceeded when the assembly, at normal conditions of transport temperature, is subjected to the simultaneous application, in all three axes, of the worst case regulatory or modal acceleration factors.
- The ability of the design to comply with the Type B(U) requirements specified in TS-R-1 shall not be impaired should the tie-down points be overloaded to failure.
- No component shall be liable to fatigue failure from normal operation during the design life of 50 years.

3.2 ASSUMPTIONS

- Loads spread over more than one component are equally distributed.
- Tie-down members are aligned with the axis of the attachment point.
- Tie-down member shackle pins are diameter 28.6 mm (1 1/8").
- Special tie-down equipment is not used.
- The contribution from friction between components clamped together is ignored.
- Upward accelerations are ignored, as the load path is straight through the pallet into the flask.
- The contribution from the dowels between the pallet and flask is ignored.

3.3 ACCELERATION DATA

Acceleration data is taken from Table IV.1 of TS-G-1.1. The worst case resultant from any modal accelerations is the rail requirement.

Mode	Acceleration (g)			
	Longitudinal	Lateral	Vertical (down)*	Resultant $\sqrt{\Sigma a^2}$
Road	2	1	2	3.00
Rail	5	2	1	5.48
Sea	2	2	1	3.00
Air	1.5	1.5	5	5.43

* Allowing for gravity.

3.4 DESIGN STRENGTHS

Under normal conditions of transport the flask tie-down eyes are at a temperature of 93°C (RTM 120). The flask is fabricated from 1.4307 (304L) plate to BS EN 10088-2. The minimum room temperature yield strength of the components in the load path is 200 N/mm². This reduces to 178 N/mm² at a temperature of 93°C (using by proportion the reduction in design strength cited in PD 5500 for a similar grade steel (304-S11) up to 100°C).

The flask feet are at a temperature of 67°C (RTM 120). The yield strength also reduces to 178 N/mm² using the above method.

The pallet pad welds are at a maximum temperature of 67°C (RTM 120). The pallet is fabricated from S355 carbon manganese steel to BS EN 10025. The minimum room temperature yield strength is 400 N/mm² (drawing R7021/004). This reduces to 371 N/mm² at a temperature of 67°C (using by proportion the reduction in design strength cited in PD 5500 for a similar grade steel (223, 490A) up to 100°C).

Yield strength data for the Grade 8.8 carbon steel studs is taken from BS 3692 and reduced for the normal conditions of transport temperature of 67°C (using by proportion the reduction in design strength cited in PD 5500 up to 100°C).

A summary of the design strengths for each component in the tie-down load path is given below:

Element	Normal Conditions Temperature (°C)	Design Strength (N/mm ²)		
		Tension		Shear* (NCT)
		RT	NCT	
Tie-down eyes	93	200	178	103
Tie-down fin welds	93	200	178	103
Pallet pad welds	67	400	371	214
Flask studs	67	640	580	335
Flask-to-feet welds	67	200	178	103

* Using a factor of 0.577 on tensile strength based on Von Mises' theorem.

3.5 LOAD PATH

Horizontal loads from the chocks are taken directly into the pallet and into the flask fixings and feet welds. Vertical loads from toppling moments and vertical accelerations are taken through the tie-down eyes and their attaching welds into the flask body.

3.6 RESTRAINED MASSES

The mass restrained by each element in the load path is:

Element	Restrained Mass (kg)
Tie-down eyes	4,600
Tie-down fin welds	
Pallet pad welds	4,350
Flask studs	
Flask-to-feet welds	

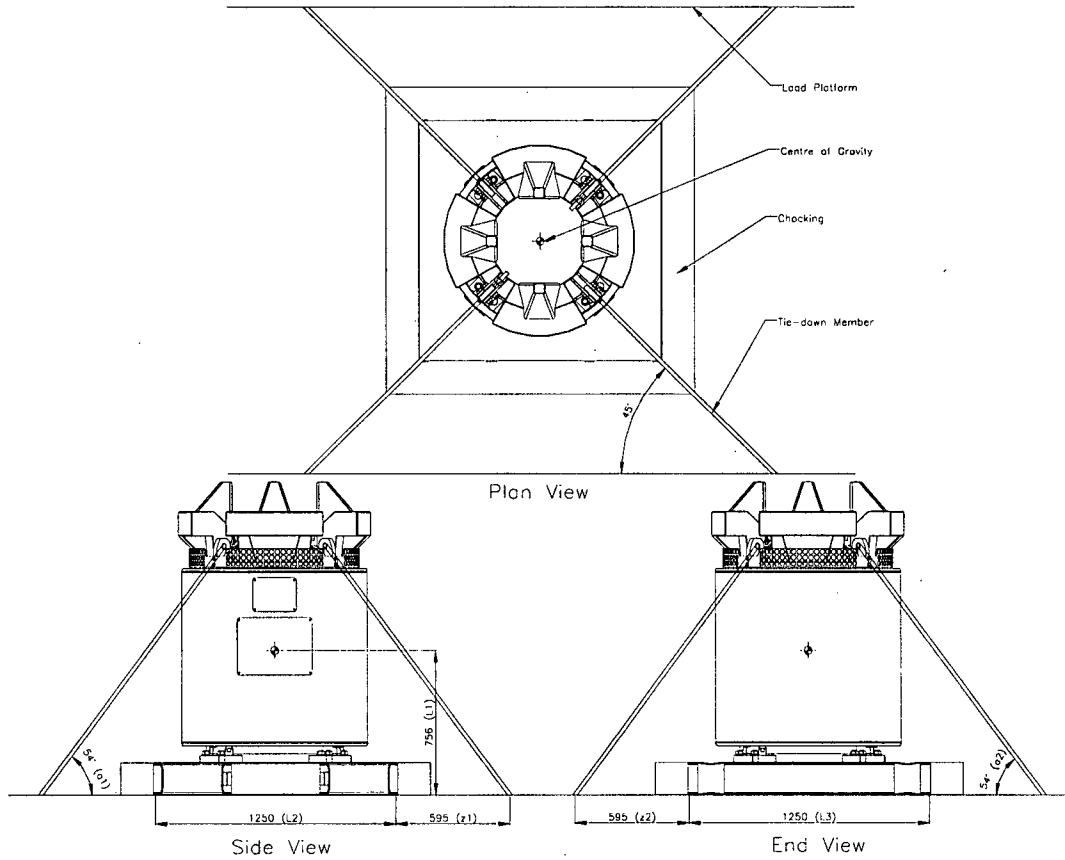


Figure 2: R7021 Tie-down Arrangement

3.7 RESTRAINT LOADS

The maximum tie-down load in each element in each of the three axes is therefore:

Element	W, Restraint Load (kN)		
	Longitudinal (W_{lon})	Lateral (W_{lat})	Vertical down (W_{ver})
Tie-down eyes	226	90.3	45.1
Tie-down fin welds			
Pallet pad welds			
Flask studs			
Flask-to-feet welds	213	85.3	42.7

4. ANALYSIS

4.1 TIE-DOWN EYES

The analysis will consider the load generated by each acceleration in turn and then combine them to arrive at the maximum stress generated in each component in the tie-down eye load path.

4.1.1 Stresses in tie-down eyes

(a) Longitudinal acceleration loads are taken primarily by the chocking but a toppling moment will be generated which will create an upwards force, W_1 , on each of the two eyes at the opposite end. The force is proportional to the height of the centre of gravity and inversely proportional to the distance from the tie-down point to the chocked edge of the pallet. This force is resisted however by gravity acting downwards on the package. The symmetry of the design puts the centre of gravity at its mid-length and mid-width and so the gravitational force may be taken as one quarter of the package mass acting at each corner. The load on each eye, W_1 , is therefore:

$$W_1 = \frac{(W_{lon} \times L_1) - (M \times g \times 0.5 \times L_2)}{N \times (L_2 + z_1) \times \sin a_1 \times \sin a_2}$$

where

W_{lon} = longitudinal acceleration load = 226 kN

L_1 = height of package CoG = 0.756 m

M = package mass = 4,600 kg

g = gravitational acceleration = 9.81 m/s²

L_2 = floor length of pallet = 1.25 m

z_1 = longitudinal distance from pallet to tie-down point = 0.595 m

N = number of tie-down eyes under load = 2

a_1 = tie-down angle from horizontal (viewed from the side) = 54°

a_2 = tie-down angle from horizontal (viewed from the end) = 54°

thus

$$W_1 = \frac{(226 \times 10^3 \times 0.756) - (4,600 \times 9.81 \times 0.5 \times 1.25)}{2 \times (1.25 + 0.595) \times 0.809 \times 0.809} = 59.1 \text{ kN}$$

(b) Lateral acceleration loads are taken primarily by the chocking but a toppling moment will be generated which will create an upwards force, W_2 , on each of the two eyes on the opposite side. The force is proportional to the height of the centre of gravity and inversely proportional to the distance from the tie-down point to the chocked edge of the pallet. Again the force is resisted by gravity. The load on each eye, W_2 , is therefore:

$$W_2 = \frac{(W_{lat} \times L_1) - (M \times g \times 0.5 \times L_3)}{N \times (L_3 + z_2) \times \sin a_1 \times \sin a_2}$$

where

W_{lat} = lateral acceleration load = 90.3 kN

L_3 = floor width of pallet = 1.25 m

z_2 = lateral distance from pallet to tie-down point = 0.595 m

N = number of tie-down eyes under load = 2

a_1 = tie-down angle from horizontal (viewed from the side) = 54°

a_2 = tie-down angle from horizontal (viewed from the end) = 54°

thus

$$W_2 = \frac{(90.3 \times 10^3 \times 0.756) - (4,600 \times 9.81 \times 0.5 \times 1.25)}{2 \times (1.25 + 0.595) \times 0.809 \times 0.809} = 16.6 \text{ kN}$$

- (c) Vertical acceleration loads create an upwards force on all of the tie-down eyes. The load on each eye, W_3 , is therefore:

$$W_3 = \frac{W_{\text{ver}}}{N \times \sin a_1 \times \sin a_2}$$

where

W_{ver} = vertical acceleration load = 45.1 kN

N = number of tie-down eyes under load = 4

a_1 = tie-down angle from horizontal (viewed from the side) = 54°

a_2 = tie-down angle from horizontal (viewed from the end) = 54°

thus

$$W_3 = \frac{45.1 \times 10^3}{4 \times 0.809 \times 0.809} = 17.2 \text{ kN}$$

- (d) Bearing stress in eye:

The combined load from each of the three accelerations above is the sum of all three. The load is resisted by the tie-down member and its shackle pin generates compressive (bearing) stress in the eye (see Fig 3). The stress, S , is therefore:

$$S = \frac{W_1 + W_2 + W_3}{A}$$

where

A = projected contact area of shackle pin = $D \times L$

Where

D = shackle pin diameter = 28.6 mm

L = length of contact = 25.0 mm

thus

$$A = 28.6 \times 25.0 = 715 \text{ mm}^2$$

thus

$$S = \frac{(59.1 + 16.6 + 17.2) \times 10^3}{715} = 130 \text{ N/mm}^2$$

- (e) Pull-out stress in eye:

The load is resisted by the tie-down member and its shackle pin may be considered to create two shear planes (Fig 3) in the eye as it attempts to pull through the eye plate. The shear stress, S_1 , in these planes is therefore:

$$S_1 = \frac{W_1 + W_2 + W_3}{A_1}$$

where

A_1 = total area of shear planes = $(25 \times 59.0) + (25 \times 84.1) = 3,580 \text{ mm}^2$

thus

$$S_1 = \frac{(59.1 + 16.6 + 17.2) \times 10^3}{3,580} = 25.9 \text{ N/mm}^2$$

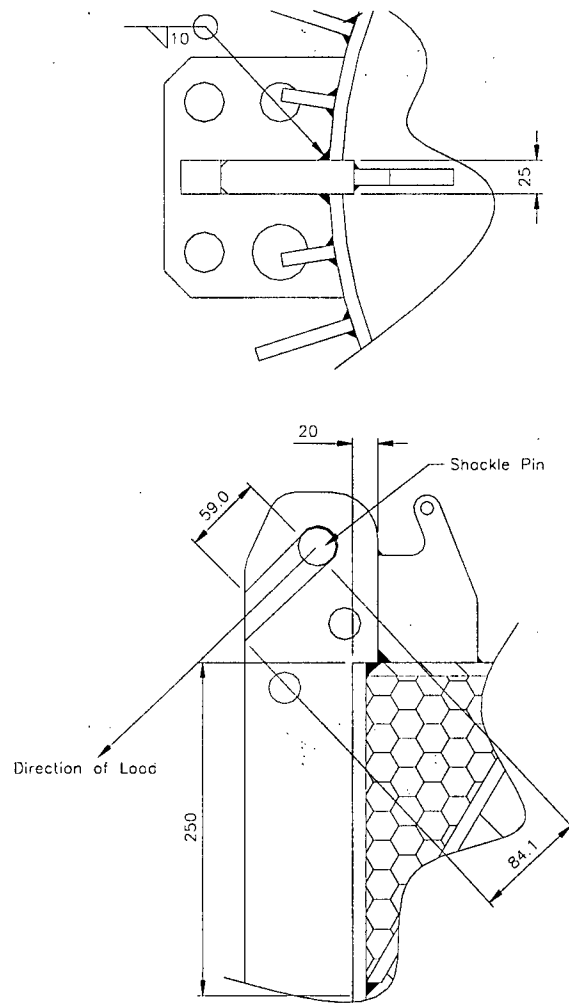


Figure 3: Tie-down eye details

4.1.2 Stress in tie-down fin weld

The load from each acceleration will be the same as above therefore the maximum load will be the sum again. The shear stress, S_2 , generated in the fin weld is therefore:

$$S_2 = \frac{W_1 + W_2 + W_3}{A_2}$$

where

A_2 = cross-sectional area of weld = $l \times t$

where

l = weld length = $2(250^* + 20) = 540$ mm

t = weld throat width = $10 \times 0.707 = 7.07$ mm

* (stressed vertical length of weld is taken as 250mm on each side of the fin)

thus $A_2 = 540 \times 7.07 = 3,820 \text{ mm}^2$

thus
$$S_2 = \frac{(59.1 + 16.6 + 17.2) \times 10^3}{3,820} = 24.3 \text{ N/mm}^2$$

4.2 PALLET

The flask is supported on a square pallet fabricated from carbon steel plate. The two are held together with twelve carbon steel, M24 studs and nuts. The studs are secured into carbon steel pads that are welded to the main pallet surface. The studs and welds are subject to shear loads from horizontal accelerations.

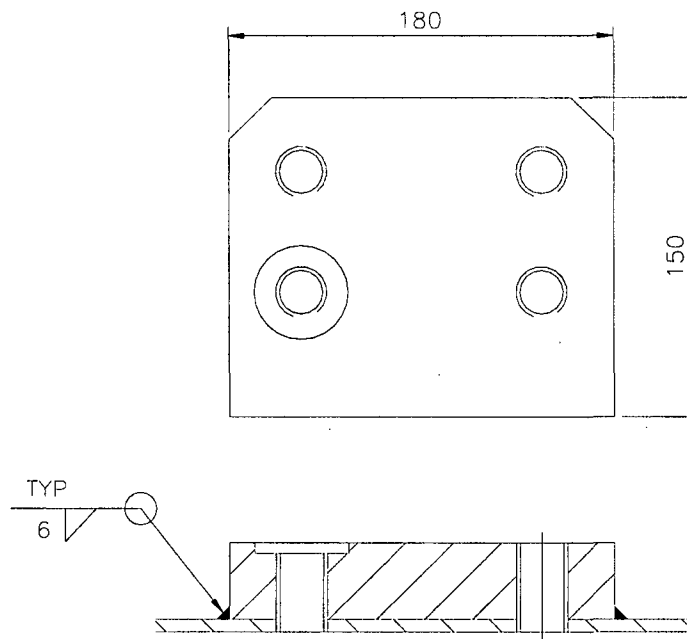


Figure 4: Pallet pad details

4.2.1 Pallet welds

- (a) Longitudinal acceleration loads generate a longitudinal shear stress, S_3 , in the welds:

$$S_3 = \frac{W_{\text{lon}}}{A_3}$$

where

$$A_3 = N \times A$$

where

N = number of pads = 4

A = cross-sectional area of weld = $l \times t$

where

l = weld length = $2(180 + 150) = 660 \text{ mm}$

t = weld throat width = $6 \times 0.707 = 4.24 \text{ mm}$

thus $A_3 = 4 \times (660 \times 4.24) = 11,200 \text{ mm}^2$

and $S_3 = \frac{213 \times 10^3}{11,200} = 19.0 \text{ N/mm}^2$

(b) Lateral acceleration loads generate a lateral shear stress, S_4 , in the welds:

$$S_4 = \frac{W_{lat}}{A_3}$$

thus $S_4 = \frac{85.3 \times 10^3}{11,200} = 7.62 \text{ N/mm}^2$

(c) Vertical acceleration loads generate no stresses in the welds.

(d) Load combination stress

The maximum stress is found when the three acceleration loads are applied simultaneously.

The maximum normal and shear stresses are found using the tri-axial stress analysis methodology. Thus:

S_x = normal longitudinal stress = 0

S_y = normal vertical stress = 0

S_z = normal lateral stress = 0

S_{xy} = vertical shear = 0 N/mm^2

S_{yz} = lateral shear = 7.62 N/mm^2

S_{zx} = longitudinal shear = 19.0 N/mm^2

A = $S_x + S_y + S_z = 0$

B = $S_x \cdot S_y + S_y \cdot S_z + S_z \cdot S_x - S_{xy}^2 - S_{yz}^2 - S_{zx}^2 = -419$

C = $S_x \cdot S_y \cdot S_z + 2 \cdot S_{xy} \cdot S_{yz} \cdot S_{zx} - S_x \cdot S_{yz}^2 - S_y \cdot S_{zx}^2 - S_z \cdot S_{xy}^2 = 0$

D = $A^2/3 - B = 419$

E = $A \times B/3 - C - 2A^3/27 = 0$

F = $\sqrt{(D^3/27)} = 1,651$

G = $\cos^{-1}(-E/2F) = 90.0^\circ$

H = $\sqrt{(D/3)} = 11.8$

the principal stresses are therefore:

I = $2 \cdot H \cdot \cos(G/3) + A/3 = 20.5 \text{ N/mm}^2$

J = $2 \cdot H \cdot \cos(G/3 + 120^\circ) + A/3 = -20.5 \text{ N/mm}^2$

K = $2 \cdot H \cdot \cos(G/3 + 240^\circ) + A/3 = 0 \text{ N/mm}^2$

S_5 , the maximum principal normal (tensile) stress, is therefore 20.5 N/mm^2

S_6 , the maximum shear stress, is $0.5(S_5 - S_{min}) = 20.5 \text{ N/mm}^2$

4.2.2 Pallet fixings

- (a) Longitudinal acceleration loads generate a longitudinal shear stress, S_7 , in the fixings:

$$S_7 = \frac{W_{\text{lon}}}{A_4}$$

where

$$A_4 = N \times A_t$$

where

N = number of bolts = 12

A_t = tensile stress area of M24 bolt = 353 mm² (BS 3643)

$$\text{thus } A_4 = 12 \times 353 = 4,240 \text{ mm}^2$$

$$\text{and } S_7 = \frac{213 \times 10^3}{4,240} = 50.2 \text{ N/mm}^2$$

- (b) Lateral acceleration loads generate a lateral shear stress, S_5 , in the flask fixings:

$$S_8 = \frac{W_{\text{lat}}}{A_4}$$

$$\text{thus } S_8 = \frac{85.3 \times 10^3}{4,240} = 20.1 \text{ N/mm}^2$$

- (c) Vertical acceleration loads generate no stresses in the fixings.

- (d) Load combination stress

The maximum stress is found when the two acceleration loads are applied simultaneously.

The maximum normal and shear stresses are found using the tri-axial stress analysis methodology. Thus:

S_x = normal longitudinal stress = 0

S_y = normal vertical stress = 0

S_z = normal lateral stress = 0

S_{xy} = vertical shear = 0

S_{yz} = lateral shear = 20.1 N/mm²

S_{zx} = longitudinal shear = 50.2 N/mm²

$$A = S_x + S_y + S_z = 0$$

$$B = S_x \cdot S_y + S_y \cdot S_z + S_z \cdot S_x - S_{xy}^2 - S_{yz}^2 - S_{zx}^2 = -2,924$$

$$C = S_x \cdot S_y \cdot S_z + 2 \cdot S_{xy} \cdot S_{yz} \cdot S_{zx} - S_x \cdot S_{yz}^2 - S_y \cdot S_{zx}^2 - S_z \cdot S_{xy}^2 = 0$$

$$D = A^2/3 - B = 2,924$$

$$E = A \times B/3 - C - 2A^3/27 = 0$$

$$F = \sqrt{(D^3/27)} = 30,430$$

$$G = \cos^{-1}(-E/2F) = 90^\circ$$

$$H = \sqrt{(D/3)} = 31.2$$

the principal stresses are therefore:

$$I = 2 \cdot H \cdot \cos(G/3) + A/3 = 54.1 \text{ N/mm}^2$$

$$J = 2 \cdot H \cdot \cos(G/3 + 120^\circ) + A/3 = -54.1 \text{ N/mm}^2$$

$$K = 2 \cdot H \cdot \cos(G/3 + 240^\circ) + A/3 = 0 \text{ N/mm}^2$$

S_9 , the maximum principal normal (tensile) stress, is therefore 54.1 N/mm^2

S_{10} , the maximum shear stress, is $0.5(S_9 - S_{\min}) = 54.1 \text{ N/mm}^2$

4.3 FLASK AND SUPPORTS

The flask is supported on four feet that are welded to its base. The feet welds will be subject to shear loads generated by horizontal accelerations.

4.3.1 Flask feet welds

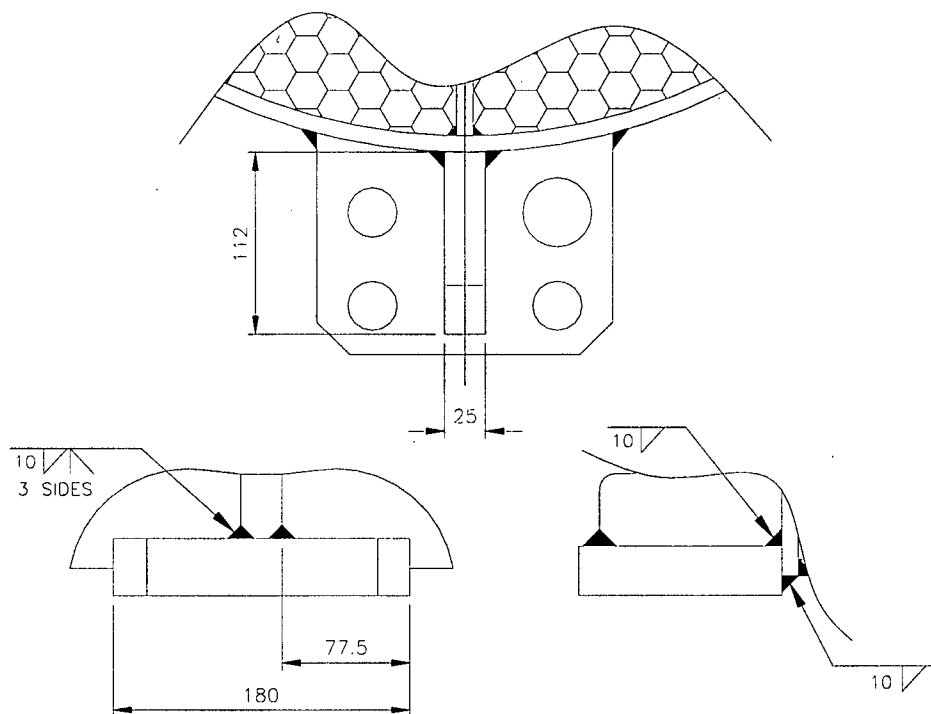


Figure 5: Flask feet details

- (a) Longitudinal acceleration loads generate a longitudinal shear stress, S_{11} , in the welds:

$$S_{11} = \frac{W_{\text{lon}}}{A_5}$$

where

$$A_5 = N \times A$$

where

$$N = \text{number of feet} = 4$$

$$A = \text{cross-sectional area of weld} = l_1 \times t_1 + l_2 \times t_2$$

where

$$l_1 = \text{fillet weld length} = 2 \times 77.5 + 180 = 335 \text{ mm}$$

$$l_2 = \text{weld length} = 2 \times 112 + 25 = 249 \text{ mm}$$

$$t_1 = \text{fillet weld throat width} = 10 \times 0.707 = 7.07 \text{ mm}$$

$$t_2 = \text{weld throat width} = 10 \text{ mm}$$

$$\text{thus } A_5 = 4 \times (335 \times 7.07 + 249 \times 10) = 19,400 \text{ mm}^2$$

$$\text{and } S_{11} = \frac{213 \times 10^3}{19,400} = 11.0 \text{ N/mm}^2$$

- (b) Lateral acceleration loads generate a lateral shear stress, S_{4} , in the flask fixings:

$$S_{12} = \frac{W_{\text{lat}}}{A_3}$$

$$\text{thus } S_{12} = \frac{85.3 \times 10^3}{19,400} = 4.40 \text{ N/mm}^2$$

- (c) Vertical acceleration loads generate no stresses in the fixings.

- (d) Load combination stress

The maximum stress is found when the two acceleration loads are applied simultaneously.

The maximum normal and shear stresses are found using the tri-axial stress analysis methodology. Thus:

$$S_x = \text{normal longitudinal stress} = 0$$

$$S_y = \text{normal vertical stress} = 0$$

$$S_z = \text{normal lateral stress} = 0$$

$$S_{xy} = \text{vertical shear} = 0$$

$$S_{yz} = \text{lateral shear} = 4.40 \text{ N/mm}^2$$

$$S_{zx} = \text{longitudinal shear} = 11.0 \text{ N/mm}^2$$

$$A = S_x + S_y + S_z = 0$$

$$B = S_x \cdot S_y + S_y \cdot S_z + S_z \cdot S_x - S_{xy}^2 - S_{yz}^2 - S_{zx}^2 = -140$$

$$C = S_x \cdot S_y \cdot S_z + 2 \cdot S_{xy} \cdot S_{yz} \cdot S_{zx} - S_x \cdot S_{yz}^2 - S_y \cdot S_{zx}^2 - S_z \cdot S_{xy}^2 = 0$$

$$D = A^2/3 - B = 140$$

$$E = A \times B/3 - C - 2A^3/27 = 0$$

$$F = \sqrt{(D^3/27)} = 320$$

$$G = \cos^{-1}(-E/2F) = 90^\circ$$

$$H = \sqrt{(D/3)} = 6.8$$

the principal stresses are therefore:

$$\begin{aligned} I &= 2.H.\cos(G/3) + A/3 = 11.8 \text{ N/mm}^2 \\ J &= 2.H.\cos(G/3 + 120^\circ) + A/3 = -11.8 \text{ N/mm}^2 \\ K &= 2.H.\cos(G/3 + 240^\circ) + A/3 = 0 \text{ N/mm}^2 \end{aligned}$$

S_{13} , the maximum principal normal (tensile) stress, is therefore 11.8 N/mm^2

S_{14} , the maximum shear stress, is $0.5(S_{13} - S_{\min}) = 11.8 \text{ N/mm}^2$

4.6 SUMMARY OF STRESSES

The stress levels and safety factors in the various elements of the R7021 structure under the worst case combined tie-down accelerations are summarised as follows:

Structural Element	Design Strength (N/mm ²)	Stress Type	Maximum Stress (N/mm ²)	Safety Factor
Tie-down eyes	178	bearing	130	1.37
	103	shear	25.9	1.80
Fin welds	103	shear	24.3	3.98
Pallet-to-pad welds	214	shear	20.5	10.4
Flask-to-pallet studs	335	shear	54.1	6.19
Flask feet welds	103	shear	11.8	8.73
Minimum Safety Factor				1.37

5. FATIGUE

TCSC 1006 Appendix, Section d), provides a method for demonstrating the likelihood of fatigue failure over the design life of a transport container. By dividing the range of accelerations experienced in any particular mode of transport into discreet subsets it is possible to calculate the stress range for each subset and hence the allowable number of cycles. Knowing the actual number of cycles likely to be experienced in the container's design life it is then possible to calculate the proportion of the fatigue life "used up" by each subset. A satisfactory fatigue case is made when the sum of the proportions is less than 1. The calculations are laid out in the Table below.

This container is shipped almost exclusively by road and sea. Of these two modes, road transport is by far the more demanding for fatigue considerations. TCSC 1006 Table 6 gives the frequency of different longitudinal, lateral and vertical accelerations recorded during a road shipment of a 20' ISO freight container with a 10 tonne load.

The highest non-compressive stress in the R7021 structure is the shear stress generated in the flask-to-pallet studs (see 4.2.2 (d)). The stress at other accelerations is calculated using the method in Section 4.2.2 of this document. Equation C-5 in PD 5500, Annex C, paragraph 3.1.2 is then used to calculate the allowable number of cycles at each stress.

The actual number of cycles is based on an estimate of the container's lifetime usage. UK shipments are entirely by road and on average 300 miles round trip. International shipments are made by sea to the nearest port, with road journeys at either end. The average distance from port to final destination does not exceed 400 miles. Therefore an average road round trip for the R7021 may reasonably be taken as 1,000 miles. Hence, for a nominal design life of fifty years and 12 shipments per year, a container could be shipped a total of 600,000 miles in

its lifetime. Assuming an average speed of 30 mph, the lifetime duration therefore would be 20,000 hours.

Table 6 gives the total number of cycles per 1,000 hours for each acceleration (load case) so these are multiplied by twenty to obtain the total number of cycles. Dividing the total number of cycles by the allowable number of cycles gives the fatigue life proportion for each load case:

Axis	Acceleration (g)	Stress range (N/mm ²)	Allowable number of cycles	Number of cycles per 1,000 hrs	Number of cycles for 20,000 hrs	Proportion of allowable cycles
Longitudinal	0.4	2.0*	NA	1.12E+07	2.23E+08	0.00E+00
	0.8	4.0*	NA	1.93E+06	3.86E+07	0.00E+00
	1.2	6.0	7.23E+08	9.95E+04	1.99E+06	2.75E-03
	1.6	8.0	3.05E+08	5.36E+03	1.07E+05	3.52E-04
	2	10.0	1.56E+08	491	9.82E+03	6.29E-05
Lateral	0.2	0.8*	NA	1.12E+07	2.23E+08	0.00E+00
	0.4	1.6*	NA	1.93E+06	3.86E+07	0.00E+00
	0.6	2.4*	NA	9.95E+04	1.99E+06	0.00E+00
	0.8	3.2*	NA	5.36E+03	1.07E+05	0.00E+00
	1	4.0*	NA	491	9.82E+03	0.00E+00
Vertical	0.4	0.0*	NA	1.12E+07	2.23E+08	0.00E+00
	0.8	0.0*	NA	1.93E+06	3.86E+07	0.00E+00
	1.2	0.0*	NA	9.95E+04	1.99E+06	0.00E+00
	1.6	0.0*	NA	5.36E+03	1.07E+05	0.00E+00
	2	0.0*	NA	491	9.82E+03	0.00E+00
Sum of fatigue life proportions						3.17E-03

* Does not exceed 5 N/mm², hence fatigue analysis is not required (para. C.2.2, PD 5500).

It is evident therefore that the tie-down points are not at risk from fatigue failure during the design life.

6. CONCLUSIONS

- Design Criteria: The R7021 transport container meets its design criteria and the tie-down requirements for Type B(U) packages as specified in TS-R-1 and TS-G-1.1 with a minimum factor of safety of 1.37.
- Overload: Should the R7021 be overloaded to the point of failure the tie-down eyes would fail first leaving all key components intact. This would not impair its ability to meet all other Type B(U) requirements specified in TS-R-1.
- Fatigue: No component is at risk from fatigue failure from tie-down loads during the design life.

7. REFERENCES

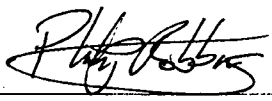
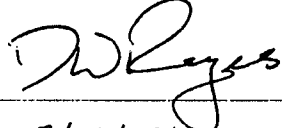
- BS 3643-1: 2007: ISO metric screw threads. Principles and basic data, British Standards Institution.
- BS 3692: 2001: ISO metric precision hexagon bolts, screws and nuts. Specification, British Standards Institution.
- BS EN 10088-2: 2005: Stainless steels. Technical delivery conditions for sheet/plate and strip of corrosion resisting steels for general purposes, British Standards Institution.
- Machinery's Handbook, 28th Edition, Industrial Press Inc, 2008.
- PD 5500: 2009: Specification for unfired fusion welded pressure vessels, British Standards Institution.
- R7021/004 issue D: Pallet manufacturing drawing, REVISS Services (UK) Ltd.
- RTM 120 issue 2: Thermal performance of the R7021 transport container, REVISS Services (UK) Ltd.
- TCSC 1006: Securing radioactive materials packages to conveyances, 2003, Transport Container Standardisation Committee.
- TS-G-1.1 (Rev. 1): "Advisory Material for the IAEA Regulations for the Safe Transport of Radioactive Material", IAEA, Vienna, 2008.
- TS-R-1: "Regulations for the Safe Transport of Radioactive Material", 2005 Edition, IAEA, Vienna.



**REVISS Services
Quality and Regulatory Group**

Technical Memorandum

**Performance of the R7021 Transport Container
Lifting Features**

Author:		Reviewer:	
Name	P J G Robbins	Name	D W Rogers
Signature		Signature	
Date	16/09/10	Date	17/09/2010

1. PURPOSE AND SCOPE

This document assesses the performance of lifting features of the R7021 transport container against various packaging regulations for the transport of radioactive materials. It analyses the stresses in the load bearing components under normal conditions of transport and quantifies their performance and their fatigue life against the design criteria.

2. DESCRIPTION

The design consists of a shielded, stainless steel flask mounted on a pallet and protected from heat and impact by a jacket and top shield (Figure 1). The maximum gross weight of the design is 4,600kg.

The flask has four lifting eyes equally disposed around its top. No other features could be used for lifting.

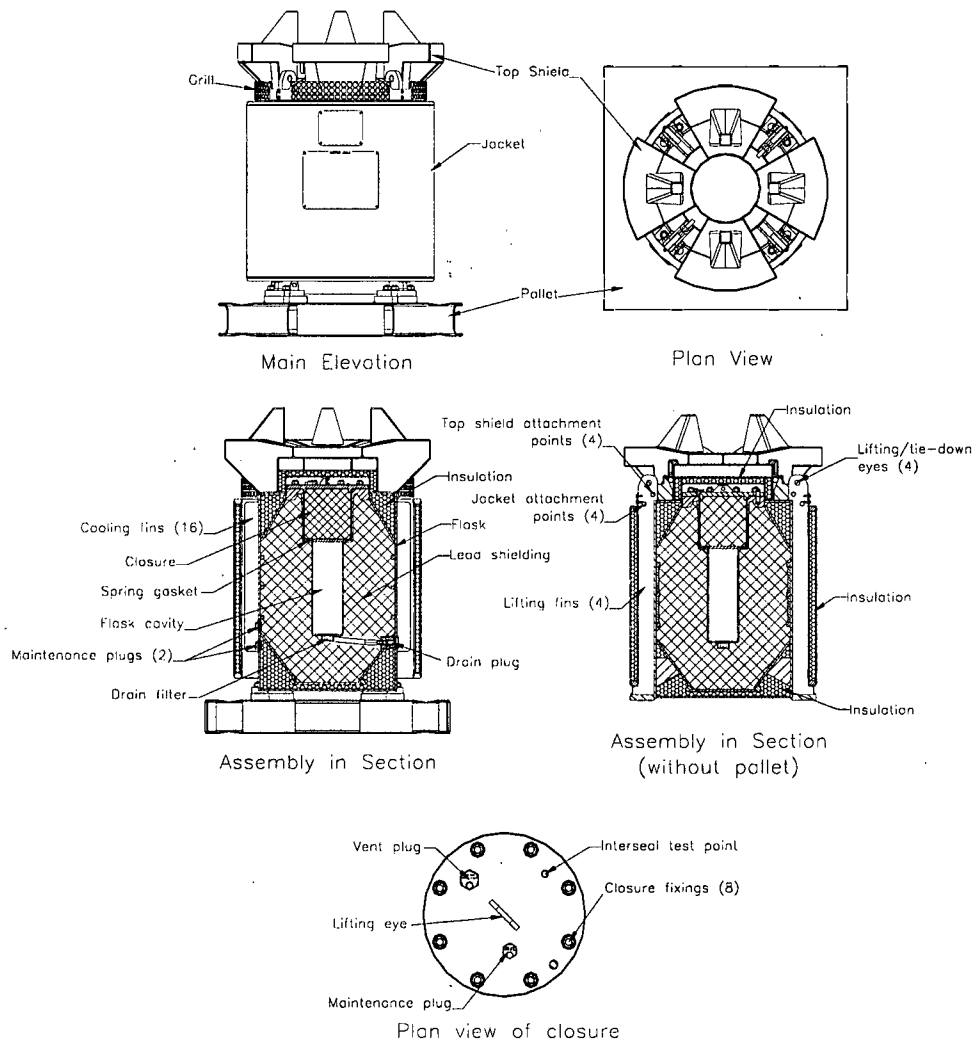


Figure 1: R7021 Assembly

3. ASSESSMENT

3.1 CRITERIA

- Factor of safety: The design strength (yield) shall not be exceeded with a snatch factor of 3. This exceeds TS-G-1.1 recommendations and the UK applicants guide requirements (snatch factor of 2) by a factor of 1.5 and satisfies the US requirements (10 CFR 71.45 (a)).
- Temperature: Material strength shall be taken at normal conditions of transport temperature.
- Failure: The ability of the design to comply with the requirements specified in TS-R-1 for Type B(U) packaging shall not be impaired should the lifting features, or any other features, be overloaded to failure.

3.2 ASSUMPTIONS

- Included angle of slings: The angle shall not exceed 90°.
- Unequal load distribution: Loads from 4-point slings will be distributed equally over two opposite lifting points.
- Shackle pin diameter: Taken as 28.6 mm (1 1/8").
- Special lifting equipment: Not required. The analysis will be based on the use of conventional multi-leg slings.

3.3 DATA

3.3.1 Design Strength

Under normal conditions of transport the flask tie-down eyes are at a maximum temperature of 93°C (RTM 120). The flask is fabricated from 1.4307 (304L) plate to BS EN 10088-2. The minimum room temperature yield strength of the lifting eyes is 200 N/mm². This reduces to 178 N/mm² at a temperature of 93°C (using by proportion the reduction in design strength cited in PD 5500 for a similar grade steel (304-S11) up to 100°C). The yield strength of the lifting fin welds similarly reduces to 141 N/mm² at their mid-height temperature of 153°C.

Element	Normal Conditions Temperature (°C)	Design Strength (N/mm ²)		
		Tension		Shear* (NCT)
		RT	NCT	
Flask lifting eyes	93	200	178	103
Flask lifting fin welds	153	200	141	81.4

* Using a factor of 0.577 on tensile strength based on Von Mises' theorem.

3.3.2 Load Paths

Lifting loads are taken by the lifting eyes and through the fin welds into the flask body.

3.3.3 Loads

Lifting Feature	Supported Mass (kg)	Maximum Load (kN)
Flask lifting eyes	4,600	135
Flask lifting fin welds	4,600	135

3.4 FLASK LIFTING POINTS

Pull-out shear stress is generated in the lifting eye and shear stresses in the welds securing the lifting fin to the flask body.

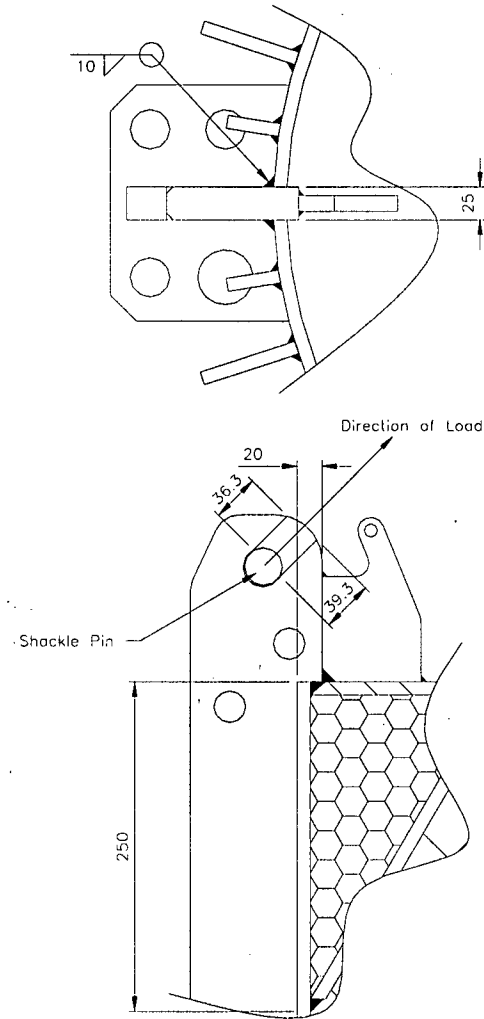


Figure 2: Flask Lifting Eye Details

3.4.1 Load on each lifting eye (W_1)

$$W_1 = \frac{W}{N \times \sin a}$$

where

W = maximum lifting load = 135 kN

N = minimum number of lifting points over which load is distributed = 2

a = angle of lifting member to horizontal (90° included angle) = 45°

thus

$$W_1 = \frac{135 \times 10^3}{2 \times \sin 45^\circ} = 95.5 \text{ kN}$$

3.4.2 Bearing stress in flask lifting eyes (S_1)

$$S_1 = \frac{W_1}{A_1}$$

where

A_1 = projected contact area of shackle pin = $D \times T$

where

D = shackle pin diameter = 28.6 mm.

T = length of contact = 25mm

thus

$$A_1 = 28.6 \times 25 = 1,120 \text{ mm}^2$$

thus

$$S_1 = \frac{95.5 \times 10^3}{1,120} = 134 \text{ N/mm}^2$$

3.4.3 Pull-out stress in flask lifting eyes (S_2)

$$S_2 = \frac{W_1}{A_2}$$

where

A_2 = total area of material in shear planes (Figure 2) = $(25 \times 36.3) + (25 \times 39.3)$
 $= 1,890 \text{ mm}^2$

thus

$$S_2 = \frac{95.5 \times 10^3}{1,890} = 50.5 \text{ N/mm}^2$$

3.4.4 Shear stress in lifting fin weld (S_3)

$$S_3 = \frac{W_1}{A_3}$$

where

A_3 = cross-sectional area of weld = $l \times t$

where

l = weld length = $2(250 + 20) = 540 \text{ mm}$ (stressed vertical length of weld is taken as 250mm on each side of the fin)

t = weld throat width = $10 \times 0.707 = 7.07 \text{ mm}$

thus

$$A_3 = 540 \times 7.07 = 3,820 \text{ mm}^2$$

thus

$$S_3 = \frac{95.5 \times 10^3}{3,800} = 25.1 \text{ N/mm}^2$$

3.7 SUMMARY:

The maximum stresses and minimum factors of safety of the key lifting components in the R7021 are:

Component	Maximum Stress (N/mm ²)	Design Stress (N/mm ²)	Safety Factor
Flask lifting eyes (bearing)	134 (S ₁)	178	1.33
Flask lifting eyes (pull-out)	50.5 (S ₂)	103	1.44
Flask lifting fin welds	25.1 (S ₃)	81.4	2.31

Failure under overload:

The table demonstrates the flask lifting eyes would fail under overload. This would have no adverse effect on the ability of the design to meet all other Type B requirements.

4. FATIGUE

An R7021 is unlikely to be shipped more than twelve times in a year. A single shipment is unlikely to require more than ten lifting operations. With a nominal design life of fifty years the lifting points therefore may reasonably be expected to be subject to a maximum of $10 \times 12 \times 50 = 6,000$ cycles.

Using Appendix C "Recommendations for the assessment of vessels subject to fatigue" and Figure C.3 in PD 5500 the maximum stress range for 6,000 cycles is 300 N/mm². It is evident therefore that the lifting points are not at risk from fatigue failure during the design life.

5. CONCLUSIONS

- Safety factor: The R7021 lifting points have a minimum factor of safety of 1.33 above any regulatory requirement.
- Overload: Should the lifting points be overloaded to the point of failure in lifting the lifting eyes would fail first leaving all key mechanical features of the assembly substantially intact. This would not impair its ability to meet all other Type B(U) requirements.
- Other features: There are no other features or attachments that could be used for lifting that, if used in their intended manner, would exceed their design limits under normal lifting conditions or, under overload conditions, would fail in manner that would impair the ability of the design to meet all other requirements.
- Fatigue: No component is at risk from fatigue failure from lifting during the design life.

6. REFERENCES

- 10 CFR: Code of Federal Regulations, Parts 51 to 199, 2004, Nuclear Regulatory Commission.

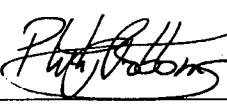
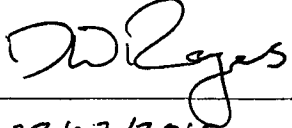
- BS EN 10088-2: 2005: Stainless steels. Technical delivery conditions for sheet/plate and strip of corrosion resisting steels for general purposes, British Standards Institution.
- DETR/RMTD/0003: Guide to an Application for UK Competent Authority Approval of Radioactive Material in Transport (IAEA 1996 Regulations).
- PD 5500: 2009: Specification for unfired fusion welded pressure vessels, British Standards Institution.
- RTM 120 issue 2: Thermal performance of the R7021 transport container, REVISS Services (UK) Ltd.
- TS-G-1.1 (Rev. 1): "Advisory Material for the IAEA Regulations for the Safe Transport of Radioactive Material", IAEA, Vienna, 2008.
- TS-R-1: "Regulations for the Safe Transport of Radioactive Material", 2005 Edition, IAEA, Vienna.



**REVISS Services
Quality and Regulatory Group**

Technical Memorandum

**Shielding Performance
of the R7021 Transport Container**

Author:		Reviewer:	
Name	P J G Robbins	Name	D W Rogers
Signature		Signature	
Date	28/07/10	Date	28/07/2010

1. PURPOSE AND SCOPE

The purpose of this document is to characterise the shielding performance of the R7021 transport container and to assess its performance under TS-R-1 normal and accident conditions tests for Type B package designs.

2. DESCRIPTION

The design consists of a lead shielded, stainless steel flask mounted on a pallet and protected from heat and impact by a jacket and top shield (Figure 1).

3. CRITERIA

1. The maximum dose level at the surface of the package shall not exceed 2.0 mSv/h (para. 531, TS-R-1).
2. The maximum dose level at 1m from the surface of the package shall not exceed 100 μ Sv/h (para. 530, TS-R-1).
3. The maximum dose level at the surface of the package shall not increase by more than 20% after normal conditions tests (para. 646(b), TS-R-1).
4. The maximum dose level at 1m from the package after accident conditions tests shall not exceed 10 mSv/h (para 657(b)(ii)(i), TS-R-1)).
5. The maximum lead temperature during accident conditions of transport shall not exceed its melting point of 327°C (Metals Handbook). Note that the latent heat of fusion of lead, 23.0 J/kg, compared to its heat capacity, 0.129 J/kg.°C (Handbook of Chemistry and Physics), means that the heat required to melt lead is equivalent to an additional temperature increase of 178°C.
6. The drain filter and spring gasket shall not allow particles greater than 100 μ m in diameter to pass through after either normal or accident conditions of transport.
7. Stresses in the spring gasket shall not exceed the design strength (yield) at maximum accident conditions temperature.
8. The spring gasket load on the underside of the closure shall not exceed 16kg (10% of the closure weight), i.e. it shall not affect closure retention in either normal or accident conditions of transport.

4. DESIGN

4.1 MAXIMUM CONTENTS

The R7021 is designed to transport a maximum of 7.40 PBq (200 kCi) of Special Form ^{60}Co and a maximum of 5.92 PBq (160 kCi) of normal form ^{60}Co .

4.2 SHIELDING

The shielding is primarily lead with a small contribution from the carbon and stainless steel structures. The design of the R7021 was modified slightly after prototype testing. Differences in lead and steel thickness are shown in the table below:

Direction	Shielding Thicknesses (mm)					
	Prototype		Modified Design		Difference	
	Lead	Steel	Lead	Steel	Lead	Steel
Radial	265	28	265	28	0	0
Up	247	53	255	59	8	6
Down	244	42	241	42	-3	0

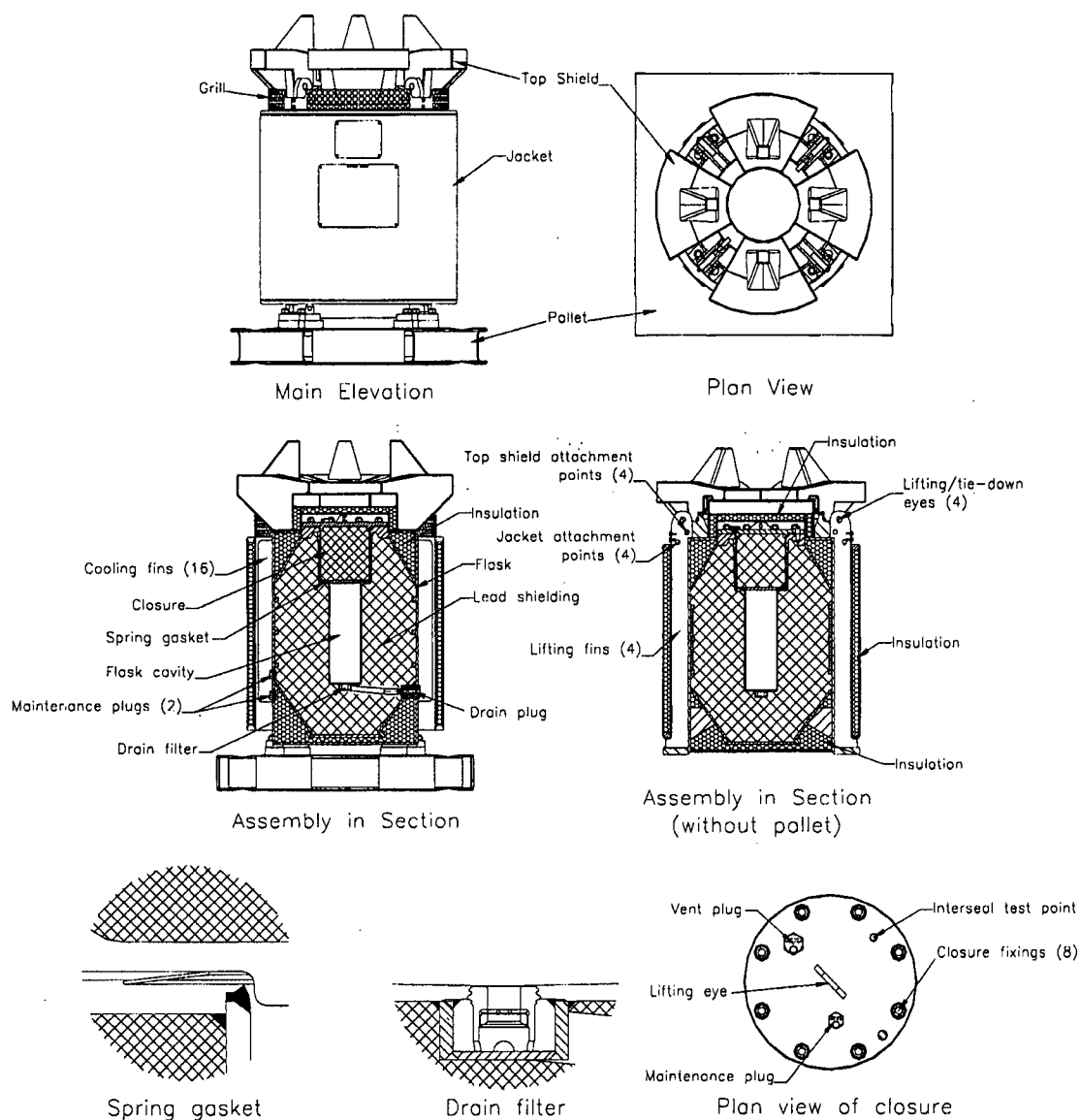


Figure 1: R7021 Constructional Details

The only other modification that could affect the shielding performance is the sleeve added to the drain tube. It is not possible to calculate the effect this will have however, as the tube

follows a double curve path through the shielding and as no raised dose rates were found on the prototype, it is unlikely there will be a problem with the modified design. In any event all units manufactured must be surveyed for shielding effectiveness, to OP 214, before they can be accepted and the procedure specifically covers potential hot spots such as the drain point.

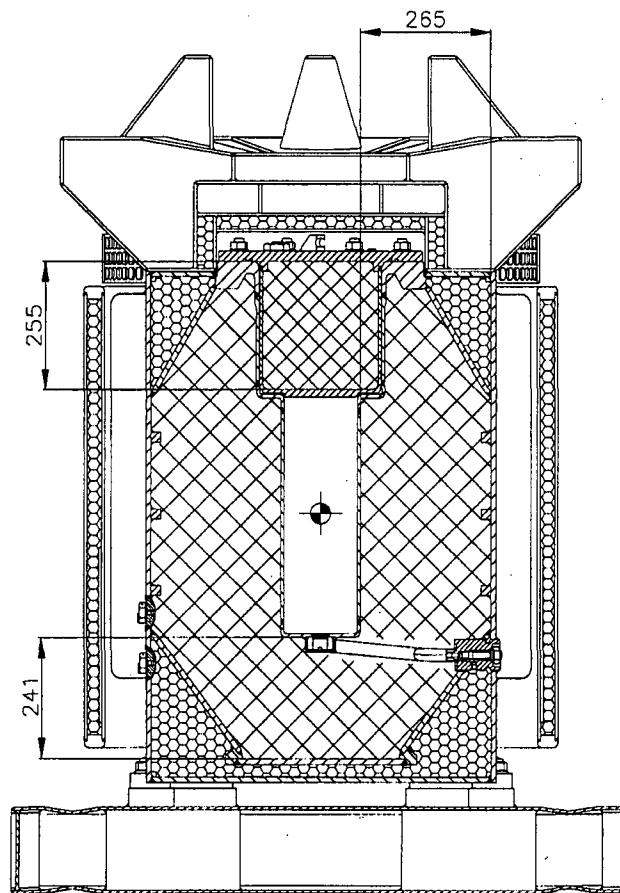


Figure 2: Package cross-section

5. CALCULATIONS

The following calculations estimate the maximum surface dose and Transport Index (TI) when the R7021 is carrying the maximum activity contents. This is achieved by adjusting measurements made on the prototype to take account of differences in contents, shielding and distance. Radiation levels at the drain, vent and closure seals are included for information only and are not subject to the criteria in section 3.

5.1 MEASUREMENTS

The prototype was surveyed for shielding efficiency after accident conditions drop testing (RTR 264) without its top shield, jacket and pallet. The results were as follows:

Direction/Location	Maximum Dose Rate* with 2.11 PBq Co ⁶⁰	
	Package Surface	1m from Flask Surface
Radial	975 µSv/h	37 µSv/h
Up	1825 µSv/h	100 µSv/h
Down	615 µSv/h	23 µSv/h
Drain Seal	775 µSv/h	-
Vent Seal	1825 µSv/h	-
Closure Seal	1825 µSv/h	-

* The 5µSv/h background dose rate has been subtracted from all readings.

5.2 RADIATION LEVEL

The radiation level, E, from BS 4094:

$$E = \frac{\Gamma Q T}{d^2} \text{ R/h}$$

where,

Γ = specific gamma ray constant = 1.32 R/Ci.h at 1m

Q = source activity in curies

T = transmission factor for shielding material.

d = distance of exposure point from point activity.

5.3 CONTENTS

The prototype shielding surveys were conducted with 2.11 PBq Co⁶⁰ in the bare flask. The equation above shows that the results require adjusting in direct proportion to the contents, i.e. by a factor of 3.51 (based on the maximum content limit; that for Special Form material).

5.4 SHIELDING

The prototype shielding surveys were conducted on the bare flask so there was no supplementary shielding from the carbon steel in the pallet, jacket and top shield. The effect of this when combined with the design changes above results in the following total variations:

Direction/ Location	Shielding Thicknesses (mm)					
	Prototype		Modified Design		Difference	
	Lead	Steel	Lead	Steel	Lead	Steel
Radial	265	16	265	28	0	12
Up	247	36	255	59	8	23
Down	244	30	241	42	-3	12
Drain Seal	265	16	265	16	0	0
Vent Seal	247	36	255	35	8	1
Closure Seal	247	36	255	35	8	1

The differences in attenuation may then be calculated using Fig 2b(i), BS 4094:

Direction/ Location	Attenuation				
	Lead		Steel		Total
	Thickness (mm)	Attenuation	Thickness (mm)	Attenuation	
Radial	0	1.00	12	0.674	0.674
Up	8	0.642	23	0.469	0.301
Down	-3	1.18	12	0.674	0.795
Drain Seal	0	1.00	0	1.00	1.00
Vent Seal	8	0.642	1	0.968	0.621
Closure Seal	8	0.642	1	0.968	0.621

5.5 DISTANCE

Radiation levels are inversely proportional to the square of the measurement distance. The difference in the source-to-surface measurements along each principal axis and the corresponding correction factor, the centre of activity being taken as the geometrical centre of the cavity, are as follows:

Direction/ Location	Measurement Distance (m)					
	Prototype		Modified Design		Ratio of squared values	
	Surface	At 1m	Surface	At 1m	Surface	At 1m
Radial	0.357	1.357	0.482	1.482	1.82	1.19
Up	0.526	1.526	0.724	1.724	1.89	1.28
Down	0.535	1.535	0.756	1.756	2.00	1.31
Drain Seal	0.357	-	0.277	-	0.60	-
Vent Seal	0.526	-	0.526	-	1.00	-
Closure Seal	0.526	-	0.526	-	1.00	-

* Dimensions derived from manufacturing drawings, QS 7021.

5.6 MAXIMUM DESIGN RADIATION LEVELS

When the correction factors calculated above are applied the dose rates at the surface and at 1m become:

Surface Radiation Levels, E					
Direction/ Location	Measurement (μ Sv/h)	Attenuation	Ratio of activities	Ratio of squared distances	Dose Rate (mSv/h)
Radial	975	0.674	3.51	1.82	1.27
Up	1825	0.301	3.51	1.89	1.02
Down	615	0.795	3.51	2.00	0.858

These are within the maximum allowable surface dose rate, 2.0 mSv/h (Section 3.1) for normal conditions of transport.

Radiation Levels at 1m from Surface, E					
Direction/ Location	Measurement ($\mu\text{Sv/h}$)	Attenuation	Ratio of activities	Ratio of squared distances	Dose Rate ($\mu\text{Sv/h}$)
Radial	37	0.674	3.51	1.19	73.6
Up	100	0.301	3.51	1.28	82.5
Down	23	0.795	3.51	1.31	49.0

These are within the maximum allowable dose rate at 1m, 100 $\mu\text{Sv/h}$ (Section 3.2) for normal conditions of transport.

Radiation Levels at Seals, E					
Direction/ Location	Measurement ($\mu\text{Sv/h}$)	Attenuation	Ratio of activities	Ratio of squared distances	Dose Rate ($\mu\text{Sv/h}$)
Drain Seal	775	1.00	3.51	0.60	4.53
Vent Seal	1825	0.621	3.51	1.00	3.98
Closure Seal	1825	0.621	3.51	1.00	3.98

6. EFFECT OF IAEA TESTING ON RADIATION LEVELS

6.1 NORMAL CONDITIONS DROP TESTING

The prototype was subjected to three normal conditions drop tests and one penetration test which caused no significant damage to the specimen (see IR 0674). The design was subsequently modified to improve accident conditions performance (see RTM 151). None of the design changes have any adverse effect on normal conditions performance and therefore there will be no change to the dose rates calculated above.

6.2 ACCIDENT CONDITIONS DROP TESTING

The prototype was subjected to nine puncture tests and four drop tests which caused no significant change to the shielding performance. The modified design has been computer modelled in the seven most damaging drop test orientations (see AMEC report C15788/TR/0001). In order for the surface dose rate to increase significantly one or more of the following would have to occur:

- Loss of the pallet, jacket or top shield.
- Failure of the closure retention system.
- Gross distortion of the flask.
- Migration of radioactive particulates past the shielding (normal form contents only).

6.2.1 Loss of the pallet, jacket or top shield

The pallet, jacket and top shield remained securely attached during drop testing (IR 0675). Computer modelling (C15788/TR/0001) demonstrated the modified design performed equally well. The 9m upright drop did however reduce the distance from the underside of the pallet. The effect of this is shown below:

Location	Dose Rate ($\mu\text{Sv/h}$)	Measurement distance (m)		Ratio of squared distances	Dose Rate
		Damaged	Undamaged		
At surface	643	0.619	0.756	0.670	0.96 mSv/h
At 1m	36.7	1.619	1.756	0.850	43.2 $\mu\text{Sv/h}$

As these are less than the values in other directions there will be no increase in the maximum dose rate, either on the surface or at 1m.

6.2.2 Failure of the closure retention system

The closure remained securely attached and there was no change in length of the closure fixings outside of normal measurement variation (IR 0671 & IR 0676) indicating all strains remained in the elastic region. Computer modelling of the modified design (C15788/TR/0001) demonstrated the closure fixings remained within their yield stress at all times.

6.2.3 Gross distortion of the flask

The only damage to the flask was superficial marking and bruising of external surfaces (see IR 0675) which was corroborated by the post drop test shielding survey. Computer modelling of the modified design (C15788/TR/0001) demonstrated the shielding remained securely supported and retained by the flask at all times.

6.2.4 Migration of radioactive particulates past the shielding (normal form contents only)

Although all normal form material must be encapsulated the possibility of a capsule rupturing under accident conditions must be considered. The smallest normal form material transported is $\varnothing 1\text{mm} \times 1\text{mm}$ cobalt pellets (see OP 381). The flask is therefore equipped with a drain filter with a 0.1 mm mesh at its inner end, whilst the gap between the underside of the closure and the flask is closed by a spring gasket. Both of these were completely undamaged and secure after accident conditions tests so there is no possibility of such material migrating past the shielding.

The possibility exists however that such material could include particulate matter generated by vibration encountered in normal transport. Such particles, if small enough, could, if the capsule was ruptured, migrate along the drain tube or the side of the closure and cause a local increase in dose rate.

A test was conducted therefore in which 76.7g of $\varnothing 1\text{mm} \times 1\text{mm}$, nickel plated, cobalt pellets (the maximum quantity that would fit), was sealed in a typical capsule and subjected to a vibration and shock regime (to Def Stan 00-35) simulating 5,000 km road transport (see report 2209). The capsule was orientated vertically, as in normal conditions of transport.

After the test the capsule was cut open and the contents presented to a 106 μm filter (see PS/W000339RL001). Chemical analysis revealed a total quantity of 129 μg of particulate material had passed the filter (see INORG/W000925RL001). This represents, by proportion of the maximum contents, an activity of 9.96 GBq. This, if it were behind the drain plug, could, using the equation in 5.2, give a dose rate at 1m of:

Radiation Levels, E, at 1m				
Location	Steel thickness (mm)	Attenuation	Distance to measurement point (m)	Dose Rate (mSv/h)
Drain Plug	26	0.425	1.126	1.19

This is comfortably less than 10mSv/h, the maximum permitted radiation level at 1m after accident conditions of transport (see 3.4).

6.2.5 Spring gasket stress

The spring gasket is a bevelled stainless steel ring designed to keep particulate material from passing into the gap between the closure and the flask body and hence circumnavigating the shielding. Its outer diameter sits in a recess in the flask body, while its inner diameter is in contact with the base of the closure. All contact surfaces are machined. The height of the gap between the flask and the closure is 3.1 - 3.1 mm while the height of the spring gasket is 5.2 - 5.4 mm. This ensures that there is always positive contact with both surfaces.

The spring gasket is deformed when the closure is in place, which generates a bending stress. The load case is a circular plate with the outer edge simply supported and the inner edge free (Case 1a, Table 24, Roark).

$$\text{Max. stress, } \sigma = \frac{6M}{t^2}$$

where:

M = maximum moment = awK_{Mib}

t = plate thickness

and:

a = outside radius

w = unit line load

K_{Mib} is related to $\frac{b}{a}$ through interpolation of special case values in Case 1a.

b = inside radius

$$\text{Max. deflection, } y = h_1 - h_2 = \frac{K_y wa^3}{D} = -2.3 \text{ mm}$$

where:

h_1 = min. height of flask/closure gap = 3.1 mm

h_2 = max. height of gasket = 5.4 mm

K_y is related to $\frac{b}{a}$ through interpolation of special case values in Case 1a.

$$D = \text{plate constant} = \frac{Et^3}{12(1-\nu^2)}$$

and:

E = modulus of elasticity = 200,000 N/mm²

ν = Poisson's ratio = 0.285

thus:

$$\sigma = \frac{6aK_{Mtb}w}{t^2} = \frac{6aK_{Mtb}\left(\frac{yD}{K_y a^3}\right)}{t^2} = \frac{6aK_{Mtb}y\left(\frac{Et^3}{12(1-\nu^2)}\right)}{K_y a^3 t^2} = \frac{6aK_{Mtb}yEt^3}{12(1-\nu^2)K_y a^3 t^2}$$

therefore:

$$\sigma = \frac{6K_{Mtb}yEt}{12(1-\nu^2)K_y a^2}$$

The highest stress in the gasket occurs when the thickness, t , and K_{Mtb} are at a maximum and the outside radius, a , and K_y at a minimum.

therefore:

$$\begin{aligned} t &= 1.15 \text{ mm} \\ a &= 114.75 \text{ mm} \end{aligned}$$

K_{Mtb} is at a maximum and K_y a minimum for higher values of $\frac{b}{a}$, i.e. when b is at a maximum.

therefore:

$$b = 85.25 \text{ mm}$$

thus:

$$\frac{b}{a} = 0.806$$

$$K_{Mtb} = 0.8814 \text{ (for } \frac{b}{a} = 0.7 \text{ (through interpolation of special case values in Case 1a))}$$

$$K_y = -0.1927 \text{ (for } \frac{b}{a} = 0.7 \text{ (through interpolation of special case values in Case 1a))}$$

therefore:

$$\sigma = 100 \text{ N/mm}^2$$

This is below the design strength, 116 N/mm^2 , based on the maximum cavity wall temperature at accident conditions of 316°C (RTM120). Taken from PD 5500, Annex K, Table K.1-4, for 304S11 as $1.35 \times f_N$, where f_N = nominal design strength and 1.35 is the factor that gives the point of transition between linear elastic and linear plastic behaviour (para. K.1.4.1.3).

6.2.6 Spring gasket load

Deformation of the gasket creates a load on the closure fixings as follows:

$$\text{Total load, } W = \frac{cw}{g}$$

where:

$$\begin{aligned} c &= \text{circumference of inside edge} = 2\pi b \\ g &= \text{gravitational acceleration} = 9.81 \text{ m/s}^2 \end{aligned}$$

therefore:

$$W = 12.3 \text{ kg}$$

6.3 ACCIDENT CONDITIONS THERMAL TESTING

RTM 120 details the thermal performance of the R7021. Peak accident conditions lead temperature is 302°C.

7. CONCLUSIONS

1. The maximum surface dose rate, when loaded with 7.40 PBq ^{60}Co , is 1.27 mSv/h.
2. The maximum dose rate at 1m, when loaded with 7.40 PBq ^{60}Co , is 82.5 $\mu\text{Sv/h}$.
3. Radiation levels are unaffected by normal conditions of transport.
4. Maximum radiation levels after accident conditions of transport.
 - Special Form contents: Are unaffected.
 - Normal form contents: Could rise to 1.19 mSv/h at 1m should all encapsulation be ruptured and all possible particulate matter less than 0.1 mm in diameter make its way to the outer end of the drain tube.
5. Lead temperature: The margin of safety to the maximum allowable design value is 25°C. This represents 23% of the temperature rise during the thermal test. This is sufficient to compensate for any calculational inaccuracy.
6. The drain filter and spring gasket will not allow particles greater than 100 μm in diameter to pass through in either normal or accident conditions of transport.
7. Stress in the spring gasket does not exceed the design strength (yield) at maximum accident conditions temperature.
8. Closure load from the spring gasket is less than 10% of the closure weight and will have no significant affect on normal or accident conditions performance.

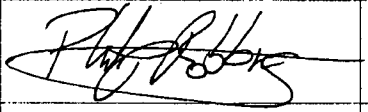

8. REFERENCES

- 2209: Test Report (Vibration and Shock Testing), Product Assessment and Reliability Centre (PARC).
- BS 4094: Part 1, 1966. Data on shielding from ionising radiation. British Standards Institution.
- C15788/TR/0001 issue 2: Impact assessment of the Reviss R7021 package, AMEC Ltd.
- Def Stan 00-35: Environmental Handbook for Defence Materiel, Part 5, Induced Mechanical Environments, MoD.
- Handbook of Chemistry and Physics: 76th Edition, 1995/6, CRC Press.
- INORG/W000925RL001: Determination of Cobalt and Nickel contents on filter papers by ICP-OES, Intertek MSG.
- IR 0673: Inspection Report on 3981/01 after normal conditions drop testing, REVISS Services (UK) Ltd.
- IR 0675: Inspection Report on 3981/01 after accident conditions drop testing, REVISS Services (UK) Ltd.
- Metals Handbook: Desk Edition, 1995, American Society for Metals.
- PD 5500: 2009: Specification for unfired fusion welded pressure vessels. British Standards Institution.
- PS/W000339RL001: Isolation and chemical analysis of fragments of metal particles produced during the vibration testing of cobalt pellets, Intertek MSG.
- OP 214 issue 7: Transport container shielding test procedure, REVISS Services (UK) Ltd.
- OP 381 issue 2: R7021 Operating and maintenance instructions, REVISS Services (UK) Ltd.
- QS 7021 issue 4: Drawings List R7021 Transport Container, REVISS Services (UK) Ltd.
- Roark's Formulas for stress and strain, 7th Edition, WC Young, McGraw-Hill, 2002.
- RTM 118 issue 2: Test plan for R7021, REVISS Services (UK) Ltd.
- RTM 120 issue 2: Thermal performance of R7021, REVISS Services (UK) Ltd.
- RTM 151 issue 1: R7021 Transport Container Design Justification, REVISS Services (UK) Ltd.
- RTR 264: 3981/01 Shielding Survey Report, REVISS Services (UK) Ltd.
- TS-R-1: Regulations for the Safe Transport of Radioactive Material, 2005 Edition, IAEA, Vienna.

REVISS

**REVISS Services
Quality and Regulatory Group
Technical Memorandum**

**Justification of the R7021
Containment System**

Author		Reviewer	
Name	P J G Robbins	Name	D W Rogers
Signature		Signature	
Date	15/09/10	Date	15/09/2010

1. PURPOSE AND SCOPE

The R7021 is a Type B transport package designed to transport both Special Form and non-SF solid radioactive material. The purpose of this document is to describe the containment system and demonstrate that it meets all its design and regulatory requirements and guidelines. It will also detail the criteria for routine and periodic testing.

2. DESCRIPTION

The R7021 consists of a lead shielded, stainless steel flask mounted on a pallet and protected from heat and impact by a pallet, jacket and top shield. The flask is an upright, cylindrical fabrication with a removable shield plug, the closure, at the top. The cavity is equipped with a drain tube at its base and a venting hole through the closure. The closure, vent and drain plugs are each sealed with an elastomer O-ring. In each case a second O-ring and an interseal test point is provided which enable the inner O-ring to be leak tested. The flask and closure are also equipped with connection points in order the containment boundary (the flask and closure internal surfaces) may be routinely leak tested. As the drain tube is enclosed by an outer sleeve the flask has two test points; one directly into the shielding space and one into the space between the drain tube and sleeve. These allow the entire containment boundary to be tested.

3. CRITERIA

1. The containment system O-ring material shall be suitable for the physical environment (DTLR guide).
2. The containment system O-ring material shall be suitable for the radiation environment (DTLR guide).
3. The containment system O-ring material shall be suitable for use at -40°C (para 637, TS-R-1) and +55°C (para 618, TS-R-1).
4. Containment system O-ring temperatures under normal conditions of transport shall not exceed 204°C (the long term limit for fluorocarbon (FKM) O-ring materials (Precision O-ring Handbook)).
5. Containment system O-ring temperatures under accident conditions of transport shall not exceed 270°C and shall not exceed 250°C for longer than 2hrs (the high temperature test results used for the FKM type V1289 seal material are 70 hrs at 250°C (Parker report ORD 5743) and 2 hrs at 270°C (Ceetak report 22550C)).
6. Containment system O-ring compression shall not be less than 10% after one year in a fully loaded flask in a mean ambient of 20°C.
7. Containment system O-ring compression shall not exceed 30% under normal conditions of transport.
8. Containment system O-ring groove fill shall not exceed 90% during accident conditions of transport.
9. The containment system shall remain leaktight after accident conditions mechanical tests.
10. Source capsule temperatures shall not exceed 800°C during the thermal test, with or without damage from the drop tests, (Special Form material may be used as the containment system and performance testing is conducted at 800°C).
11. Routine and periodic leak testing shall comply with the DfT and ANSI N15.5 requirements and recommendations.
12. Closure O-ring compression shall not be reduced by more than 1% as a result of thermal distortion during the thermal test.

4. ASSESSMENT

4.1 DATA

4.1.1 O-Ring details

Position	Material	Dimensions (mm)		
		Inside Diameter	Cross-Section	C/S Tolerance (\pm)
Closure	FKM V1289	279	5.33	0.13
Vent Plug	FKM V1289	20.3	2.62	0.09
Drain Plug	FKM V1289	9.19	2.62	0.09

Note: Tolerances are taken from the Precision O-Ring Handbook.

4.1.2 Coefficients of thermal expansion

Material	Coefficient, α ($\times 10^{-6}$)
FKM	160
300 series stainless steel	16

Note: The FKM coefficient is taken from the Precision O-Ring Handbook, the stainless steel from ASME II.

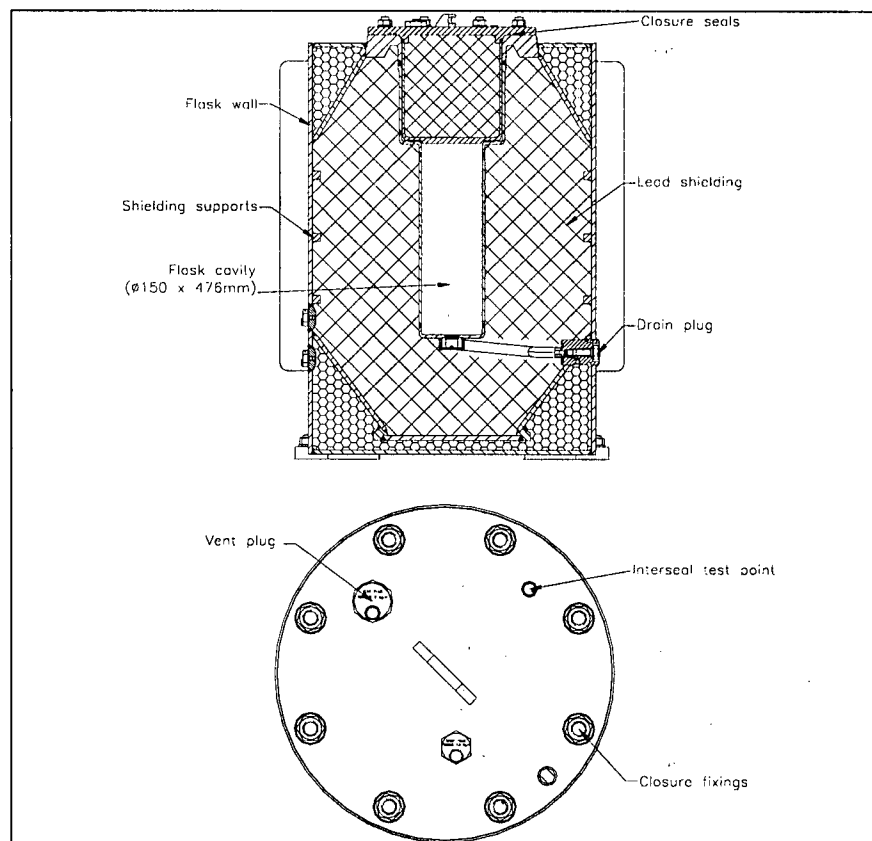


Figure 1: R7021 Flask Section

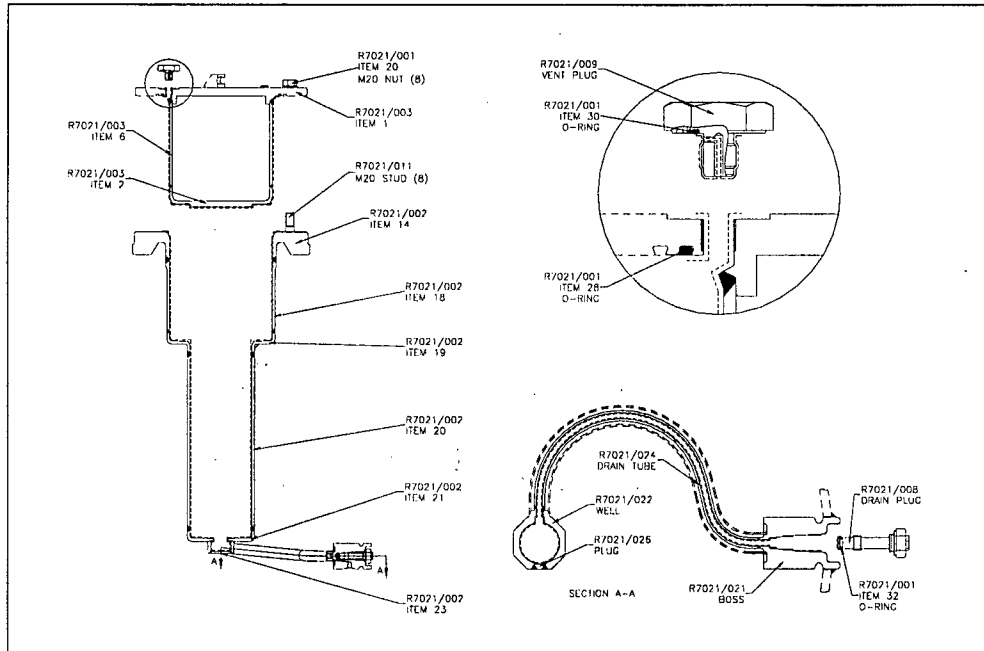


Figure 2: R7021 Containment Boundary (shown in small chain dot)

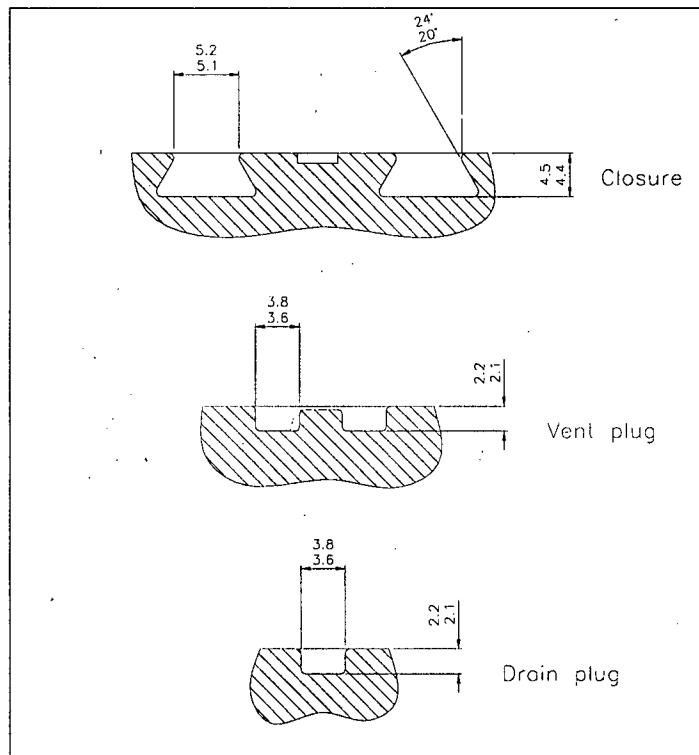


Figure 3: O-Ring Groove Details

Note: Drain plug groove depth is measured from the bottom of the groove to the internal diameter of the cylinder as it is a piston seal.

4.1.3 Physical environment

The physical environment is inside stainless steel housings where the seals will be containing an inert noble gas such as helium or neon (see OP 381). Although the flask is dried thoroughly after pond operations (see OP 381) the seals could be exposed to water vapour from any residue.

4.1.4 Long term heat load

The ^{60}Co contents generate an internal heat load. The nuclide has a half life of 5.271 years (TS-G-1.1). After one year the contents activity will have reduced to 87.7% (the mean activity over the year being 93.9%) and flask and seal temperatures will be reduced proportionally.

4.1.5 Operating temperatures

Environment	Seal Temperature (°C)
Normal Conditions of Transport	144
Accident Conditions of Transport	262
20°C Ambient and 93.9% Content Activity	120
-40°C Ambient and 87.7% Content Activity	46
55°C Ambient	75

Notes:

- Normal (144°C) and accident conditions (262°C) O-ring temperatures are taken from the R7021 thermal analysis report, RTM 120.
- The O-ring temperature in a 20°C ambient is derived from the normal conditions temperature by deducting the effect of insolation together with the 18°C temperature difference i.e. $144 - 18 - 6 = 120^\circ\text{C}$
- The O-ring temperature in a -40°C ambient, when the flask contains an 87.7% heat load from the contents (the heat load after one year of decay), is derived as follows: The effect of insolation and the 38°C ambient are deducted from the normal conditions O-ring temperature to give the temperature difference caused by the contents heat load alone, i.e. $(144 - 8 - 38 = 98^\circ\text{C})$. Multiplying by 0.877 allows for decay of the cobalt contents and adding the resulting temperature difference to the -40°C ambient gives the seal temperature, i.e. $(98 \times 0.877) - 40 = 46^\circ\text{C}$.
- The O-ring temperature at 55°C ambient is only important for air shipments, when the content activity will be limited to 32.4 kCi (3000 x the A_2 limit for ^{60}Co (para 433 and Table 2, TS-R-1). It is derived as follows: The effect of insolation and the 38°C ambient are deducted from the normal conditions O-ring temperature to give the temperature difference caused by the contents heat load alone, i.e. $(144 - 8 - 38 = 98^\circ\text{C})$. Multiplying by the air shipment limit and dividing by the license limit reduces this temperature in proportion to the content activity, i.e. $(98 \times 32.4) / 160 = 20^\circ\text{C}$. Adding the new ambient gives the seal temperature, i.e. $20 + 55 = 75^\circ\text{C}$. This value is lower than the seal temperature under normal conditions of transport, hence any subsequent calculations for normal conditions will always present a worst case.

4.2 ASSESSMENT AGAINST CRITERIA

4.2.1 O-Ring suitability for physical environment

FKM seals are compatible with air to 204°C (Precision O-Ring Handbook). They are susceptible to acids, alkalis, mineral oils and hydrocarbons. The R7021 Operating and Maintenance Instructions, OP 381, alert the operator to this issue.

4.2.2 O-Ring suitability for radiation environment

FKM is unaffected by exposures of up to about 10^6 Rads (Precision O-Ring Handbook). The containment system O-rings are all outside the flask shielding so are exposed to the minimum dose. A maximum radiation level of 4.53 mSv/hr will occur at the drain O-ring when fully loaded (RTM 124). This will give rise to a cumulative dose over a period of one year of $4.53 \times 10^{-3} \times 24 \times 365 = 40$ Sv. This is broadly equivalent to $40 \times 100 = 4,000$ Rad.

4.2.3 O-Ring suitability for low temperature

FKM V1289 has a low temperature limit of -50°C for static seals (Ceetak report RC 19356A). This exceeds the normal conditions low temperature limit of -40°C and agrees with the manufacturers recommendations (ORD5743).

4.2.4 O-Ring suitability for long term normal conditions temperature

FKM has a long term temperature limit of 204°C (DTLR/RMTD/0004). This comfortably exceeds the normal conditions temperature of 144°C. Note: There is an additional 18°C margin of safety as the maximum long term mean ambient temperature may reasonably be assumed to be 20°C rather than 38°C.

RTM 120 gives the temperature of the drain plug seal, the hottest of the three seals, as 144°C. The margin of safety to the maximum allowable design value is $204 - 144 = 60^\circ\text{C}$. The temperature difference from ambient is $144 - 38 = 106^\circ\text{C}$. This affords a safety margin of 57%, which is sufficient to compensate for any calculational inaccuracy.

4.2.5 O-Ring suitability for short term accident conditions temperature

R7110/1.1 provides the following time/temperature data for the seals:

Peak Seal Temperature and Duration over 250°C			
Package Orientation	Condition	Closure and Vent Plug	Drain Plug
Upright	Undamaged	259°C, 67 mins	236°C, 0
Inverted		251°C, 25 mins	262°C, 83 mins
Angled Side		252°C, 33 mins	257°C, 80 mins
Upright	With damage	253°C, 33 mins	228°C, 0
Inverted		253°C, 33 mins	261°C, 80 mins
Angled Side		253°C, 42 mins	256°C, 70 mins
Maximum		262°C, 83 mins	

Peak temperature: The peak seal temperature is 262°C. The minimum margin of safety to the design limit is $270 - 262 = 8^\circ\text{C}$. The temperature increase over normal conditions is $262 - 144 = 118^\circ\text{C}$. This affords a safety margin of 7%, which is sufficient to compensate for any calculational inaccuracy.

Duration over 250°C: The maximum temperature duration over 250°C is 83 minutes. This affords a safety margin of 45%, which is sufficient to compensate for any calculational inaccuracy.

4.2.6 Minimum O-ring compression

Containment system O-ring compression shall not be less than 10%:

- After one year with the flask fully loaded in an ambient temperature of 20°C and subsequently in an ambient of -40°C or:
- The minimum flask loading (empty) in an ambient of -40°C.

In both instances the manufacturing tolerances shall be worst case, i.e. O-rings at minimum diameter and housings at maximum depth.

The minimum O-ring compression will occur at -40°C (the elastomer will shrink more than the groove due to its much higher coefficient of expansion) either with the seal having the maximum compression set (after a year, fully loaded in an ambient of 20°C) or with the minimum contents heat load and no compression set.

In the first case the seal/groove temperature in an ambient of -40°C with maximum contents after a year's decay is 46°C. Thus:

- Maximum Groove Depth:

The formula used is $D_{\max 46} = (D + \text{tol}) \times (1 + \alpha(46 - 20))$

Position	Maximum Depth (mm)	
	@ 20°C	@ 46°C
Closure	4.50	4.50
Vent Plug	2.20	2.20
Drain Plug	2.22	2.22

- Minimum Seal Diameter:

The formula used is $XS_{\min 46} = (XS - \text{tol}) \times (1 + \alpha(46 - 20))$

Position	Minimum Cross-Section Diameter (mm)	
	@ 20°C	@ 46°C
Closure	5.20	5.22
Vent Plug	2.53	2.54
Drain Plug	2.53	2.54

- Effect of Compression Set:

The Precision O-Ring Handbook gives the compression set, CS, for FKM (FKM) at 134°C after 70 hrs (at which time the set has stabilised) as 10%. The formula for calculating the effect of compression set on seal compression is:

$$CS = \frac{h_0 - h_2}{h_0 - h_1}$$

where

h_0 = original seal cross-section = $XS_{\min 46}$

h_1 = height of deformed seal = maximum groove depth at 46°C = $D_{\max 46}$

h_2 = height of released seal

re-arranging

$$h_2 = h_0 - CS(h_0 - h_1) = XS_{\min 46} - CS(XS_{\min 46} - D_{\max 46})$$

and the minimum compression at 46°C, $C_{\min 46} = 1 - \frac{h_1}{h_2}$

Position	$XS_{\min 46}$ (h_0)	$D_{\max 46}$ (h_1)	h_2	$C_{\min 46}$ (%)
Closure	5.22	4.50	5.15	12.6
Vent Plug	2.54	2.20	2.51	12.2
Drain Plug	2.54	2.22	2.51	11.5

In the second case the seal/groove temperature in an ambient of -40°C with minimum contents is -40°C. Thus:

- Maximum Groove Depth:
 $D_{\max -40} = (D + \text{tol}) \times (1 + \alpha(-40 - 20))$

Position	Maximum Depth (mm)	
	@ 20°C	@ -40°C
Closure	4.50	4.50
Vent Plug	2.20	2.20
Drain Plug	2.22	2.22

- Minimum Seal Diameter:
 $XS_{\min -40} = (XS - \text{tol}) \times (1 + \alpha(-40 - 20))$

Position	Minimum Cross-Section Diameter (mm)	
	@ 20°C	@ -40°C
Closure	5.20	5.15
Vent Plug	2.53	2.51
Drain Plug	2.53	2.51

- Effect of Compression Set:
Compression set will not exceed 10% for FKM at temperatures below 100°C (Fig 6.5, Precision O-Ring Handbook).

Position	$XS_{\min -40}$ (h_0)	$D_{\max -40}$ (h_1)	h_2	$C_{\min -40}$ (%)
Closure	5.15	4.50	5.09	11.6
Vent Plug	2.51	2.20	2.48	11.2
Drain Plug	2.51	2.22	2.48	10.4

4.2.7 Maximum O-ring compression

Containment system O-ring compression shall not exceed 30% under normal conditions of transport (manufacturing tolerances at worst case):

The maximum O-ring compression will occur in the maximum ambient (the elastomer will

expand more than the groove due to its much higher coefficient of expansion) with the flask fully loaded, the minimum groove depth and no compression set.

The seal/groove temperature in an ambient of 38°C with maximum contents and insulation is 144°C. Thus:

- Minimum Groove Depth:

The formula used is $D_{\min 144} = (D - \text{tol}) \times (1 + \alpha(144 - 20))$

Position	Minimum Depth (mm)	
	@ 20°C	@ 144°C
Closure	4.40	4.41
Vent Plug	2.10	2.10
Drain Plug	2.10	2.10

- Maximum Seal Diameter:

The formula used is $XS_{\max 144} = (XS + \text{tol}) \times (1 + \alpha(144 - 20))$

Position	Maximum Cross-Section Diameter (mm)	
	@ 20°C	@ 144°C
Closure	5.46	5.57
Vent Plug	2.71	2.76
Drain Plug	2.71	2.76

- Maximum Compression:

$$C_{\max 204} = 1 - \frac{D_{\min 144}}{XS_{\max 144}}$$

Position	$D_{\min 144}$	$XS_{\max 144}$	$C_{\max 144}$ (%)
Closure	4.41	5.57	20.8
Vent Plug	2.10	2.76	23.9
Drain Plug	2.10	2.76	23.9

4.2.8 Maximum groove fill

Containment system O-ring groove fill shall not exceed 90% under accident conditions of transport thermal test (manufacturing tolerances worst case, i.e. O-rings at maximum diameter and housings at minimum depth and width).

The maximum groove fill will occur at the maximum temperature (accident conditions) with the minimum groove width, depth and side angle.

The maximum seal/groove temperature in accident conditions is 262°C with maximum contents and insulation. Thus:

- Minimum Groove Depth:

The formula used is $D_{\min 262} = (D - \text{tol}) \times (1 + \alpha(262 - 20))$

Position	Minimum Depth (mm)	
	@ 20°C	@ 262°C
Closure	4.40	4.42
Vent Plug	2.10	2.11
Drain Plug	2.10	2.11

- Minimum Groove Width:

The formula used is $W_{\min 262} = (W - \text{tol}) \times (1 + \alpha(262 - 20))$

Position	Minimum Width (mm)	
	@ 20°C	@ 262°C
Closure	5.10	5.02
Vent Plug	3.60	3.61
Drain Plug	3.60	3.61

- Minimum Groove Area:

The cross-sectional area of the trapezoidal groove is taken as the rectangular area in the centre plus the two triangular fillets to each side. Thus:

$$GA_{\min 262} = D_{\min 262}(W_{\min 262} + D_{\min 262} \tan \theta)$$

Position	$D_{\min 262}$	$W_{\min 262}$	θ (Groove Angle)	$GA_{\min 262}$ (mm ²)
Closure	4.42	5.02	20°	29.3
Vent Plug	2.11	3.61	0°	7.62
Drain Plug	2.11	3.61	0°	7.62

- Maximum Seal XS Area:

$$SA_{\max 262} = 0.25\pi((XS + \text{tol}) \times (1 + \alpha(262 - 20)))^2$$

Position	Maximum Diameter (mm ²)		Maximum Cross-Section Area (mm ²)
	@ 20°C	@ 262°C	@ 262°C
Closure	5.46	5.67	25.3
Vent Plug	2.71	2.82	6.23
Drain Plug	2.71	2.82	6.23

- Maximum Groove Fill:

$$GF_{\max 262} = \frac{SA_{\max 262}}{GA_{\min 262}}$$

Position	$GA_{\min 262}$ (mm ²)	$SA_{\max 262}$ (mm ²)	$GF_{\max 262}$ (%)
Closure	29.3	25.3	86.4
Vent Plug	7.62	6.23	81.7
Drain Plug	7.62	6.23	81.7

4.2.9 Accident conditions mechanical tests

- The length of the eight M20 closure studs was measured before and after drop testing (see IR 0671 & 0676). The results show only normal measurement variation. The calculated mean lengths were respectively 87.04 mm and 87.01mm. The pass criteria was no permanent elongation exceeding 0.2mm (RTM 118). There was no permanent elongation.
- Helium leak test measurements on the seals were taken after drop testing (see RTR 263). The results were:

Position	Leakrate after testing (mbar.l/s)
Closure	1×10^{-8}
Drain Plug	6×10^{-8}
Vent Plug	1×10^{-7}

The pass criteria was that flask seals remained leaktight to 2.65×10^{-7} mbar.l/s (RTM 118).

4.2.10 Containment boundary

Accident conditions mechanical testing caused no physical damage to the closure or the vent and drain plugs (see inspection report, IR 0675). However, failure of the outer drain tube weld caused the containment boundary to fail its leak test (RTR 263). Computer modelling identified the cause as movement of the lead shielding (AMEC report C15578/TR/0001). The drain tube was subsequently fitted with an outer sleeve to isolate it from lead movement. At the same time a number of minor modifications were made to the impact limiters to improve their performance in the mechanical tests. The modified design was then modelled in seven different drop test orientations. The results demonstrate that all significant stresses in the drain and its welds have been eliminated. It also demonstrates that strains in the rest of the containment boundary, including the closure fixings, are within acceptable limits.

4.2.11 Capsule temperature (accident conditions)

RTM 120 gives the peak mean capsule temperature under accident conditions as 471°C. The margin of safety to the maximum allowable design value is $800 - 471 = 329^\circ\text{C}$. This is sufficient to compensate for any calculational inaccuracy.

4.2.12 Thermal distortion of closure flange

The normal flow of heat through the closure flange is outwards, i.e. the temperature of its upper face will be lower than the underside. During the thermal test when the heat flow is inwards this is reversed which could lead to an upwards distortion (hogging), resulting in a reduction of O-ring compression.

The environment enclosing closure flange is primarily the disc on the underside of the top shield. Heat from the thermal test has to pass through the top shield and then a layer of insulation of uniform thickness to reach the disc. The conductivity of the steel disk and presence of an air gap beneath it ensure that any variations in temperature distribution outside the insulation are not able to manifest themselves in the disc. This will therefore present a surface of essentially uniform temperature to the closure flange.

The closure flange is a disc of more or less constant thickness retained by a ring of fixings set inside its diameter. It may therefore best be considered a disc of the same diameter as the PCD of its fixings with its outer edge fixed. Roark (Table 11.2, Case No 15b) states that when

such a plate is subjected to a uniform temperature gradient bending moments are the same throughout and the plate will not distort. Therefore there will be no reduction in O-ring compression.

RTM 120 shows that the maximum reverse temperature gradient is 3°C, hence even if the temperature distribution across the closure flange were not to be completely uniform it would not be conceivable for it to have any significant effect.

5. LEAKTESTING

5.1 ROUTINE ASSEMBLY AND LEAKTESTING

The operating instructions, OP 381, require checklists to be used for all operations. Turnround inspection, Section 10, requires each package to be inspected before loading to ensure all components are present, correct and in a serviceable condition. The assembly procedure, Section 5.4, requires all components to be correctly positioned and secured and includes leaktesting each of the three O-ring seals to verify a maximum helium leak rate of 5.0×10^{-4} mbar.l/s at 1 bar differential, the value accepted by the DfT for solids and particulates. This also complies with ANSI N14.5.

5.2 PERIODIC LEAKTESTING

Scheduled inspection, Section 11, requires each of the three O-ring seals and the containment boundary to be leaktested annually to verify a maximum helium leak rate of 1×10^{-6} mbar.l/s at 1 bar differential, the value recommended in TS-G-1.1 para. 657.13 as representing leaktightness for solid particulate material.

6. CONCLUSIONS

Design Aspect	Performance	Criteria
Material Compatibility	Suitable	Compatible with water, water vapour, air and noble gases
Radiation Resistance	4,000 Rads	$\leq 10^6$ Rads
Long Term Temperature	144°C	$\leq 204^\circ\text{C}$
Peak Temperature	262°C	$\leq 270^\circ\text{C}$
Temperature Duration Over 250°C	83 mins	≤ 120 mins
Minimum Compression	10.4%	$\geq 10\%$
Maximum Compression	23.9%	$\leq 30\%$
Maximum Groove Fill	86.4%	$\leq 90\%$
Accident Conditions	Unaffected	Unaffected by mechanical tests
Capsule Temperature	471°C	$\leq 800^\circ\text{C}$
Thermal Compression Reduction	0	$< 1\%$

- The table above demonstrates that the R7021, O-ring material and the design of the seal housings meets all relevant Type B(U) regulatory containment criteria and guidelines for transporting up to 160 kCi of ^{60}Co as normal form material.
- Routine and periodic leaktesting comply with the DfT requirements and ANSI N14.5.

7. REFERENCES

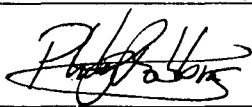
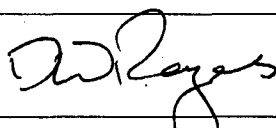
- 22550C: Compression Set testing on V1289-75 compound using Type A Buttons at 270°C, Ceetak Ltd, 2009.
- ANSI N14.5-1997: Radioactive Materials - Leakage Tests On Packages For Shipment.
- ASME II: Part D: 1995: ASME boiler and pressure vessel code. Properties.
- C15578/TR/0001 issue 2: Impact assessment of the Reviss R7021 package, AMEC Ltd, 2010.
- DTLR/RMTD/0004: "An Applicant's Guide to the Suitability of Elastomeric Seal Materials for Use in Radioactive Materials Transport Packages", RMTD, DTLR, Feb 2002.
- IR 0671 issue 1: Inspection report, 3981/01 closure bolt lengths before normal conditions drop testing, REVISS Services (UK) Ltd.
- IR 0675 issue 1: Inspection report, 3981/01 after accident conditions drop testing, REVISS Services (UK) Ltd.
- IR 0676 issue 1: Inspection report, 3981/01 closure bolt lengths after accident conditions drop testing, REVISS Services (UK) Ltd.
- OP 381: R7021 Operating and Maintenance Instructions, REVISS Services (UK) Ltd.
- ORD 5743: Technical Bulletin – Low Temperature FKM V1289-75, Parker Hannifin Corporation, 2006.
- Precision O-Ring Handbook: Catalogue 5705 E, March 1997, Parker Seals, Parker Hannifin GmbH.
- R7110/1.1: Thermal Analysis of the R7021 Radioactive Materials Transport Container, FTT Technology, July 2010.
- RC 13256A: Low Temperature testing of Parker V1289-75 O-rings, Ceetak Ltd, 2009.
- Roark's Formulas for stress and strain, 7th Edition, WC Young, McGraw-Hill, 2002.
- RTM 120 issue 2: Thermal performance of the R7021 transport container, REVISS Services (UK) Ltd.
- RTR 263: Test report, 3981/01 leak testing after accident conditions drop testing, REVISS Services (UK) Ltd.
- TS-R-1: Regulations for the Safe Transport of Radioactive Material, 2005 Edition, IAEA, Vienna.
- TS-G-1.1 (Rev. 1): Advisory Material for the IAEA Regulations for the Safe Transport of Radioactive Material, IAEA, Vienna, 2008.



**REVISS Services
Quality and Regulatory Group**

Technical Memorandum

**Compression Performance
of the R7021 Transport Container**

Author:		Reviewer:	
Name	P J G Robbins	Name	D W Rogers
Signature		Signature	
Date	28/07/10	Date	28/07/2010

1. PURPOSE AND SCOPE

This document analyses the stresses generated in the R7021 transport container in the IAEA compression test. It calculates the stresses in the load path and compares them with the design criteria.

2. DESCRIPTION

The R7021 consists of a lead shielded, stainless steel flask, with carbon steel top shield, jacket and pallet (Figure 1). The maximum gross weight is 4,600 kg.

3. ASSESSMENT

3.1 DESIGN CRITERIA

Stresses shall not exceed yield when the R7021, at normal conditions temperature, is subjected to the compression load test specified in TS-R-1, para 723.

3.2 TEST LOAD

The assembly must withstand the greater of either:

- Five times the maximum gross weight, i.e. $5 \times 4,600 = 23,000$ kg
- $1,300 \text{ kg/m}^2$ over the package vertically projected area, i.e. $1,300 \times 1.26^2 = 2,064$ kg

Therefore the test load is 23,000 kg.

3.3 ASSUMPTIONS

The load is evenly distributed.

3.4 LOAD PATH

With the R7021 in its normal upright position the compression load is taken on the four top shield cones, comprising a mixture of vertical and angled plates, from whence it passes into the top shield and there to the flask outer wall. The load is then transferred from the flask into the flask feet and thence to the pallet top plate, from which it passes through the channels and into the pallet base.

3.5 YIELD STRENGTHS

Under normal conditions of transport the upper surfaces of the top shield and pallet may reach temperatures up to 100°C (RTM 120). The minimum room temperature yield strength of these components is 400 N/mm^2 (drawings R7021/004 & R7021/005). This reduces to 371 N/mm^2 at a temperature of 100°C (using by proportion the reduction in design strength cited in PD 5500 for a similar grade steel (223, 490A) up to 100°C).

The flask wall is at a maximum temperature of 153°C (RTM 120). The flask is fabricated from 1.4307 (304L) plate to BS EN 10088-2 (drawing R7021/002). The minimum room temperature yield strength is 200 N/mm^2 . This reduces to 141 N/mm^2 at a temperature of 153°C (using by proportion the reduction in design strength cited in PD 5500 for a similar grade steel (304-S11) up to 200°C).

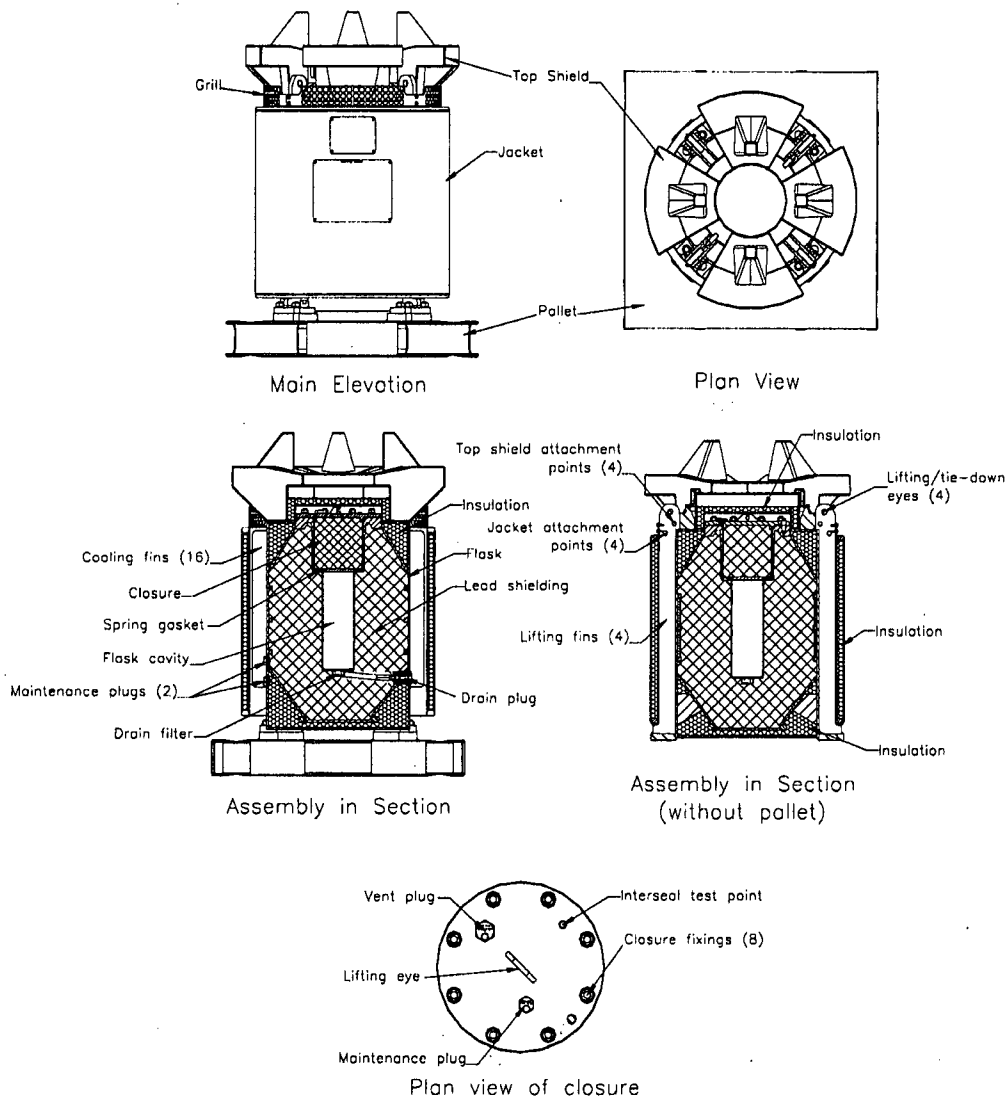


Figure 1: R7021 Assembly

4. ANALYSIS

4.1 TOP SHIELD CONES

The cones consist of a vertical plate and three angled plates welded to each other and to the top shield. The highest stress will be where the cross section is least, i.e. at the top. The compressive stress, S_1 , is calculated as follows:

$$S_1 = \frac{W}{A}$$

where

W = compression load = $23,000 \times 9.81 = 226 \text{ kN}$

A = cross-sectional area of load path

$$= N \times ((w \times t) + (w \times t \times \cos \alpha^\circ) + (2 \times w \times t \times \cos \beta^\circ))$$

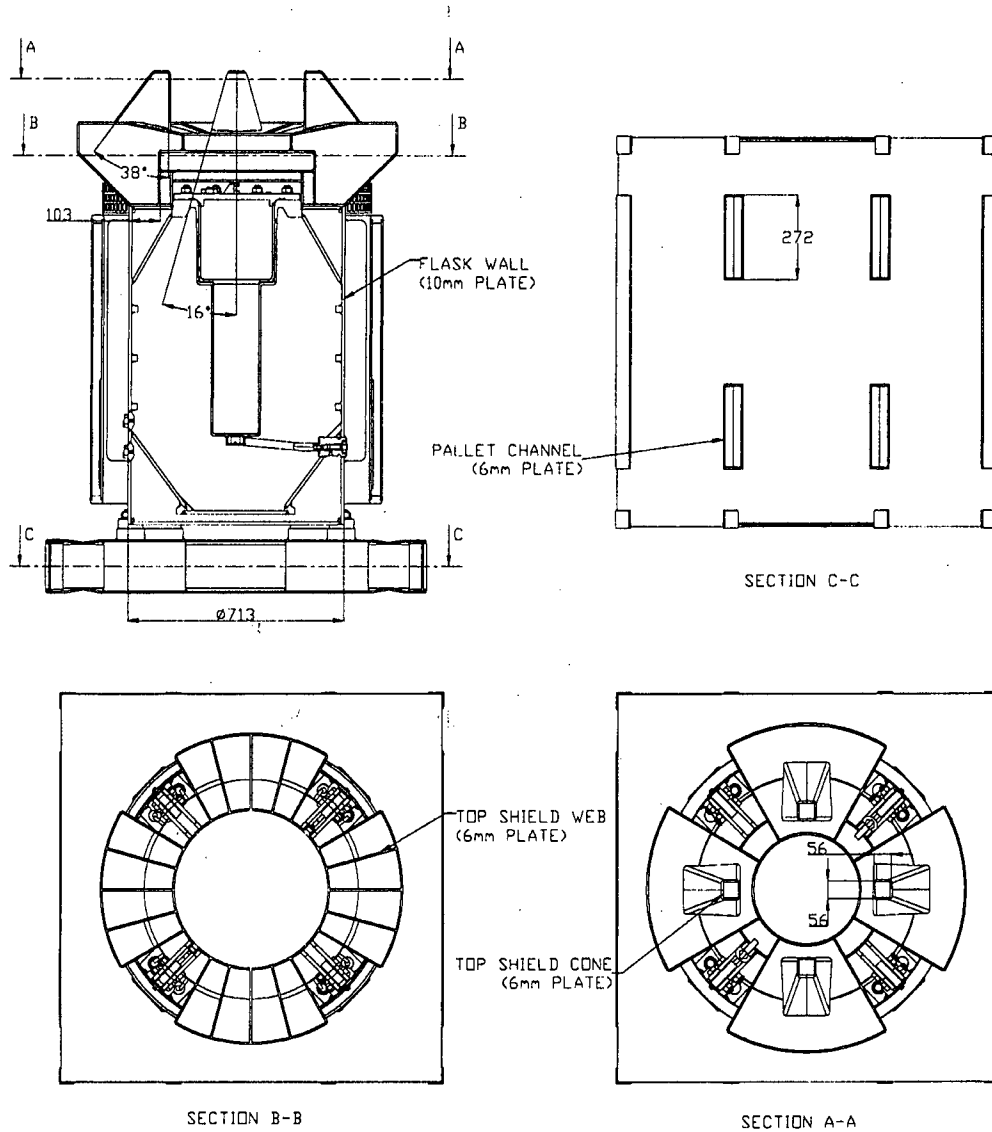


Figure 2: Load Path

where

N = number of cones = 4

w = plate width = 56 mm

t = plate thickness = 6 mm

α = angle from vertical of outboard plate = 40°

β = angle from vertical of side plates = 18°

thus

$$S_1 = \frac{W}{N \times ((w \times t) + (w \times t \times \cos \alpha^\circ) + (2 \times w \times t \times \cos \beta^\circ))}$$

$$= \frac{226 \times 10^3}{4 \times ((56 \times 6) + (56 \times 6 \times \cos 38^\circ) + (2 \times 56 \times 6 \times \cos 16^\circ))} = 45.3 \text{ N/mm}^2$$

4.2 TOP SHIELD

The top shield load path comprises four quadrants inside each of which are five vertical webs, three of which are under the cone. The webs are constrained against buckling by being welded on all sides, except the top horizontal, to the surrounding structure. The compressive stress in the plates, S_2 , is calculated as follows:

$$S_2 = \frac{W}{A}$$

where

W = compression load = 226 kN

A = cross-sectional area of load path = $N \times w \times t$

where

N = number of load bearing vertical plates = 12

w = load bearing width of plates = 103 mm

t = plate thickness = 6 mm

thus

$$S_2 = \frac{226 \times 10^3}{12 \times 103 \times 6} = 30.5 \text{ N/mm}^2$$

4.3 FLASK

The outer wall of the flask is an upright cylinder. The compressive stress in the wall, S_3 , is calculated as follows:

$$S_3 = \frac{W}{A}$$

where

W = compression load = 226 kN

A = cross-sectional area of load path = $D \times \pi \times t$

where

D = diameter of outer wall = 703 mm

t = wall thickness = 10 mm

thus

$$S_3 = \frac{226 \times 10^3}{703 \times 3.14 \times 10} = 10.2 \text{ N/mm}^2$$

4.4 PALLET

The pallet has channel sections directly beneath the flask feet. The compressive stress in these sections, S_4 , is calculated as follows:

$$S_4 = \frac{W}{A}$$

where

W = compression load = 226 kN

A = cross-sectional area of load path = $N \times l \times t$

where

N = number of vertical channel sections = 8

l = length of channels = 272 mm

t = plate thickness = 6 mm

thus

$$S_4 = \frac{226 \times 10^3}{8 \times 272 \times 6} = 17.3 \text{ N/mm}^2$$

4.5 SUMMARY

Component	Stress (N/mm ²)		Safety Factor
	Calculated	Yield	
Top shield cones, S ₁	45.3	371	8.19
Top shield structure, S ₂	30.5	371	12.2
Flask wall, S ₃	10.2	141	13.8
Pallet channels, S ₄	17.3	371	21.4

5. CONCLUSIONS

The R7021 is capable of supporting the compression load specified in TS-R-1, para 723, with a minimum factor of safety of 8.19. This is sufficient to compensate for any calculational inaccuracies or simplifications.

6. REFERENCES

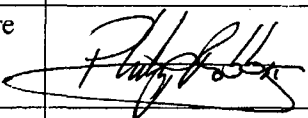
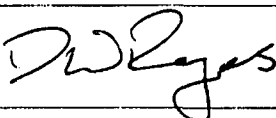
- BS EN 10088-2: 2005: Stainless steels. Technical delivery conditions for sheet/plate and strip of corrosion resisting steels for general purposes, British Standards Institution.
- Machinery's Handbook, 28th Edition, Industrial Press Inc, 2008.
- PD 5500: 2009: Specification for unfired fusion welded pressure vessels, British Standards Institution.
- R7021/002 issue D: Flask manufacturing drawing, REVISS Services (UK) Ltd.
- R7021/004 issue E: Pallet manufacturing drawing, REVISS Services (UK) Ltd.
- R7021/005 issue E: Top Shield manufacturing drawing, REVISS Services (UK) Ltd.
- RTM 120 issue 2: Thermal performance of the R7021 transport container, REVISS Services (UK) Ltd.
- TS-R-1: Regulations for the Safe Transport of Radioactive Material, 2005 Edition, IAEA, Vienna.



**REVISS Services
Quality and Regulatory Group**

Technical Memorandum

**R7021 Transport Container
Design Justification**

Author:		Reviewer:	
Name	P J G Robbins	Name	D W Rogers
Signature		Signature	
Date	15/09/10	Date	15/09/2010

1. PURPOSE AND SCOPE

This document details the changes to the R7021 transport container manufacturing drawings from the prototype onwards and justifies them with respect to the thermal, shielding, containment and mechanical performance of the design.

2. DESCRIPTION

The design consists of a shielded, stainless steel flask mounted on a pallet and protected from heat and impact by a jacket and top shield (Figure 1). The maximum gross weight is 4,600 kg.

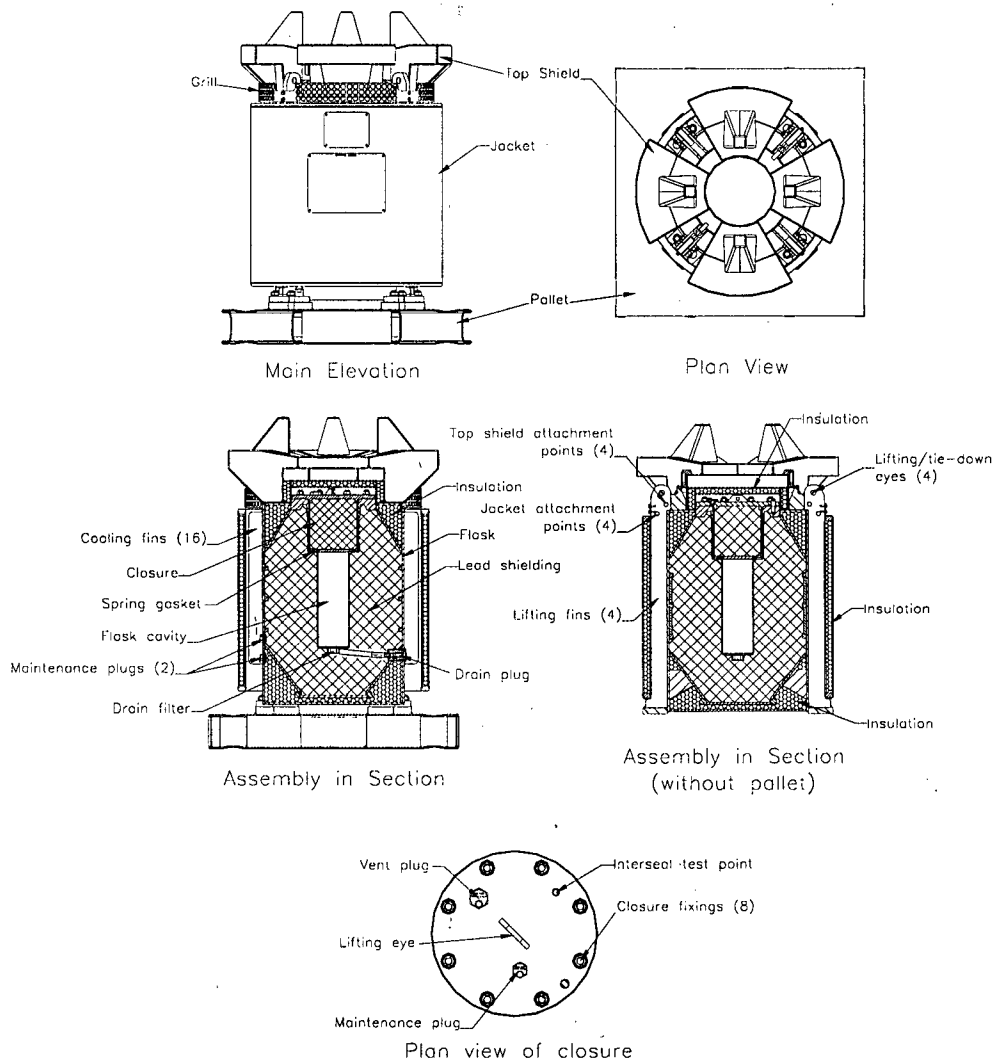


Figure 1: R7021 Assembly

3. ASSESSMENT

3.1 CHANGES FROM DRAWINGS LIST ISSUE 2 TO ISSUE 3

3.1.1 Pallet - R7021/004 issue C

Ref.	Change	Reason	Justification
3.1.1.1	Lateral folds added to upper and lower plates (items 1 & 14).	To give similar energy absorption in both axis.	See report C15578/TR/0001.
3.1.1.2	Projections on ends of channels (items 5) removed.	No value during impact.	
3.1.1.3	Thread size for dowel holes (in items 8) increased to M30, counterbore depth increased by 21mm and diameter reduced by 4mm.	To better support dowels.	
3.1.1.4	All fillet welds increased to 5mm.	To eliminate weld failure during drop testing.	
3.1.1.5	Fillet welds removed from central sections of outer channels (items 6) and inner ends of centre channels (items 10).	To improve welding access.	
3.1.1.6	Centre channels (items 10) no longer continuous between folds on upper and lower plates.	To provide more consistent energy absorption.	
3.1.1.7	Full penetration welds added top and bottom between components of each centre channel (items 10).	To minimise the risk of weld failure during drop testing.	
3.1.1.8	Items 12 added.	To fill in holes required when folding upper and lower plates.	
3.1.1.9	Weight reduced by 4kg.	Result of other changes.	Label has no effect on thermal, shielding, containment or mechanical performance.
3.1.1.10	Item 13 added and marking details (note 4) changed to engraving.	Label replaces stamping on prototype for better control of marking.	
3.1.1.11	Plan view added.	For clarity, to define unwelded lengths of outer channels (see 3.1.1.5).	Pictorial changes only.
3.1.1.12	Reference dimension (450) added for items 3.	For clarity.	
3.1.1.13	Lower plate becomes item 14.	For clarity.	Finish has no effect on thermal, shielding, containment or mechanical performance.
3.1.1.14	Paint specification reinstated.	To replace simplified specification on prototype.	

3.1.2 Top Shield - R7021/005 issue C

Ref.	Change	Reason	Justification
3.1.2.1	Outer diameter of component increased by 60mm.	For increased energy absorption.	See report C15578/TR/0001.
3.1.2.2	Height of cones (items 25 & 26) increased by 15mm. Reference dimensions amended.	For increased energy absorption.	

Ref.	Change	Reason	Justification
3.1.2.3	Length and width of cone caps (items 27) increased by 10mm. Reference dimensions amended.	For smoother energy absorption.	
3.1.2.4	Angle of outer cone face to vertical reduced by 2°. Reference dimensions amended.	To accommodate increased height (ref. 3.1.2.2).	
3.1.2.5	Height of outer face (items 13) reduced by 30mm.	To accommodate increase in outer diameter (ref. 3.1.2.1).	
3.1.2.6	Angle of items 10 to vertical reduced by 1.2°.	To accommodate increased height to items 14 caused by ref. 3.1.2.5.	
3.1.2.7	Items 3-6 removed and items 29-32 added.	To improve punch and drop test performance.	
3.1.2.8	Intermittent fillet welds around webs (items 16) changed to continuous both sides.	To eliminate weld failure during drop testing.	
3.1.2.9	Weld between items 12 & 13 becomes full thickness fillet.	To eliminate weld failure during drop testing.	
3.1.2.10	All fillet welds except to lifting points (items 20) increased to 6mm.	To eliminate weld failure during drop testing.	
3.1.2.11	Weight increased by 11kg.	Result of other changes.	
3.1.2.12	Item 23 moved to side view and item 27 becomes item 28.	For clarity and correction of error.	Pictorial change only.
3.1.2.13	Note 5 removed and st/st 304L added to materials box.	To better specify material grade.	No change to material specification.
3.1.2.14	Item 21 added and marking details (note 7) changed to engraving.	Label replaces stamping on prototype for clearer marking.	No effect on thermal, shielding, containment or mechanical performance.
3.1.2.15	Item 19 quantity reduced to 4 and item 33 quantity 4 added.	Correction of error.	Change to part numbering only.
3.1.2.16	Supplier details added to note 8.	For information.	No change to part specification.
3.1.2.17	Item 23 becomes stainless steel.	To realise original design intent.	No effect on thermal, shielding, containment or mechanical performance.
3.1.2.18	Paint specification reinstated.	To replace simplified specification on prototype.	No effect on thermal, shielding, containment or mechanical performance.
3.1.2.19	Outer diameter of item 8 and inner diameter of item 2 become 506mm and item numbers added to dimensions.	To rationalise dimensions and for clarity.	No change to design.
3.1.2.21	Angle 32° added to items 25 & 26.	To allow cone to be developed.	
3.1.2.22	Dimension 123/127 added to items 25 & 26.	To position cones.	

3.1.3 Jacket - R7021/006 issue C

Ref.	Change	Reason	Justification
3.1.3.1	Items 13 added, along with section F-F for positioning.	To reduce punch penetration near drain point.	See report C15578/TR/0001.
3.1.3.2	Weight increased by 17kg.	Result of other change.	
3.1.3.3	NDT2 (radiography – note 1) added to seam welds in inner (item 3) and outer (item 2) surfaces.	For improved weld assurance.	No change to design.
3.1.3.7	Angular position of seam welds in items 2 & 3 and joins in items 9 added.	For clarity.	
3.1.3.4	Item 12 added and marking details (note 8) changed to engraving.	Label replaces stamping on prototype for clearer marking.	No effect on thermal, shielding, containment or mechanical performance.
3.1.3.5	Weld preparation between items 9 & 2 and 9 & 3 becomes single-V.	For optimum welding access.	No effect on thermal, shielding, containment or mechanical performance.
3.1.3.6	Distance to item 9 weld root from top of component increased to 17mm.	To maintain clearance between the edge of the weld and radius.	
3.1.3.8	Angular tolerance relaxed for positioning items 8.	Over-specified.	No effect on thermal, shielding, containment or mechanical performance.
3.1.3.10	Weld of items 6 & 7 increased to 6mm.	For ease of manufacture and robustness.	
3.1.3.9	Paint specification reinstated.	To replace simplified specification on prototype.	No effect on thermal, shielding, containment or mechanical performance.

3.2 CHANGES FROM DRAWINGS LIST ISSUE 3 TO ISSUE 4

3.2.1 R7021 Container Assembly - R7021/001 issue C

Ref.	Change	Reason	Justification
3.2.1.1	Material of O-rings (items 28, 30 & 32) becomes FKM V1289-75.	For required performance.	See report 22550C.
3.2.1.2	Cross-section of O-rings (items 30, 31 & 32) increased by 0.22mm.	To allow use of new material.	See RTM 126.
3.2.1.3	Maintenance plugs (items 40) and O-rings (items 41 & 42) added, along with leak-testing of containment boundary (note 4A).	Requirement for production design.	
3.2.1.4	Item 12 becomes M30 dowel and material becomes c/st.	To reflect revised design.	
3.2.1.5	Items 13, 14, 18 & 24 reinstated.	Omitted from prototype for test purposes.	No effect on thermal, shielding, containment or mechanical performance.
3.2.1.6	Item 26 quantity increased to 6.	To protect interseal test points in maintenance plugs.	
3.2.1.7	Item 33 removed and quantity of item 30 becomes 2.	Rationalisation of O-rings.	
3.2.1.8	Item 16 finish becomes cadmium plate.	Omitted from prototype for test purposes.	No change to design.
3.2.1.9	Weighing requirement added to note 1.	To ensure compliance.	
3.2.1.10	Reference height becomes 1685 and reference diameter becomes 1060.	To reflect new top shield design.	See report C15578/TR/0001.
3.2.1.11	Stud (item 27) used for plugging temporary leak-test port removed.	No longer required.	Change has no effect on thermal, shielding, containment or mechanical performance.
3.2.1.12	Section A-A and drain plug detail added.	For clarity.	Pictorial change only.
3.2.1.13	Calculated weight (4390 kg) replaces measured weight (note 2).	To update data.	Changes affecting weight justified elsewhere in this document.
3.2.1.14	Supplier details added to note 5.	For information.	No change to part specification.

3.2.2 Body - R7021/002 issue C

Ref.	Change	Reason	Justification
3.2.2.1	Lifting fin (items 11) chamfers lengthened to 1050mm.	To remove sharp edges.	See report C15578/TR/0001.
3.2.2.2	Edge radius added to fins (items 7).		
3.2.2.3	Lifting fin (items 11) fillet welds increased to 10mm.	To improve strength and thermal conductivity.	
3.2.2.4	Items 27 added.	To better secure lead.	
3.2.2.5	Additional item 8 added.	For ease of manufacture.	
3.2.2.6	Feet (items 12) welds increased to 10mm fillet.	To maximise strength of joint.	
3.2.2.7	Minimum stainless steel properties added (note 11).	To bring into line with modelling.	
3.2.2.8	Weld between items 14 & 18	To allow a more	

Ref.	Change	Reason	Justification
	moved and becomes full penetration single V-butt.	consistent weld to be made and tested.	
3.2.2.9	Welds between cones (items 4 & 5) and outer wall (item 1) increased to 12mm fillet.	To maximise strength.	
3.2.2.10	Welds between feet (items 12) and lifting fins (items 11) changed to bevel-butt beneath 10mm fillet.		
3.2.2.11	Items 14, 18, 19, 20, & 21 modified.	To allow UT inspection, remove sharp corners, return depth of closure counterbore and cavity to original dimensions and increase strength of connection to item 14.	
3.2.2.12	Items 4 to 14 register reduced.	To ensure full penetration.	
3.2.2.13	Drain tube assembly (item 29) replaces items 16, 17 & 22. Note 9 item numbers updated.	To better represent manufacturing process.	
3.2.2.14	Item 23 details modified.	To suit new drain tube assembly.	
3.2.2.15	Item 29 to 21 welds enlarged.	To maximise strength of joint.	
3.2.2.16	Major revision to item 29.	To provide annulus around drain tube, improve thermal connection to item 5 and reduce projection outside item 1.	
3.2.2.17	Calculated weight (3418 kg) replaces measured weight (note 2).	To update data.	
3.2.2.18	Fin (items 7) welds increased to 5mm.	To maximise thermal conduction.	See RTM 120.
3.2.2.19	Tie-down holes in lifting fins (items 11) increased to 30mm diameter.	To reduce tie-down contact stress.	See RTM 122.
3.2.2.20	Items 28 added.	To provide leak-test points.	See RTM 126.
3.2.2.21	Register in cavity base (item 21) increased in diameter by 10mm.	To accommodate item 29.	Changes have no effect on thermal, shielding, containment or mechanical performance.
3.2.2.22	Item 10 fillet weld increased to 5mm.	For ease of welding.	
3.2.2.23	Seam weld in item 1 moved 90°.	To avoid test points.	
3.2.2.24	UT inspection added to note 1 and welds in items 1, 3, 5, 9, 13 & 14. Items 14, 19, 21 & 23 increased in thickness to allow for UT inspection.	For improved assurance.	
3.2.2.25	Weld between items 9 & 13 becomes a single-V.	For ease of manufacture.	
3.2.2.26	Angle of dish on item 21 becomes 2.1/1.9°.	To better control angle.	
3.2.2.27	Item 24 added and marking details (note 7) changed to engraving.	Label replaces stamping on prototype for clearer	No effect on thermal, shielding, containment or

Ref.	Change	Reason	Justification
		marking.	mechanical performance.
3.2.2.28	St/st now to BS EN 10088.	For clarity.	No change to design.
3.2.2.29	Fin radius (20mm) added.	To correct omission.	
3.2.2.30	Finish now refers to note 3.	For clarity.	
3.2.2.31	Note 10 added.	To avoid risk of container being overweight.	
3.2.2.32	Reference to BS2779 (note 6) deleted.	No longer required.	
3.2.2.33	Item 8 to 1 weld updated.	Correction of error.	
3.2.2.34	Depth of item 14 from item 3 changed to 25.1/24.9mm, thickness of item 21 changed to 8.2/7.8mm, depth from item 19 to item 21, 482.2/481.8mm, and depth from item 19 to item 14, 217.1/216.8mm, added. Thickness of item 19 (8mm) and projection of item 14 (20mm) become reference.	To better control build-up of tolerances.	Pictorial change only.
3.2.2.35	View M added.	To show test points.	
3.2.2.36	Part-fabrication details added.	For ease of manufacture.	

3.2.3 Closure - R7021/003 issue C

Ref.	Change	Reason	Justification
3.2.3.1	Section E-E added.	To provide test point for containment boundary.	No effect on thermal, shielding, containment or mechanical performance.
3.2.3.2	4mm diameter hole added to lifting point (item 4).	To enable test point plug to be wired.	
3.2.3.3	Item 1 to 6 weld preparation modified.	To improve access.	
3.2.3.4	UT inspection added to note 1 and welds in items 1, 2 & 6. Item 2 increased in thickness to allow for UT inspection. Item 6 adjusted to compensate. Section E-E weld preparation also modified.	For improved assurance.	
3.2.3.5	Item 7 added and marking details (note 5) changed to engraving.	Label replaces stamping on prototype for clearer marking.	No effect on thermal, shielding, containment or mechanical performance.
3.2.3.6	St/st now to BS EN 10088.	For clarity.	No change to design.
3.2.3.7	Finish now refers to note 3.	For clarity.	
3.2.3.8	Items 3, 9, 10 & 11 deleted.	No longer necessary.	See report C15578/TR/0001.
3.2.3.9	Calculated weight (156 kg) replaces measured weight (note 2).	To update data.	
3.2.3.10	Minimum stainless steel properties added (note 11).	To bring into line with modelling.	
3.2.3.11	Depth dimension and final thickness of base of item 2 revert to issue A values.	To re-balance shielding.	
3.2.3.12	Half section titles and shrinkage warning note added.	For clarity.	Pictorial change only.

3.2.4 Pallet - R7021/004 issue D

Ref.	Change	Reason	Justification
3.2.4.1	Finish becomes galvanising.	Access for painting restricted due to items 16.	No effect on thermal, shielding, containment or mechanical performance. See report C15578/TR/0001.
3.2.4.2	Items 16 and associated details added.	To provide structural support to channel sections.	
3.2.4.3	Calculated weight becomes 240 kg (note 2). Engraved weight is 248kg.	To reflect changes. Weight includes studs and dowels.	
3.2.4.4	Minimum c/st properties added to note 3.	To ensure adequate strength and ductility.	
3.2.4.5	Dimensions of central channels reduced to 33.5/31.5mm & 18.5/16.5mm.	To bring centre of effort of flask feet more centrally over channels in upright drop test.	

3.2.5 Top Shield - R7021/005 issue D

Ref.	Change	Reason	Justification
3.2.5.1	Minimum st/st properties added to note 5.	To ensure adequate strength and ductility.	See report C15578/TR/0001.
3.2.5.2	Minimum c/st properties added to note 6.	To ensure adequate strength and ductility.	
3.2.5.3	Paint specification changed to SS023.	Correction of error.	No change to design.

3.2.6 Jacket - R7021/006 issue D

Ref.	Change	Reason	Justification
3.2.6.1	Minimum st/st properties added to note 3.	To ensure materials are of sufficient strength and ductility.	See report C15578/TR/0001.
3.2.6.2	Minimum c/st properties added to note 4.	To ensure materials are of sufficient strength and ductility.	
3.2.6.3	Paint specification changed to SS023.	Correction of error.	No change to design.

3.2.7 Drain Plug - R7021/008 issue B

Ref.	Change	Reason	Justification
3.2.7.1	Overall length increased.	To locate main seal deeper within container.	See RTM 120.
3.2.7.2	Increased depth of tap drill hole.	To minimise conduction of heat along plug.	
3.2.7.3	Change in seal groove dimensions.	To accommodate imperial seal sizes.	See RTM 126.
3.2.7.4	Backup seal changed to chamfer-type.	For ease of manufacture.	No effect on thermal, shielding, containment or mechanical performance.
3.2.7.5	Engraving added to head of plug.	For operator information.	

3.2.8 Vent Plug - R7021/009 issue B

Ref.	Change	Reason	Justification
3.2.8.1	Change in seal groove dimensions.	To accommodate imperial seal sizes.	See RTM 126.
3.2.8.2	Hex head angle 60° added.	For clarity.	No change to design.
3.2.8.3	Thread standard now to ISO 228.		
3.2.8.4	Material specification changed to 300 series st/st.		
3.2.8.5	Engraving added to head of plug.	For operator information.	No effect on thermal, shielding, containment or mechanical performance.

3.2.9 M20 Stud - R7021/011 issue C

Ref.	Change	Reason	Justification
3.2.9.1	Material grade changed to A2-80 or A4-80.	Lower grade used on prototype for test purposes.	See report C15578/TR/0001.
3.2.9.2	Calculated weight 0.2kg added.	For information.	No change to design.
3.2.9.3	Engraving updated.	To reflect new issue status.	

3.2.10 M24 Stud - R7021/012 issue C

Ref.	Change	Reason	Justification
3.2.10.1	Thread length increased to 40mm and overall length increased to 99mm.	To allow stud to engage with pallet top plate.	See report C15578/TR/0001.
3.2.10.2	Calculated weight 0.4kg added.	For information.	No change to design.
3.2.10.3	Engraving updated.	To reflect new issue status.	

3.2.11 M30 Dowel - R7021/013 issue B

Ref.	Change	Reason	Justification
3.2.11.1	Thread size increased to M30. Undercut diameter becomes 25.5/25.3mm and thread chamfer becomes 2.5mm x 45°.	To maximise strength.	See report C15578/TR/0001.
3.2.11.2	OD changed to 39.8/39.7mm.	To improve fit in pallet counterbore.	
3.2.11.3	Body length changed to 91mm and length to flats changed to 71mm.	To increase depth of engagement with counterbore.	
3.2.11.4	Lengths of threaded portion become 15.5mm and 6mm.	To maintain overall engagement depth of dowel.	
3.2.11.5	Material changed to c/st grade 8.8. Finish becomes cadmium plate and passivate.	For increased strength.	No change to design.
3.2.11.6	Calculated weight 1.1kg added.	For information.	

3.2.12 Identity Plate - R7021/015 issue B

Ref.	Change	Reason	Justification
3.2.12.1	Maximum gross weight becomes 4600kg.	To reflect new maximum design weight.	See report C15578/TR/0001.
3.2.12.2	Assembly net weight and jacket weight removed.	For simplicity.	No change to design.
3.2.12.3	Note 2 NN changed to XX.	To bring into line with similar drawings.	

3.2.13 M16 Shoulder Bolt - R7021/016 issue C

Ref.	Change	Reason	Justification
3.2.13.1	Minimum c/st properties added to note 1.	To ensure adequate strength and ductility.	See report C15578/TR/0001.
3.2.13.2	Reference to manufacture from M10 x 100mm bolt removed.	To allow manufacture from bar stock.	No change to design.
3.2.13.3	Plain portion diameter 20.1/19.9mm, head depth 13mm, across flats width 30.0/29.8mm and hex head angle 60° added.		
3.2.13.4	Finish changed to cadmium plate and passivate.	Omitted from prototype for test purposes.	No effect on thermal, shielding, containment or mechanical performance.

3.2.14 Drain Filter - R7021/017 issue B

Ref.	Change	Reason	Justification
3.2.14.1	Components detailed separately.	For clarity.	No change to design.
3.2.14.2	Overall height increased.	To allow for increased depth of well due to drain to drain tube sleeve.	No effect on thermal, shielding, containment or mechanical performance.

3.2.15 1/8" BSP Maintenance Plug - R7021/019 issue A

Ref.	Change	Reason	Justification
3.2.15.1	New drawing.	New requirement.	No effect on thermal, shielding, containment or mechanical performance.

3.2.16 Drain Tube Assembly - R7021/020 issue A

Ref.	Change	Reason	Justification
3.2.16.1	New sub-assembly drawing created from details previously on body, R7021/002.	To better suit manufacturing process.	No change to design.
3.2.16.2	Design modified.	To incorporate drain tube sleeve, interspace leak-test point, improved NDT and leak-testing.	See report C15578/TR/0001.

3.2.17 Boss - R7021/021 issue A

Ref.	Change	Reason	Justification
3.2.17.1	New drawing created from details previously on body, R7021/002.	To better suit manufacturing process.	No change to design.
3.2.17.2	Design modified.	To incorporate drain tube sleeve, radiography of drain tube joint, interspace leak-test point, longer drain plug (with imperial seals), to update thread standard and to minimise protrusion of plug head.	See report C15578/TR/0001.

3.2.18 Well - R7021/022 issue A

Ref.	Change	Reason	Justification
3.2.18.1	New drawing created from details previously on body, R7021/002.	To better suit manufacturing process.	No change to design.
3.2.18.2	Design modified.	For drain tube sleeve and radiography of drain tube joint.	See report C15578/TR/0001.

3.2.19 Outer Tube - R7021/023 issue A

Ref.	Change	Reason	Justification
3.2.19.1	New drawing.	To protect drain tube from lead movement.	See report C15578/TR/0001.

3.2.20 Drain Tube - R7021/024 issue A

Ref.	Change	Reason	Justification
3.2.20.1	New drawing created from details previously on body, R7021/002.	To better suit manufacturing process.	No change to design.
3.2.20.2	Design modified.	To allow radiography of joints.	See report C15578/TR/0001.

3.2.21 Sheath - R7021/025 issue A

Ref.	Change	Reason	Justification
3.2.21.1	New drawing.	To protect drain tube from lead movement.	See report C15578/TR/0001.

3.2.22 Plug - R7021/026 issue A

Ref.	Change	Reason	Justification
3.2.22.1	New drawing.	Allows inside of drain tube to be machined after welding.	No effect on thermal, shielding, containment or mechanical performance.

3.2.23 Filter Body - R7021/027 issue A

Ref.	Change	Reason	Justification
3.2.23.1	New drawing created from details previously on drain filter, R7021/017.	For clarity.	No change to design.
3.2.23.2	Height increased.	To allow for increased depth of well due to drain tube sleeve.	No effect on thermal, shielding, containment or mechanical performance.

3.2.24 Backing Ring - R7021/028 issue A

Ref.	Change	Reason	Justification
3.2.24.1	New drawing created from details previously on drain filter, R7021/017.	For clarity.	No change to design.

3.2.25 Washer - R7021/029 issue A

Ref.	Change	Reason	Justification
3.2.25.1	New drawing created from details previously on drain filter, R7021/017.	For clarity.	No change to design.

3.2.26 Mesh - R7021/030 issue A

Ref.	Change	Reason	Justification
3.2.26.1	New drawing created from details previously on drain filter, R7021/017.	For clarity.	No change to design.

3.3 CHANGES FROM DRAWINGS LIST ISSUE 4 TO ISSUE 5

3.3.1 R7021 Container Assembly - R7021/001 issue D

Ref.	Change	Reason	Justification
3.3.1.1	Item 18 becomes M8 x 10 skt pan hd screw. Quantity of item 23 becomes 24. Item 24 removed.	Correction of error. Thread size mismatch between fasteners and label holes on jacket.	Change has no effect on thermal, shielding, containment or mechanical performance.
3.3.1.2	Note 6 added.	Correction of omission.	No change to design.
3.3.1.3	Item 20 specification becomes to BS EN ISO 3506-2.	Correction of error.	

3.3.2 Body - R7021/002 issue D

Ref.	Change	Reason	Justification
3.3.2.1	Diameter of spring gasket recess in item 19 becomes 232mm.	To accommodate increased outer diameter of spring gasket.	Changes have no effect on thermal, shielding, containment or mechanical performance.
3.3.2.2	Angular dimension on item 14 becomes 65°/55°.	Dimension over-specified.	
3.3.2.3	Note 13 added.	To permit alternative machining processes.	
3.3.2.4	Dimensions of holes through leak-test points (items 28) changed (minimum thread depth becomes 12mm, tap drill max depth becomes 16mm). Diameter 6mm hole added to break through with max drill point 31mm and note 14 added.	Correction of omission. Necessary to maintain cleanliness of shielding and insulation.	
3.3.2.5	External radius (7mm) at the base of items 11 removed.	Unnecessary feature.	316L is compatible with 304L and has identical mechanical and thermal properties.
3.3.2.6	Alternative material grade 1.4404 (316L) added.	For ease of procurement.	
3.3.2.7	NDT2 removed from fillet weld between items 5 & 13.	UT requirement is not essential.	
3.3.2.8	NDT3 (Radiography) added to note 1. NDT2 changed to NDT3 on two welds between items 21 & 29.	Radiography is more appropriate for the material geometry and thickness.	Weld is a back-up for the full penetration weld between these items and as such is not a key structural weld.
3.3.2.9	NDT3 added to welds between items 4 & 1 and items 5 & 1.	Radiography is needed to cover volumetric and horizontal side wall defects.	
3.3.2.10	NDT2 removed from weld between items 11 & 12.	UT not practicable.	
3.3.2.11	NDT2 changed to NDT3 for item 18 seam weld and welds between items 14 & 18, 18 & 19, 19 & 20, and 20 & 21.	UT not practicable for all circumferential welds.	

Ref.	Change	Reason	Justification
3.3.2.12	Note 11 removed.	Redundant information. Minimum properties for 304L in BS EN 10088 are the same as those specified.	
3.3.2.13	Note 12 added specifying coupon for welds between items 21 and 29.	Not practicable to inspect root of welds using volumetric NDT.	
3.3.2.14	Dimension 28mm (position of chamfer on item 18) removed.	Insufficient raw material thickness in item 18 to accommodate chamfer.	No effect on structural strength or shielding. Wall thickness maintained at junction with main flange and transition remains well clear of junction.
3.3.2.15	Spotface added to diameter 30 holes on items 12 (diameter 51/49mm, depth such that thickness under spotface is 31/28mm).	To ensure flask securing nuts are tightened onto a flat and perpendicular surface. Eliminates sensitivity of design to distortion of feet from welding.	No change to net thickness of feet, hence no change to shear area. Thus mechanical performance is not affected.
3.3.2.16	10mm radius on item 19 moved to corner of machined rebate.	Correction of error.	Pictorial change only.

3.3.3 Closure - R7021/003 issue D

Ref.	Change	Reason	Justification
3.3.3.1	Alternative material grade 1.4404 (316L) added.	For ease of procurement.	316L is compatible with 304L and has identical mechanical and thermal properties.
3.3.3.2	Note 6 removed.	Redundant information. Minimum properties for 304L in BS EN 10088 are the same as those specified.	No change to design.
3.3.3.3	Note 7 added.	To permit alternative machining processes.	No effect on thermal, shielding, containment or mechanical performance.
3.3.3.4	Dimensions of hole through leak-test point (section E-E) changed (minimum thread depth becomes 12mm, tap drill max depth becomes 16mm). Diameter 6mm hole added to break through with max drill point 32mm and note 8 added.	Correction of omission. Necessary to maintain cleanliness of shielding and insulation.	
3.3.3.5	Section showing seam weld through item 6 becomes F-F.	Correction of error. Section E-E already details leak-test point.	Pictorial change only.

3.3.4 Pallet - R7021/004 issue E

Ref.	Change	Reason	Justification
3.3.4.1	C/st yield strength becomes 400 N/mm ² (note 3).	To reflect modelled properties.	See report C15578/TR/0001.
3.3.4.2	Galvanising omitted from counterbores on items 8.	Not practicable to maintain tolerance on diameter.	No effect on thermal, shielding, containment or mechanical performance.
3.3.4.3	Alternative material grade (P460NL1/2 to EN 10028-3) added to note 3.	For ease of procurement.	Chemical and mechanical properties comply fully with drawing requirements.

3.3.5 Top Shield - R7021/005 issue E

Ref.	Change	Reason	Justification
3.3.5.1	C/st yield strength becomes 400 N/mm ² (note 3).	To reflect modelled properties.	See report C15578/TR/0001.
3.3.5.2	Alternative material grade (P460NL1/2 to EN 10028-3) added to note 3.	For ease of procurement.	Chemical and mechanical properties comply fully with drawing requirements.
3.3.5.3	Item 19 becomes item 20 in note 3	Correction of error.	No change to design.
3.3.5.4	Minimum stainless steel requirements and 'or equivalent' removed from note 5.	Redundant information. Minimum properties for 304L (1.4307) in BS EN 10088 are the same as those specified.	No change to design.

3.3.6 Jacket - R7021/006 issue E

Ref.	Change	Reason	Justification
3.3.6.1	C/st yield strength becomes 400 N/mm ² (note 3).	To reflect modelled properties.	See report C15578/TR/0001.
3.3.6.2	Alternative material grade (P460NL1/2 to EN 10028-3) added to note 3.	For ease of procurement.	Chemical and mechanical properties comply fully with drawing requirements.
3.3.6.3	Note 10 added.	Flush weld finish only required opposite lifting fins.	No reduction in strength of weld and no difference to the weight.
3.3.6.4	Dimension 24°/0° and 10° added positioning items 10.	To give more flexibility during manufacture.	No effect on thermal, shielding, containment or mechanical performance.
3.3.6.5	Minimum stainless steel requirements and 'or equivalent' removed from note 3.	Redundant information. Minimum properties for 304L (1.4307) in BS EN 10088 are the same as those specified.	No change to design.

3.3.7 Drain Plug - R7021/008 issue C

Ref.	Change	Reason	Justification
3.3.7.1	Diameter 13.4 becomes 13.45/13.25.	To ensure clearance between the plug and boss when assembled.	No effect on thermal, shielding, containment or mechanical performance.

3.3.8 M24 Stud - R7021/012 issue D

Ref.	Change	Reason	Justification
3.3.8.1	Charpy V-notch impact requirement added (note 4).	Correction of omission.	No change to design.
3.3.8.2	Marking updated.	To reflect new issue level.	

3.3.9 M30 Dowel - R7021/013 issue C

Ref.	Change	Reason	Justification
3.3.9.1	Charpy V-notch impact requirement added (note 3).	Correction of omission.	No change to design.

3.3.10 Shipping Plate - R7021/014 issue B

Ref.	Change	Reason	Justification
3.3.10.1	Hole diameters become 11/10mm.	Correction of error.	No effect on thermal, shielding, containment or mechanical performance.

3.3.11 Identity Plate - R7021/015 issue C

Ref.	Change	Reason	Justification
3.3.11.1	Hole diameters become 11/10mm.	Correction of error.	No effect on thermal, shielding, containment or mechanical performance.

3.3.12 M16 Shoulder Bolt - R7021/016 issue D

Ref.	Change	Reason	Justification
3.3.12.1	Charpy V-notch impact requirement added (note 1).	Correction of omission.	No change to design.

3.3.13 Spring Gasket - R7021/018 issue B

Ref.	Change	Reason	Justification
3.3.13.1	Marking requirement becomes engraving (note 2).	Engraving is more durable.	No effect on thermal, shielding, containment or mechanical performance.
3.3.13.2	Outer diameter becomes 230mm, diameter of lower, inner edge becomes 227.4mm and angle becomes 8.9°.	To reduce bending stress when compressed and allow margin to yield strength at high temperature.	

3.3.14 1/8" BSP Maintenance Plug - R7021/019 issue B

Ref.	Change	Reason	Justification
3.3.14.1	Diameter 3mm hole becomes diameter 2.2mm. Hole position becomes 18.25mm.	To facilitate manufacture.	No effect on thermal, shielding, containment or mechanical performance.

3.3.15 Drain Tube Assembly - R7021/020 issue B

Ref.	Change	Reason	Justification
3.3.15.1	Alternative material grade 316L added.	For ease of procurement.	316L is compatible with 304L and has identical mechanical properties.
3.3.15.2	NDT1 removed from welds concerning items 3, 5, 6, & 8.	Visual inspection is sufficient to reveal any surface defects that might lead to lead ingress during casting.	Outer sleeve is not required to perform a structural function, just to ensure there is a gap around the inner tube after lead casting.
3.3.15.3	Note 8 added.	For ease of manufacture. Helps to control concentricity during assembly.	Change has no effect on thermal, shielding, containment or mechanical performance.

3.3.16 Boss - R7021/021 issue B

Ref.	Change	Reason	Justification
3.3.16.1	Alternative material grade 1.4404 (316L) added.	For ease of procurement.	316L is compatible with 304L and has identical mechanical properties.
3.3.16.2	Diameter 2.0mm in alternative detail becomes 4.0mm.	Ease of machining. Minimises risk of tool breakage.	Changes have no effect on thermal, shielding, containment or mechanical performance.
3.3.16.3	2mm x 90° countersink added to holes diameter 4.0mm.	Ease of welding.	

3.3.17 Well - R7021/022 issue B

Ref.	Change	Reason	Justification
3.3.17.1	Alternative material grade 1.4404 (316L) added.	For ease of procurement.	316L is compatible with 304L and has identical mechanical properties.

3.3.18 Outer Tube - R7021/023 issue B

Ref.	Change	Reason	Justification
3.3.18.1	Alternative material grade 316L added.	For ease of procurement.	316L is compatible with 304L and has identical mechanical properties.

3.3.19 Drain Tube - R7021/024 issue B

Ref.	Change	Reason	Justification
3.3.19.1	Alternative material grade 316L added.	For ease of procurement.	316L is compatible with 304L and has identical mechanical properties.

3.3.20 Sheath - R7021/025 issue B

Ref.	Change	Reason	Justification
3.3.20.1	Alternative material grade 316L added.	For ease of procurement.	316L is compatible with 304L and has identical mechanical properties.

3.3.20.1	Drawing title becomes 'Sheath'.	'Outer Tube' already in use (R7021/023).	No change to design.
----------	---------------------------------	--	----------------------

3.3.21 Plug - R7021/026 issue B

Ref.	Change	Reason	Justification
3.3.21.1	Alternative material grade 1.4404 (316L) added.	For ease of procurement.	316L is compatible with 304L and has identical properties.

3.3.22 Mesh - R7021/030 issue B

Ref.	Change	Reason	Justification
3.3.22.1	'Plain weave' removed from description. Material becomes 304 or 316 st/st. Wire diameter becomes 0.1mm max. Aperture becomes 0.1mm max. Open area becomes 0.3 min. 'Mesh' and 'microns' removed. 'May be part no.' added.	For ease of procurement.	No effect on mechanical performance.

4. CONCLUSIONS

All changes affecting mechanical, thermal, containment and shielding performance made between issues 2 (prototype) and issue 4 (production) are justified through modelling and calculation. Changes made between issues 4 and 5 (as manufactured) have no adverse effect any of these criteria.

5. REFERENCES

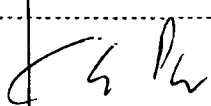
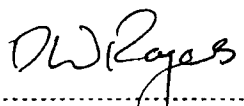
- 22550C: Compression Set testing on V1289-75 compound using Type A Buttons at 270°C, Ceetak Ltd, 2009.
- C15578/TR/0001 issue 2: Impact assessment of the REVISS R7021 package, AMEC Ltd.
- QS 7021 issue 2: R7021 Transport container drawings List and drawings, REVISS Services (UK) Ltd.
- QS 7021 issue 3: R7021 Transport container drawings List and drawings, REVISS Services (UK) Ltd.
- QS 7021 issue 4: R7021 Transport container drawings List and drawings, REVISS Services (UK) Ltd.
- QS 7021 issue 5: R7021 Transport container drawings List and drawings, REVISS Services (UK) Ltd.
- RTM 120 issue 2: Thermal performance of the R7021 transport container, REVISS Services (UK) Ltd.
- RTM 122 issue 2: Performance of the R7021 (GB 3981) transport container under IAEA tie-down loads, REVISS Services (UK) Ltd.
- RTM 126 issue 2: Justification of the R7021 containment system, REVISS Services (UK) Ltd.



**REVISS Services
Quality And Operations Group**

Technical Memorandum

Nuclide Heating

Author:		Reviewer:	
Name	C. Pyne	Name	DW ROGERS
Signature		Signature	
Date	11/4/00	Date	11/04/00

1. PURPOSE AND SCOPE

The purpose of this document is to define the decay heat output of a variety of nuclides for use in thermal calculations and analysis.

2. INTRODUCTION

When radiation is emitted by a decaying nucleus, energy is carried away by a combination of particles and electromagnetic radiation. When that radiation is absorbed, e.g. by shielding, its' energy is dissipated in the form of heat. The maximum amount of heating will occur when all of the energy of the radiation is absorbed. Any emitted neutrinos can be discounted, as they interact only weakly with matter and are not considered to contribute to heating effects.

3. CALCULATION OF NUCLIDE HEATING

In order to determine the total energy emitted by a decaying radioactive isotope, we must consider all possible decay routes that emit particles, except neutrinos, or photons.

Browne *et al*¹ have published a table of experimental values for the average energy released, per disintegration, for a range of radioactive isotopes; they consider electromagnetic radiation, α -particles, electrons and positrons. Summing the average energies per disintegration, for all of these radiation types, gives the total average energy per disintegration that is available for conversion to heat.

Average energies emitted for a range of isotopes are listed in the Table of Radioactive Isotopes in units of keV. The total energy has been converted to power using the following relationships:

$$\begin{aligned} 1 \text{ keV} &= 1.60 \times 10^{-16} \text{ J} \\ 1 \text{ W} &= 1 \text{ Js}^{-1} \\ 1 \text{ Bq} &= 1 \text{ disintegration per second} \\ 1 \text{ Ci} &= 3.7 \times 10^{10} \text{ Bq} \end{aligned}$$

$$\begin{aligned} \therefore \text{Power} &= 1.60 \times 10^{-16} \text{ WBq}^{-1} \\ &= 0.160 \text{ mWTBq}^{-1} \\ &= 5.92 \times 10^{-3} \text{ mWCi}^{-1} \end{aligned}$$

4. REFERENCES

Table of Radioactive Isotopes, E Browne & R B Firestone (ed Virginia S Shirley), John Wiley & Sons, 1986.

Average Energies and Power Dissipation

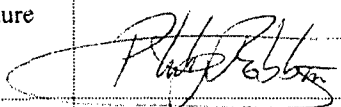
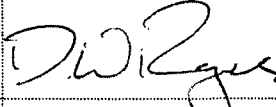
Nuclide	Symbol	Half-Life	Average Energy Per Disintegration / keV					Power Dissipation	
			alpha	electron	positron	e.m	Total	mW / Ci	mW / TBq
Actinium-227	²²⁷ Ac	21.77 yr	67.3	12.5		0.168	80	0.47	13
Americium-241	²⁴¹ Am	432.7 yr	5480	30.4		28.7	5539	32.79	886
Americium-243	²⁴³ Am	7380 yr	5270			48.1	5318	31.48	851
Antimony-122	¹²² Sb	2.70 dy		566		434	1000	5.92	160
Antimony-124	¹²⁴ Sb	60.20 dy		390		1850	2240	13.26	358
Bismuth-210	²¹⁰ Bi	5.013 dy		389		0.45	389	2.31	62
Bismuth-214	²¹⁴ Bi	19.9 min	1.43	662		1510	2173	12.87	348
Cadmium-109	¹⁰⁹ Cd	1.267 yr		81.3		26	107	0.64	17
Caesium-134	¹³⁴ Cs	2.062 yr		164		1550	1714	10.15	274
Caesium-137	¹³⁷ Cs	30.0 yr		250		566	816	4.83	131
Californium-252	²⁵² Cf	2.64 yr	5930	5.14		1.14	5936	35.14	950
Cobalt-56	⁵⁶ Co	77.7 dy		3.6	120	3580	3704	21.93	593
Cobalt-57	⁵⁷ Co	271.77 dy		17.6		125	143	0.84	23
Cobalt-58	⁵⁸ Co	70.92 dy		3.6	30	977	1011	5.98	162
Cobalt-60	⁶⁰ Co	5.271 yr		96		2500	2596	15.37	415
Curium-242	²⁴² Cm	162.9 dy	6040	8.95		1.75	6051	35.82	968
Curium-244	²⁴⁴ Cm	18.11 yr	5800			1.6	5802	34.35	928
Europium-152	¹⁵² Eu	13.33 yr		127	8.70E-02	1160	1287	7.62	206
Europium-154	¹⁵⁴ Eu	8.8 yr		279		1250	1529	9.05	245
Europium-155	¹⁵⁵ Eu	4.96 yr		65		63	128	0.76	20
Europium-156	¹⁵⁶ Eu	15.2 dy		425		1330	1755	10.39	281
Gadolinium-153	¹⁵³ Gd	241.6 dy		39.9		102	142	0.84	23
Gold-198	¹⁹⁸ Au	2.6935 dy		421		403	824	4.88	132
Hydrogen-3	³ H	12.3 yr		5.7		1.12E-04	6	0.03	1
Iodine-125	¹²⁵ I	60.1 dy		17.9		42.4	60	0.36	10
Iodine-131	¹³¹ I	8.04 dy		192		382	574	3.40	92
Iridium-192	¹⁹² Ir	73.83 dy		216		813	1029	6.09	165
Iridium-194	¹⁹⁴ Ir	19.15 hr		811		92	903	5.35	144
Iron-59	⁵⁹ Fe	44.5 dy		118		1190	1308	7.74	209
Krypton-85	⁸⁵ Kr	10.72 yr		251		2.4	253	1.50	41
Lead-201	²⁰¹ Pb	9.33 hr		60.9	9.70E-02	760	821	4.86	131
Lead-210	²¹⁰ Pb	22.3 yr		34.2		4.67	39	0.23	6
Lead-214	²¹⁴ Pb	27 min		294		250	544	3.22	87
Molybdenum-99	⁹⁹ Mo	2.7477 dy		408		273	681	4.03	109
Neptunium-237	²³⁷ Np	2.14E06 yr	4760	64		32.7	4857	28.75	777
Phosphorus-32	³² P	14.282 dy		695		1.18	696	4.12	111

Nuclide	Symbol	Half-Life	Average Energy Per Disintegration / keV					Power Dissipation	
			alpha	electron	positron	e.m.	Total	mW / Ci	mW / TBq
Plutonium-238	²³⁸ Pu	87.7 yr	5490	9.92		1.76	5502	32.57	880
Plutonium-239	²³⁹ Pu	2.411E+04 yr	5100			6.60E-02	5100	30.19	816
Plutonium-240	²⁴⁰ Pu	6.54E+03 yr	5160			2.86E-02	5160	30.55	826
Plutonium-241	²⁴¹ Pu	14.4 yr	0.118	5.2		1.46E-03	5	0.03	1
Polonium-210	²¹⁰ Po	138.376 dy	5300				5300	31.38	848
Polonium-214	²¹⁴ Po	163.7 ms	7690			8.30E-02	7690	45.53	1230
Polonium-218	²¹⁸ Po	3.11 min	6000				6000	35.52	960
Promethium-147	¹⁴⁷ Pm	2.6234 yr		62		1.86E-02	62	0.37	10
Protactinium-231	²³¹ Pa	3.28E+04 yr	4920	48		39.9	5008	29.65	801
Radium-226	²²⁶ Ra	1.60E+03 yr	4770	3.53		6.74	4780	28.30	765
Radon-222	²²² Rn	3.825 dy	5490				5490	32.50	878
Samarium-151	¹⁵¹ Sm	90 yr		125		6.71E-02	125	0.74	20
Selenium-75	⁷⁵ Se	119.77 dy		14.2		392	406	2.40	65
Silver-110m	¹¹⁰ Ag	249.76 dy		75.5		2740	2816	16.67	450
Sodium-24	²⁴ Na	14.659 hr		554		4120	4674	27.67	748
Strontium-90	⁹⁰ Sr	28.5 yr		196		0.124	196	1.16	31
Sulphur-35	³⁵ S	87.5 dy		48.6		8.60E-03	49	0.29	8
Technetium-99m	⁹⁹ Tc	6.006 hr		14.2		124	138	0.82	22
Tellurium-131m	¹³¹ Te	1.2 dy		52.3		1420	1472	8.72	236
Thorium-228	²²⁸ Th	1.913 yr	5400	20.1		3.4	5424	32.11	868
Thorium-230	²³⁰ Th	7.54E+04 yr	4660			0.371	4660	27.59	746
Thulium-170	¹⁷⁰ Tm	128.6 dy		330		5.73	336	1.99	54
Tin-119m	¹¹⁹ Sn	293 dy		78.3		11.4	90	0.53	14
Tritium	See Hydrogen-3						0	0.00	0
Uranium-233	²³³ U	1.59E+05 yr	4810	5.5		1.29	4817	28.52	771
Uranium-235	²³⁵ U	7.04E+08 yr	4380	42		156	4578	27.10	732
Uranium-238	²³⁸ U	4.468E+09 yr	4190	9.5		1.3	4201	24.87	672
Ytterbium-169	¹⁶⁹ Yb	32.022 dy		112		312	424	2.51	68

REVISS

**REVISS Services (UK) Ltd
Quality and Regulatory Group
Technical Memorandum**

**RTM 130 – Analysis of High-Speed Video Footage
from R7021 Drop Testing**

Author:		Reviewer:	
Name	P J G Robbins	Name	D W Rogers
Signature		Signature	
Date	29/12/09	Date	29/12/2009

1. PURPOSE AND SCOPE

The purpose of this document is to characterise the impact event of the R7021 flask, 3981/01, in each of four 9m drop tests, using data from two high speed cameras.

2. INTRODUCTION

The outer components of the R7021 are the jacket, top shield and pallet. These components are fastened to the flask which is a stainless steel, lead filled, upright cylinder.

The 9m drops were part of a programme of 17 drop tests performed on the 3981/01. Details of the programme may be found in RTM118. A summary of the 9m drops is given below:

Drop Test No.	Orientation	Test Report
6	Upright	RTR 240
9	Inverted	RTR 243
12	Angled Inverted	RTR 246
15	Side	RTR 249

Table 1 - Test Summary

The test reports detail the external condition after each test. A more thorough record, IR 0675, was made when the specimen was given a strip down inspection after completion of the test program.

3. CAMERA SETUP

Two Olympus i-Speed cameras were used, one colour and the other monochrome. In the first three drop tests the cameras were aimed at the impact point from two directions at right angles to one another. For the fourth, the side drop, one camera was aimed at the pallet and the other at the top shield. Appendix 1 gives extracts from the footage.

4. ANALYSIS

This section details the calculational processes (Appendix 3 details the data extracted from the footage and the results of the calculations). See Appendix 2 for graphs of displacement, velocity, deceleration and work done.

The position of the flask may be measured by tracking the position of individual points and counting the number of pixels moved between frames. To translate that to real units the relationship between pixels and distance has to be established. Once the position at each time step is known the velocity, and thence the deceleration and energy absorbed, may be calculated.

4.1 RELATIONSHIP BETWEEN PIXELS AND DISTANCE

This is a three stage process:

1. The time to impact is calculated from the drop height.
2. The displacement at a prior point in time is calculated.
3. The difference between this displacement and the drop height is divided by the number of pixels to calibrate the readings.

4.1.1 Time to impact, t_0

The equation relating time, t , acceleration, a , and displacement, s , is:

$$s = ut + \frac{1}{2}at^2$$

At frame 0; the moment of impact:

$$s_0 = ut_0 + \frac{1}{2}at_0^2$$

Where: s_0 = drop height = 9.26 m (see RTR 240)

u = initial velocity = 0 m/s

t_0 = time to impact

a = gravitational acceleration = 9.81 m/s²

Thus the equation may be simplified as follows:

$$s_0 = \frac{1}{2}at_0^2$$

Rearranging for t_0 gives:

$$t_0 = \sqrt{\frac{2s_0}{a}} = \sqrt{\frac{2 \times 9.26}{9.81}} = 1.374 \text{ s}$$

4.1.2 Displacement, s_i at prior point in time, t_i

The prior point (0.01s before impact) was selected to give not less than 50 pixels of movement to minimise the potential for inaccuracy. The time at prior point, t_i , is therefore 1.364 s.

Thus the displacement, $s_i = \frac{1}{2}at_i^2 = \frac{1}{2} \times 9.81 \times 1.364^2 = 9.126 \text{ m}$

4.1.3 Pixel/displacement relationship, k

$$k = \frac{n_i}{s_i}$$

Where: k = number of pixels per metre

n_i = number of pixels between t_i and t_0

4.2 DISPLACEMENT, VELOCITY, DECELERATION AND ABSORBED ENERGY

For each drop four different points on the specimen were tracked. The average displacement was derived for each time step and used in the following calculations.

The change in displacement enabled the velocity, deceleration and energy absorbed to be calculated.

4.2.1 Velocity

4.2.1.1 Velocity at impact, v_0

The equation relating velocity to acceleration and time is:

$$v = u + at$$

At frame 0; the moment of impact:

$$v_0 = u + at_0$$

Where: v_0 = velocity at impact

As in section 4.1.1, the equation may be simplified as follows:

$$v_0 = at_0$$

Thus:

$$v_0 = 9.81 \times 1.374 = 13.48 \text{ m/s}$$

4.2.1.2 Velocity after impact, v_t

The velocity after impact, v_t , may be calculated as follows:

$$v_t = \frac{dy}{dt}$$

Where: dy = change in displacement = $y_t - y_{t-dt}$

y_t = displacement at time t

y_{t-dt} = displacement at time $t - dt$

dt = time step

4.2.1.3 Velocity at impact of top shield in side drop

The side drop is a special case where there are two impact points hitting the target at different times. The pallet hits the ground first (see A.1.7) and some of the kinetic energy is converted into rotational energy, causing the opposite end of the container to accelerate up until the moment of impact (see A.1.8). The velocity of the top shield at impact (A.2.4) is calculated in exactly the same way as the velocity after impact, v_t .

4.2.2 Deceleration, a_t ,

Deceleration is calculated as follows:

$$a_t = \frac{dv}{dt}$$

Where: dv = change in velocity = $v_t - v_{t-dt}$

v_t = velocity at time t

v_{t-dt} = velocity at time $t - dt$

Expressed as a function of the gravitational acceleration, g :

$$g_t = \frac{a_t}{g} = \frac{a_t}{9.81}$$

4.2.3 Potential energy of the container, U

The equation for potential energy is:

$$U = mgh$$

Where: U = potential energy

m = mass of container = 4374 kg

h = total displacement = 9.26m + total crush distance

The different crush distances meant that the potential energy varied between 401 and 409kJ in the four drops.

4.2.4 Energy absorbed, W ,

The energy absorbed by the external structures is the work done to slow the flask. The equation is:

$$W = F \cdot x$$

Where: W = work done

F = force = $m_t \cdot a_t$

x = distance over which force is applied = change in displacement, dy

And: m_t = estimated mass being decelerated by impact limiter

Thus:

$$W = m_t \cdot a_t \cdot dy$$

4.3 ACCURACY

The analysis relies tracking on the displacement of the flask. As the flask comes to a halt the number of pixels between each frame approaches zero causing a significant reduction in accuracy.

4.3 CAMERA SENSITIVITY

The colour camera required a longer exposure, which consequently gave less sharp images than the monochrome camera. This reduced tracking accuracy making the results from the colour camera likely to be less reliable than those from the monochrome.

5. RESULTS

Plots of the results may be found in Appendix 2 and tabulated data, in Appendix 3.

Drop	Camera	Impact Duration (s)	Deformation (mm)		Peak Deceleration (g)	Energy Absorbed (kJ)
			Measured	Actual		
6- Upright	Mono	0.020	133	130	133g	320 (79%)
	Colour	0.018	133		183g	329 (82%)
9- Inverted	Mono	0.020	138	135	131g	330 (82%)
	Colour	0.018	136		122g	341 (85%)
12- Angled inverted	Mono	0.015	113	105	157g	312 (78%)
	Colour	0.018	112		143g	315 (78%)
15-Side Top Shield	Mono	0.023	100	90	138g	405 (100%)*
	Colour	0.025	118	120	183g	

Table 2 – Summary of Results

* For simplicity the mass in the side drop is assumed to be divided equally between the two points of impact and the energy absorbed is then combined to give the total.

6. CONCLUSIONS

1. The 2.5ms interval between data points means that the results do not capture short impulses such as shockwaves.
2. Where the results from each camera differ markedly those from the monochrome camera are likely to be the more reliable indicator.
3. Displacement:
 - a) All four drops show good agreement between the camera measured displacement and the actual crush deformation.
 - b) The first three drops have indicated impact durations of 15 – 20ms. The side drop shows a longer duration, 25ms, for the pallet, which struck first, and 15ms for the top shield.
 - c) In the side drop the top shield plot agrees with the distance it has to move, following the initial pallet impact, before it hits the target and starts to absorb energy.
4. Velocity:
 - a) The velocity graphs derived from each camera in first three drops show reasonable agreement.
 - b) The side drop clearly shows the slap down effect as the top shield velocity increases from 13.5m/s to approximately 17m/s immediately following pallet impact.
5. Deceleration:
 - a) At each differentiation of the data relatively insignificant measurement inaccuracies become progressively exaggerated. This is most marked in the acceleration overlays for Drops 6, 9 & 12. Nevertheless the results do show a broad measure of agreement between the cameras and should serve to provide an indication of the impact process.
 - b) The results indicate peak decelerations in the order of 130g (Drop 6), 130g (Drop 9), 155g (Drop 12), 155g (Drop 15, pallet) and 130g (Drop 15, top shield).
6. Energy absorption:
 - a) The energy plots from each camera generally show good agreement in the total energy absorbed and the form of the graph.
 - b) Within the limitations of the calculation process most of the energy in the system is accounted for.

7. REFERENCES

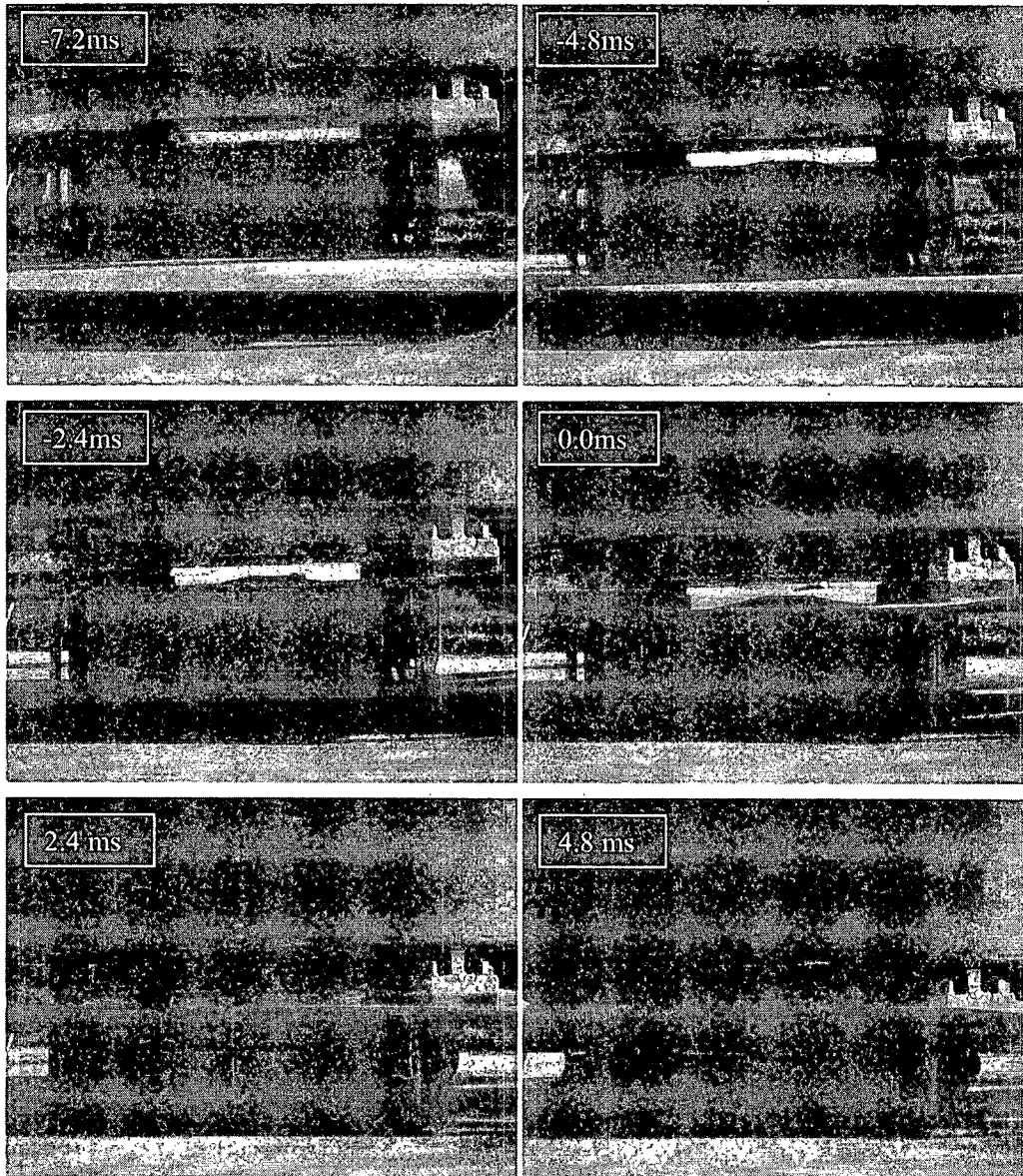
- RTM118 – Test Plan for the R7021 Transport Container, REVISS Services (UK) Ltd.
- RTR233 – 3981/01 1.2 m Free Drop Test – Upright, REVISS Services (UK) Ltd.
- RTR235 – 3981/01 1.2 m Free Drop Test – Vertical Inverted, REVISS Services (UK) Ltd.
- RTR240 – 3981/01 9.0m Free Drop Test – Upright, REVISS Services (UK) Ltd.
- RTR243 – 3981/01 9.0m Free Drop Test – Inverted, REVISS Services (UK) Ltd.
- RTR245 – 3981/01 1.0m Punch Test – Angled Inverted, REVISS Services (UK) Ltd.
- RTR246 – 3981/01 9.0m Free Drop Test – Angled Inverted, REVISS Services (UK) Ltd.
- RTR249 – 3981/01 9.0m Free Drop Test – Side, REVISS Services (UK) Ltd.
- IR0675 – 3981/01 Inspection After Accident Conditions Drop Testing, REVISS Services (UK) Ltd.

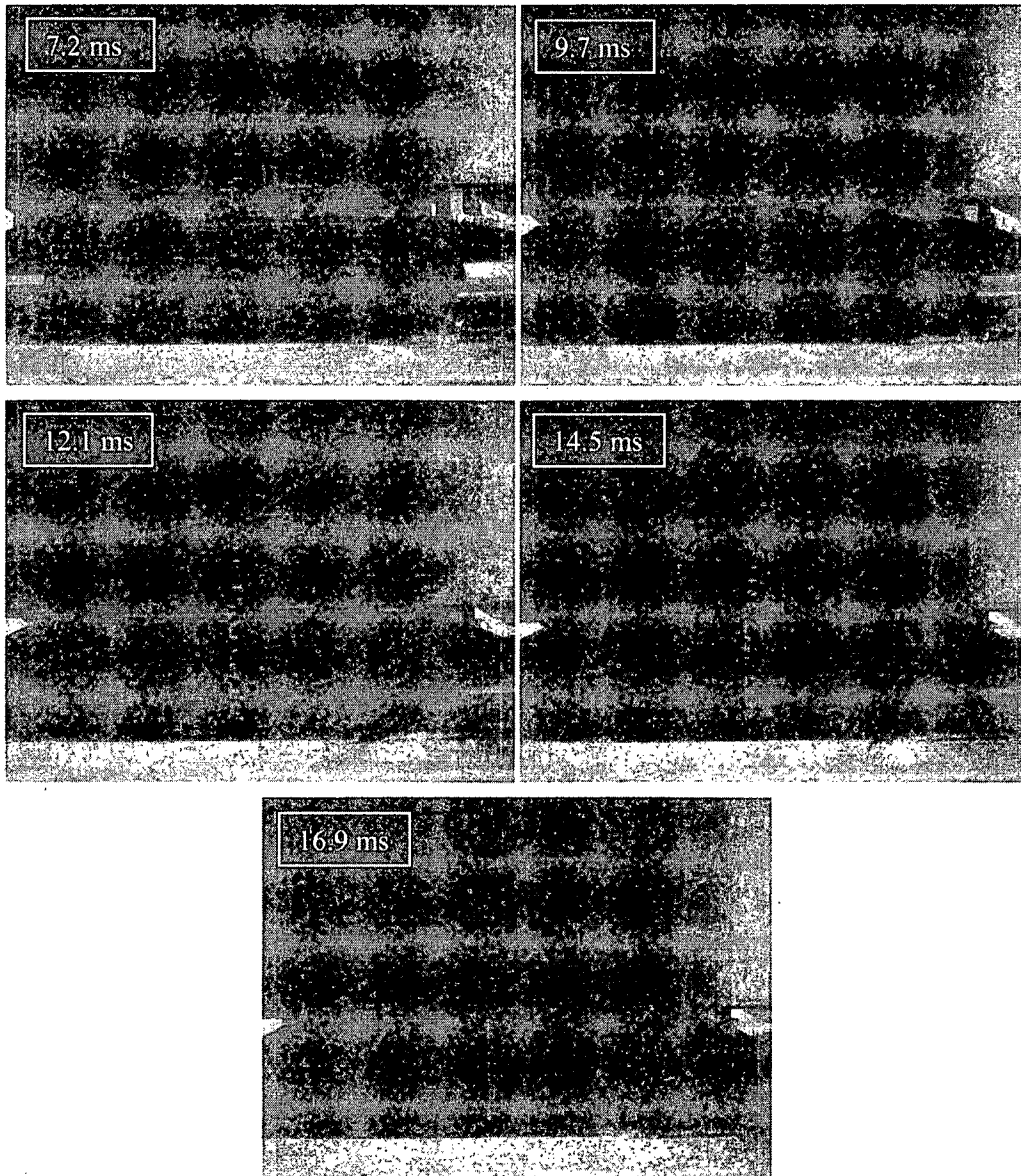
A.1 APPENDIX 1 – HIGH SPEED FOOTAGE

As these tests formed part of a series, the impact points may have sustained damage from a previous drop. This is highlighted for each test and more details may be found in the associated RTR.

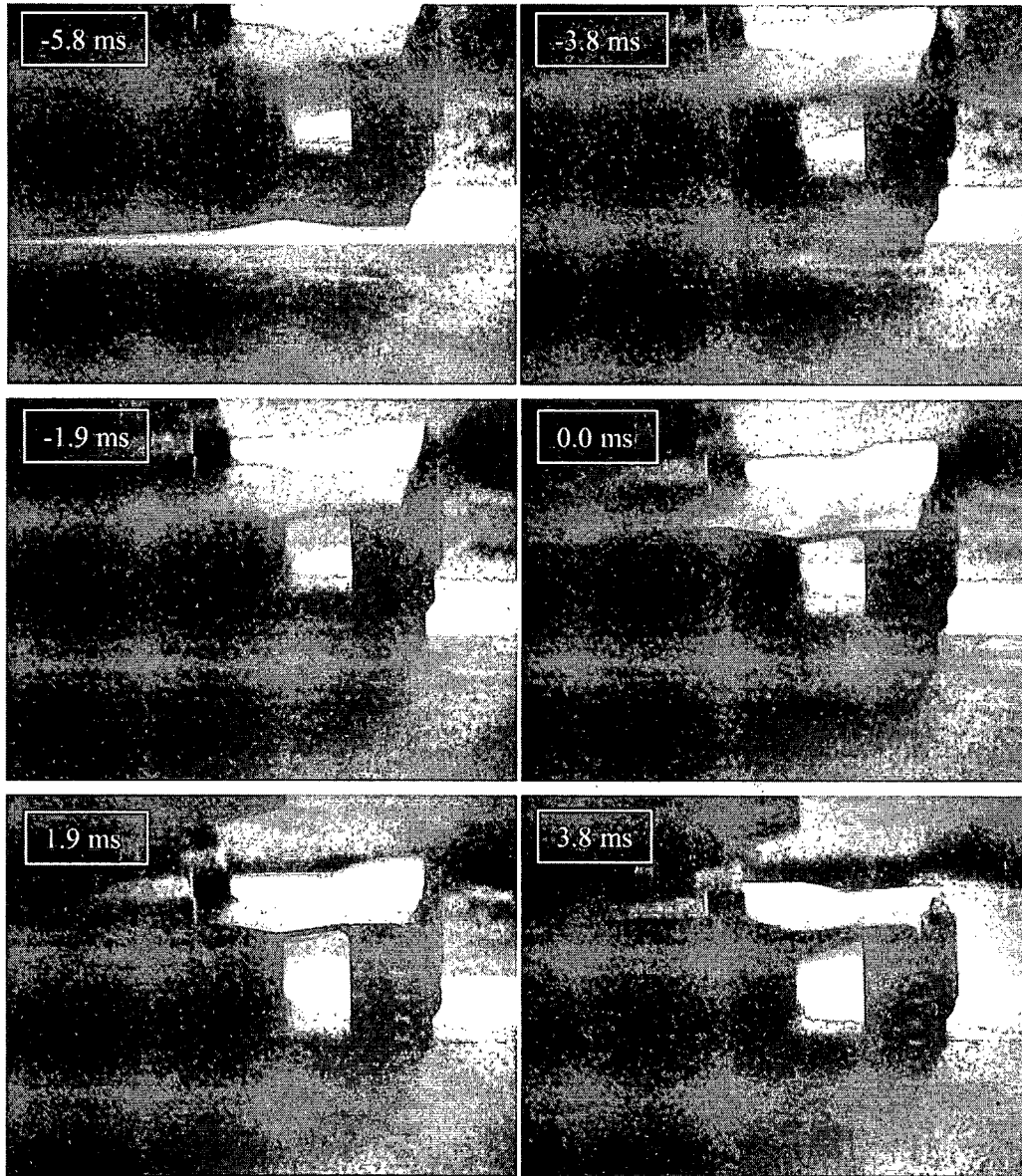
A.1.1 Drop 6 (Upright), mono camera, 2000fps

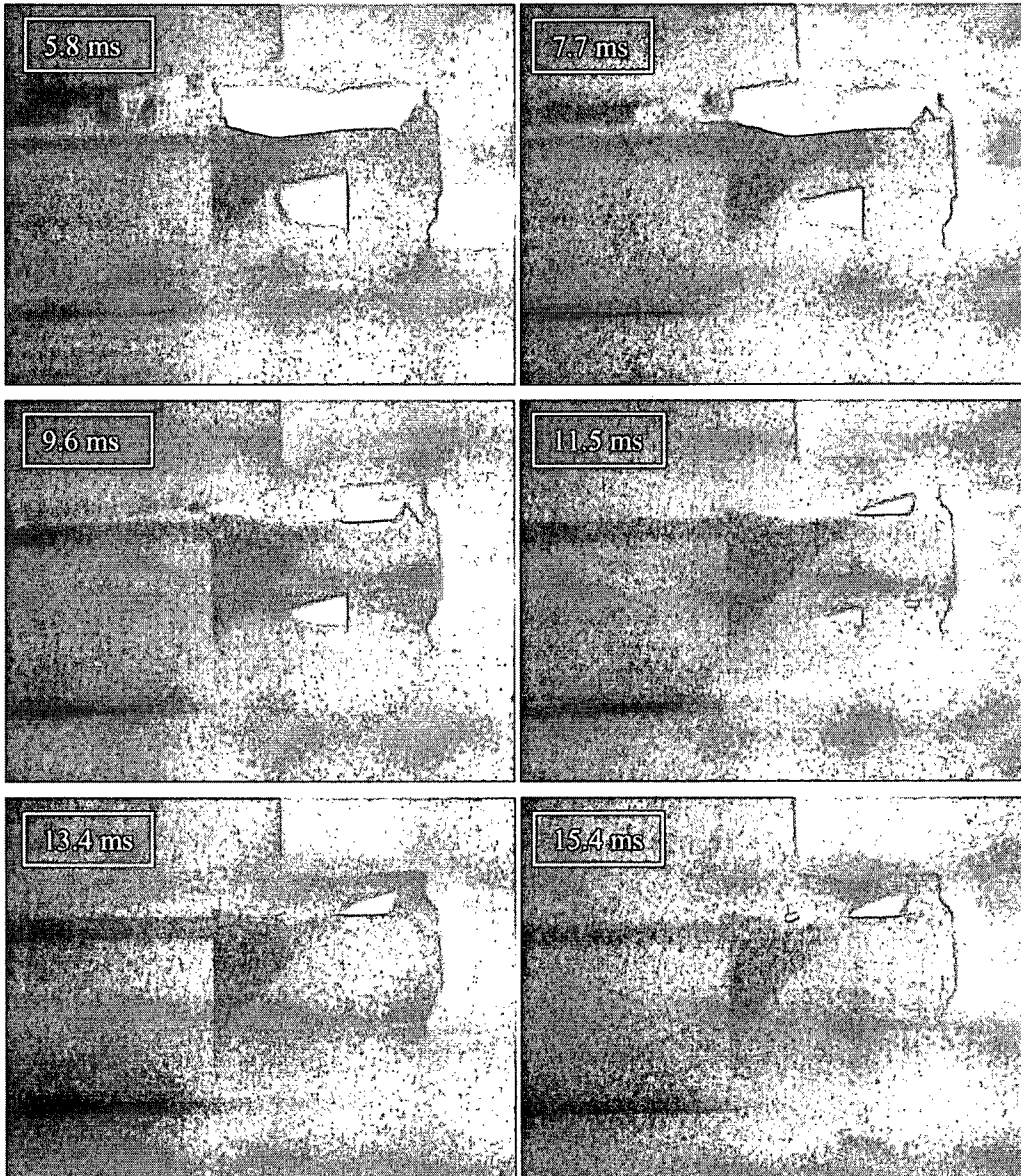
Prior damage: none.





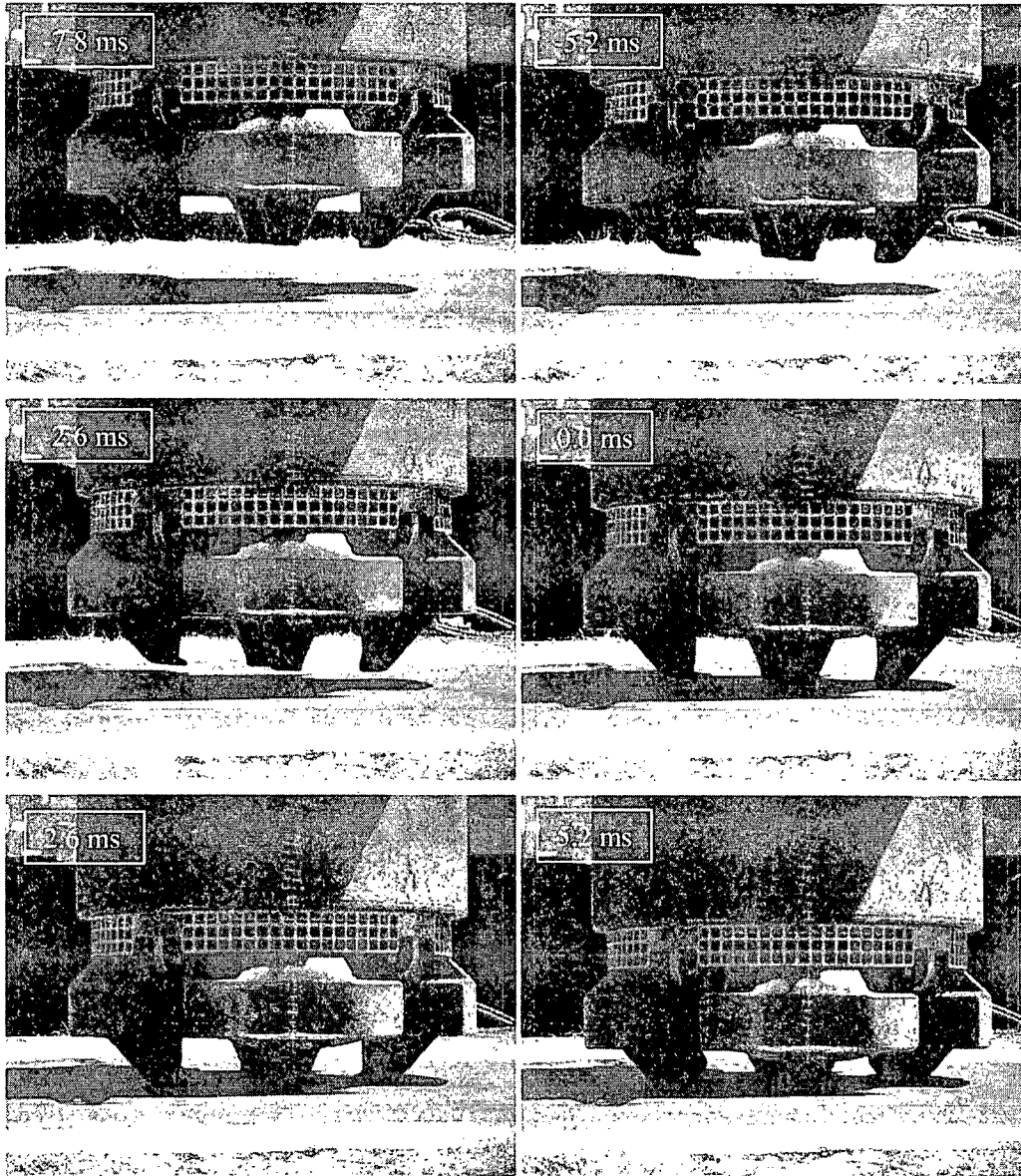
A.1.2 Drop 6 (Upright), colour camera, 1000fps

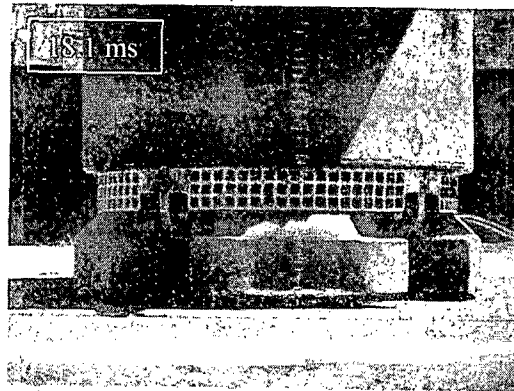
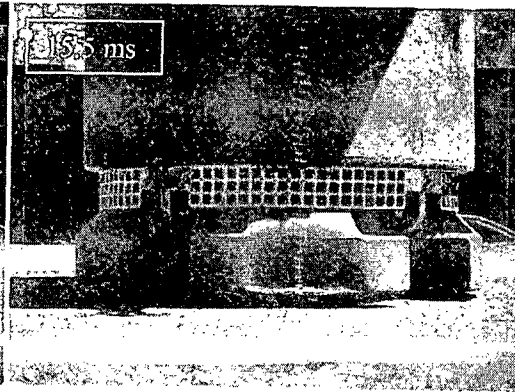
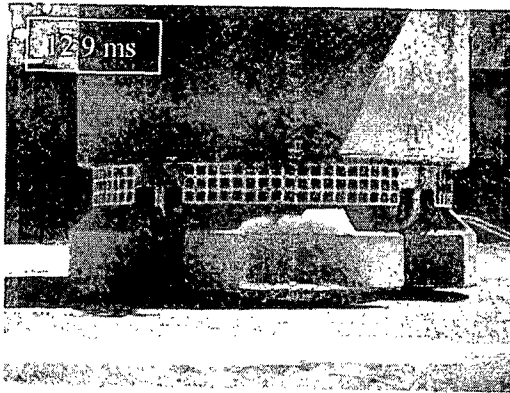
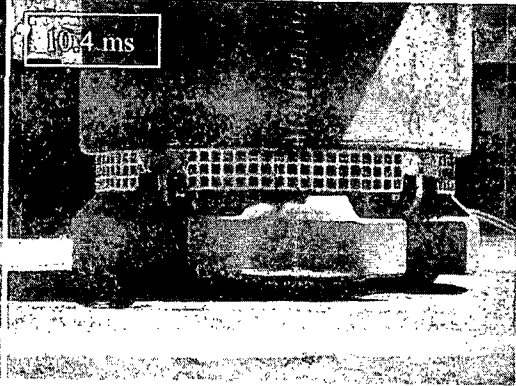
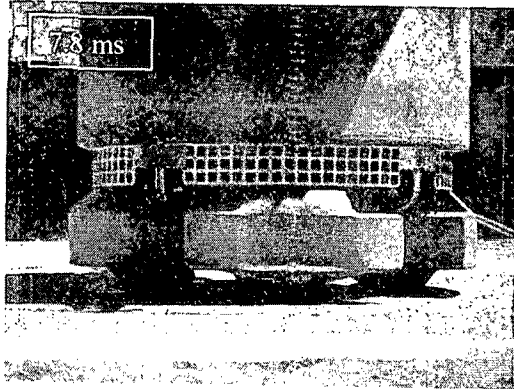




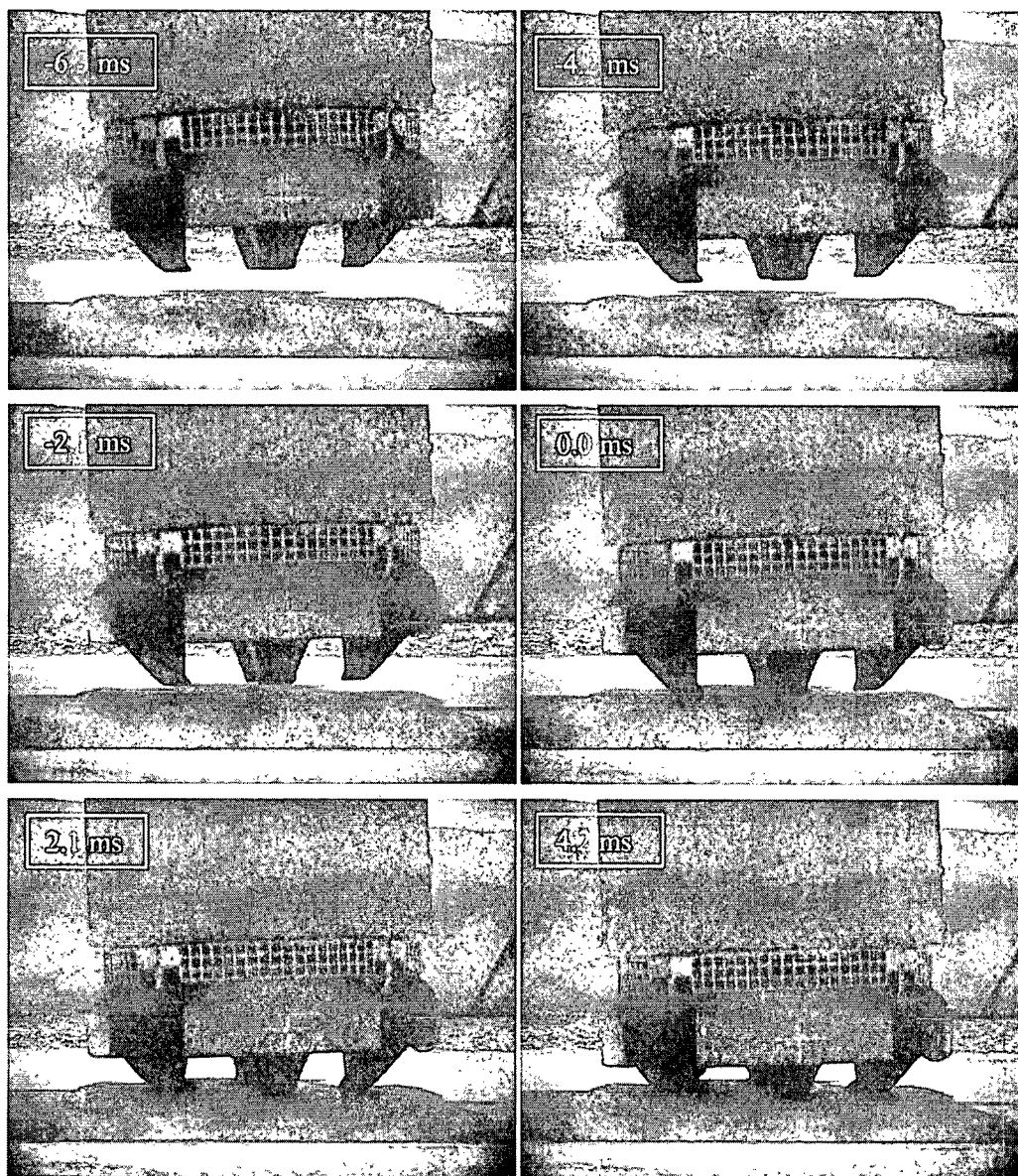
A.1.3 Drop 9 (Inverted), mono camera, 2000fps

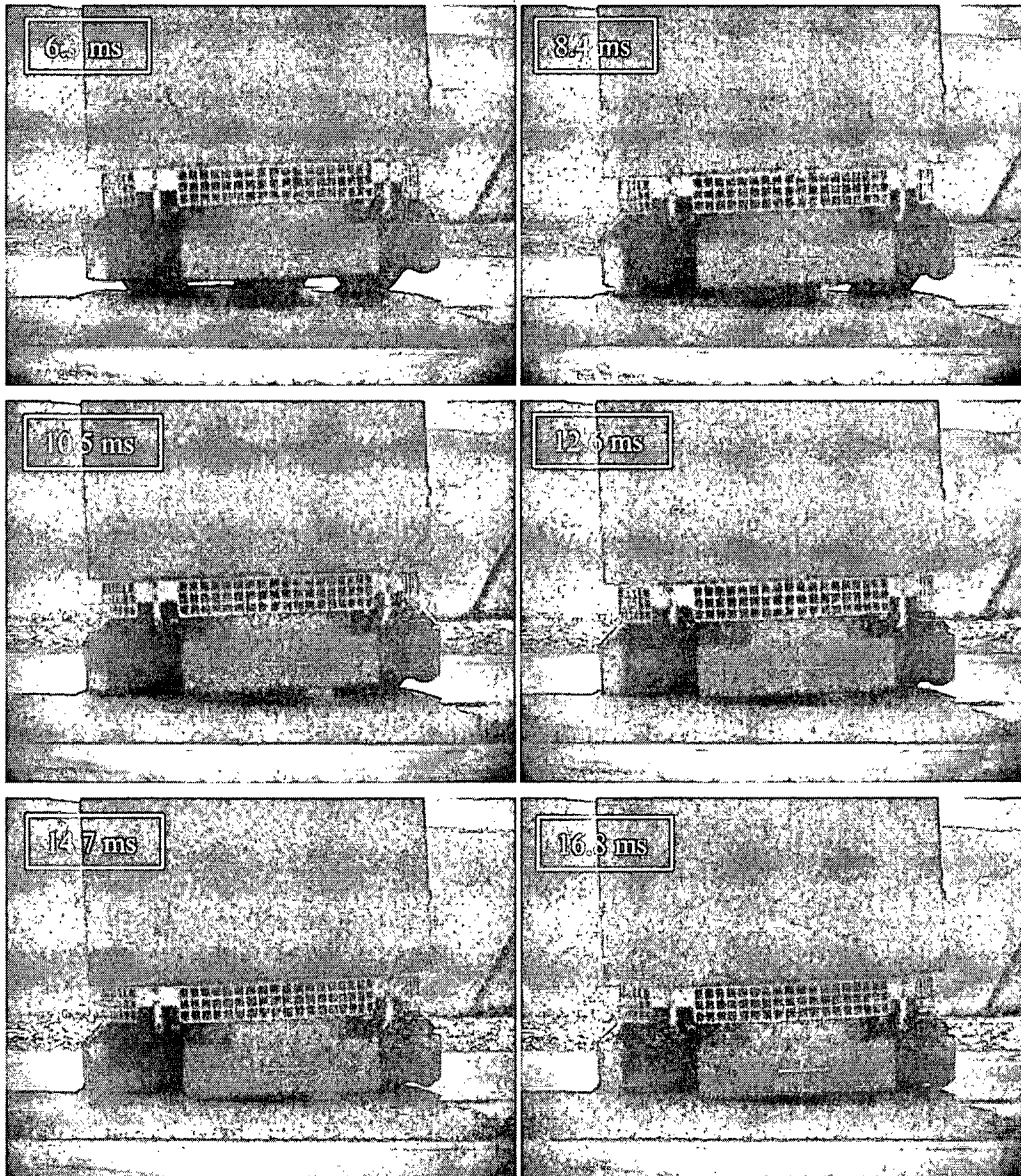
Prior damage: minor distortion of cones – from 1.2m inverted free drop test (see RTR235).





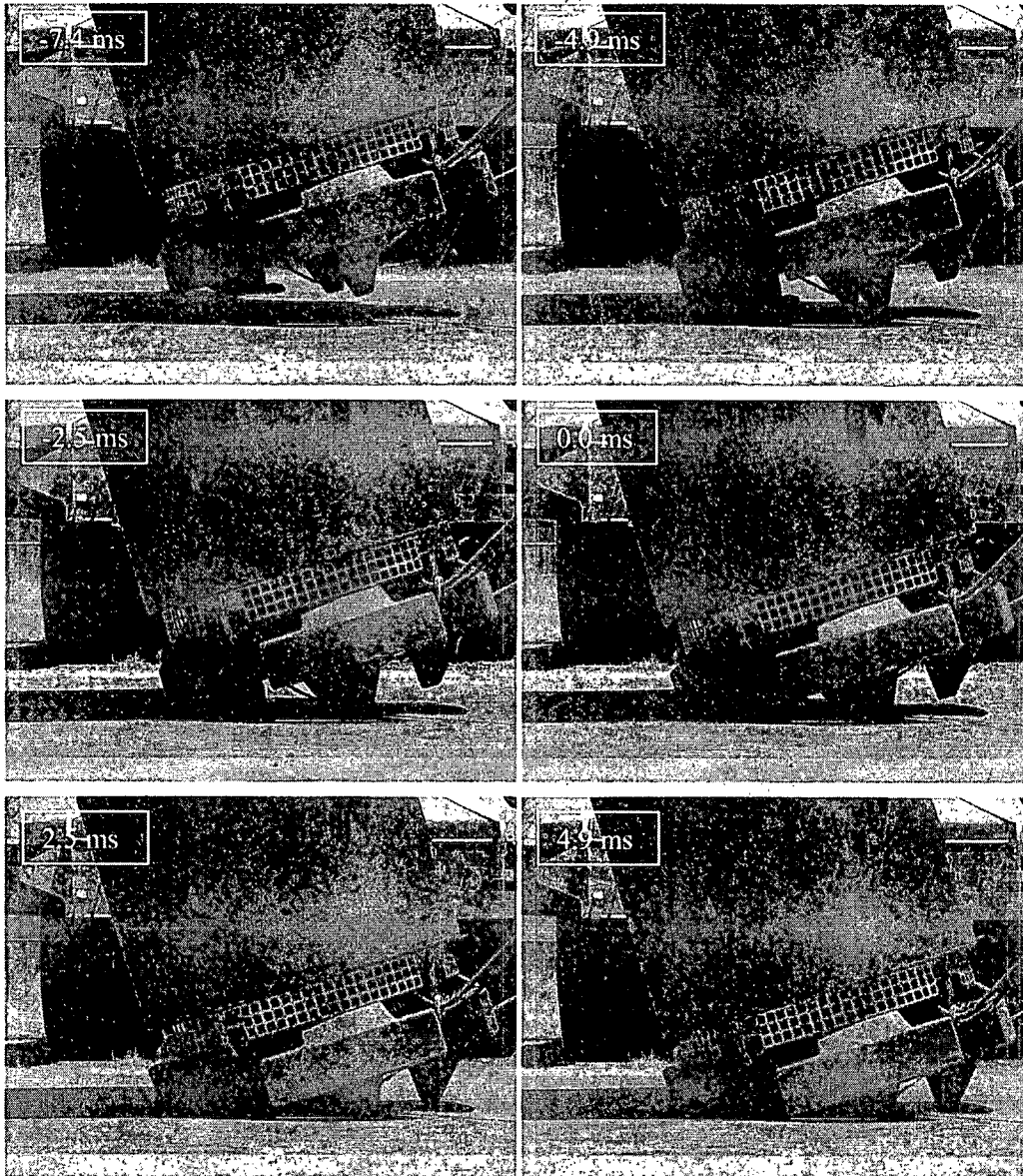
A.1.4 Drop 9 (Inverted), colour camera, 2000fps

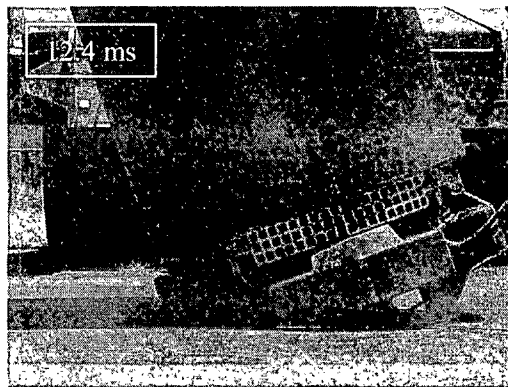




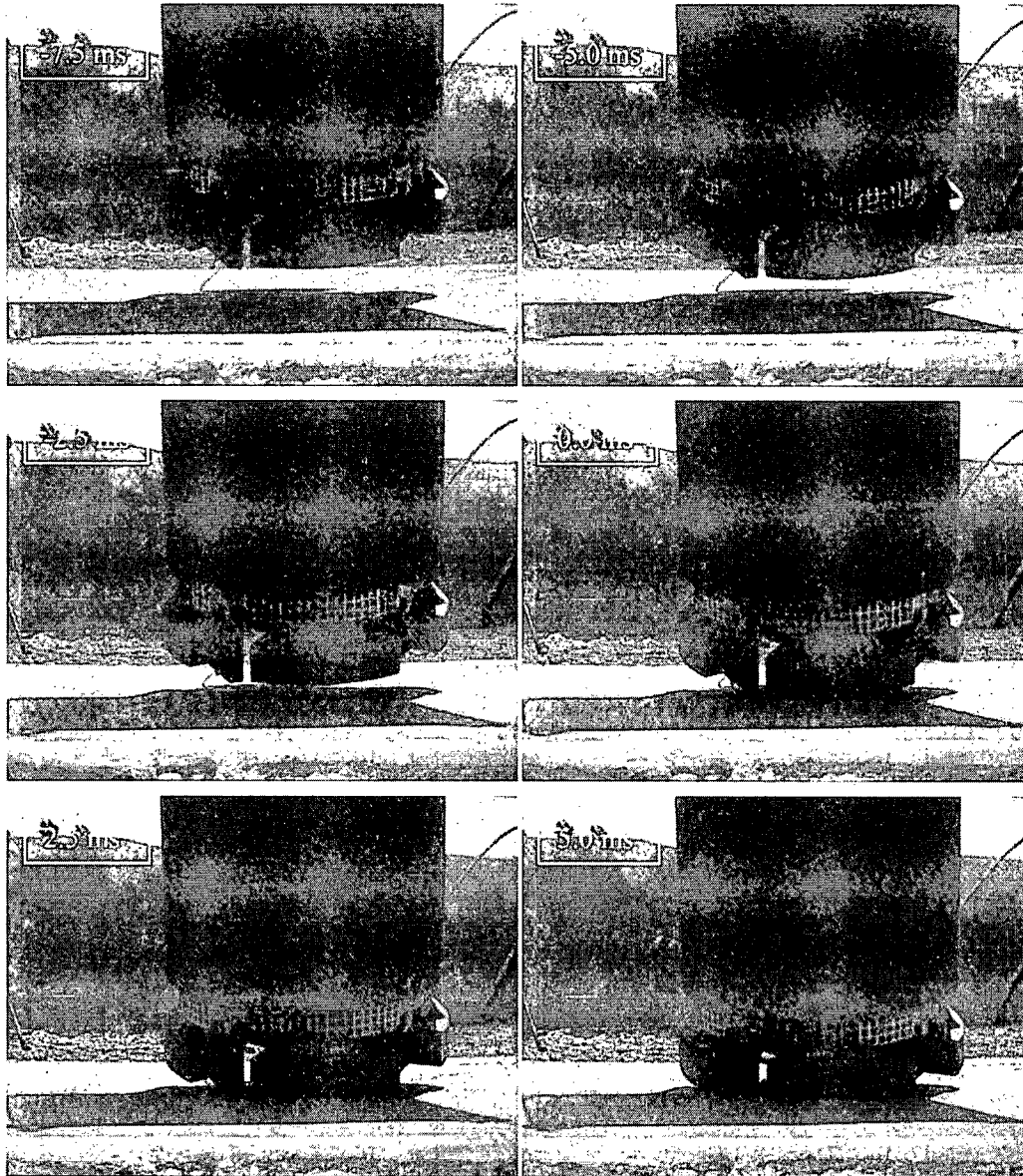
A.1.5 Drop 12 (Angled Inverted), mono camera, 2000fps

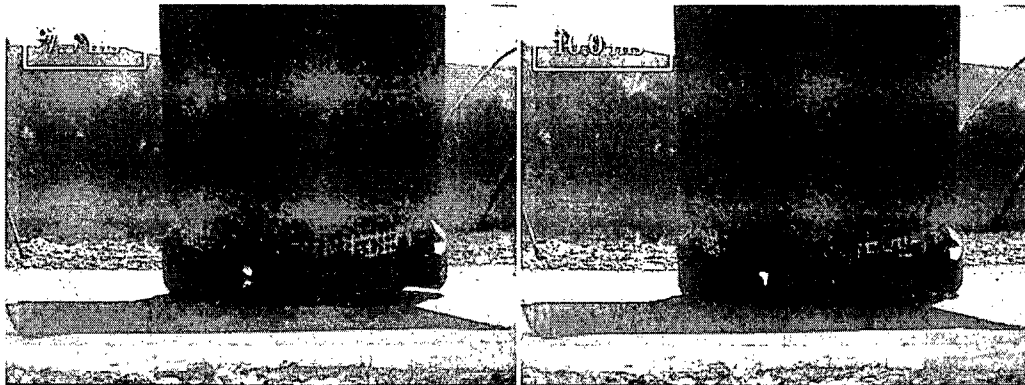
Prior damage: moderate distortion of cone taking initial impact – from 1.0m angled inverted punch test (see RTR245).





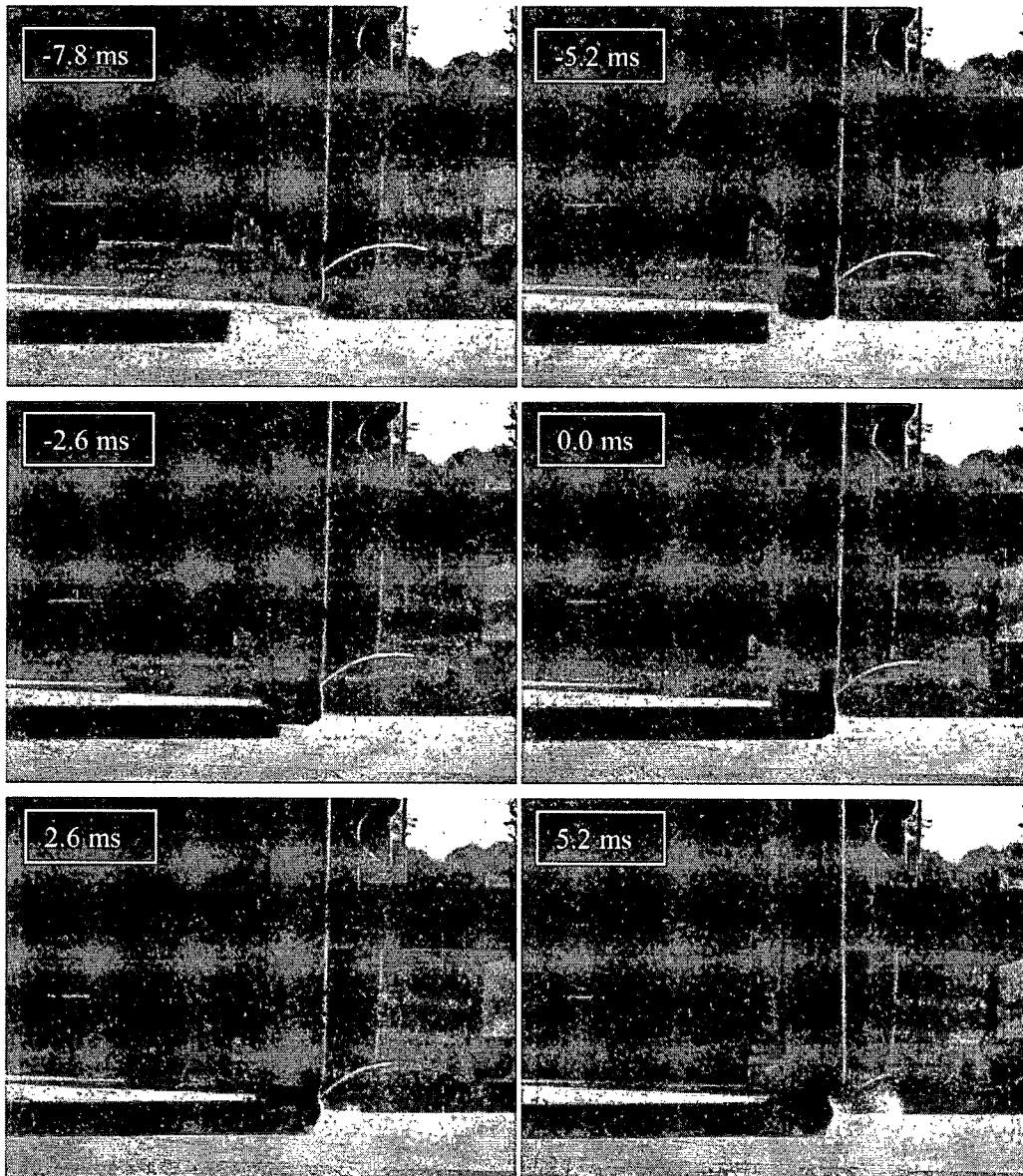
A.1.6 Drop 12 (Angled Inverted), colour camera, 2000fps

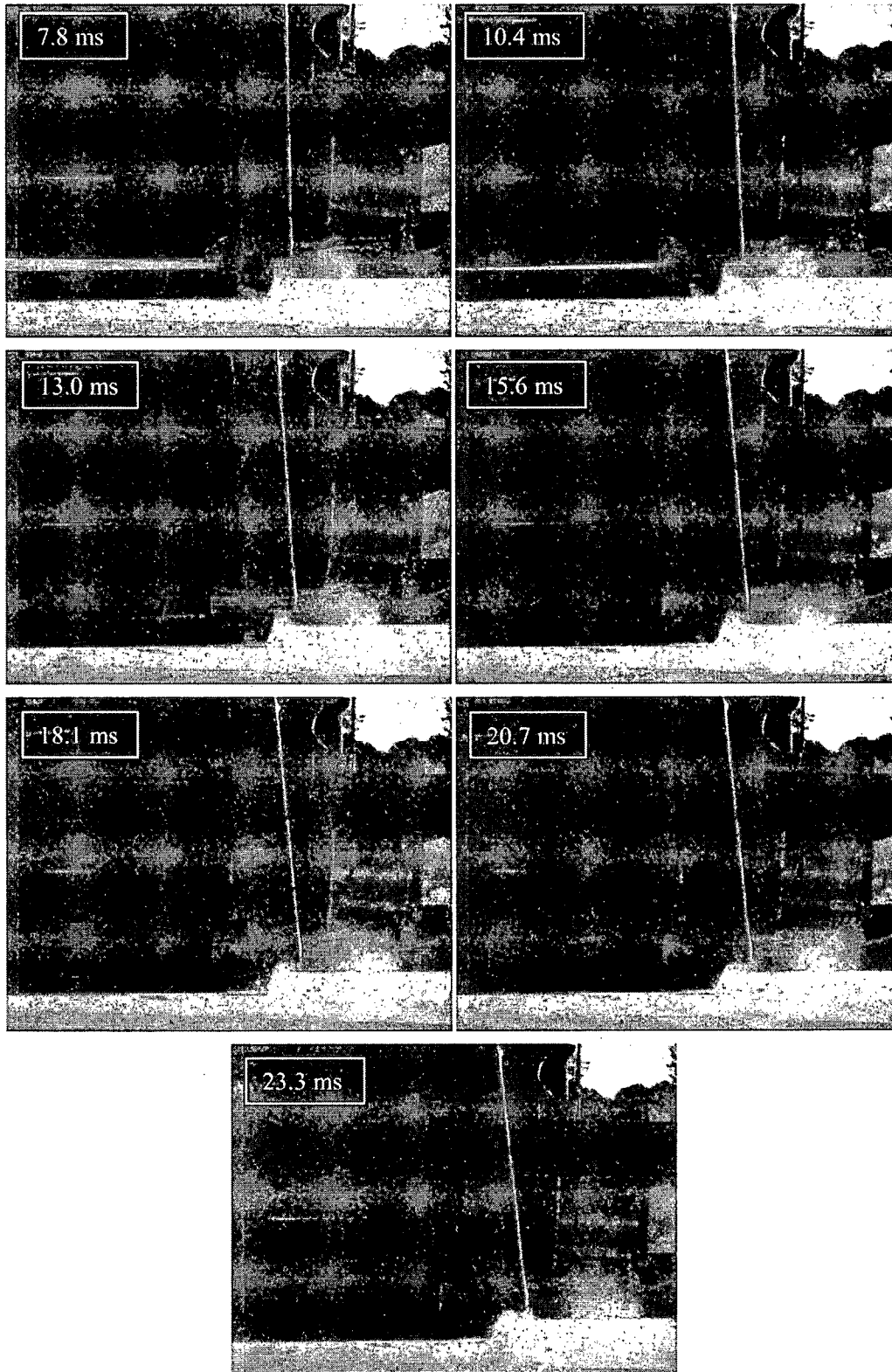




A.1.7 Drop 15 (Side), colour footage, camera, 2000fps

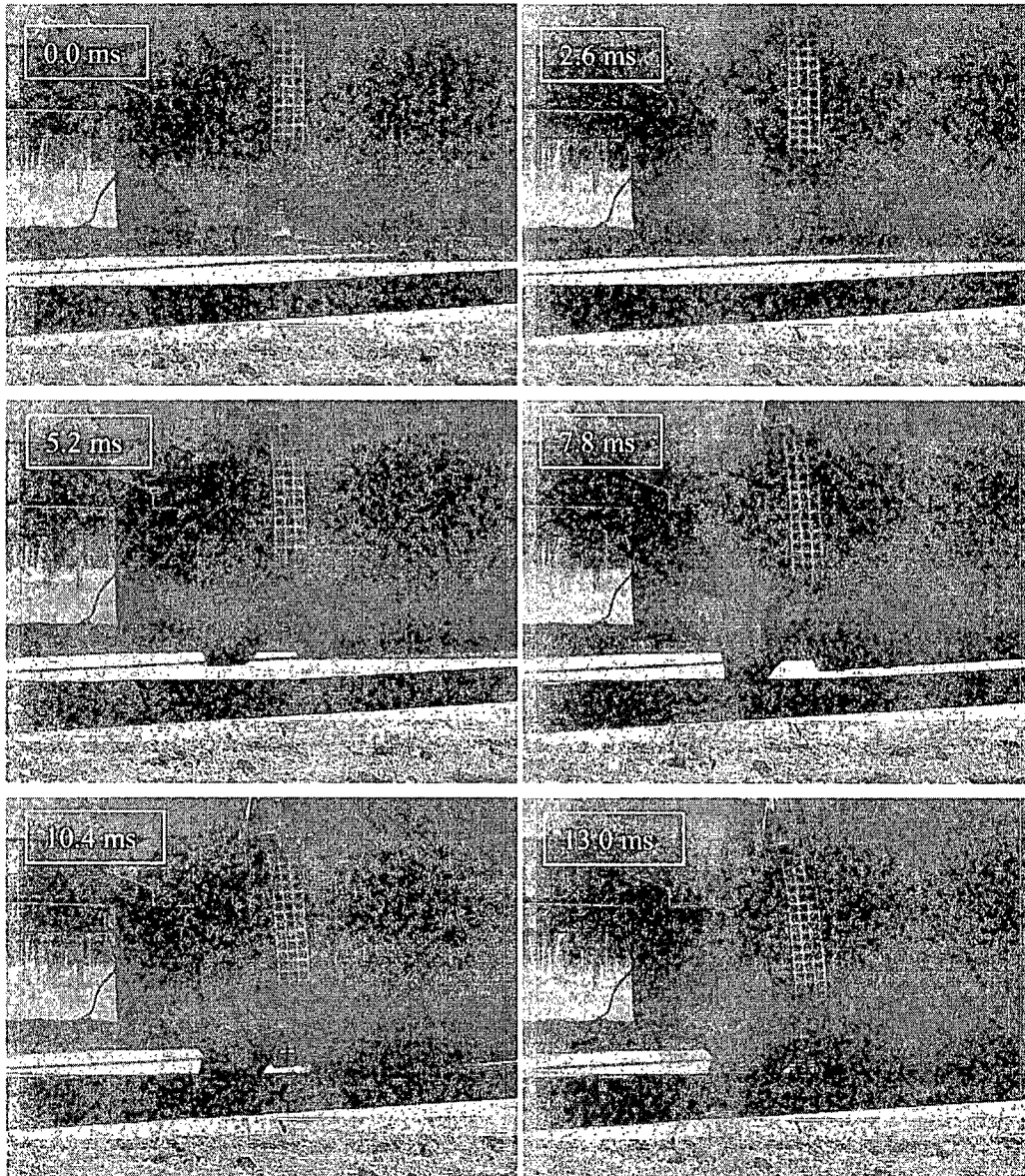
Prior damage: minor crushing of upper pallet surface – from 1.2m upright free drop test (see RTR233).

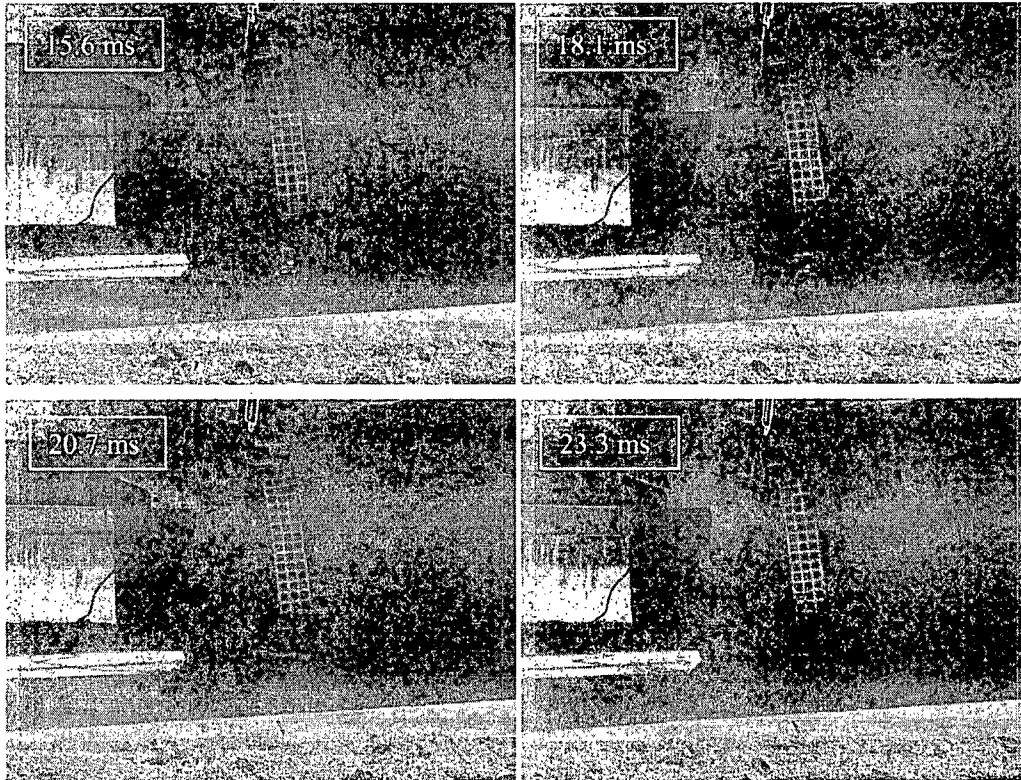




A.1.8 Drop 15 (Side), mono camera, pallet, 2000fps

Note that this sequence has been synchronised with Drop 15 (Pallet). The time line has been zeroed at the moment of pallet impact.

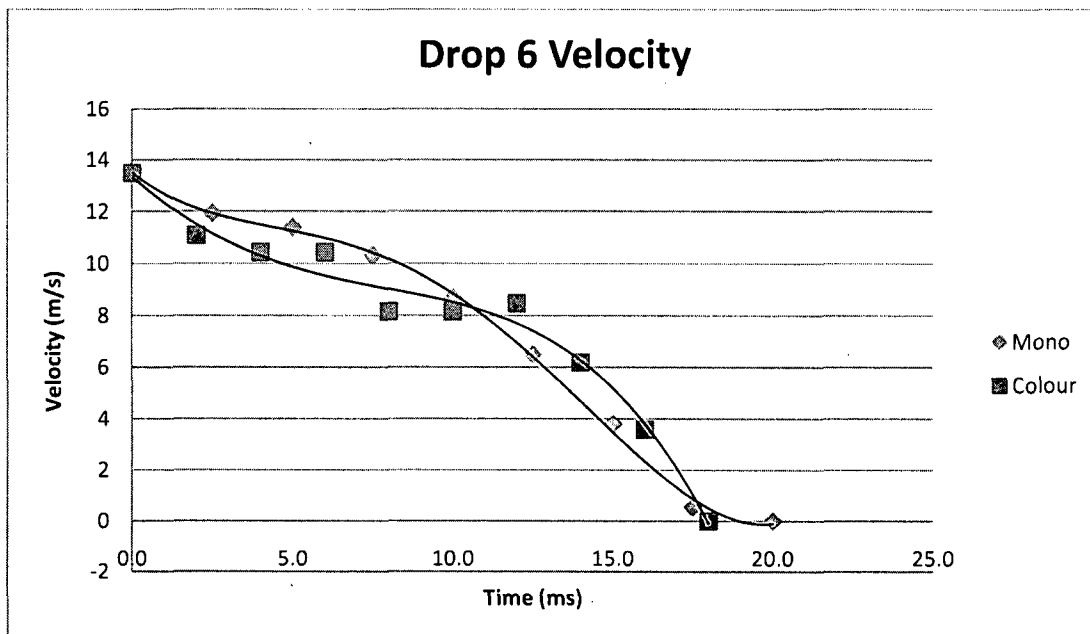
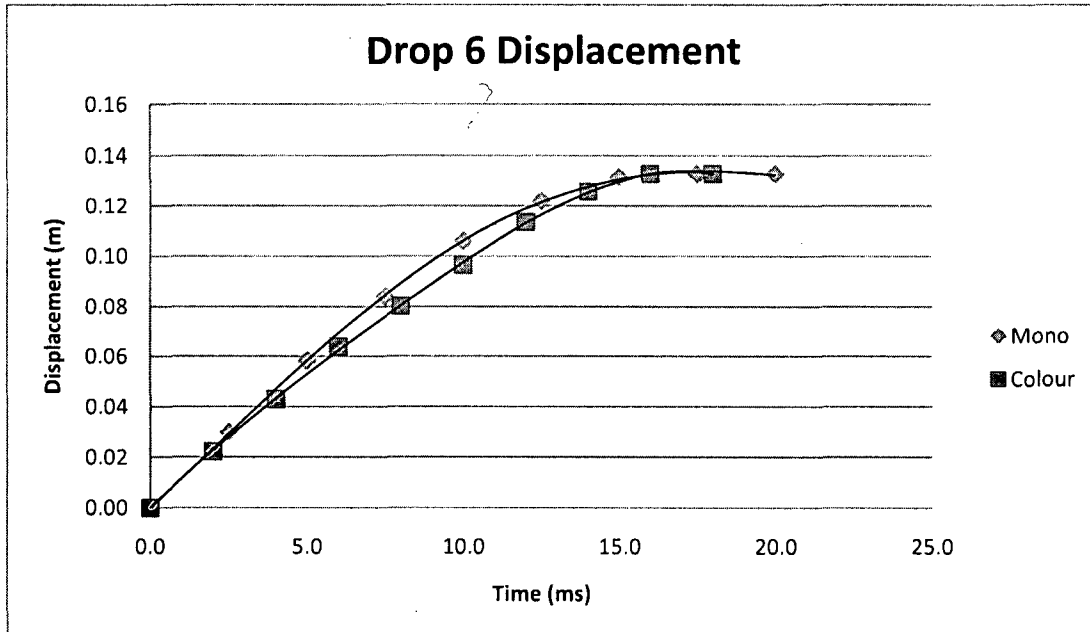


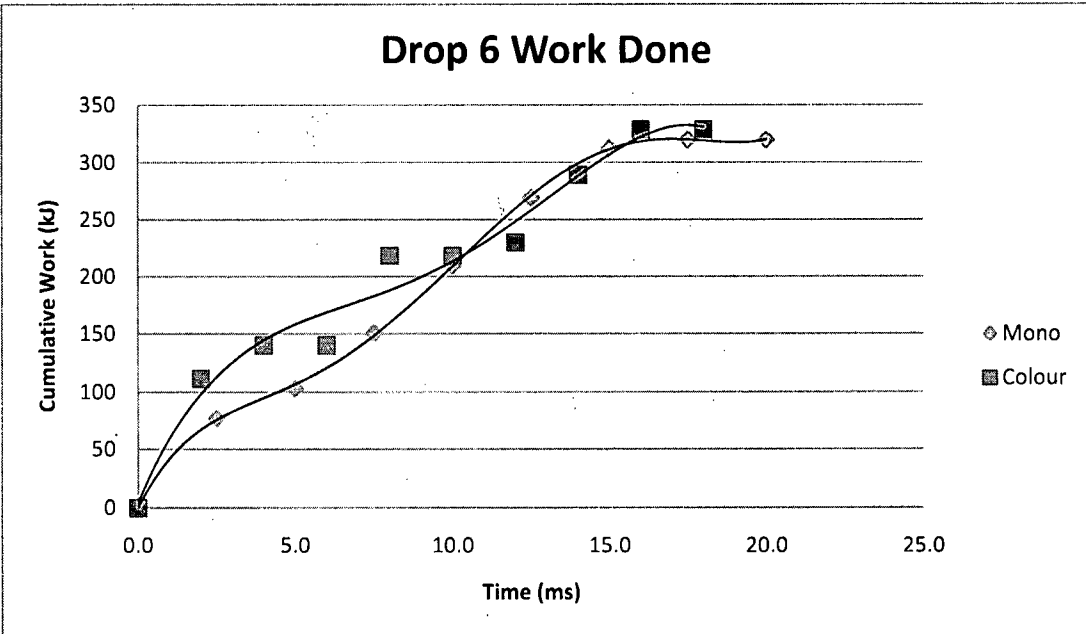
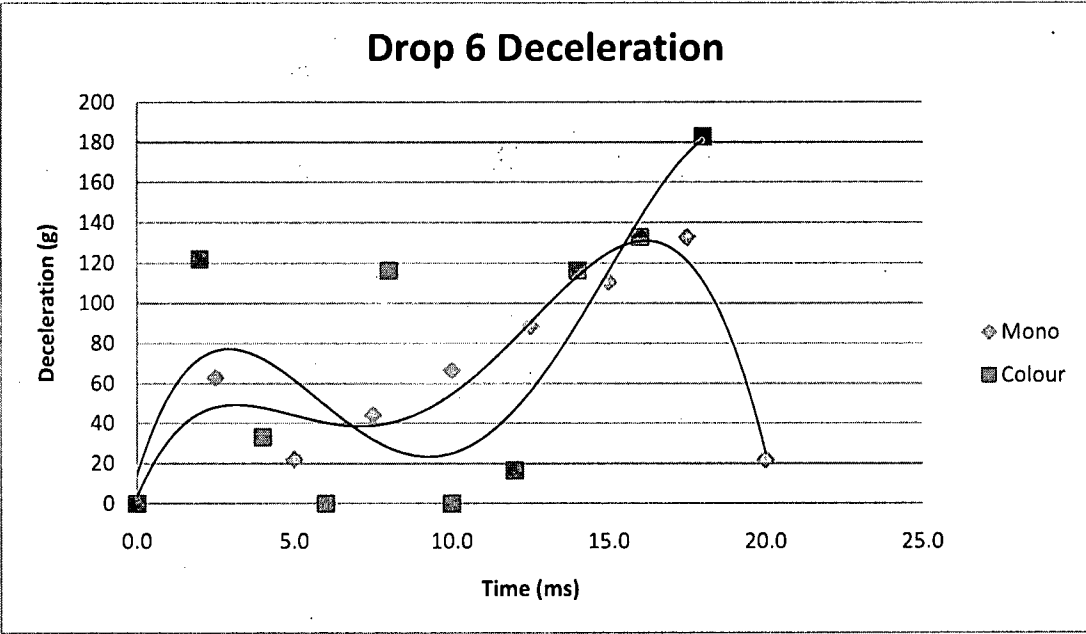


A.2 APPENDIX 2 – DISPLACEMENT, VELOCITY, DECELERATION AND ERROR CHARTS

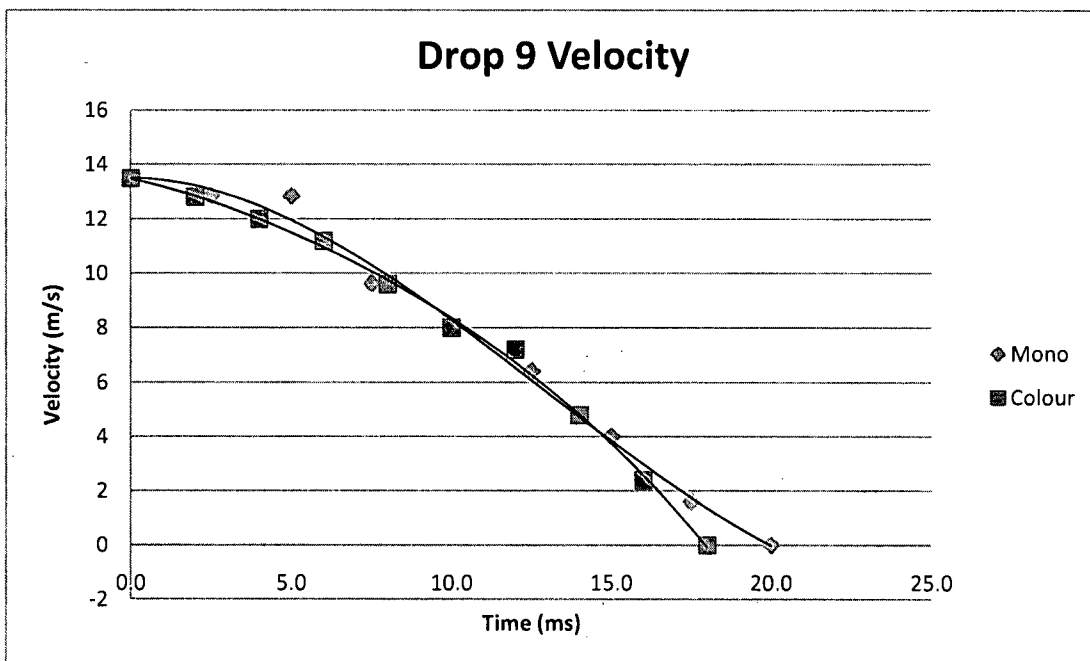
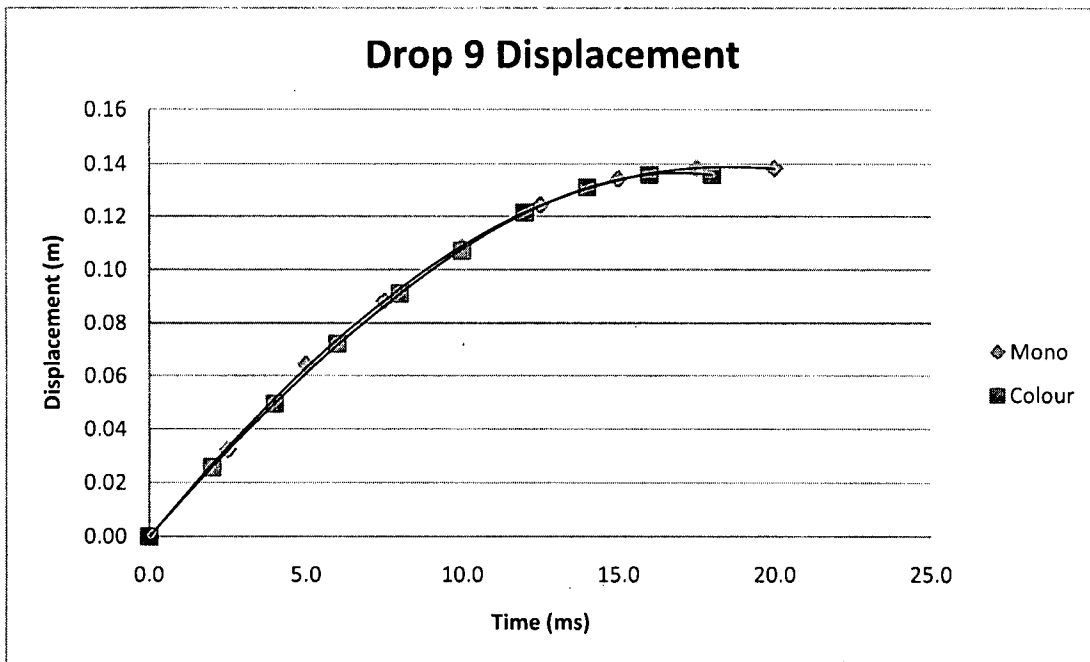
The curves are all best fit and are typically 4th order polynomials. Note that for drop 15 the results have been plotted separately as the cameras were filming separate impact points.

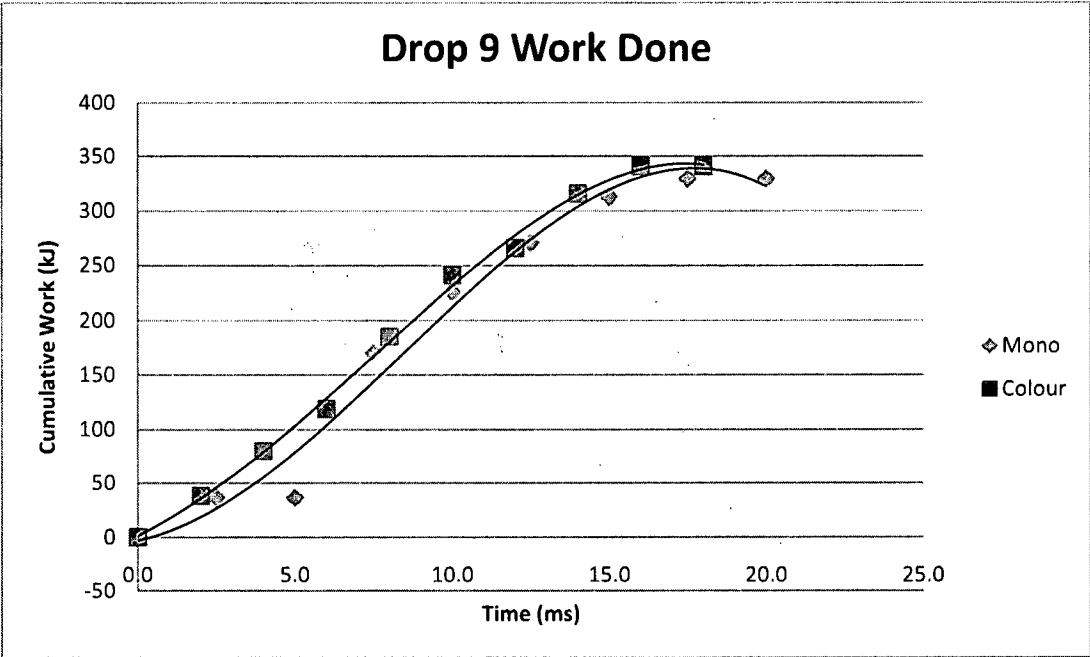
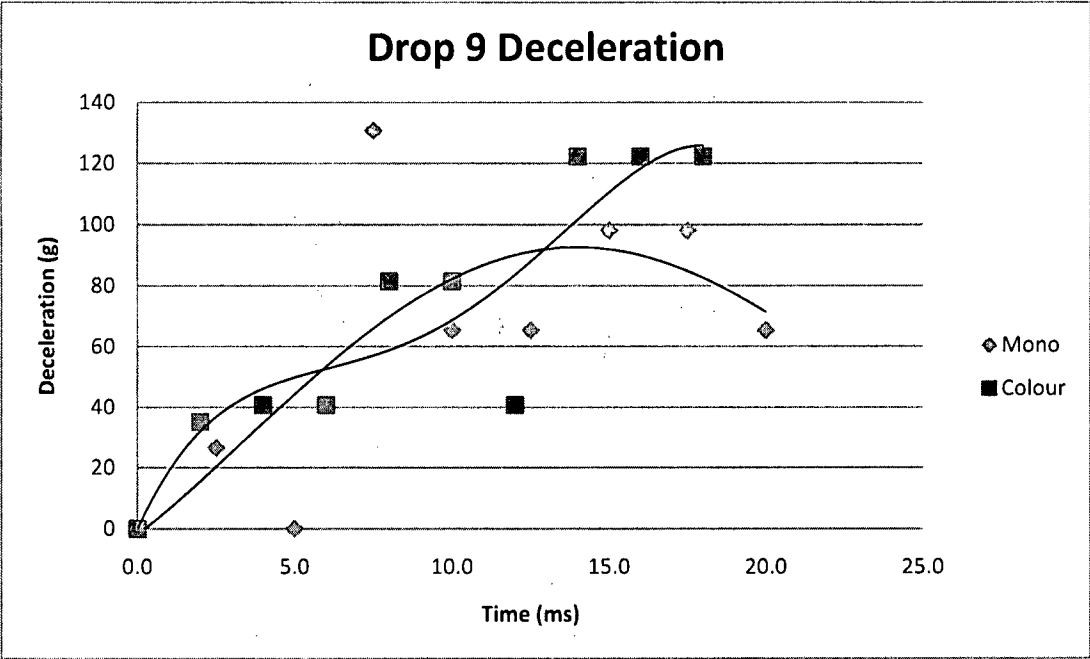
A.2.1 Drop 6 (Upright)



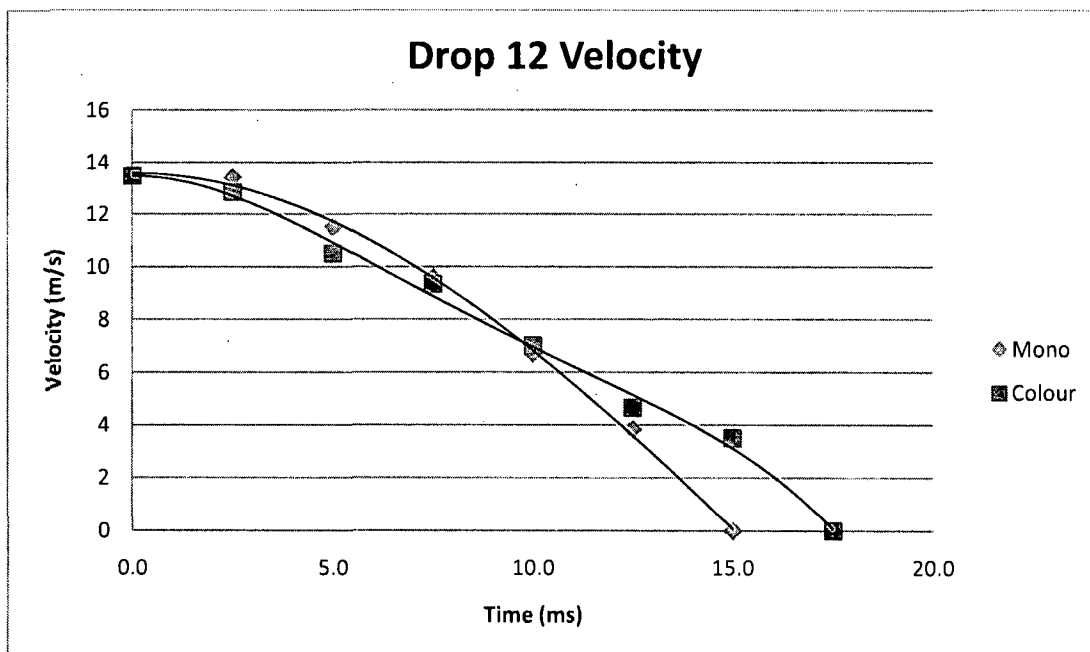
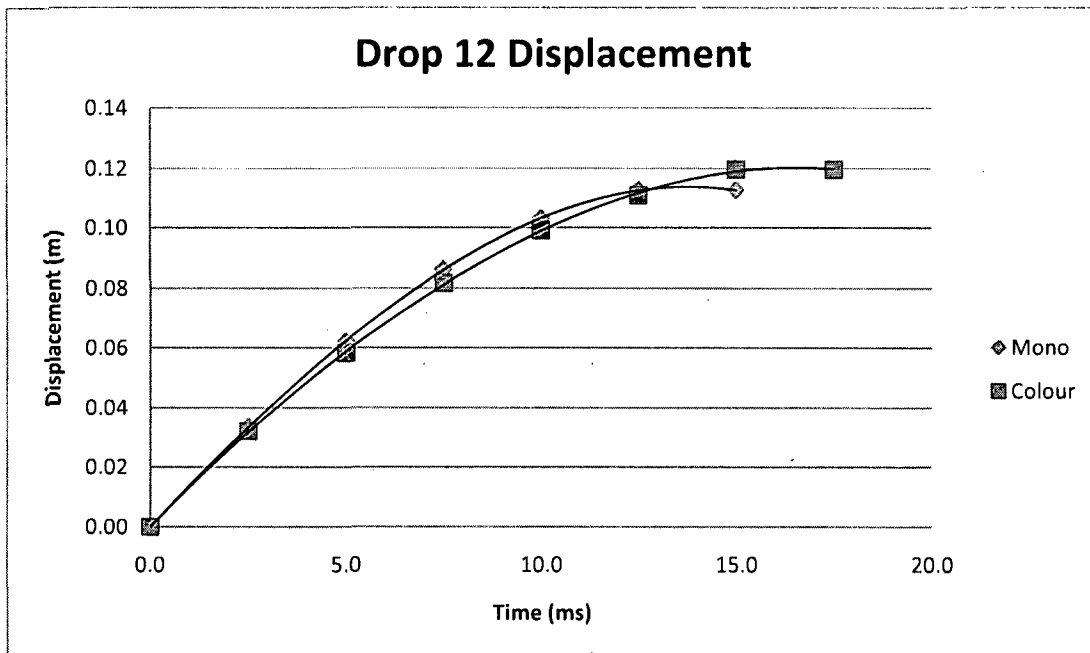


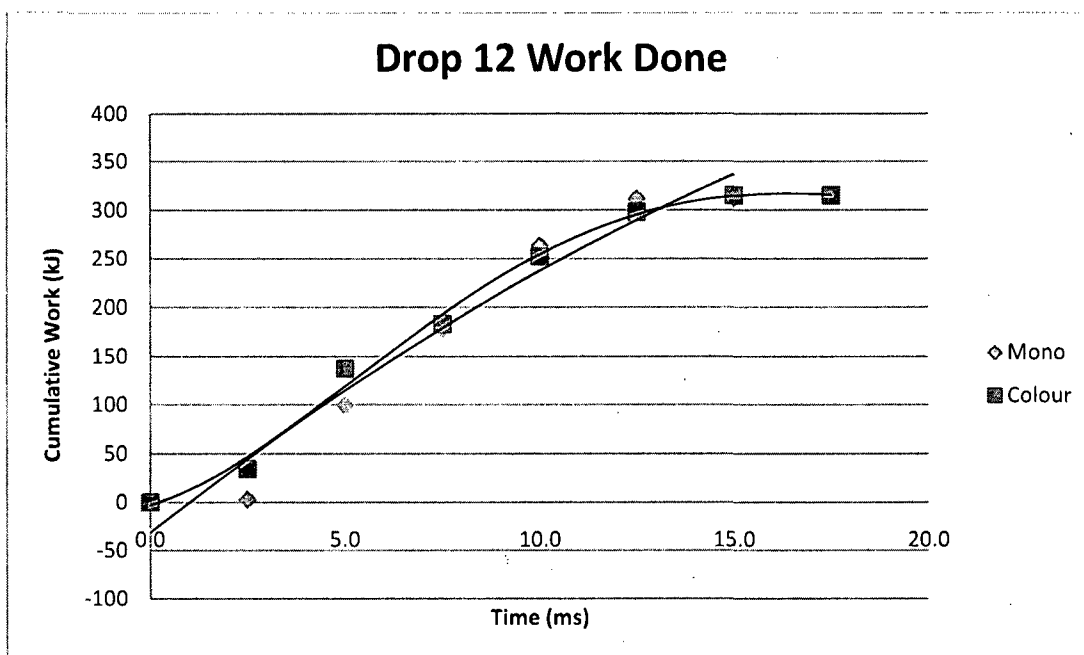
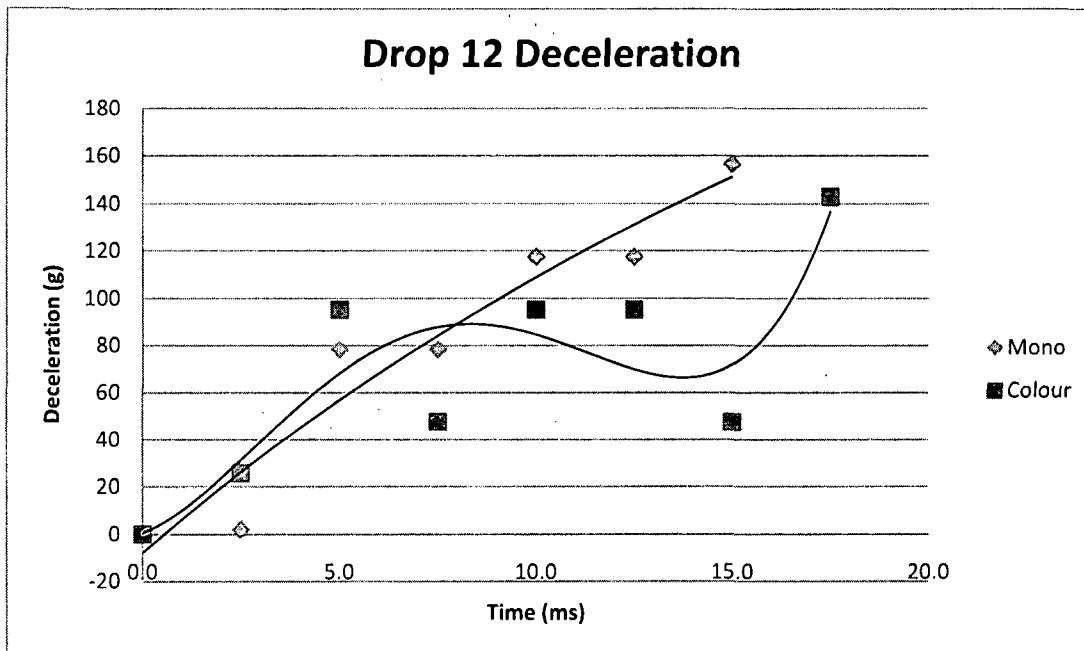
A.2.2 Drop 9 (Inverted)



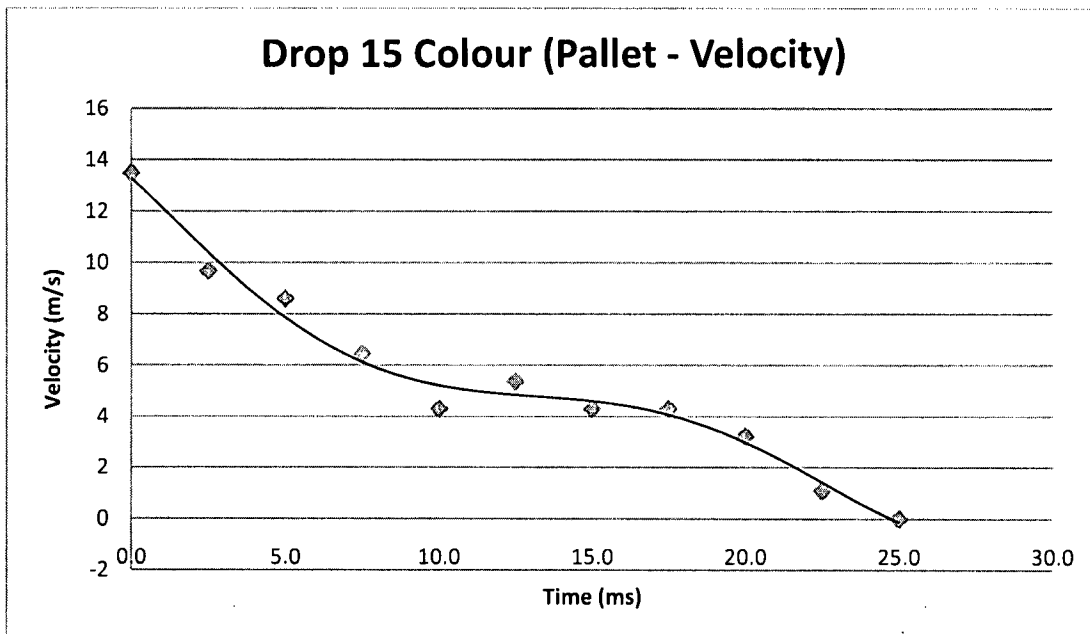
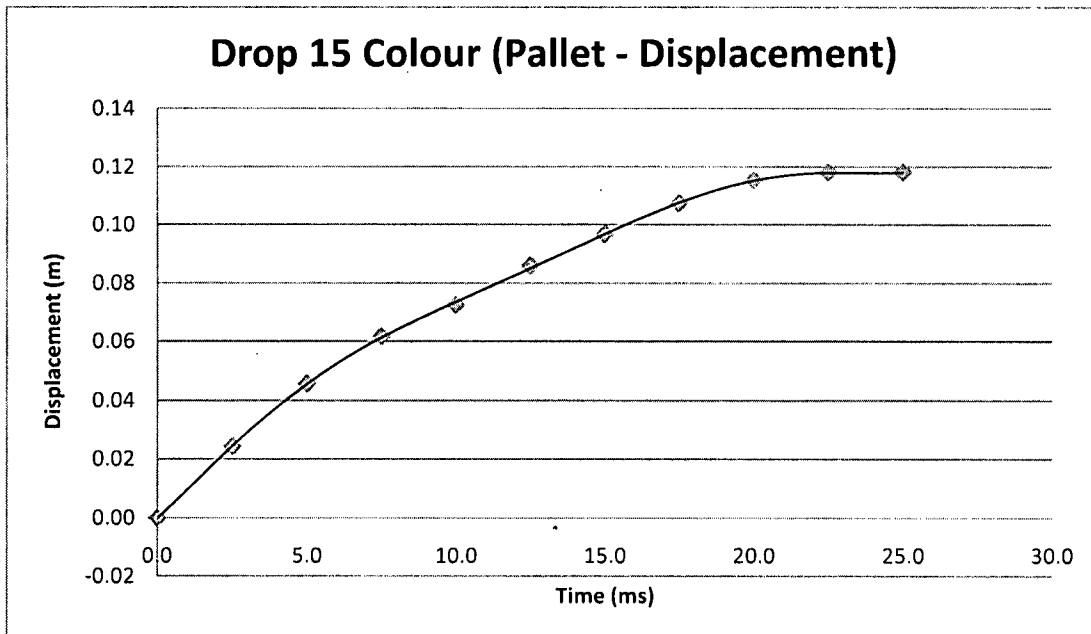


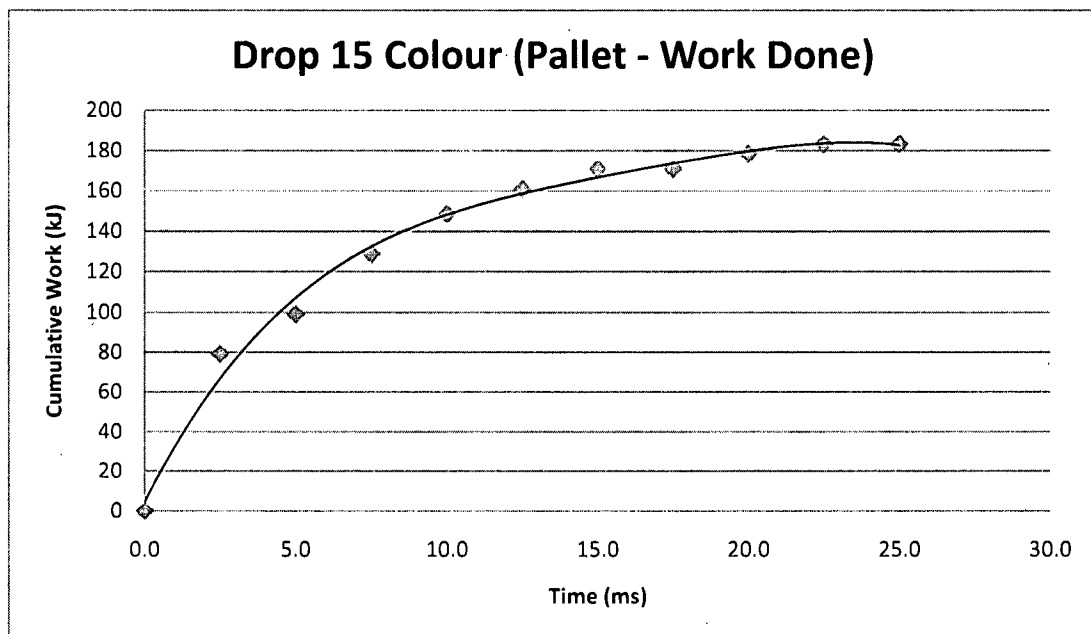
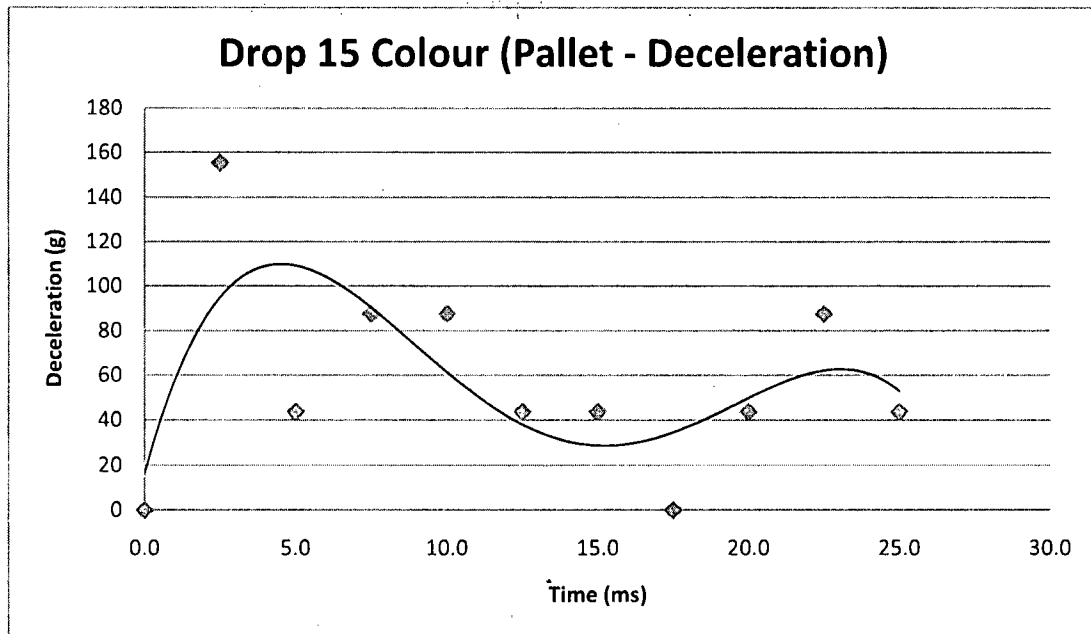
A.2.3 Drop 12 (Angled Inverted)

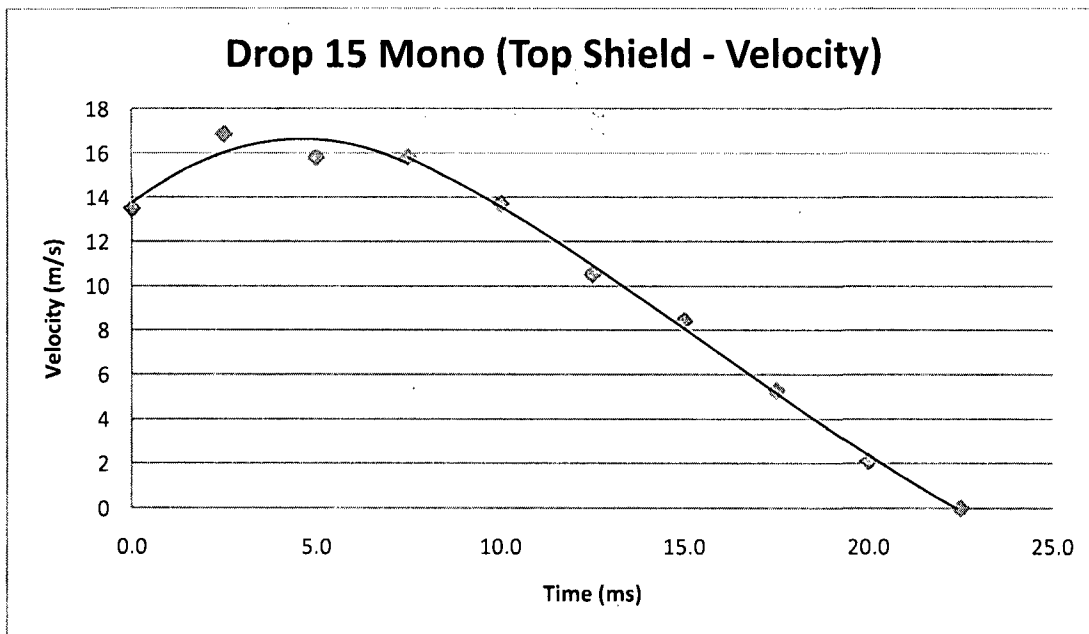
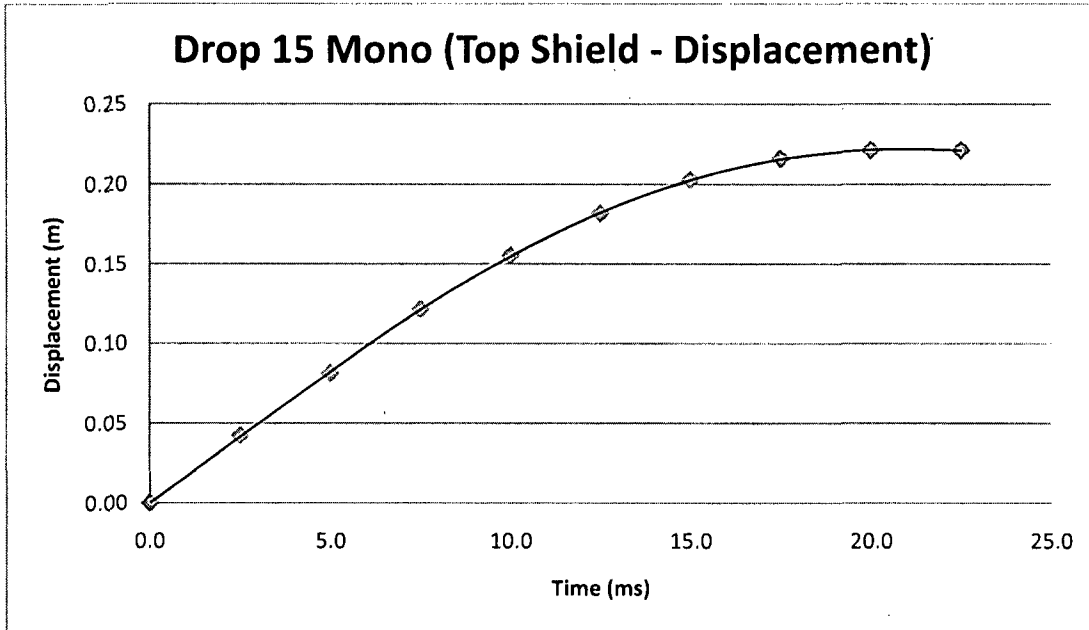


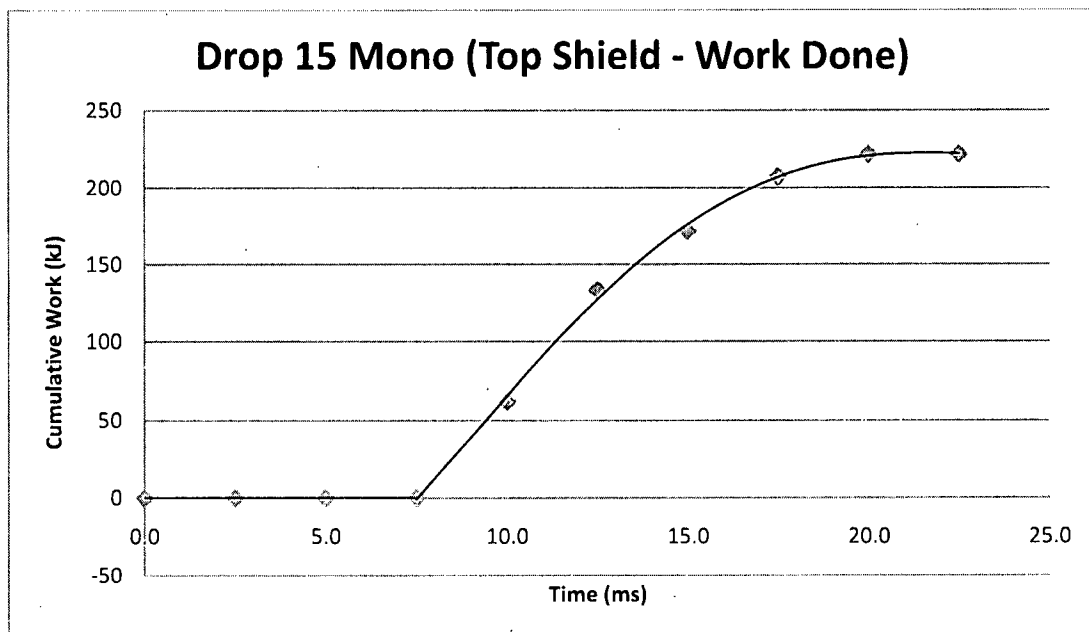
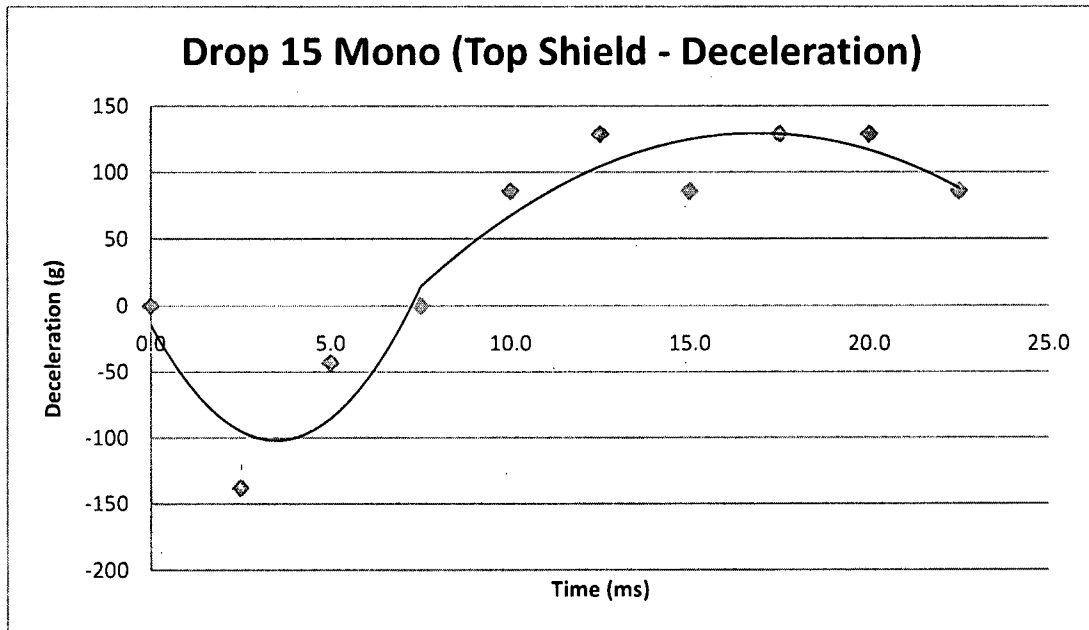


A.2.4 Drop 15 (Side)









A.3 APPENDIX 3 – DISPLACEMENT, VELOCITY AND DECELERATION DATA

A.3.1 Drop 6 (Upright)

Analysis Data Sheet - Drop 6 (9m Upright) Mono

Calibration

Frame rate:	2000 fps	Total container mass:	4374 kg	Equations used: $s = ut + 0.5at^2$
Time step per frame:	0.0005 s	Total pallet mass:	260 kg	$v = u + at$
Gravitational acceleration:	9.81 m/s ²	Stationary pallet mass (2/3):	173 kg	(where $u = 0$)
Drop distance:	9.26 m	Moving mass on impact:	4201 kg	$F = ma$
Time to impact:	1.37 s	Crush distance:	0.1329 m	$W = Fx$
Distance at t = -20 frames:	9.13 m	Total distance travelled:	9.393 m	
Distance moved to impact:	0.13 m	Total energy (m x g x h):	403.0 kJ	
Distance calibration:	737.2 pixels/m			

Tracking Data

Frame	Point 1		Point 2		Point 3		Point 4		Average
	y	dy	y	dy	y	dy	y	dy	dy
42	49		37		23		8		
62	148	99	135	98	122	99	107	99	99
67	170	22	157	22	144	22	130	23	22
72	191	21	178	21	165	21	150	20	21
77	210	19	197	19	183	18	169	19	19
82	225	15	213	16	199	16	185	16	16
87	238	13	224	11	210	11	196	11	12
92			231	7	217	7	203	7	7
97			232	1	218	1	203	0	1
102									0

Results from averaged displacements

Frame	Time, t (s)	dt	dy (pixels)	y norm (pixels)	y (m)	dy (m)	v (m/s)	dv (m/s)	a (m/s ²)	a (g)	m (kg)	F (kN)	W (kJ)	Cum. W (kJ)	Error	Time (ms)
42	-0.0100	-0.0100		-99	-0.1343		13.4									
62	0.0000	0.0100	99	0	0.0000	0.1343	13.5		0.0	0.0				0	1.0%	0.0
67	0.0025	0.0025	22	22	0.0298	0.0298	11.9	-1.5	-616.5	62.8	4201	2589.9	77.3	77.3	4.5%	2.5
72	0.0050	0.0025	21	43	0.0583	0.0285	11.4	-0.5	-217.0	22.1	4201	911.8	26.0	103.3	4.8%	5.0
77	0.0075	0.0025	19	62	0.0841	0.0258	10.3	-1.1	-434.1	44.3	4201	1823.6	47.0	150.3	5.3%	7.5
82	0.0100	0.0025	16	78	0.1058	0.0217	8.7	-1.6	-651.1	66.4	4201	2735.5	59.4	209.6	6.3%	10.0
87	0.0125	0.0025	12	90	0.1221	0.0163	6.5	-2.2	-868.2	88.5	4201	3647.3	59.4	269.0	8.3%	12.5
92	0.0150	0.0025	7	97	0.1316	0.0095	3.8	-2.7	-1085.2	110.6	4201	4559.1	43.3	312.3	14.3%	15.0
97	0.0175	0.0025	1	98	0.1329	0.0014	0.5	-3.3	-1302.3	132.8	4201	5470.9	7.4	319.7	100.0%	17.5
102	0.0200	0.0025	0	98	0.1329	0.0000	0.0	-0.5	-217.0	22.1	4201	911.8	0.0	319.7	#DIV/0!	20.0

Analysis Data Sheet - Drop 6 (9m Upright) Colour

Calibration

Frame rate:	1000 fps	Total container mass:	4374 kg	Equations used:	$s = ut + 0.5at^2$
Time step per frame:	0.001 s	Total pallet mass:	260 kg		$v = u + at$
Gravitational acceleration:	9.81 m/s ²	Stationary pallet mass (2/3):	173 kg		(where $u = 0$)
Drop distance:	9.26 m	Moving mass on impact:	4201 kg		$F = ma$
Time to impact:	1.37 s	Crush distance:	0.1330 m		$W = Fx$
Distance at t = -10 frames:	9.13 m	Total distance travelled:	9.393 m		
Distance moved to impact:	0.13 m	Total energy (m x g x h):	403.0 kJ		
Distance calibration:	1533.9 pixels/m				

Tracking Data

Frame	Point 1		Point 2		Point 3		Point 4		Average
	y	dy	y	dy	y	dy	y	dy	dy
10	233		203		173		141		
20	441	208	409	206	378	205	345	204	206
22	20		28		33		38		34
24	52	32	58	30	66	33	72	34	32
26	83	31	89	31	99	33	105	33	32
28	108	25	116	27	123	24	130	25	25
30	131	23	138	22	151	28	157	27	25
32	159	28	165	27	174	23	181	24	26
34	176	17	186	21	194	20	199	18	19
36	187	11	198	12	203	9	210	11	11
38									0

Note: It was not possible to track four points for the full duration of the drop, hence the average for frame 22 is an estimate.

Results from averaged displacements

Frame	Time, t (s)	dt	dy (pixels)	y norm (pixels)	y (m)	dy (m)	v (m/s)	dv (m/s)	a (m/s ²)	a (g)	m (kg)	F (kN)	W (kJ)	Cum. W (kJ)	Error	Time (ms)
10	-0.0100	-0.0100		-206	-0.1343		13.4									
20	0.0000	0.0100	206	0	0.0000	0.1343	13.5		0.0	0.0				0	0.5%	0.0
22	0.0020	0.0020	34	34	0.0222	0.0222	11.1	-2.4	-1198.0	122.1	4201	5032.8	111.6	111.6	2.9%	2.0
24	0.0040	0.0020	32	66	0.0430	0.0209	10.4	-0.7	-326.0	33.2	4201	1369.4	28.6	140.1	3.1%	4.0
26	0.0060	0.0020	32	98	0.0639	0.0209	10.4	0.0	0.0	0.0	4201	0.0	0.0	140.1	3.1%	6.0
28	0.0080	0.0020	25	123	0.0802	0.0163	8.1	-2.3	-1140.9	116.3	4201	4792.9	78.1	218.2	4.0%	8.0
30	0.0100	0.0020	25	148	0.0965	0.0163	8.1	0.0	0.0	0.0	4201	0.0	0.0	218.2	4.0%	10.0
32	0.0120	0.0020	26	174	0.1134	0.0170	8.5	0.3	163.0	16.6	4201	684.7	11.6	229.8	3.8%	12.0
34	0.0140	0.0020	19	193	0.1258	0.0124	6.2	-2.3	-1140.9	116.3	4201	4792.9	59.4	289.2	5.3%	14.0
36	0.0160	0.0020	11	204	0.1330	0.0072	3.6	-2.6	-1303.9	132.9	4201	5477.6	39.3	328.5	9.1%	16.0
38	0.0180	0.0020	0	204	0.1330	0.0000	0.0	-3.6	-1792.8	182.8	4201	7531.6	0.0	328.5	#DIV/0!	18.0

A.3.2 Drop 9 (Inverted)

Analysis Data Sheet - Drop 9 (9m Inverted) Mono

Calibration

Frame rate:	2000 fps	Total container mass:	4374 kg	Equations used:	$s = ut + 0.5at^2$
Time step per frame:	0.0005 s	Total top shield mass:	194 kg		$v = u + at$
Gravitational acceleration:	9.81 m/s ²	Mass of cones:	30 kg		(where $u = 0$)
Drop distance:	9.26 m	Moving mass on impact:	4344 kg		$F = ma$
Time to impact:	1.37 s	Crush distance:	0.1383 m		$W = Fx$
Distance at t = -20 frames:	9.13 m	Total distance travelled:	9.398 m		
Distance moved to impact:	0.13 m	Total energy (m x g x h):	403.3 kJ		
Distance calibration:	498.9 pixels/m				

Tracking Data

Frame	Point 1		Point 2		Point 3		Point 4		Average
	y	dy	y	dy	y	dy	y	dy	dy
43	41		32		22		13		
63	107	66	99	67	89	67	80	67	67
68	124	17	115	16	105	16	96	16	16
73	139	15	131	16	121	16	111	15	16
78	151	12	142	11	133	12	123	12	12
83	161	10	153	11	143	10	133	10	10
88	169	8	161	8	151	8	141	8	8
93	174	5	165	4	156	5	145	4	5
98	176	2	167	2	158	2	148	3	2
103									0

Results from averaged displacements

Frame	Time, t (s)	dt	y (pixels)	y norm (pixels)	y (m)	dy (m)	v (m/s)	dv (m/s)	a (m/s ²)	a (g)	m (kg)	F (kN)	W (kJ)	Cum. W (kJ)	Error	Time (ms)
43	-0.0100	-0.0100		-67	-0.1343		13.4									
63	0.0000	0.0100	67	0	0.0000	0.1343	13.5		0.0	0.0				0	1.5%	0.0
68	0.0025	0.0025	16	16	0.0321	0.0321	12.8	-0.7	-260.2	26.5	4344	1130.1	36.2	36.2	6.3%	2.5
73	0.0050	0.0025	16	32	0.0641	0.0321	12.8	0.0	0.0	0.0	4344	0.0	0.0	36.2	6.3%	5.0
78	0.0075	0.0025	12	44	0.0882	0.0241	9.6	-3.2	-1282.9	130.8	4344	5572.7	134.0	170.3	8.3%	7.5
83	0.0100	0.0025	10	54	0.1082	0.0200	8.0	-1.6	-641.4	65.4	4344	2786.4	55.9	226.1	10.0%	10.0
88	0.0125	0.0025	8	62	0.1243	0.0160	6.4	-1.6	-641.4	65.4	4344	2786.4	44.7	270.8	12.5%	12.5
93	0.0150	0.0025	5	67	0.1343	0.0100	4.0	-2.4	-962.1	98.1	4344	4179.5	41.9	312.7	20.0%	15.0
98	0.0175	0.0025	2	69	0.1383	0.0040	1.6	-2.4	-962.1	98.1	4344	4179.5	16.8	329.5	50.0%	17.5
103	0.0200	0.0025	0	69	0.1383	0.0000	0.0	-1.6	-641.4	65.4	4344	2786.4	0.0	329.5	#DIV/0!	20.0

Analysis Data Sheet - Drop 9 (9m Inverted) Colour

Calibration

Frame rate:	1000 fps	Total container mass:	4374 kg	Equations used:	$s = ut + 0.5at^2$
Time step per frame:	0.001 s	Total top shield mass:	194 kg		$v = u + at$
Gravitational acceleration:	9.81 m/s ²	Mass of cones:	30 kg		(where $u = 0$)
Drop distance:	9.26 m	Moving mass on impact:	4344 kg		$F = ma$
Time to impact:	1.37 s	Crush distance:	0.1311 m		$W = Fx$
Distance at t = -10 frames:	9.13 m	Total distance travelled:	9.391 m		
Distance moved to impact:	0.13 m	Total energy (m x g x h):	403.0 kJ		
Distance calibration:	625.5 pixels/m				

Tracking Data

Frame	Point 1		Point 2		Point 3		Point 4		Average
	y	dy	y	dy	y	dy	y	dy	dy
17	114		82		58		33		
27	197	83	166	84	141	83	117	84	84
29	214	17	182	16	157	16	133	16	16
31	229	15	198	16	172	15	148	15	15
33	243	14	211	13	186	14	162	14	14
35	255	12	222	11	198	12	173	11	12
37	264	9	233	11	207	9	183	10	10
39	274	10	241	8	216	9	191	8	9
41	279	5	247	6	221	5	197	6	6
43	282	3	249	2	224	3	199	2	3
45									0

Results from averaged displacements

Frame	Time, t (s)	dt	y (pixels)	y norm (pixels)	y (m)	dy (m)	v (m/s)	dv (m/s)	a (m/s ²)	a (g)	m (kg)	F (kN)	W (kJ)	Cum. W (kJ)	Error	Time (ms)
17	-0.0100	-0.0100		-84	-0.1343		13.4									
27	0.0000	0.0100	84	0	0.0000	0.1343	13.5		0.0	0.0				0	1.2%	0.0
29	0.0020	0.0020	16	16	0.0256	0.0256	12.8	-0.7	-344.3	35.1	4344	1495.6	38.3	38.3	6.3%	2.0
31	0.0040	0.0020	15	31	0.0496	0.0240	12.0	-0.8	-399.7	40.7	4344	1736.3	41.6	79.9	6.7%	4.0
33	0.0060	0.0020	14	45	0.0719	0.0224	11.2	-0.8	-399.7	40.7	4344	1736.3	38.9	118.8	7.1%	6.0
35	0.0080	0.0020	12	57	0.0911	0.0192	9.6	-1.6	-799.4	81.5	4344	3472.6	66.6	185.4	8.3%	8.0
37	0.0100	0.0020	10	67	0.1071	0.0160	8.0	-1.6	-799.4	81.5	4344	3472.6	55.5	240.9	10.0%	10.0
39	0.0120	0.0020	9	76	0.1215	0.0144	7.2	-0.8	-399.7	40.7	4344	1736.3	25.0	265.9	11.1%	12.0
41	0.0140	0.0020	6	82	0.1311	0.0096	4.8	-2.4	-1199.1	122.2	4344	5208.9	50.0	315.9	16.7%	14.0
43	0.0160	0.0020	3	85	0.1359	0.0048	2.4	-2.4	-1199.1	122.2	4344	5208.9	25.0	340.8	33.3%	16.0
45	0.0180	0.0020	0	85	0.1359	0.0000	0.0	-2.4	-1199.1	122.2	4344	5208.9	0.0	340.8	#DIV/0!	18.0

A.3.3. Drop 12 (Angled Inverted)

Analysis Data Sheet - Drop 12 (9m Angled Inverted) Mono

Calibration

Frame rate:	2000 fps	Total container mass:	4374 kg	Equations used:	$s = ut + 0.5at^2$
Time step per frame:	0.0005 s	Total top shield mass:	194 kg		$v = u + at$
Gravitational acceleration:	9.81 m/s ²	Mass of cones:	15 kg		(where $u = 0$)
Drop distance:	9.26 m	Moving mass on impact:	4359 kg		$F = ma$
Time to impact:	1.37 s	Crush distance:	0.1127 m		$W = Fx$
Distance at t = -20 frames:	9.13 m	Total distance travelled:	9.373 m		
Distance moved to impact:	0.13 m	Total energy (m x g x h):	402.2 kJ		
Distance calibration:	417.0 pixels/m				

Tracking Data

Frame	Point 1		Point 2		Point 3		Point 4		Average
	y	dy	y	dy	y	dy	y	dy	dy
54	108		92		76		60		
74	164	56	149	57	132	56	116	56	56
79	178	14	163	14	146	14	130	14	14
84	190	12	175	12	158	12	142	12	12
89	200	10	185	10	168	10	152	10	10
94	207	7	192	7	175	7	158	6	7
99	211	4	196	4	179	4	162	4	4
104	211	0	196	0	179	0	163	1	0

Results from averaged displacements

Frame	Time, t (s)	dt	dy (pixels)	y norm (pixels)	y (m)	dy (m)	v (m/s)	dv (m/s)	a (m/s ²)	a (g)	m (kg)	F (kN)	W (kJ)	Cum. W (kJ)	Error	Time (ms)
54	-0.0100	-0.0100		-56	-0.1343		13.4									
74	0.0000	0.0100	56	0	0.0000	0.1343	13.5		0.0	0.0				0	1.8%	0.0
79	0.0025	0.0025	14	14	0.0336	0.0336	13.4	0.0	-19.6	2.0	4359	85.5	2.9	2.9	7.1%	2.5
84	0.0050	0.0025	12	26	0.0624	0.0288	11.5	-1.9	-767.4	78.2	4359	3345.2	96.3	99.1	8.3%	5.0
89	0.0075	0.0025	10	36	0.0863	0.0240	9.6	-1.9	-767.4	78.2	4359	3345.2	80.2	179.4	10.0%	7.5
94	0.0100	0.0025	7	43	0.1031	0.0168	6.7	-2.9	-1151.1	117.3	4359	5017.8	84.2	263.6	14.3%	10.0
99	0.0125	0.0025	4	47	0.1127	0.0096	3.8	-2.9	-1151.1	117.3	4359	5017.8	48.1	311.7	25.0%	12.5
104	0.0150	0.0025	0	47	0.1127	0.0000	0.0	-3.8	-1534.8	156.5	4359	6690.4	0.0	311.7	100.0%	15.0

Analysis Data Sheet - Drop 12 (9m Angled Inverted) Colour

Calibration

Frame rate:	2000 fps	Total container mass:	4374 kg	Equations used:	$s = ut + 0.5at^2$
Time step per frame:	0.0005 s	Total top shield mass:	194 kg		$v = u + at$
Gravitational acceleration:	9.81 m/s ²	Mass of cones:	15 kg		(where $u = 0$)
Drop distance:	9.26 m	Moving mass on impact:	4359 kg		$F = ma$
Time to impact:	1.37 s	Crush distance:	0.1109 m		$W = Fx$
Distance at $t = -20$ frames:	9.13 m	Total distance travelled:	9.371 m		
Distance moved to impact:	0.13 m	Total energy (m x g x h):	402.1 kJ		
Distance calibration:	342.5 pixels/m				

Tracking Data

Frame	Point 1		Point 2		Point 3		Point 4		Average
	y	dy	y	dy	y	dy	y	dy	
77	183		195		191		188		
97	229	46	241	46	237	46	234	46	46
102	242	13	252	11	247	10	245	11	11
107	249	7	261	9	258	11	254	9	9
112	257	8	269	8	265	7	262	8	8
117	263	6	274	5	270	5	268	6	6
122	267	4	277	3	274	4	273	5	4
127	269	2	280	3	278	4	276	3	3
132									0

Results from averaged displacements

Frame	Time, t (s)	dt	dy (pixels)	y norm (pixels)	y (m)	dy (m)	v (m/s)	dv (m/s)	a (m/s ²)	a (g)	m (kg)	F (kN)	W (kJ)	Cum. W (kJ)	Error	Time (ms)
77	-0.0100	-0.0100		-46	-0.1343		13.4									
97	0.0000	0.0100	46	0	0.0000	0.1343	13.5		0.0	0.0				0	2.2%	0.0
102	0.0025	0.0025	11	11	0.0321	0.0321	12.8	-0.6	-253.2	25.8	4201	1063.6	34.2	34.2	9.1%	2.5
107	0.0050	0.0025	9	20	0.0584	0.0263	10.5	-2.3	-934.3	95.2	4201	3924.8	103.1	137.3	11.1%	5.0
112	0.0075	0.0025	8	28	0.0817	0.0234	9.3	-1.2	-467.1	47.6	4201	1962.4	45.8	183.1	12.5%	7.5
117	0.0100	0.0025	6	34	0.0993	0.0175	7.0	-2.3	-934.3	95.2	4201	3924.8	68.8	251.9	16.7%	10.0
122	0.0125	0.0025	4	38	0.1109	0.0117	4.7	-2.3	-934.3	95.2	4201	3924.8	45.8	297.7	25.0%	12.5
127	0.0150	0.0025	3	41	0.1197	0.0088	3.5	-1.2	-467.1	47.6	4201	1962.4	17.2	314.9	33.3%	15.0
132	0.0175	0.0025	0	41	0.1197	0.0000	0.0	-3.5	-1401.4	142.9	4201	5887.2	0.0	314.9	#DIV/0!	17.5

A.3.4 Drop 15 (Side)

Analysis Data Sheet - Drop 15 (9m Side) Mono

Calibration

Frame rate:	2000 fps	Total container mass:	4374 kg	Equations used: $s = ut + 0.5at^2$
Time step per frame:	0.0005 s	Half container mass:	2187 kg	$v = u + at$
Gravitational acceleration:	9.81 m/s ²	Mass of top shield quadrant:	39 kg	(where $u = 0$)
Drop distance:	9.26 m	Moving mass on impact:	2148 kg	$F = ma$
Time to impact:	1.37 s	Drop distance (incl. offset):	9.39 m	$W = Fx$
Distance at $t = -20$ frames:	9.13 m	Crush distance:	0.2212 m	
Distance moved to impact:	0.13 m	Total distance travelled:	9.611 m	
Distance calibration:	379.8 pixels/m	Total energy ($m \times g \times h$):	206.2 kJ	

Tracking Data

Frame	Point 1		Point 2		Point 3		Point 4		Average
	y	dy	y	dy	y	dy	y	dy	dy
558	10		21		32		43		
578	60	50	72	51	83	51	94	51	51
583	76	16	87	15	99	16	109	15	16
588	91	15	102	15	113	14	125	16	15
593	107	16	117	15	127	14	140	15	15
598	120	13	130	13	140	13	153	13	13
603	129	9	140	10	150	10	163	10	10
608	137	8	148	8	158	8	171	8	8
613	143	6	152	4	163	5	176	5	5
618	145	2	155	3	164	1	178	2	2
623									0

Results from averaged displacements

Frame	Time, t (s)	dt	dy (pixels)	y norm (pixels)	y (m)	dy (m)	v (m/s)	dv (m/s)	a (m/s ²)	a (g)	m (kg)	F (kN)	W (kJ)	Cum. W (kJ)	Error	Time (ms)
558	-0.0100	-0.0100		-51	-0.1343		13.4									
578	0.0000	0.0100	51	0	0.0000	0.1343	13.5		0.0	0.0				0	2.0%	0.0
583	0.0025	0.0025	16	16	0.0421	0.0421	16.9	3.4	1349.7	-137.6	2148			0.0	6.3%	2.5
588	0.0050	0.0025	15	31	0.0816	0.0395	15.8	-1.1	-421.3	-42.9	2148			0.0	6.7%	5.0
593	0.0075	0.0025	15	46	0.1211	0.0395	15.8	0.0	0.0	0.0	2148	-0.0	0.0	0.0	6.7%	7.5
598	0.0100	0.0025	13	59	0.1554	0.0342	13.7	-2.1	-842.7	85.9	2148	1810.0	62.0	62.0	7.7%	10.0
603	0.0125	0.0025	10	69	0.1817	0.0263	10.5	-3.2	-1264.0	128.8	2148	2715.0	71.5	133.5	10.0%	12.5
608	0.0150	0.0025	8	77	0.2028	0.0211	8.4	-2.1	-842.7	85.9	2148	1810.0	38.1	171.6	12.5%	15.0
613	0.0175	0.0025	5	82	0.2159	0.0132	5.3	-3.2	-1264.0	128.8	2148	2715.0	35.7	207.3	20.0%	17.5
618	0.0200	0.0025	2	84	0.2212	0.0053	2.1	-3.2	-1264.0	128.8	2148	2715.0	14.3	221.6	50.0%	20.0
623	0.0225	0.0025	0	84	0.2212	0.0000	0.0	-2.1	-842.7	85.9	2148	1810.0	0.0	221.6	#DIV/0!	22.5

Analysis Data Sheet - Drop 15 (9m Side) Colour

Calibration

Frame rate:	2000 fps	Total container mass:	4374 kg	Equations used:	$s = ut + 0.5at^2$
Time step per frame:	0.0005 s	Half container mass:	2187 kg		$v = u + at$
Gravitational acceleration:	9.81 m/s ²	Mass of pallet edge:	43 kg		(where $u = 0$)
Drop distance:	9.26 m	Moving mass on impact:	2144 kg		$F = ma$
Time to impact:	1.37 s	Crush distance:	0.1182 m		$W = Fx$
Distance at $t = -20$ frames:	9.13 m	Total distance travelled:	9.378 m		
Distance moved to impact:	0.13 m	Total energy ($m \times g \times h$):	201.2 kJ		
Distance calibration:	372.3 pixels/m				

Tracking Data

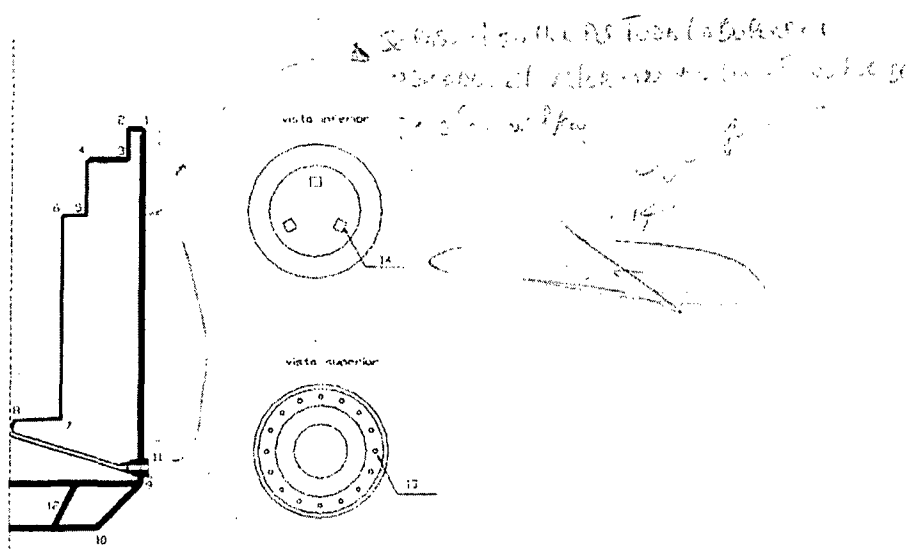
Frame	Point 1		Point 2		Point 3		Point 4		Average
	y	dy	y	dy	y	dy	y	dy	dy
118	177		199		214		229		
138	226	49	250	51	264	50	279	50	50
143	235	9	258	8	273	9	288	9	9
148	243	8	266	8	280	7	295	7	8
153	249	6	272	6	286	6	302	7	6
158	253	4	277	5	290	4	306	4	4
163	257	4	281	4	295	5	311	5	5
168	262	5	285	4	299	4	315	4	4
173	265	3	289	4	303	4	319	4	4
178	268	3	291	2	306	3	321	2	3
183	269	1	292	1	307	1	322	1	1
188									0

Results from averaged displacements

Frame	Time, t (s)	dt	dy (pixels)	y norm (pixels)	y (m)	dy (m)	v (m/s)	dv (m/s)	a (m/s ²)	a (g)	m (kg)	F (kN)	W (kJ)	Cum. W (kJ)	Error	Time (ms)
118	-0.0100	-0.0100		-50	-0.1343		13.4									
138	0.0000	0.0100	50	0	0.0000	0.1343	13.5		0.0	0.0				0	2.0%	0.0
143	0.0025	0.0025	9	9	0.0242	0.0242	9.7	-3.8	-1523.8	155.3	2148	3273.0	79.1	79.1	11.1%	2.5
148	0.0050	0.0025	8	17	0.0457	0.0215	8.6	-1.1	-429.8	43.8	2148	923.1	19.8	99.0	12.5%	5.0
153	0.0075	0.0025	6	23	0.0618	0.0161	6.4	-2.1	-859.5	87.6	2148	1846.2	29.8	128.7	16.7%	7.5
158	0.0100	0.0025	4	27	0.0725	0.0107	4.3	-2.1	-859.5	87.6	2148	1846.2	19.8	148.5	25.0%	10.0
163	0.0125	0.0025	5	32	0.0860	0.0134	5.4	1.1	429.8	43.8	2148	923.1	12.4	160.9	20.0%	12.5
168	0.0150	0.0025	4	36	0.0967	0.0107	4.3	-1.1	-429.8	43.8	2148	923.1	9.9	170.9	25.0%	15.0
173	0.0175	0.0025	4	40	0.1074	0.0107	4.3	0.0	0.0	0.0	2148	0.0	0.0	170.9	25.0%	17.5
178	0.0200	0.0025	3	43	0.1155	0.0081	3.2	-1.1	-429.8	43.8	2148	923.1	7.4	178.3	33.3%	20.0
183	0.0225	0.0025	1	44	0.1182	0.0027	1.1	-2.1	-859.5	87.6	2148	1846.2	5.0	183.3	100.0%	22.5
188	0.0250	0.0025	0	44	0.1182	0.0000	0.0	-1.1	-429.8	43.8	2148	923.1	0.0	183.3	#DIV/0!	25.0

DIOXITEK SA SISTEMA DE GESTIÓN DE LA CALIDAD		Ensayo de estanqueidad en cavidad de blindaje de embalajes/bultos Shielding cavity leakage test for flask/packing		Reporte No: Report No. RTR260
1.0 Equipamiento (Equipment & Data)				
1.1	Contenedor Flask	Modelo / N° de serie: 3962 / 05 Model / Serial N°:		
1.2	Detector de helio Helium Detector	Modelo / N° de serie: 1011 / A0000 SSP7226 Model / Serial N°:		
1.3	Pérdida calibrada Calibrated leakage	N° de serie: FLH / 1742 Serial N°:	Vencimiento de calibración: 4/1 Calibration Due:	
1.3	Manovacuometro Manovacuumeter	Modelo / N° de serie: 1011 / A0000 SSP7226 Model / Serial N°:	Vencimiento de calibración: 4/1 Calibration Due:	
	Operación (Operation)	Resultado o ✓ (Results or ✓)	Inicial (Initial)	
2.0 Procedimiento (Leak testing)				
2.1	Calibrar el detector de helio con la pérdida controlada y chequear el funcionamiento del sniffer antes de realizar el ensayo según II14JZ33 Punto 1.2 Calibrate the Helium Detector with external calibrated leak and check the sniffer probe before perform the test according to II14JZ33 Point 1.2	3.28 x 10 ⁻³ mbar.l/s	20	
2.2	Conectar en el orificio de la pared del cuerpo del contenedor la bomba de vacío, el manovacuometro y el tanque de helio mediante una válvula de tres vías. Connect the vacuum pump, manovacuumeter and the helium tank in the hole on the flask wall through a three way valve.	✓	20	
2.3	Hacer vacío hasta que el manovacuometro indique 1mbar. Cerrar el vacío y abrir la válvula del helio hasta que la presión interna sea la atmosférica. Vacuum until the manovacuumeter indicates 1mbar. Close the vacuum and open the helium valve until the inner atmospheric pressure value.	0.6 mbar.l/s	20	
2.4	Repetir el paso 2.2 como mínimo dos veces. Repeat operation 2.2 at least two times.	✓	20	
2.5	Cerrar la válvula de tres vías, y mantener la presión atmosférica dentro de la cavidad del blindaje durante el ensayo. Close the three way valve, and to maintain the pressure atmospheric within the cavity of the shield during the test.	0.6 mbar.l/s	20	
2.6	Conectar el espectrómetro de masas en el punto de drenaje, con el tapón de cierre y el de venteo colocados. Connect mass spectrometer to drain point with closure and vent plug in place	NA		
2.7	Dejar que se establezca la lectura o frenar en 1.10 ⁻³ mbar.l/s si decrece. Tomar nota de los valores máximos encontrados. Let readings setter or stop at 1.10 ⁻³ mbar.l/s if decreasing. Take note of the maximum values found	NA		
2.8	Desconectar el espectrómetro de masas, quitar el tapón de cierre y pasar el sniffer del detector de helio lentamente por los cordones de soldadura indicadas en el esquema adjunto Disconnect mass spectrometer, remove closure and slowly pass the sniffer of the helium detector on the indicated fillets welds in the attached scheme.	✓	20	
2.9	Tomar nota los valores máximos encontrados y marcar el punto donde fue encontrado en la siguiente tabla de resultados. Take note of the maximum values found and to mark the point where it was found in the following table of results.	0.6 mbar.l/s	20	
2.10	Calibrar el detector de helio con la pérdida controlada y chequear el funcionamiento del sniffer después de realizar el ensayo según II14JZ33 Punto 1.2 Calibrate the Helium Detector with external calibrated leak and check the sniffer probe after perform the test according to II14JZ33 Point 1.2	3.28 x 10 ⁻³ mbar.l/s	20	

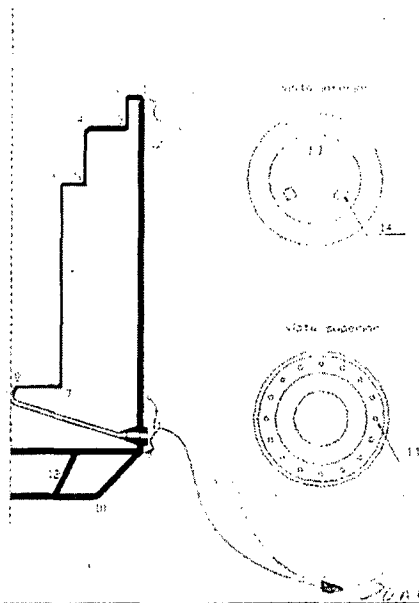
DIOXITEK SA SISTEMA DE GESTIÓN DE LA CALIDAD	Ensayo de estanqueidad en cavidad de blindaje de embalajes/bultos Shielding cavity leakage test for flask/packing	Reporte No: Report No. RTR-260
--	---	--



3.0 Resultado (Results)			
3.1	Valor máximo encontrado con el espectrómetro de masas: <u>1.5 x 10⁻⁶ mbar.l/s</u> (mbar.l/s)		
3.2	Valores máximos encontrados con el sniffer:		
	Posición	Valor (mbar.l/s)	Ubicación (en grados respecto la punto de drenaje sentido horario)
3.2.1	1	<u>1.5 x 10⁻⁶ mbar.l/s</u>	Tapa lateral izquierda
3.2.2	2	<u>1.5 x 10⁻⁶ mbar.l/s</u>	
3.2.3	3	<u>1.5 x 10⁻⁶ mbar.l/s</u>	
3.2.4	4	<u>1.5 x 10⁻⁶ mbar.l/s</u>	
3.2.5	5	<u>1.5 x 10⁻⁶ mbar.l/s</u>	
3.2.6	6	<u>1.5 x 10⁻⁶ mbar.l/s</u>	
3.2.7	7	<u>1.5 x 10⁻⁶ mbar.l/s</u>	
3.2.8	8	<u>1.5 x 10⁻⁶ mbar.l/s</u>	
3.2.9	9	<u>1.5 x 10⁻⁶ mbar.l/s</u>	
3.2.10	10	<u>1.5 x 10⁻⁶ mbar.l/s</u>	
3.2.11	11	<u>1.5 x 10⁻⁶ mbar.l/s</u>	
3.2.12	12	<u>1.5 x 10⁻⁶ mbar.l/s</u>	
3.2.13	16 Agujeros M20 de tornillos del tapón de cierre	<u>1.5 x 10⁻⁶ mbar.l/s</u>	Tapa lateral izquierda
3.2.14	3 tapas de la base	<u>1.5 x 10⁻⁶ mbar.l/s</u>	Tapa lateral izquierda
3.2.15	Valor de fondo (Background)	<u>1.5 x 10⁻⁶ mbar.l/s</u>	
APROBADO si el valor máximo encontrado es 1×10^{-6} mbar.l/s o inferior. sino RECHAZADO PASS if maximum results is 1×10^{-6} mbar.l/s or less, if not FAILED			APROBADO (PASS) ✓ RECHAZADO (FAILED)
Realizó: Signed:	<u>A. Fernández Salazar</u> Date: <u>17/11/08</u>		Fecha: <u>17/11/08</u> Date: <u>17/11/08</u>
Supervisó: Reviewed:	<u>[Signature]</u> Date: <u>17/11/08</u>		Fecha: <u>17/11/08</u> Date: <u>17/11/08</u>

DIOXITEK SA SISTEMA DE GESTIÓN DE LA CALIDAD		Ensayo de estanqueidad en cavidad de blindaje de embalajes/bultos Shielding cavity leakage test for flask/packing		Reporte No: Report No. 276.20.
1.0 Equipamiento (Equipment & Data)				
1.1	Contenedor Flask	Modelo / N° de serie: 353 3962 / 01 Model / Serial N°:		
1.2	Detector de helio Helium Detector	Modelo / N° de serie: ALKATEL MSN 170 T Model / Serial N°:		
1.3	Pérdida calibrada Calibrated leakage	N° de serie: FEIN 02 2993 Serial N°:	Vencimiento de calibración: 0/4 Calibration Due:	
1.3	Manovacuometro Manovacuumeter	Modelo / N° de serie: PEARL 070064-52515 Model / Serial N°: B2000-4000 107	Vencimiento de calibración: 26-01-05 Calibration Due: 02-05-05	
	Operación (Operation)		Resultado o ✓ (Results or ✓)	Inicial (Initial)
2.0 Procedimiento (Leak testing)				
2.1	Calibrar el detector de helio con la pérdida controlada y chequear el funcionamiento del sniffer antes de realizar el ensayo según II14JZ33 Punto 1.2 Calibrate the Helium Detector with external calibrated leak and check the sniffer probe before perform the test according to II14JZ33 Point 1.2		2.47 mbar.l/s	OK
2.2	Conectar en el orificio de la pared del cuerpo del contenedor la bomba de vacío, el manovacuometro y el tanque de helio mediante una válvula de tres vías. Connect the vacuum pump, manovacuumeter and the helium tank in the hole on the flask wall through a three way valve.			OK
2.3	Hacer vacío hasta que el manovacuometro indique 1mbar. Cerrar el vacío y abrir la válvula del helio hasta que la presión interna sea la atmosférica. Vacuum until the manovacuumeter indicates 1mbar. Close the vacuum and open the helium valve until the inner atmospheric pressure value.		0.3 mbar (Válvula) 0.7 " " 0.9 mbar (Pump)	OK
2.4	Repetir el paso 2.2 como mínimo dos veces. Repeat operation 2.2 at least two times.		Sombra controlada	OK
2.5	Cerrar la válvula de tres vías, y mantener la presión atmosférica dentro de la cavidad del blindaje durante el ensayo. Close the three way valve, and to maintain the pressure atmospheric within the cavity of the shield during the test.		✓	OK
2.6	Conectar el espectrómetro de masas en el punto de drenaje, con el tapón de cierre y el de venteo colocados. Connect mass spectrometer to drain point with closure and vent plug in place		✓	
2.7	Dejar que se establezca la lectura o frenar en 1.10 ⁻⁵ mbar.l/s si decrece. Tomar nota de los valores máximos encontrados. Let readings setter or stop at 1.10 ⁻⁵ mbar.l/s if decreasing. Take note of the maximum values found		1.10	
2.8	Desconectar el espectrómetro de masas, quitar el tapón de cierre y pasar el sniffer del detector de helio lentamente por los cordones de soldadura indicadas en el esquema adjunto Disconnect mass spectrometer, remove closure and slowly pass the sniffer of the helium detector on the indicated fillets welds in the attached scheme.			OK
2.9	Tomar nota los valores máximos encontrados y marcar el punto donde fue encontrado en la siguiente tabla de resultados. Take note of the maximum values found and to mark the point where it was found in the following table of results.			OK
2.10	Calibrar el detector de helio con la pérdida controlada y chequear el funcionamiento del sniffer después de realizar el ensayo según II14JZ33 Punto 1.2 Calibrate the Helium Detector with external calibrated leak and check the sniffer probe after perform the test according to II14JZ33 Point 1.2			OK

DIOXITEK SA SISTEMA DE GESTIÓN DE LA CALIDAD	Ensayo de estanqueidad en cavidad de blindaje de embalajes/bultos Shielding cavity leakage test for flask/packing	Reporte No: Report No. <i>RTE 261</i>
--	---	---



3.0 Resultado (Results)			
3.1	Valor máximo encontrado con el espectrómetro de masas: <i>5.10⁻⁶ mbar.l/s</i>		
3.2	Valores máximos encontrados con el sniffer:		
	Posición	Valor (mbar.l/s)	Ubicación (en grados respecto la punto de drenaje sentido horario)
3.2.1	1	<i>5.10⁻⁶ mbar.l/s</i>	<i>Toca la del agujero</i>
3.2.2	2	<i>5.10⁻⁶ mbar.l/s</i>	"
3.2.3	3	<i>5.10⁻⁶ mbar.l/s</i>	"
3.2.4	4	<i>5.10⁻⁶ mbar.l/s</i>	"
3.2.5	5	<i>5.10⁻⁶ mbar.l/s</i>	"
3.2.6	6	<i>5.10⁻⁶ mbar.l/s</i>	"
3.2.7	7	<i>5.10⁻⁶ mbar.l/s</i>	"
3.2.8	8	<i>5.10⁻⁶ mbar.l/s</i>	"
3.2.9	9	<i>5.10⁻⁶ mbar.l/s</i>	"
3.2.10	10	<i>5.10⁻⁶ mbar.l/s</i>	"
3.2.11	11	<i>5.10⁻⁶ mbar.l/s</i>	"
3.2.12	12	<i>5.10⁻⁶ mbar.l/s</i>	"
3.2.13	16 Agujeros M20 de tornillos del tapón de cierre	<i>5.10⁻⁶ mbar.l/s</i>	"
3.2.14	3 tapas de la base	<i>5.10⁻⁶ mbar.l/s</i>	"
3.2.15	Valor de fondo (Background)	<i>5.10⁻⁶ mbar.l/s</i>	"
APROBADO si el valor máximo encontrado es 1.10^{-5} mbar.l/s o inferior, sino RECHAZADO PASS if maximum results is 1.10^{-5} mbar.l/s or less, if not FAILED			APROBADO (PASS) ✓
Realizó: <i>[Signature]</i> Signed: <i>[Signature]</i> Superviso: <i>[Signature]</i> Reviewed: <i>[Signature]</i>			Fecha: <i>17/11/08</i> Date: <i>17/11/08</i>

CINDELVAC RUVAC

VACUUM

RUVAC S.R.L. Terrada 2562 C1417GV Di. Zavina 5563 C1439 BEAII Concordia 2041 C1407DJOI
Código Federal: Bs As Teléfono: 4501-5129 / 4504-4122 Fax: Int. 36

Aut. Gubernativa N° 1111/00 del 10/01/00. Reg. N° 22.000.000/00
Reg. Federal N° 1111/00 del 10/01/00. Reg. N° 22.000.000/00
Reg. N° 1111/00 del 10/01/00. Reg. N° 22.000.000/00

Dioxtek S.A.		Ensayo de la estanquidad en la cavidad de blindaje de embalajes/bultos		Reporte N° RTR 852
		Sealing cavity leakage test for Bulkpackaging		Report N°
1.0 Equipamiento (Equipment & Data)				
1.1	Combinador	Modelo / Nº de serie	3131 / 01	
	Mark	Modelo / Serial Nº		
1.2	Detector de Fugas	Modelo / Nº de serie	ALCATEL 4601 1987	
	Leak Detector	Modelo / Serial Nº		
1.3	Patilla Calibrada	Modelo / Nº de serie	F E 11	Verificación de la calibración
	Calibrated Fork	Modelo / Serial Nº	Nº 2743	Calibration Date
1.4	Manómetro de vacío	Modelo / Nº de serie	PA-300 07.04.03.14	Verificación de la calibración
	Vacuum Gauge	Modelo / Serial Nº	PA-300 07.04.03.14	Calibration Date
Operación		Resultado b		Final
Operation		Observations		Grade
2.0 Pruebas de la Cavidad del Blindaje (Test containment boundary, cavity wall and drum tight)				
2.1	Calibrar el Detector de Fugas con la pérdida calibrada y verificar el funcionamiento del sistema antes de realizar el ensayo. Calibrate the Leak Detector with the calibrated leakage and check the system operation before the test.			OK
2.2	Conectar en el punto de la pared del cuerpo del contenedor la sonda de vacío, el transmisor de aire y el tanque de nitrógeno para la prueba de tres vías. Connect the vacuum probe, the transmitter and the nitrogen tank at the body wall for the three-way test.			OK
2.3	Hacer vacío hasta que el manómetro indique 1 mbar. Cerrar el vacío y medir la pérdida de fuga hasta que la presión interna sea la atmosférica. Vacuum until the gauge indicates 1 mbar. Close the vacuum and measure the leakage until the internal pressure is atmospheric.			OK
2.4	Cerrar la válvula de tres vías y mantener a presión atmosférica dentro de la cavidad del blindaje durante el ensayo. Close the three-way valve and maintain the atmospheric pressure inside the containment cavity during the test.			OK
2.5	Conectar el detector de fuga en el punto de la pared del cuerpo del contenedor y de la sonda de vacío. Connect the leak detector at the body wall and the vacuum probe.			OK
2.6	Dejar que se estabilice la lectura a menos de 1 mbar. Medir la pérdida de fuga hasta que la presión interna sea la atmosférica. Let the reading stabilize at less than 1 mbar. Measure the leakage until the internal pressure is atmospheric.			OK
2.7	Hacer vacío de nuevo a una presión de 1 mbar y verificar el funcionamiento del detector de fuga, medir la pérdida de fuga y poner el sistema al detectar un mal funcionamiento por las condiciones de operación de la cavidad. Vacuum again to 1 mbar and check the leak detector operation, measure the leakage and put the system at work when a malfunction occurs due to the operating conditions of the cavity.			OK
2.8	Tomar nota de los valores lecturas estabilizadas y registrar los datos. Take note of the stabilized reading values and record the data.			OK
2.9	Calibrar el Detector de Fugas con la pérdida calibrada y verificar el funcionamiento del sistema después de realizar el ensayo. Calibrate the Leak Detector with the calibrated leakage and check the system operation after the test.			OK

CINDEL VACUUM

VACUUM

RUVAC S.R.L. Terrado 2562C 1417 CV D. #2400 5862G C1430 UCA B. Concordia 20410 C1400 D. J. Capital Federal - Bs. As. Teléfono: 4501-5129 / 4504-4122 Fax. int. 30

Pruebas del espacio entre sellos de O ring (Test O-ring seals closure with plug and drain plug)		
1.1	Instalar el Detector de Fugas en la posición calibrada y chequear el funcionamiento del sistema antes de realizar el ensayo. Instalar el Detector de Fugas en posición calibrada y chequear el funcionamiento del sistema.	Ver 3.1
3.2	Conectar en el punto de llenado del sistema la bomba de vacío y el Detector de Fugas en posición calibrada y chequear el funcionamiento del sistema.	Ver 3.2
3.3	Aplicar la presión de vacío, hasta alcanzar el nivel de vacío requerido en el punto de llenado del sistema.	Ver 3.3
3.4	Aplicar la presión de vacío, hasta alcanzar el nivel de vacío requerido en el punto de llenado del sistema.	Ver 3.4
3.5	Aplicar la presión de vacío, hasta alcanzar el nivel de vacío requerido en el punto de llenado del sistema.	Ver 3.5
3.6	Aplicar la presión de vacío, hasta alcanzar el nivel de vacío requerido en el punto de llenado del sistema.	Ver 3.6
3.7	Aplicar la presión de vacío, hasta alcanzar el nivel de vacío requerido en el punto de llenado del sistema.	Ver 3.7
3.8	Aplicar la presión de vacío, hasta alcanzar el nivel de vacío requerido en el punto de llenado del sistema.	Ver 3.8
3.9	Aplicar la presión de vacío, hasta alcanzar el nivel de vacío requerido en el punto de llenado del sistema.	Ver 3.9
3.10	Aplicar la presión de vacío, hasta alcanzar el nivel de vacío requerido en el punto de llenado del sistema.	Ver 3.10
3.11	Aplicar la presión de vacío, hasta alcanzar el nivel de vacío requerido en el punto de llenado del sistema.	Ver 3.11
3.12	Aplicar la presión de vacío, hasta alcanzar el nivel de vacío requerido en el punto de llenado del sistema.	Ver 3.12

Referencias

APROBADO en el <u>18/11/2018</u> por <u>Diego C. C. C.</u> en la <u>18/11/2018</u> .	APROBADO	✓
RECHAZADO	RECHAZADO	
FECHA: <u>18/11/2018</u>	FECHA: <u>18/11/2018</u>	
ROBADA: <u>Diego C. C. C.</u>	FECHA: <u>18/11/2018</u>	
RECHAZADA: <u>Diego C. C. C.</u>	FECHA: <u>18/11/2018</u>	

ROBADA: Diego C. C. C.

RECHAZADA: Diego C. C. C.

INTEL VACUUM

PERIPHERAL VACUUM

RUVAC S.R.L. Ferrada 2562 (C1417CW) Zúñiga 5863 (C1417D) B.E.A. Concordia 2041 (C1407D) (C1407D)
Capital Federal - Bto. Ato. Teléfono: 4501-5129 / 4504-4122 Fax: Int. 36

Int. 36
www.intelvac.com.ar
mailto:ventas@intelvac.com.ar

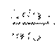
ventas@intelvac.com.ar

Dioxtek S.A.		Ensayo de la estanqueidad en la cavidad de blindaje de embalajes/bultos		Reporte N°: RTR 263
		Splicing cavity leakage test for bulkpacking		Report 263
1.0 Equipamiento (Equipment & Data)				
1.1	Contenedor	Modelo / N° de serie	3981/01	
1.1	Flask	Model / Serial N°		
1.2	Detector de helio	Modelo / N° de serie	ALCATEL ASM 180 T	
1.2	Helium Detector	Model / Serial N°		
1.3	Pérdida Calorada	Modelo / N° de serie	7E 14	
1.3	Calorated Leak	Model / Serial N°	N° 2743	
1.4	Manovacuómetro	Modelo / N° de serie	PIRANI N° 046235K	
1.4	Manovacuumeter	Model / Serial N°	VACUOMETRO 102	
		Verificación de la calibración		Calibration Due
		Verificación de la calibración		26-05-05
		Calibration Due		07-05-05
Operación		Resultado	Inicial	
(Operation)		(Vacuum or V)	(Initial)	
2.0 Pruebas de la Cavidad del Blindaje (Test containment boundary, cavity wall and drain tube)				
2.1	Calibrar el Detector de Helio con la pérdida calibrada y chequear el funcionamiento del sifón antes de realizar el ensayo.	3.67 x 10 ⁻⁸ mbar L/s R		
2.1	Calibrate the Helium Detector with calibrated leak and check the siphon before the test.			
2.2	Conectar en el centro de la pared del cuerpo del contenedor la bomba de vacío, el manovacuómetro y el tapón de helio mediante una válvula de tres vías.	✓ R		
2.2	Connect the vacuum pump, manovacuumeter and the helium leak to the hole of the flask wall through a three-way valve.			
2.3	Hacer vacío hasta que el manovacuómetro indique 1 mbar. Cerrar el vacío y abrir la válvula de helio hasta que la presión alcance sea la atmosférica.	No largos cambios de R		
2.3	Evacuate until the manovacuumeter indicates 1 mbar. Close the vacuum and open the helium valve until the pressure reaches the atmospheric.			
2.4	Cerrar la válvula de tres vías y mantener a presión atmosférica dentro de la cavidad del blindaje durante el ensayo.	N/A (2.3) R		
2.4	Close the three-way valve and maintain the atmospheric pressure inside the cavity during the test.			
2.5	Conectar el detector de helio en el punto de escape con el tapón de cierre y de venteo calibrado.	N/A (2.3) R		
2.5	Connect the helium detector to the leak point with the calibrated closure and venting.			
2.6	Dejar que se establezca la lectura e iniciar un 2.0 x 10 ⁻⁸ mbar L/s durante el ensayo. Tomar nota de los valores observados.	N/A (2.3) R		
2.6	Let the reading stabilize and start a 2.0 x 10 ⁻⁸ mbar L/s during the test. Take note of the observed values.			
2.7	Si el valor es mayor a 2.0 x 10 ⁻⁸ mbar L/s desconectar el detector de helio, quitar el tapón de cierre y pasar el sifón del detector de helio lentamente por los conductos de escape de la cavidad.	R N/A (2.3) R		
2.7	If the value is greater than 2.0 x 10 ⁻⁸ mbar L/s disconnect the helium detector, remove the closure and pass the siphon of the helium detector slowly through the cavity escape ducts.			
2.8	Tomar nota de los valores máximos encontrados y registrar en ubicación.	N/A (2.3) R		
2.8	Take note of the maximum values found and register in the location.			
2.9	Calibrar el Detector de Helio con la pérdida calibrada y chequear el funcionamiento del sifón después de realizar el ensayo.	N/A (2.3) R		
2.9	Calibrate the Helium Detector with calibrated leak and check the siphon after the test.			

CONDELVAC/CF/0000

FEELIFER - VACUUM

RUVAC S.R.L. Ferrada 2562 (C1477CWD) / Zúñiga 5663 (C1439 BEA) / Concordia 204 (C1407D) /
 Capital Federal - Bs. As. Teléfonos: 4501-5129 / 4504-4122 Fax: Int. 30

Logo:  RUVAC S.R.L. / Zúñiga 5663 (C1439 BEA) / Concordia 204 (C1407D) /
 Capital Federal - Bs. As. Teléfonos: 4501-5129 / 4504-4122 Fax: Int. 30

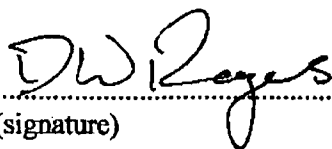
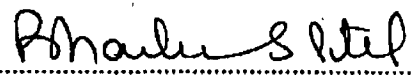
Entrega: 1.1.2007 / 01/01/07

3.0 Pruebas del espacio entre sellos de O-ring (Test O-ring seals, closure vent plug and drain plug)		
3.1	Calibrar el Detector de Hielo con la pérdida calibrada y chequear el funcionamiento del indicador antes de realizar el ensayo. Calibrate the ice detector with the calibrated leakage and check the operation of the indicator before the test.	N/A
3.2	Conectar en el punto de llenado del contenedor la bomba de vacío, al mismo tiempo y el tanque de nitrógeno una válvula de cierre. Connect the vacuum pump to the filling point of the container, at the same time and the nitrogen tank a shut-off valve.	✓
3.3	Hacer vacío hasta que el manómetro indique 1 mbars. Cerrar el vacío y abrir la válvula de helio hasta que la presión alcance una atmósfera. Vacuum until the manometer indicates 1 mbar. Close the vacuum and open the helium valve until the pressure reaches one atmosphere.	N/A
3.4	Cerrar la válvula de tres vías y mantener a presión atmosférica dentro de la cavidad del contenedor durante el ensayo. Close the three-way valve and maintain atmospheric pressure inside the cavity during the test.	1 Kg
3.5	Conectar el detector de helio en el punto de prueba entre sellos del tapón de cierre. Connect the helium detector to the test point between seals of the closure plug.	✓
3.6	Dejar que se establezca la lectura o leer en 2.0x10 ⁻⁸ mbar/s el detector. Tomar nota de los valores encontrados. Let the reading stabilize or read on the detector 2.0x10 ⁻⁸ mbar/s. Take note of the values found.	2 x 10 ⁻⁸ mbar/s
3.7	Desconectar el detector de helio, colocar el tapón en el punto entre sellos del tapón de cierre y conectar el detector de helio en el punto entre sellos del drenaje. Disconnect the helium detector, place the plug in the point between seals of the closure plug and connect the helium detector to the point between seals of the drain plug.	✓
3.8	Dejar que se establezca la lectura o leer en 2.0x10 ⁻⁸ mbar/s el detector. Tomar nota de los valores encontrados. Let the reading stabilize or read on the detector 2.0x10 ⁻⁸ mbar/s. Take note of the values found.	6 x 10 ⁻⁸ mbar/s
3.9	Desconectar el detector de helio, colocar el tapón en el punto entre sellos del drenaje y conectar el detector de helio en el punto entre sellos del drenaje. Disconnect the helium detector, place the plug in the point between seals of the drain plug and connect the helium detector to the point between seals of the drain plug.	✓
3.10	Dejar que se establezca la lectura o leer en 2.0x10 ⁻⁸ mbar/s el detector. Tomar nota de los valores encontrados. Let the reading stabilize or read on the detector 2.0x10 ⁻⁸ mbar/s. Take note of the values found.	1 x 10 ⁻⁸ mbar/s
3.11	Desconectar el detector de helio, colocar el tapón en el punto entre sellos del drenaje. Abrir la válvula de tres vías para conectar el punto de llenado con la bomba y hacer un vacío menor a 1 mbars. Luego abrir a la atmósfera para hacer ingresar aire. Repetir la operación 2 veces más. Disconnect the helium detector, place the plug in the point between seals of the drain plug. Open the three-way valve to connect the filling point with the pump and make a vacuum less than 1 mbar. Then open to atmosphere to let air enter. Repeat the operation 2 more times.	N/A
3.12	Calibrar el Detector de Hielo con la pérdida calibrada después de realizar el ensayo. Calibrate the ice detector with the calibrated leakage after the test.	4 x 10 ⁻⁸ mbar/s

Referencias: *Terminando el punto 3.9, se retiro el Tapón de Drenaje y se colocó el sniffel detectando una pérdida en el menos 5cm de profundidad.*

APROBADO si el valor máximo observado es 2.0x10 ⁻⁸ mbar/s e inferiores. Si no RECHAZADO.	APROBADO (PASS)	
RECHAZADO si el valor máximo observado es mayor a 2.0x10 ⁻⁸ mbar/s e inferiores. Si no RECHAZADO.	RECHAZADO (FAIL)	✓
Realizado por: <i>A. Jaramila Salazar</i>	Fecha: <i>21/11/08</i>	
Revisado por: <i>Roberto Pablo</i>	Fecha: <i>21-11-08</i>	

After finishing point 3.9, The drain plug was taken apart and with the sniffel it was detected a leak in at least 5 cm of depth.

TRANSPORT CONTAINER SHIELDING TEST PROCEDURE	
Design Approval	D W Rogers  (signature) date: 20/06/2008
Quality System Approval	B S Patel  (signature) date: 23 June 2008
Date implemented	31 JUL 2008
Controlled file number	

1.0 PURPOSE AND SCOPE

The purpose of this procedure is to survey and quantify the shielding performance of transport containers for gamma emitting nuclides. The results may be used for manufacturing quality control using the pass/fail criteria or, without them, for design validation.

2.0 REFERENCES

TS-R-1 : Regulations for the Safe Transport of Radioactive Material, current edition, IAEA, Vienna.

3.0 EQUIPMENT

3.1 INSTRUMENTATION

- Package monitor (gamma), minimum range 1 - 2,000 $\mu\text{Sv/h}$.
- Finger probe (gamma), maximum detector dia 40 mm., minimum range 50 - 2,000 $\mu\text{Sv/h}$.
- Beta/ Gamma contamination probe (optional).

3.2 OTHER EQUIPMENT

- Transport container.
- Total content activity not less than 33% of licensed capacity, unless otherwise specified, in the form normally carried and evenly distributed inside the container.
- Metre rule.

4.0 PROCEDURE

4.1 SAFETY

- This procedure carries the risk of collecting a large radiation dose if it is not conducted in the right sequence.
- Barrier off an area around the container sufficiently large to maintain perimeter doserates at levels acceptable to personnel not involved in this operation.
- Ensure all operations comply with your local safety rules and procedures.

4.2 DESCRIPTION

Unless otherwise specified the test is performed in three parts on the fully assembled package:

- As soon as practicable after the container is loaded approach container cautiously and monitor for unusually high radiation readings. If safe to continue, scan entire surface, including base, for short paths and hot spots. Pay particular attention to areas of potential design/manufacturing weakness such as drain points, clearances between interlocking components, likely positions of casting defects etc. Record peak readings.
- Only when it has been established that all dose levels are within permitted limits record measurements at regular intervals along four vertical equi-spaced lines from top to bottom and their joining lines across top and bottom faces.
- Survey at one metre from surface, including base, and record maximum levels.

4.3 NOTES

- Perform the test in as low a background radiation area as possible.

- Containers with depleted uranium shielding should also have their surface dose rates in the centre of each side and the top surface recorded when unloaded.

4.5 PASS/FAIL CRITERIA

This is only applicable when the procedure is applied as a manufacturing acceptance test. When the results are scaled up linearly to the maximum licensed content activity:

- Maximum surface dose rate must not exceed 2.0 mSv/h (TS-R-1).
- Maximum dose rate at one metre from the surface must not exceed 100 μ Sv/h (TS-R-1).
- In the event of a FAIL result label flask clearly "Failed QC" or "Quarantine" unless otherwise specified.

5.0 DOCUMENTATION

5.1 CHECKLIST

To ensure all operations are adequately planned it is recommended that a checklist be used. This should contain all key instructions together with the data logging requirements, pass/fail criteria and space for observations.

5.2 RECORDS

- Complete report as the test progresses.
- Quote all activities in content activity, not output, referenced to the day of the test.
- Record all pertinent observations, if necessary taking photographs.
- Ensure completed report is reviewed and countersigned by either a test witness or your supervisor.
- Unless otherwise specified file report in manufacturing dossier or maintenance log.

Test RTR No.

RTR 264

R7021 SHIELDING SURVEY RECORD (ref. OP 214)**Equipment**

Flask Serial No.	3981/01	Serial No.	Calibration Date
Package Monitor	AUTOMESS 6150 ADS/H	121977	07/11/08
Finger probe			

Loading

Step	Description	Result or ✓
1	Measure background dose rate in area to be used for the test prior to moving container into the area.	S $\mu\text{Sv/h}$
2	Load basket and record loading plan.	✓

Loading Plan

Activity ref. date

Posn. *	Source No	Content (kCi)	Posn.	Source No	Content (kCi)	Posn.	Source No.	Content (kCi)
1			17	786	9,445	33		
2	782	9,160	18			34		
3			19			35		
4			20			36		
5			21			37		
6			22	760	9,529	38		
7	764	9,670	23			39		
8			24			40		
9			25			41		
10			26			42		
11			27	766	9,593	43		
12	774	9,593	28			44		
13			29			45		
14			30			46		
15			31			47		
16			32			48		
TOTAL		28423	TOTAL		28567	TOTAL		
* Counting clockwise from notch when viewed from above. Start on the outer ring and move to the inner ring from 30 onwards.						GRAND TOTAL		56,990

Step	Description	Result or ✓
3	Load and re-assemble flask.	✓
4	Using contamination monitor or package monitor scan entire flask surface, including underside, for any reading over 1,000 $\mu\text{Sv/h}$. Check particularly the drain and vent plugs. If found record dose rate and position and continue only if safe to do so. If none found, record 'none'. Mark highest spots on the side, top and base for future reference.	N

Test RTR No.

RT12 264

Notes:

Las mediciones se realizaron DESPUES DEL Drop Test.
No se colocaron los elementos que cubren al cuerpo.
(Socket, Pallet).

Las mediciones fueron hechas DIRECTAMENTE SOBRE LA
PARED DEL CUERPO.

Se utilizó la grilla R8062 (48 AGUJEROS)

Pages attached: Yes ☒ No ☐

If Yes how many?.....

Signed



Date

23-12-08

Witnessed/Reviewed



Date

23-12-08

Test RTR No.

RTR 264

Base Surface Scan

8 Using the monitor scan the surface in 100 mm steps in two lines across the base of the pallet in an 'X' shape continuing the line of the vertical scans.							
North		East		South		West	
Posn. *	Dose ($\mu\text{Sv/h}$)	Posn.	Dose ($\mu\text{Sv/h}$)	Posn.	Dose ($\mu\text{Sv/h}$)	Posn.	Dose ($\mu\text{Sv/h}$)
0	350	-	-	-	-	-	-
100	740	100	240	100	270	100	325
200	150	200	215	200	210	200	170
300	620	300	560	300	500	300	590
400		400		400		400	

* distance from centre, starting from below drain point and moving anti-clockwise seen from below.

Special Areas Scan

Step	Description	Result
9	Use the finger probe to measure the dose rate on the jacket directly over the drain plug.	160 $\mu\text{Sv/h}$
10	Use the finger probe to measure the dose rate on the top shield directly over the vent plug.	1540 $\mu\text{Sv/h}$
11	Use a package monitor to measure the maximum dose rate around the mid-height of the grill.	$\mu\text{Sv/h}$

Maximum Surface dose rate

12	Maximum surface dose rate from all surveys above.	1540 $\mu\text{Sv/h}$
13	Subtract background from maximum dose rate, multiply by 140 and divide by total test activity (kCi).	3770 $\mu\text{Sv/h}$

Transport Index Scan

14	Using a metre rule and the package monitor scan the flask at a distance of one metre from the surface on the sides, top and base. Record the maximum dose rate observed and its position. Pay particular attention to high dose areas identified in the previous surveys.	Top: 105 $\mu\text{Sv/h}$ Sides: 42 $\mu\text{Sv/h}$ Base: 28 $\mu\text{Sv/h}$
15	Subtract background from maximum dose rate above, multiply by 140 and divide by total test activity (kCi).	245 $\mu\text{Sv/h}$

Test RTR No.

RTR 264

Vertical Scans

5 Using package monitor scan vertically up the side of the jacket (starting in line with the drain point) in 100mm steps from base along four equi-spaced lines moving clockwise around the flask.

1st Vertical (North)		2nd Vertical (East)		3rd Vertical (South)		4th Vertical (West)	
Height (mm)	Dose ($\mu\text{Sv/h}$)	Height (mm)	Dose ($\mu\text{Sv/h}$)	Height (mm)	Dose ($\mu\text{Sv/h}$)	Height (mm)	Dose ($\mu\text{Sv/h}$)
900	980	900	750	900	900	900	960
800	300	800	200	800	245	800	220
700	320	700	220	700	250	700	280
600	300	600	260	600	300	600	300
500	310	500	300	500	344	500	390
400	280	400	235	400	340	400	220
300	250	300	150	300	180	300	180
200	750	200	520	200	510	200	620
100	820	100	830	100	800	100	930
0	760	0	570	0	540	0	780

Circumferential Scan

6 Identify the height at which the highest dose is measured above and scan horizontally around the circumference in 200 mm steps at this height starting in line with the drain point

Height 900 mm

Posn	Dose ($\mu\text{Sv/h}$)	Posn	Dose ($\mu\text{Sv/h}$)	Posn	Dose ($\mu\text{Sv/h}$)	Posn	Dose ($\mu\text{Sv/h}$)
1	990	5	830	9	590	13	
2	650	6	890	10	770	14	
3	930	7	810	11		15	
4	810	8	800	12			

Top Surface Scan

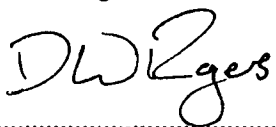
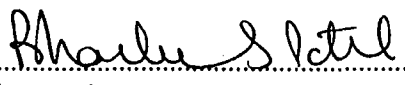
7 Using the monitor scan the surface in 100 mm steps in two lines across the top shield in an 'X' shape continuing the line of the vertical scans.

North		East		South		West	
Posn. *	Dose ($\mu\text{Sv/h}$)	Posn.	Dose ($\mu\text{Sv/h}$)	Posn.	Dose ($\mu\text{Sv/h}$)	Posn.	Dose ($\mu\text{Sv/h}$)
0	140	-	-	-	-	-	-
50	200	50	280	50	260	50	280
100	440	100	290	100	260	100	330
150	1120	150	860	150	780	150	1830
200	400	200	360	200	290	200	520
250	530	250	600	250	620	250	740

* distance from centre, starting from above drain point and moving clockwise seen from above.

300 | 530 | 300 | 630 | 300 | 630 | 300 | 740



SUPPLY SPECIFICATION WELDING FOR TRANSPORT CONTAINERS	
Design Approval	D W Rogers  (signature) date: 12/02/04
Quality System Approval	B S Patel  (signature) date: 26 February 2004
Date Implemented	25 MAR 2004
Controlled file number	



1.0 PURPOSE AND SCOPE

This document specifies the requirements for arc welding, resistance spot welding, brazing and soldering and the associated inspection processes used in the fabrication of transport containers for radioactive materials. It is not necessarily restricted to this application. It applies to both stainless and carbon steels. It does not cover the welding or joining of non-ferrous materials.

2.0 REFERENCES

- SS 028: current issue: Quality assurance requirements for controlled purchases.
- BS 499: Part 2C: 1980: Welding symbols.
- BS 1140: 1993: Specification for resistance spot welding of uncoated and coated low carbon steel.
- BS 1723: Part 1: 1986: Specification for brazing.
- BS 1723: Part 2: 1986: Guide to Brazing.
- BS 5500: 2000: Specification for unfired fusion welded pressure vessels.
- BS EN 287-1: 1992: Approval testing of welders for fusion welding. Steels.
- BS EN 288-2: 1992: Welding procedure specification for arc welding.
- BS EN 288-3: 1992: Welding procedure tests for the arc welding of steels.
- BS EN 571-1: 1997: Non-destructive testing. Penetrant testing. General principles.
- BS EN 875: 1995: Destructive tests on welds. Impact testing.
- BS EN 876: 1996: Destructive tests on welds. Longitudinal tensile test.
- BS EN 895: 1995: Destructive tests on welds. Transverse tensile test.
- BS EN 910: 1996: Destructive tests on welds. Bend testing.
- BS EN 1043-1: 1996: Destructive tests on welds. Hardness testing.
- BS EN 1043-2: 1997: Destructive tests on welds. Micro-hardness testing.
- BS EN 1320: 1997: Destructive tests on welds. Fracture testing.
- BS EN 1321: 1997: Destructive tests on welds. Macro- and microscopic examination.
- BS EN 1435: 1997: Non-destructive examination of welds. Radiographic examination.
- BS EN 1712: 1997: Non-destructive examination of welds. Ultrasonic examination. Acceptance levels.
- BS EN 1714: 1998: Non-destructive examination of welds. Ultrasonic examination.
- BS EN 12517: 1998: Non-destructive examination of welds. Radiographic examination. Acceptance levels.
- BS EN 24063: 1992: Welding, brazing, soldering and braze welding of metals. Nomenclature of processes and reference numbers for symbolic representation on drawings.
- BS EN 25817: 1992: Arc-welded joints in steel. Quality levels for imperfections.
- ASME V: Boiler and pressure vessel code. Non-destructive examination.
- ASME IX: Boiler and pressure vessel code. Welding and brazing qualifications.

3.0 DEFINITIONS

- Purchaser : REVISS Services (UK) Ltd.
- Supplier : Organisation named in the purchase order
- Welder : Person performing a manual welding operation
- Operator : Person controlling a welding machine.



4.0 QUALITY ASSURANCE

- See SS 028 for general quality assurance and documentation requirements.
- See purchase order and any specifications referenced therein for any supplementary requirements.

5.0 GENERAL

- The purchase order takes precedence over the manufacturing drawing.
- The manufacturing drawing takes precedence over this specification.
- The manufacturing drawing specifies the weld form, size and, if necessary, the process, the inspection technique and any pre- or post-heat treatment.
- Welding, brazing and soldering terms and symbols comply with BS 499 and BS EN 24063. Any drawing using the current, 1999, issue of BS 499 will carry a note to that effect.
- Brazing and soldering procedures do not require procedure approval by the Purchaser.
- The Supplier is responsible for planning the order of operations to minimise distortion.

6.0 ARC WELDING

6.1 STANDARDS AND ALTERNATIVES

This specification follows the general principles and appropriate requirements of BS5500. Other national or international pressure vessel standards may be considered technically equivalent, subject to approval by the Purchaser. As an example ASME IX (weld and welder approval) and ASME V (inspection) are acceptable. In any event the Supplier must be able to demonstrate a basic similarity in procedure and welder tests, methods of inspection and acceptance criteria. Weld procedure and welder qualification tests that may be required are BS EN 875 (impact), BS EN 876 (longitudinal tensile), BS EN 895 (transverse tensile), BS EN 910 (bend), BS EN 1043-1 & 2, (hardness), BS EN 1320 (fracture) and BS EN 1321 (macroscopic examination).

6.2 GENERAL

- All welding shall be performed in accordance with a welding procedure specification or other work instruction that conforms to BS EN 288-2. The only exception to this being for the welding of non-structural items such as source holders, mesh panels, labels etc.
- The Supplier may deviate from the drawing specification for weld preparation in order to comply with established welding procedures subject to Purchaser approval.
- All weld spatter shall be removed.
- Discolouration shall be removed from stainless steel fabrications. If discolouration is removed by chemical etching the surface must be cleaned of all residue following the manufacturer's instructions.

6.3 WELDING PROCEDURE APPROVAL

- Approval testing of welding procedures shall be conducted and recorded in accordance with BS EN 288-3 except for non-structural items.
- In addition, for butt welds in plate over 10 mm thick, a longitudinal tensile test should be conducted.
- Weld yield strength shall not be less than the specified minimum value for the parent metal. Elongation shall not be less than 80% of the specified minimum value for the parent metal.



- Impact tests in ferritic steels with specified low temperature properties shall be conducted at a temperature not exceeding that recommended by BS5500, Appendix D, or equivalent national standard. Unless otherwise specified the minimum design temperature shall be taken to be -40°C.

6.4 WELDER APPROVAL

- Approval testing of welders shall be conducted and recorded in accordance with BS EN 287-1, except for non-structural items, where the supplier shall certify that the welder is competent and adequately trained.
- A welder who successfully welds all the test pieces for a weld procedure test need not be required to undertake the welder prolongation test for a subsequent period of six months.

6.5 CONSUMABLES

- Welding consumables shall be the same as those used in the weld qualification procedure except when alternative consumables are permitted within the grouping schemes specified in BS EN 288-3.
- The storing and handling of welding consumables shall be controlled in accordance with procedures written on the basis of the maker's information.
- Welding consumables and their packaging shall be marked in accordance with the welding standard.

6.6 ALIGNMENT

Joint, i.e. parent metal, alignment must comply with the welding procedure.

6.7 TACK WELDS

Tack welds may be incorporated into the weld only if permitted by the weld procedure.

6.8 TEMPORARY ATTACHMENTS

- Any temporary attachments or supports welded to the structure shall be of the same nominal chemical composition as the structure in that area.
- The location of such attachment welds shall be chosen, as far as is practicable, to avoid existing welds and areas to be subsequently welded.
- The welding process shall follow a welding procedure or be approved by the Purchaser.
- The weld area shall be dressed smooth after removal of the attachment.

6.9 HEAT TREATMENT

- Any pre-or post-weld heat treatment requirements will be specified on the manufacturing drawing.
- No welding is to take place if parent metal temperature is less than 0°C.

6.10 WELD PROFILE

- The weld profile will be specified on the manufacturing drawing.
- Any dressing or machining requirements will be specified on the manufacturing drawing.



6.11 INSPECTION

6.11.1 General

- Non-destructive testing of the parent materials or fusion faces prepared for welding is not required.
- The manufacturing drawing will specify the final inspection technique. Intermediate inspection such as for the root run shall be in accordance with the welding procedure.
- Inspection personnel for visual and dye penetrant inspection shall be certified by the Supplier to be trained to the required standard.
- Inspection personnel for ultrasound and radiography shall hold an appropriate certificate of competence from an independent inspection authority.
- Batch inspection:
 - 1) A batch shall be considered to be two or more identical components welded by the same welder following the same procedure using the same equipment with the same settings without significant delay between consecutive welding operations.
 - 2) Visual and dye penetrant inspection requirements may not be modified.
 - 3) Radiographic and ultrasound inspection requirements may be modified to take account of the additional control afforded by the continuity of the production process. This is considered on a case by case basis and is subject to written agreement from the Purchaser.

6.11.2 Visual Inspection

- All welds, with the exception of any surfaces that are subsequently machined, shall be visually inspected. Machined surfaces need only meet the dimensional and surface finish requirements specified on the manufacturing drawing.
- Acceptance criteria: Table 5.7 (3), BS 5500 or BS EN 25817 (quality level B, stringent) to the extent permitted by access.
- Excess reinforcement is acceptable provided overall dimensions are within tolerance.

6.11.3 Dye/liquid Penetrant Inspection

- To be carried out on the weld surface in its final condition, i.e. after any subsequent machining operation, in accordance with BS EN 571-1.
- Acceptance criteria: No indications permitted.

6.11.4 Radiographic Inspection

- To be carried out in accordance with BS EN 1435, Class B technique.
- Surfaces may be dressed only where weld surface ripples or irregularities will interfere with interpretation of the radiograph.
- Acceptance criteria: Table 5.7 (1), BS 5500 or BS EN 12517, Level 1.
- Where geometry or design make radiography impractical or unreliable the Supplier has several options:
 - 1) Prepare a coupon of the same geometry and materials and not less than the greater of 10% of the length of the production weld or 200 mm. The welder, or operator, shall weld the coupon at the same time as the production weld, run for run, without changing any machine settings. The coupon shall then be machined as necessary to allow a satisfactorily clear radiograph. The production weld may then be sentenced on the coupon results.
 - 2) Use ultrasound inspection in accordance with 6.11.5 below.
 - 3) Use dye penetrant inspection on each weld run in accordance with 6.11.3 above.



6.11.5 Ultrasound Inspection

- To be carried out in accordance with BS EN 1714, Level B.
- The condition of surfaces in contact with the probe must comply with the requirements of BS EN 1714.
- Acceptance criteria: Table 5.7 (2) BS 5500 or BS EN 1712, Level 2.
- Where geometry or design make ultrasound impractical or unreliable the Supplier has several options:
 - 1) Prepare a coupon of the same geometry and materials and not less than the greater of 10% of the length of the production weld or 200 mm. The welder, or operator, shall weld the coupon at the same time as the production weld, run for run, without changing any machine settings. The coupon shall then be machined as necessary to allow a satisfactory ultrasound scan. The production weld may then be sentenced on the coupon results.
 - 2) Use radiographic inspection in accordance with 6.11.4 above.
 - 3) Use dye penetrant inspection on each weld run in accordance with 6.11.3 above.

6.12 REPAIRS

- Repair welds shall be carried out to an approved procedure and are subject to the same acceptance criteria as the original work.

6.13 TRACEABILITY MARKINGS

- All materials, other than those less than 6 mm thick or those used in non-structural fabrications, shall be permanently marked on an external surface, for instance by stamping, vibro-engraving or equivalent process, with the cast or heat number for that material.
- Welds in materials so marked shall be permanently marked in their vicinity with the welder's identity mark.
- Where possible a marking shall be sited on an unmachined external surface. If all external surfaces are machined the marking shall avoid areas of 0.8 μ m surface finish and shall be only be deep enough to be legible. If there is no accessible external surface the marking may be omitted.
- Temporary markings shall be removed after manufacture but before any acceptance testing.

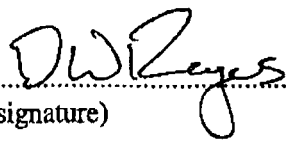
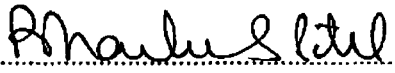
7.0 RESISTANCE SPOT WELDING

- Spot welding shall comply with the general principles of BS 1140.
- Welder/operator and inspector shall be certified by the Supplier to be trained to the required standard.
- The procedure shall be established using identical samples (materials, thicknesses, surface condition or coatings and number and size of welds).
- Weld samples shall be clearly identified with the procedure, issue status and date.
- Samples shall be tested destructively by splitting apart the joint with a hammer and chisel.
- A plug of metal from one side shall be retained on the other side of the joint.
- Prior to any production spot welding the welder shall check the machine settings by destructively testing a sample as above. No production spot welding may take place until the settings have been satisfactorily rechecked.
- After continuous production welding for a period of two hours, and subsequently every two hours, the welder shall check the machine settings by retesting a sample as above.



8.0 BRAZING AND SOLDERING

- Brazing shall comply with the general principles of BS 1723, Parts 1 & 2.
- The welder/operator and inspector shall be certified by the Supplier to be trained to the required standard.
- The Supplier shall be able to show that the consumables are suitable for the process and materials being joined.
- The storing and handling of welding consumables shall be controlled in accordance with procedures written on the basis of the maker's information.
- The brazing/soldering procedure shall be established using identical samples (materials, thicknesses and surface condition).
- The procedure shall include the removal of corrosive fluxes and cleaning agents.
- Samples shall be examined visually with a 2-4 times magnifying lens. The joint shall show no evidence of lack of flow or cracks in or around the joint.

SUPPLY SPECIFICATION	
SURFACE FINISH REQUIREMENTS FOR TRANSPORT CONTAINERS	
Design Approval	D Rogers  (signature) date: 03/07/2008
Quality System Approval	B Patel  (signature) date: 03 July 2008
Date implemented	31 JUL 2008
Controlled file number	

1.0 PURPOSE AND SCOPE

This document specifies the surface coating or finish requirements (painting, galvanising, electroplating, clean and matt) of components for transport containers for radioactive materials. It is not necessarily restricted to this application.

2.0 REFERENCES

- BS 1706: Method for specifying electroplated coatings of zinc and cadmium onto iron and steel.
- BS 4800: Schedule of paint colours for building purposes.
- BS EN ISO 1461: Hot dip galvanized coatings on fabricated iron and steel articles.

3.0 DEFINITIONS

- Purchaser : REVISS Services (UK) Ltd.
- Supplier : Organisation named in the purchase order

4.0 QUALITY ASSURANCE

See purchase order and any specifications referenced therein for any supplementary requirements.

5.0 GENERAL

- The purchase order takes precedence over the manufacturing drawing.
- The manufacturing drawing takes precedence over this specification.
- The manufacturing drawing will specify the treatment, the applicable area and any special instructions.

6.0 PROTECTIVE COATINGS

6.1 CARBON STEEL (GENERAL)

- Paint: Zinga (obtainable from Zinga UK Ltd, 3 Arkwright Way, North Newmoor, Irvine).
 - Preparation: Ensure all surfaces are free from rust, moisture, oil or other surface contamination and blast clean to 60-80µm profile.
 - Application: Apply in accordance with manufacturer's instructions.
 - Thickness: Nominal 120µm dry film thickness.

6.2 CARBON STEEL (FLATRACKS AND ASSOCIATED COMPONENTS)

- Undercoat: Quick drying zinc phosphate high build primer (e.g. Product 51L25, Fiesta Industrial Paints Ltd, Burnley Road, Hapton, Lancs BB11 5QR).
 - Colour: Light grey.
 - Preparation: Ensure all surfaces are free from rust, moisture, oil or other surface contamination and blast clean to 60-80µm profile.
 - Application: Apply in accordance with manufacturer's instructions.
 - Thickness: Nominal 75µm dry film thickness.
- Top coat: Modified chlorinated rubber paint (e.g. Product 58L300, Fiesta Paints).
 - Colour: Light grey (e.g. BS 4800, 18B17).
 - Application: Apply in accordance with manufacturer's instructions.
 - Thickness: Nominal 75µm dry film thickness.

6.3 GALVANISING

- Prepare surface and hot dip galvanise in accordance with BS EN ISO 1461. Nominal thickness 0.1 mm.
- No drips or spikes permitted.

6.4 ZINC PLATING

Prepare surface, zinc electroplate and passivate in accordance with BS 1706, Zn-3.

7.0 STANDARD SURFACE FINISHES

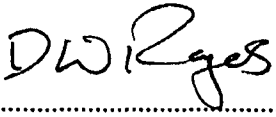
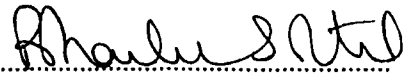
Applies to corrosion resistant materials such as stainless steel, brass and lead:

7.1 CLEAN

Surfaces are to be wiped clean of all visible traces of lubricants, machining fluids, swarf, loose particles and dirt.

7.2 MATT

- Often used on stainless steel surfaces for glare control it may be achieved using bead blasting. Clean glass or plastic beads are necessary to avoid iron contamination and will avoid the surface becoming too rough.
- A matt finish may be achieved by mechanical or chemical means if not otherwise specified. Chemical techniques must include an appropriate cleansing procedure.
- The procedure and a sample of the finish must be submitted for approval by the Purchaser before application.

SUPPLY SPECIFICATION MARKING TECHNIQUES FOR TRANSPORT CONTAINERS	
Design Approval	D W Rogers  (signature) date: 01/05/02
Quality System Approval	B S Patel  (signature) date: 01 May 2002
Controlled file number	

1.0 PURPOSE AND SCOPE

This document specifies the requirements for the permanent marking (engraving, stamping, laser etching, vibro-engraving and paint marking) of components for transport containers for radioactive materials. It is not necessarily restricted to this application.

2.0 REFERENCES

SS 028: current issue: Quality assurance requirements for controlled materials.

3.0 DEFINITIONS

- Purchaser : REVISS Services (UK) Ltd.
- Supplier : Organisation named in the purchase order

4.0 QUALITY ASSURANCE

- See SS 028 for general quality assurance and documentation requirements.
- See purchase order and any specifications referenced therein for any supplementary requirements.

5.0 GENERAL

- The purchase order takes precedence over the manufacturing drawing.
- The manufacturing drawing takes precedence over this specification.
- The manufacturing drawing and/or associated supply specification will specify the content, size, position and marking technique.
- All text shall be in an upright, non-ornate (sans-serif) typeface. The capital letter height will be specified on the drawing or associated specification.
- All text and symbols must be faithfully reproduced. It is not permissible to change the case, omit, add or otherwise modify what is shown on the drawing or associated specification.
- Care should be observed in reading the drawing notes or associated specification. Variable text is usually shown as dashes or crosses with an instruction where to find the actual text (for instance "See purchase order for serial number").

6.0 MARKING TECHNIQUES

6.1 ENGRAVING

- Engraving is the machining of a U-shaped groove in the surface of a component.
- The groove width shall be 12-20% of the specified text height unless otherwise specified on the manufacturing drawing or specification.
- The groove depth shall be 0.10 - 0.30 mm.
- If "back-fill in black" is specified the Supplier shall use a waterproof paint or paint system recommended by the paint manufacturer for the base metal to ensure adequate adhesion.
- If a trefoil (the standard radiation warning symbol) is required and the drawing gives only the outer diameter the proportions defined in Figure 1 shall be used.
-

6.2 LASER ETCHING

- Laser etching is the computer controlled oxidation of a stainless steel surface with a scanning laser.

- Line width shall be 12-20% of the specified text height unless otherwise specified on the manufacturing drawing or specification.
- If a trefoil (the standard radiation warning symbol) is required and the drawing gives only the outer diameter the proportions defined in Figure 1 shall be used.

6.3 STAMPING

- Stamping is the indentation of a surface, one character at a time, by the impact of a shaped punch tool.
- The minimum depth shall be determined by legibility. The maximum depth shall be 0.5mm.
- Engraving is an acceptable alternative technique.

6.4 VIBRO-ENGRAVING

- Vibro-engraving is the indentation of a surface using a hand tool with a vibrating hardened tip.
- Text shall be non-ornate and clearly legible to the naked eye.
- Engraving or stamping is an acceptable alternative technique..

6.5 MARKING

- Marking is the application of text using paint and a stencil.
- It may be applied to metallic or organic base materials.
- The Supplier shall use a waterproof paint or paint system recommended by the paint manufacturer for the base material to ensure adequate adhesion.

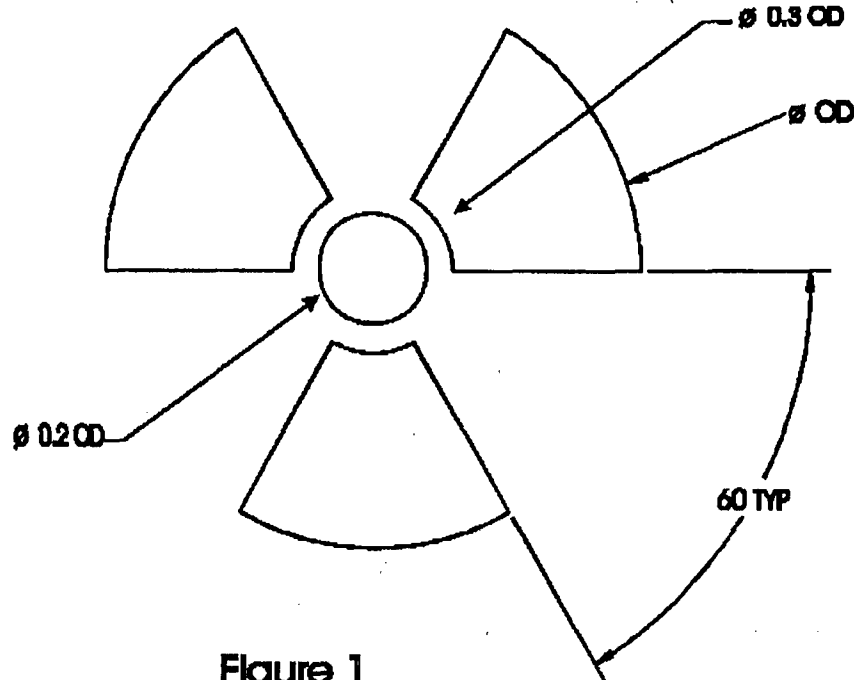


Figure 1
Trefoil Proportions

SUPPLY SPECIFICATION
LOW CARBON STAINLESS STEELS

Design
Approval

D W Rogers



(signature)

date: 11/07/00

Management
Approval

D A Coppel

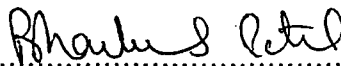


(signature)

date: 18/7/2000

Quality System
Approval

B S Patel



(signature)

date: 20/7/2000

Controlled file number



1.0 PURPOSE AND SCOPE

This purpose of this document is to define the essential physical and chemical properties of the group of materials generally known as low carbon, austenitic stainless steels. It also provides guidance for manufacturers in the selection and use of these materials. It applies only to the raw material forms of sheet, plate, strip, rod, bar, tube and pipe. It does not apply to proprietary items such as fasteners and mesh.

2.0 REFERENCES

- SS 028: current issue: Quality assurance requirements for controlled purchases.
- BS 970: Part 3: 1991: Bright bars for general engineering purposes.
- BS 1449: Part 2: 1983: Specification for stainless and heat resisting steel plate, sheet and strip.
- BS 1501: Part 3: 1990: Specification for corrosion and heat resisting steels: plates, sheet and strip.
- BS 3605: Pt 1: 1991: Specification for seamless tubes.
- BS 3605: Pt 2: 1992: Specification for longitudinally welded tubes.
- BS EN ISO 3651-2: 1998: Ferritic, austenitic, and ferritic-austenitic (duplex) stainless steels. Corrosion tests in media containing sulphuric acid.

3.0 DEFINITIONS

- Purchaser : REVISS Services (UK) Ltd.
- Supplier or Manufacturer : Organisation named in the purchase order.

4.0 QUALITY ASSURANCE

- General requirements are detailed in SS 028.
- See purchase order and any specifications referenced therein for any supplementary requirements.

5.0 GENERAL

- The purchase order takes precedence over the manufacturing drawing.
- The manufacturing drawing takes precedence over this specification.
- The manufacturing drawing will specify the principle dimension(s) and form of the raw material and any additional requirements.

6.0 SPECIFICATION

6.1 STANDARDS

The table lists acceptable UK standards and a selection of German and US equivalents current at the time of writing:

Material Form	UK	German	USA
Sheet and Strip	BS 1449, Pt 1	DIN 17440 DIN 17441	ASTM A240
Plate	BS 1449, Pt 2	DIN 17440	ASTM A240

Material Form	UK	German	USA
	BS 1501, Pt 3		
Rod and Bar	BS 970, Pt 3	-	ASTM A479
Tube	BS 3605	DIN 50049 3.1.B	ASTM A269 ASTM A213 ASTM A511
Pipe	BS 3605	DIN 50049 3.1.B	ASTM A312 ASTM A376 ASTM A358 ASME SA312

6.2 MATERIAL GRADES

The table lists acceptable UK grades and a selection of equivalent grades current at the time of writing:

UK (BS 970)	French (AFNOR)	German (WNR)	Italian	Japanese (JIS)	Swedish (SIS)	USA (SAE)
304S11	Z2CN18.10	1.4306	X2CrNi 18 11	SUS304L	14 23 52	304L
316S11 316S13	Z2CND17.12	1.4404 1.4435	X2CrNiMo 17 12	SUS316L	14 23 53 14 23 48	316L

6.3 INTERGRANULAR CORROSION

All materials must be capable of passing the intergranular corrosion test specified in BS EN ISO 3651-2, Method A, or equivalent.

6.4 OTHER STANDARDS AND GRADES

Materials conforming to other equivalent national or international standards may be used subject to written permission from the Purchaser. Such materials shall meet the following chemical and mechanical requirements and the intergranular corrosion test specified above:

6.4.1 304L

Composition (% maximum unless stated)								Strength (min MPa)		Elongation
C	Si	Mn	P	S	Cr	Mo	Ni	Tensile	0.2% Strain	5.65√So*
0.030	1.00	2.00	0.045	0.030	20.0 17.0	-	13.0 8.0	480	173	40% min

* or 50 mm gauge length (So = cross-sectional area, thus length is equivalent to 5D on cylindrical test piece).

CONTROLLED DOCUMENT

(when in red)



6.4.2 316L

Composition (% maximum unless stated)								Strength (min MPa)		Elongation
C	Si	Mn	P	S	Cr	Mo	Ni	Tensile	0.2% Strain	5.65 $\sqrt{S_0}$
0.030	1.00	2.00	0.045	0.030	18.5 16.5	3.0 2.0	15.0 10.0	480	173	40% min

7.0 RAW MATERIAL SIZES

The manufacturing drawing will state the stock material sizes in one system of units. The manufacturer may deviate from the specification in two instances:

Machined items:

Where the primary dimension (thickness, width or diameter) is subsequently machined down the size may be taken as a guide only. The manufacturer may use any appropriate stock size.

Imperial/metric parity:

Where the item is not machined, and materials are not available in the unit system specified, the manufacturer may use the following equivalent sizes. It is the manufacturer's responsibility to ensure that all mating dimensions are adjusted so that fits and clearances are maintained.

Imperial (inch)	1/8	3/16	1/4	3/8	1/2	5/8	3/4	7/8	1.0	1.5	2.0
Metric (mm)	3	5	6	10	12	16	20	22	25	40	50

Imperial (swg)	22	20	18	16	14	12	10	8	6	4	2
Metric (mm)	0.75	1	1.25	1.5	2	2.5	3.5	4	5	6	7

8.0 DOCUMENTATION

The Supplier shall provide certified evidence from the manufacturer or from his own testing that the chemical composition and mechanical properties meet this specification or one of the equivalents cited previously. All documentation shall reference the original cast or heat number.

TRANSPORT CONTAINER THERMAL SURVEY PROCEDURE	
Design Approval	<p>D W Rogers</p> <p><i>DWRogers</i></p> <p>.....</p> <p>(signature)</p> <p>date: 20/03/07</p>
Quality System Approval	<p>B S Patel</p> <p><i>Bhaskar S Patel</i></p> <p>.....</p> <p>(signature)</p> <p>date: 23 March 2007</p>
Date implemented 13 APR 2007	
Controlled file number	

1.0 PURPOSE AND SCOPE

The purpose of this procedure is to survey the temperature profile of a transport container with an internal heat load. The results may be used to validate a thermal model or calculations.

2.0 EQUIPMENT

2.1 INSTRUMENTATION

- Thermometer and/or temperature recorder.
- Ambient air thermometer.

2.2 OTHER EQUIPMENT

- Transport container and capsule basket.
- Thermocouples and appropriate adhesive(s), as required.
- Thermocoupled capsules, as required.
- Spacers, as required, to allow exit of thermocouple leads.
- Internal heat load of nominal 50% of maximum licensed capacity in normal form.

3.0 PROCEDURE

3.1 SAFETY

Ensure all operations do not conflict with your local safety rules and procedures.

3.2 CHECKLIST

To ensure all operations are adequately planned it is recommended that a checklist be used. This is normally provided by the Design Authority and should contain all key instructions together with the data logging requirements and space for observations.

3.3 PROCEDURE

- Complete checklist as the test progresses.
- Record all pertinent observations, if necessary taking photographs.
- Site the container in a clear area at least twice as wide and free from continuous drafts.
- Use sufficient thermocouples to measure the axial and radial temperature distribution and the temperature at critical points such as fasteners or known hot spots. On large containers use duplicate, evenly spaced sensors to average key readings.
- Load basket to loading plan.
- Record temperatures when rise is less than 0.25% per hour.
- Ensure completed report is reviewed and countersigned by either a test witness or your supervisor.
- Unless otherwise specified send report to Design Authority.

TRANSPORT CONTAINER THERMAL TEST PROCEDURE

Design
Approval

D W Rogers

DW Rogers

.....
(signature)

date: 14/04/05

Quality System
Approval

B S Patel

Bharat S Patel

.....
(signature)

date: 15 April 2005

Date implemented

24 MAY 2005

Controlled file number

1.0 PURPOSE AND SCOPE

The purpose of this procedure is to test the thermal performance of a transport container with an internal heat load. The results may be used in manufacturing quality control, routine inspection or at any other time. It is not necessarily restricted to this application.

2.0 EQUIPMENT

2.1 INSTRUMENTATION

- Thermocouples and thermometer.
- Ambient air thermometer.

2.2 OTHER EQUIPMENT

- Transport container.
- Internal heat load of nominal 50% of maximum licensed capacity in normal form.
- Spacers, if required, to allow exit of thermocouple leads.

3.0 PROCEDURE

3.1 SAFETY

- The container surface may get hot enough to burn unprotected skin.
- Dose levels around the lid may be higher than normal if the lid has to be supported on spacers to allow access for thermocouple leads.
- Ensure all operations comply with your local safety rules and procedures.

3.2 DESCRIPTION

Unless otherwise instructed:

- Assemble the container in accordance with its Certificate of Approval (if none then the assembly drawing).
- Site the test in a clear area at least twice as wide as the container and free from continuous drafts.
- Use sufficient thermocouples to measure the temperature at critical points. On large containers use sufficient duplication to average key readings.
- Load basket to the loading plan and check doserates are within acceptable limits before proceeding.
- Record temperatures when rise is less than 0.25% per hour.

3.3 PASS/FAIL CRITERIA

- To be specified by Design Authority.
- In the event of a fail result label flask clearly "Failed QC" or "Quarantine" unless otherwise specified.

4.0 DOCUMENTATION

4.1 CHECKLIST

To ensure the test is adequately planned and recorded a checklist should be used. This should contain all key instructions together with any deviations from the normal assembly



procedure (or assembly drawing), the data logging requirements, pass/fail criteria and space for observations.

4.2 RECORDS

- Record any deviations from the checklist instructions.
- Complete report as the test progresses.
- Record all pertinent observations, if necessary taking photographs.
- Ensure completed report is reviewed and countersigned by either a test witness or your supervisor.
- Unless otherwise specified file report in manufacturing dossier or maintenance log.

Test RTR No.	12TR 225	Chr. Serial No.	3981/01
--------------	----------	-----------------	---------

R7021 THERMAL SURVEY RECORD (Ref. OP 215)

Equipment	
Thermometer:	TES 1303 K/J
Calibration Due:	03/10/09

Preparation		
Step	Operation	Result or ✓
1	Prepare flask with thermocouples as in table below.	✓
2	Load basket and record loading plan.	✓

Loading Plan					Activity ref. date:		29/10/08	
Posn. No.	Source No.	Content (kg)	Posn. No.	Source No.	Content (kg)	Posn. No.	Source No.	Content (kg)
1	769	9.683	17			33		
2	776/608	9.300	18	516/586	9.193	34		
3			19	963	9.555	35		
4	779	9.593	20	960	9.679	36		
5			21			37		
6	764	9.670	22	966	9.583	38		
7	762	9.606	23			39		
8	780	9.509	24	936	10.059	40		
9			25			41		
10	756/696	9.300	26			42		
11			27			43		
12	779	10.022	28			44		
13	767	9.395	29			45		
14	786	9.445	30			46		
15			31			47		
16	782	9.160	32			48		
TOTAL			TOTAL			TOTAL		
* Counting clockwise from notch when viewed from above. Start on the outer ring and move to the inner ring from 30 onwards.						GRAND TOTAL		152,582

Loading and assembly		
Step	Operation	Result or ✓
3	Load flask using spacers under closure to allow leads to exit flask and assemble into transport crate.	✓
4	Site container in area not less than 3.6 m square, free from continuous drafts and with a stable ambient temperature.	✓

Test RTR No.	12TR 225	Contr. Serial No.	3981/01
--------------	----------	-------------------	---------

Thermocouples			
Identity	Location	Drop/Part No.	Adhesive
X1	Dummy R2089 #1, 280mm from bottom, equi-spaced	R8096/301	Brass
X2	Dummy R2089 #1, 280mm from bottom, equi-spaced		
X3	Dummy R2089 #1, 280mm from bottom, equi-spaced		
Y1	Dummy R2089 #2, 280mm from bottom, equi-spaced	R8096/301	Brass
Y2	Dummy R2089 #2, 280mm from bottom, equi-spaced		
Y3	Dummy R2089 #2, 280mm from bottom, equi-spaced		
Z1	Dummy R2089 #3, 280mm from bottom, equi-spaced	R8096/301	Brass
Z2	Dummy R2089 #3, 280mm from bottom, equi-spaced		
Z3	Dummy R2089 #3, 280mm from bottom, equi-spaced		
A1	Cavity wall, 50mm below top, equi-spaced	12-K-2000-11E-05-21-3PZLB-2MTRS C40KX	Silver-loaded epoxy: RS 186-3616
A3	Cavity wall, 50mm below top, equi-spaced		
B1	Cavity wall, mid-height, equi-spaced		
B2	Cavity wall, mid-height, equi-spaced		
B3	Cavity wall, mid-height, equi-spaced	R5219-4321	Heat sink adhesive: RS 850 55-1
B4	Cavity wall, mid-height, equi-spaced		
C1	Cavity wall, 50mm above base, equi-spaced		
C3	Cavity wall, 50mm above base, equi-spaced		
F1	Closure top surface, 10mm from outer edge		
F2	Vent plug		
G1	Lifting fin, at top shield attachment point		
G3	Lifting fin, at top shield attachment point		
H1	Lifting fin, at lifting point		
H3	Lifting fin, at lifting point		
I1	Lifting fin, at jacket attachment point		
I3	Lifting fin, at jacket attachment point		
L1	Plank side, 600mm from base, equi-spaced, between fins		
L2	Plank side, 600mm from base, equi-spaced, between fins		
L3	Plank side, 600mm from base, equi-spaced, between fins		
L4	Plank side, 600mm from base, equi-spaced, between fins		
N	Drain plug		
P1	Plank front, top surface, 20mm from outer edge		
P3	Plank front, top surface, 20mm from outer edge		
R1	Jackets, top edge, mid-way between lifting fins		
K1	Jackets, top edge, mid-way between lifting fins		
S1	Civil, mid-height, mid-way between lifting fins		
S3	Civil, mid-height, mid-way between lifting fins		
T1	Top shield, mid-height, outermost vertical face		
T3	Top shield, mid-height, outermost vertical face		
U1	Top shield, halfway across topmost horizontal face		
U3	Top shield, halfway across topmost horizontal face		
V	Top shield, centre, outer surface		
	Ambient air temperature		

Equilibration						
Step	Operation	Time	Cavity wall temperature (°C)			
			B1	B2	B3	B4
5	Take readings (not less than 24 hrs later).					
6	Take readings 1 hr later.					
7	Calculate difference as a percentage.					

R7021 Thermal Survey

page 2 of 3

BACKGROUND AND SIGNATURE TAB

**USE THIS SIDE OF THE SHEET TO PRECEDE
THE BACKGROUND MATERIAL
WHEN ASSEMBLING CORRESPONDENCE**

(USE REVERSE SIDE FOR SIGNATURE TAB)

BACKGROUND AND SIGNATURE TAB

**USE THIS SIDE OF THE SHEET TO PRECEDE
THE SIGNATURE PAGE
WHEN ASSEMBLING CORRESPONDENCE**

(USE REVERSE SIDE FOR BACKGROUND TAB)